



INEL-96/0439

November 1996

## **Innovative Subsurface Stabilization Project—Final Report**

**MASTER**

DISTRIBUTION OF THIS DOCUMENT IS UNLIMITED

***Guy G. Loomis  
Andrew P. Zdinak  
Carolyn W. Bishop***

**LOCKHEED MARTIN** 

#### DISCLAIMER

This report was prepared as an account of work sponsored by an agency of the United States Government. Neither the United States Government nor any agency thereof, nor any of their employees, makes any warranty, express or implied, or assumes any legal liability or responsibility for the accuracy, completeness, or usefulness of any information, apparatus, product or process disclosed, or represents that its use would not infringe privately owned rights. References herein to any specific commercial product, process, or service by trade name, trademark, manufacturer, or otherwise, does not necessarily constitute or imply its endorsement, recommendation, or favoring by the United States Government or any agency thereof. The views and opinions of authors expressed herein do not necessarily state or reflect those of the United States Government or any agency thereof.

## **DISCLAIMER**

**Portions of this document may be illegible electronic image products. Images are produced from the best available original document.**

Errata  
to  
INEL-96/0439  
November 1996

**Innovative Subsurface Stabilization Project - Final Report**

Guy G. Loomis  
Andrew P. Zdinak  
Carolyn W. Bishop

p vii 24,000 holes = 14,000 holes  
p viii \$21,866,000 = \$13.1 M  
\$12,514,000 = \$8.2 M  
\$10,730,000 = \$6.6 M  
\$1704 = \$816  
\$1045 = \$514  
\$829 = \$413

p 77 4 9/16 = 3 9/16

p 247 24,000 = 14,000  
\$22 M = \$13.1 M  
\$13.5 M = \$8.2 M  
\$10.7 M = \$6.6 M  
1704 = 816  
1045 = 514  
829 = 413

p 248 6000K = 3500 K  
24,000 = 14,000  
12,000 = 7,000  
4800 = 2800  
2400 = 1400  
18,850 = 11,350  
11,600 = 7,100  
9200 = 5750  
1,885 = 1135  
1165 = 715  
925 = 575  
1131 = 681  
699 = 429  
555 = 345  
21,866 = 13,166  
13,514 = 8,294  
10,730 = 6,670

## **Innovative Subsurface Stabilization Project—Final Report**

**Guy G. Loomis  
Andrew P. Zdinak  
Carolyn W. Bishop**

**Published November 1996**

**Idaho National Engineering Laboratory  
Environmental Restoration Technologies Department  
Lockheed Martin Idaho Technologies Company  
Idaho Falls, Idaho 83415**

**Prepared for the  
U.S. Department of Energy  
Assistant Secretary for Environmental Management  
Under DOE Idaho Operations Office  
Contract DE-AC07-94ID13223**

**Innovative Subsurface Stabilization  
Project—Final Report**

**INEL-96/0439**

Reviewed by:

*Rick Farnsworth*

Rick Farnsworth  
Advisory Engineer

*2-21-97*

Date

*Gretchen E Matthern*

Gretchen Matthern  
Integrated Product Team Leader—Stabilization

*2-22-97*

Date

Approved by:

*Kevin M Kostelnik*

Kevin Kostelnik  
Environmental Restoration Technologies Department Manager

*2/13/97*

Date



## ABSTRACT

This is a report of results of applying four innovative grouting materials and one commercially available material for creating monoliths out of buried waste sites using jet grouting. The four innovative materials included a proprietary water-based epoxy, an Idaho National Engineering Laboratory-developed two-component grout that resembles hematite when cured with soil, molten low-temperature paraffin, and a proprietary iron oxide cement-based grout called TECT. The commercial grout was Type-H high-sulfate-resistant cement. These materials were tested in specially designed cold test pits that simulate buried transuranic waste at the Idaho National Engineering Laboratory. In addition to the grouting studies, specially designed field-scale permeameters were constructed to perform full-scale controlled mass balance hydraulic conductivity studies. An ungrouted field-scale permeameter contained simulated buried waste and soil and was left ungrouted, and a second identical field-scale permeameter was grouted with commercial-grade Type-H cement. The field demonstrations were performed in an area referred to as the Cold Test Pit at the Idaho National Engineering Laboratory. The Cold Test Pit is adjacent to the laboratory's Radioactive Waste Management Complex. At the complex, 2 million ft<sup>3</sup> of transuranic waste is commingled with 6–8 million ft<sup>3</sup> of soil in shallow land burial, and improving the confinement of this waste is one of the options for final waste disposition. By creating monoliths out of the waste using jet grouting of encapsulating materials, the waste is simultaneously protected from subsidence and contained against further migration of contaminants. This report gives results of grouting, coring, hydraulic conductivity, and destructive examination of the grouted buried waste matrix.



## EXECUTIVE SUMMARY

The Innovative Subsurface Stabilization Project is a series of applied research tests involving stabilizing simulated buried waste sites with grouting agents using jet-grouting techniques. The purpose of this research is to prove that the technology is valid for application to hot buried waste sites. The basic jet-grouting technique is to make the waste into a solid monolith, which is the same effect as simultaneous horizontal and vertical barriers while also providing stabilization against subsidence. The monolith is created by jet grouting adjacent columns with the grouting material such that the soil-and-waste matrix forms a solid monolith, which should be an improved containment over a combination of vertical and horizontal barriers.

In FY-94, the Subsurface Stabilization Project first examined the proof of concept of stabilizing the waste by jet grouting then retrieving the resultant monolith. In this innovative retrieval concept, the grouted matrix agglomerated the waste into a matrix that reduced dust spread during retrieval. During this demonstration, it was shown that simple Type-1 Portland cement was jet groutable, the resultant monolith was free of voids, and there was a reduction in dust spread during retrieval compared with using conventional mining techniques to control dust. Next, in FY-95, the technology examined jet grouting a two-component acrylic polymer grout with two different formulations. One formulation resulted in a hard durable monolith for long-term confinement, and the other formulation resulted in a rubber-like monolith that was easily retrieved with little dust spread. Finally, the subject study was designed to expand the list of grouts that are jet groutable and to examine the use of a thrust block for controlling secondary waste. All of these studies are used as background information to support demonstrations or treatability studies for stabilizing contaminated buried waste sites.

During a full-scale field study, one commercially available grouting material and four innovative materials were evaluated for use in creating monoliths out of buried waste sites using jet grouting. The four innovative materials included a proprietary water-based epoxy, an Idaho National Engineering Laboratory (INEL)-developed two-component grout that resembles hematite when cured with soil, molten low-temperature paraffin, and a proprietary iron oxide cement-based grout called TECT. The commercial grout was high-sulfate-resistant Portland cement (Type-H cement). These materials were tested in specially designed cold test pits that simulate buried transuranic waste at the INEL.

In addition to the grouting studies, specially designed field-scale permeameters were constructed to perform full-scale controlled mass balance hydraulic conductivity studies. An ungrouted field-scale permeameter contained simulated buried waste and soil, and a second identical field-scale permeameter was grouted with commercial-grade Type-H high-sulfate-resistant cement. The field demonstrations were performed at the INEL in an area referred to as the Cold Test Pit, which is adjacent to the INEL's Radioactive Waste Management Complex (RWMC). At the RWMC, 2 million ft<sup>3</sup> of transuranic waste is commingled with 6–8 million ft<sup>3</sup> of soil in shallow land burial, and improving the confinement of this waste is one of the options for final waste disposition. By creating monoliths out of the waste using jet grouting of encapsulating materials, the waste is simultaneously protected from subsidence and contained against further contaminant migration.

## Field Testing Results and Recommendations

Both the TECT and paraffin grout were successfully grouted in a typical buried waste scenario. Grouting of the TECT material was accomplished with minimal grout returns while still filling voids in the pit. The paraffin grouting operation resulted in copious grout returns (about 33% of injected volume). However, the long-term multiday cooling of the molten interior of the grouted pit resulted in considerable permeation of ungrouted soils, leaving all contents of the pit, both soil and waste, virtually saturated in paraffin. Use of both TECT and paraffin in jet grouting of buried waste sites resulted in a cohesive (stand-alone) monolith with essentially no voids. The TECT material is difficult to retrieve because the resultant mixture of soil and grout (soilcrete) in the monolith cures to a hard high-compressive-strength (greater than 1,000 psi) material. The paraffin monolith, while freestanding, is easily retrieved with a standard backhoe with minimal dust spread. Both of these materials can be recommended for jet-grouting buried transuranic waste sites or radioactive-contaminated soil zones.

It is recommended that the TECT grout be used in applications where the monolith is left in an undisturbed state and that the paraffin material be applied for interim storage followed by retrieval at a later date. It is recommended that a spoils return management strategy be refined for application of the molten paraffin grout and that modifications to the drilling system be engineered for radioactive applications.

The TECT grout readily mixed with the organic sludge simulant (common canola oil/kitty litter) and formed a cured cohesive monolith. This is in contrast to poor results with the Type-1 cement and the acrylic polymer grouting performed in previous experiments.

The TECT pit showed a solid monolith with small inclusions of ungrouted soil completely surrounded by grout. These inclusions represent approximately 15% of the volume of the pit. For the paraffin, however, the inclusions of soil were completely permeated with paraffin prior to solidification, and there were virtually no regions not encapsulated with paraffin.

Also successfully grouted was the Type-H cement in both a field-scale permeameter full of simulated waste and a pit. The Type-H cement is jet groutable in field applications and forms a cohesive monolith following jet grouting, except (as observed during destructive examinations) in regions of high concentrations of a nitrate salt simulator sodium sulfate. The jet-grouting action did not form a cured mixture in the vicinity of a sodium sulfate drum located on the edge of a pit. Even though the Type-H cement is considered high sulfate resistant, it is designed to accommodate only a few percent sulfates in the total volume. In the jet-grouting operation in the pit, the grout encountered pure sodium sulfate and therefore did not form a solid cured monolith. Even though the monolith was quite porous in this region, there were no visible voids and the waste was stabilized against subsidence. Although jet groutable, the Type-H cement tends to cake on filters and to intermittently plug nozzles during injection.

The INEL-developed hematite material could not be jet grouted because of "filter caking" of the slaked lime slurry mixture.

The proprietary epoxy material could not be jet grouted because the B part of the mixture was too viscous.

Core and TV video log data in drilled core holes are in general agreement with destructive examination data. TV logs show the sides of the core hole to exhibit a solid walled monolith, indicating that coring and the use of TV video logs may replace destructive examinations.

Use of a thrust-block concept for secondary waste management works well for controlling grout returns for the TECT grout. However, application of this idea for paraffin may require some modification or expansion of the volume within the thrust block. In either case, the concept appears workable for field applications.

Packer testing of the grouted permeameter grouted with Type-H cement, the TECT pit, and the paraffin pit showed positions with hydraulic conductivity of  $10^{-7}$  cm/s or less. These tests involved local hydraulic conductivity measurements using core holes and standard packer systems.

Hydraulic conductivity testing using the falling head method in a specially prepared full-scale permeameter has shown that the ungrouted condition in an INEL-simulated buried transuranic waste pit has a hydraulic conductivity of about  $10^{-5}$  cm/s, which does not agree with previous data of  $10^{-3}$  cm/s. In the previous data, water was free to flow isotropically through the matrix as well as horizontally away from the matrix, which could explain the difference.

The overall hydraulic conductivity of the permeameter grouted with Type-H cement is inconclusive. The packer data for this permeameter showed less than  $10^{-7}$  cm/s. However, the falling head method showed an unsteady flow between what was put into the permeameter and what was taken out. Based on outflow data, the falling head technique resulted in  $10^{-6}$  cm/s hydraulic conductivity. It is most likely that shrinkage of the grouted matrix from the wall of the permeameter allowed the too high calculation of hydraulic conductivity because of too much flow in the gap. When conducting the packer tests in the permeameter, the access ports were opened and no water flowed. This indicated a "tight" matrix.

It is recommended that the potential gap formed by shrinkage of the grouted soil-and-waste matrix be sealed at the top of the grouted permeameter and that the falling head tests be rerun. In addition, it is recommended that the falling head test be rerun for the ungrouted permeameter and that more of the access ports be used to track the flow of water.

A cost estimate was made for application of TECT, paraffin, and Type-H cement grouts. For cost and schedule assumption purposes, an acre-sized transuranic waste pit 8 ft deep jet grouted in staged phases 2 years at the INEL Subsurface Disposal Area is assumed. In general, it is assumed that a single-component grout is jet grouted at a rate of 12.5 gal per vertical foot of hole, resulting in 100 gal per 8-ft hole injected. In addition, a 2-ft triangular pitch matrix results in 24,000 holes per acre. Also, it is assumed that there will be an engineered cap placed atop the waste by another program. It is further assumed that this technology is either a Record of Decision or a treatability study. Costs for permitting and any interaction with state and local governments is not included but is assumed half the cost of the actual remediation. Estimates for grouting are based on operations by the same vendor that supplied grouting for this demonstration using government-supplied equipment, with some additional parts purchased as capital equipment. If another vendor is selected for this technology, an additional \$2 million in capital costs should be added to all estimates. The total for a 2-year project is \$21,866,000 for TECT, \$13,514,000 for paraffin, and \$10,730,000 for Type-H cement. These numbers equate to

\$1,704 per cubic yard for TECT, \$1,045 per cubic yard for paraffin, and \$829 per cubic yard for Type-H cement.

On an overall basis, the technology of jet grouting buried waste sites to provide stabilization and containment has been shown to be practicable. In the subject test, a variety of grouting materials have been demonstrated to be field implementable, including TECT, paraffin, and Type-H cement. In prior studies, the viability of both Type-1 cement and two-component acrylic polymer has likewise been demonstrated. The technology is ready to be considered for buried waste sites.

## **ACKNOWLEDGMENTS**

The authors would like to thank Joel Hubbell and Rick Farnsworth. Joel provided the thermocouple recording system to evaluate core temperatures of the grouted matrix and an excellent critical review of this document. Rick provided excellent project management and technical guidance during project planning and evaluation.



## CONTENTS

ABSTRACT .....	iii
EXECUTIVE SUMMARY .....	v
ACKNOWLEDGMENTS .....	ix
1. INTRODUCTION .....	1
2. TEST OBJECTIVES .....	4
3. PROCEDURES AND SEQUENCE OF EVENTS .....	6
3.1 Pit and Field-Scale Permeameter Construction .....	6
3.1.1 Implementation Pits .....	6
3.1.2 Hydraulic Conductivity Field-Scale Permeameters .....	25
3.2 Grouting Phase .....	43
3.3 Coring/Hydraulic Conductivity Testing .....	53
3.3.1 Grouted Field-Scale Permeameter .....	53
3.3.2 Packer Testing on Pits .....	55
3.3.3 Falling Head Hydraulic Conductivity Testing on Permeameters .....	55
3.4 Destructive Examination of Pits .....	61
4. TEST RESULTS .....	65
4.1 Grouting the Field-Scale Permeameter and Pits .....	65
4.1.1 Grouted Field-Scale Permeameter .....	65
4.1.2 TECT Pit (Pit A) .....	77
4.1.3 Paraffin Pit (Pit B) .....	91
4.1.4 Hematite Pit (Pit C) .....	108
4.1.5 Epoxy Pit (Pit D) .....	131
4.1.6 Type-H Cement Pit (Pit D) .....	131
4.2 Temperature Time History of TECT and Paraffin Pits .....	135
4.3 Evaluation of Cores Taken in the Pits and Field-Scale Permeameter .....	135
4.3.1 Grouted Field-Scale Permeameter .....	137
4.3.2 TECT Pit .....	145
4.3.3 Paraffin Pit .....	151

4.3.4 Type-H Cement Pit .....	151
4.3.5 Discussion of the TV Video Log of the Core Holes .....	159
4.4 Destructive Examination of Pits .....	159
4.5 TECT Pit .....	159
4.6 Paraffin Pit .....	175
4.7 Type-H Cement Pit .....	193
4.8 Hydraulic Conductivity Testing Results .....	213
4.8.1 Packer Testing in Pits and Grouted Field-Scale Permeameter .....	213
4.8.2 Hydraulic Conductivity Testing on the Grouted and Ungrounded Permeameters .....	223
4.9 Water Migration Study During Grouting .....	240
5. DISCUSSION OF RESULTS-RELEVANCE OF TECHNOLOGY .....	245
6. FULL-SCALE IMPLEMENTATION .....	247
7. CONCLUSIONS/RECOMMENDATIONS .....	249
REFERENCES .....	252
Appendix A—Programmatic Issues .....	A-1
Appendix B—Details of Pit and Field-Scale Permeameter Construction .....	B-1
Appendix C—Packer Test Data/Calculations and Falling Head Test Data .....	C-1
Appendix D—Results of Field-Scale Permeameter Water Emissions .....	D-1
Appendix E—Monitoring for Water Migration Following Jet Grouting .....	E-1

## **FIGURES**

1. Subsurface stabilization testing area (Graphic M96 0431) .....	7
2. Relative position of field-scale permeameters and pits in FY-97 testing (Graphic M96 0432) .....	8
3. Sodium sulfate in drum (simulates nitrate salts) (Photo 96-417-2-1) .....	13
4. Concrete (cinder blocks) in drums (Photo 96-417-2-2) .....	15

5. Metal material in a drum (Photo 96-417-2-10) .....	17
6. Pit construction showing bottom layer (Photo 96-417-1-8) .....	19
7. Backfilling for second layer in a pit (Photo 96-417-1-20) .....	21
8. Handfilling interstitial soil in a pit (Photo 96-373-1-7) .....	23
9. Concrete rebar-reinforced pad for field-scale permeameter with first ring being placed (Photo 96-428-1-13) .....	27
10. Field-scale permeameter with third ring being installed (Photo 96-471-1-16) .....	29
11. Metal water deflection ring with "tar" sealant and over water access hole inside view (Photo 96-450-1-17) .....	31
12. Outside view of water access ports in bottom ring (Photo 96-428-1-17) .....	33
13. Top of field-scale permeameter showing three access ports and head pipe port (Photo 96-511-1-4) .....	35
14. Workers installing seals on access ports (Photo 96-498-1-10) .....	37
15. Field-scale permeameter with head pipe installed, including safety ladders and railing (Photo 96-658-2-26) .....	39
16. Placement of simulated waste in field-scale permeameter's bottom ring (Photo 96-450-1-4) .....	45
17. Final compaction of ungrouted baseline field-scale permeameter (Photo 96-503-1-8) .....	47
18. Thrust block backfilled with soil ready for field trials (Photo 96-503-1-13) .....	49
19. Schematic of field-trial grouting, showing thrust block with spacer blocks (Graphic M96 0445) .....	51
20. Relative position of four core holes for grouted field-scale permeameter (Graphic M96 0433) .....	54
21. Packer testing of grouted field-scale permeameter (Graphic M96 0452) .....	57
22. Packer test hole location in Pits A, B, and D (Graphic M96 0434) .....	59
23. Backhoe during destructive examination (Photo 96-587-9-17) .....	63
24. CASA GRANDE Jet 5 pump (Graphic M95 0469) .....	67

25. CASA GRANDE C65 drill system (Photo 94-715-1-12) .....	69
26. Drill stem used for Type-H cement, TECT, and paraffin (Photo 96-503-1-1) .....	71
27. Heave of top surface of field-scale permeameter during grouting of Type-H cement (Photo 96-511-1-8) .....	75
28. Orientation of grout holes for grouted field-scale permeameter (order of grouting) (Graphic M96 0435) .....	79
29. White film on spoils collection pit for grouted field-scale permeameter (Photo 96-512-2-3) .....	81
30. Thrust block in use during field trials for injection of TECT grout (Photo 96-512-2-18) .....	83
31. Hole orientation of TECT Pit A (Graphic M96 0437) .....	87
32. Grouting operation for TECT Pit A (Photo 96-512-1-2) .....	89
33. Grout returns during grouting of TECT pit (trickle flow of grout shown emanating from nozzles) (Photo 96-512-1-10) .....	93
34. Heater tape applied to high-pressure hose (Photo 96-512-2-8) .....	95
35. Insulation applied over heater tape on high-pressure hose (Photo 96-512-2-10) .....	97
36. System in operation during injection of paraffin grout (Photo 96-517-3-4) .....	99
37. Detail of supply lines during grouting of paraffin (Photo 96-517-2-13) .....	101
38. Tanker truck containing hot paraffin (140°F) and hot water for cleanout (180°F) (Photo 96-517-2-11) .....	103
39. Paraffin grout emanating from an uncovered crack in the thrust block during the paraffin field trials (Photo 96-517-2-18) .....	105
40. Spoils collection pit for paraffin (Graphic M96 0438) .....	109
41. Grout returns during grouting of the paraffin pit (Photo 96-517-3-32) .....	111
42. Schwing, Jet 5 pump, and two Ready Mix trucks with slaked lime slurry and ferrous sulfate slurry during hematite pit injection (Photo 96-529-1-14) .....	115
43. Feed from Ready Mix truck on the ferrous sulfate side (Photo 96-529-1-25) .....	117
44. Feed from Ready Mix truck on the ferrous sulfate side (Photo 96-529-1-27) .....	119

45. Dual concentric annulus drill stem (Graphic M95 0315) .....	121
46. Ferrous sulfate flow above ground (in position to attempt field trial) (Photo 96-529-2-5) .....	123
47. Line slurry flow just prior to plugging (Photo 96-529-2-3) .....	125
48. Line slurry flow completely plugged (Photo 96-529-2-1) .....	127
49. Filter caking of line slurry on B pump intake screen (Photo 96-529-2-6) .....	129
50. Schematic of two-component setup for epoxy jet grouting (Graphic M95 0447) .....	132
51. Grouting hole orientation for Type-H cement (Pit D) (Graphic M96 0440) .....	134
52. Temperature/time history of TECT/paraffin pit (Graphic M96 0441) .....	136
53. Relative position of core holes for the grouted field-scale permeameter, Type-H, TECT, paraffin grout (Graphic M96 0442) .....	138
54. Core holes 2 and 3, grouted field-scale permeameter (Graphics M96 0456 and M96 0457) .....	141
55. Core holes 5 and 6, grouted field-scale permeameter (Graphics M96 0458 and M96 0459) .....	143
56. Core holes 1, 2, and 3, TECT pit (Graphics M96 0464, M96 0465, and M96 0466) .....	147
57. Example of blocked injector during jet grouting (Portland Type-1 cement 1994) (Photo 94-715-2-1) .....	149
58. Core holes 1 and 2, paraffin pit (Graphics M96 0460 and M96 0461) .....	153
59. Core holes 1 and 2, Type-H pit (Graphics M96 0463 and M96 0462) .....	157
60. Interface between ungrouted soil and the TECT monolith (Photo 96-587-9-30) .....	161
61. Inclusions of clay soil in TECT monolith (Photo 96-584-2-23) .....	163
62. TECT monolith 30 in. from east face showing drums of office trash embedded in the face (Photo 96-587-9-4) .....	165
63. Outline of encapsulated oil sludge drum in TECT pit at 30 in. from east face (Photo 96-587-9-13) .....	167
64. Detail of encapsulated sludge showing kitty litter inclusion (Photo 96-587-9-15) .....	169

65. UngROUTed canola oil-based sludge simulant in southern end of TECT pit (ungrouted portion) (Photo 96-587-4-3) .....	171
66. Overview of TECT pit at 36 in. from east face (Photo 96-587-9-22) .....	173
67. Detail of core hole 3 and soil cavity in TECT pit at 36 in. from east face (Photo 96-587-9-24) .....	177
68. Drum of wood at the 42-in. level from the east face of the TECT pit (Photo 96-584-2-28) .....	179
69. Sodium sulfate in ungrouted drum at the 42-in. level from the east face for the TECT pit (Photo 96-587-10-35) .....	181
70. Top of paraffin pit prior to destructive examination (Photo 96-587-2-10) .....	183
71. Paraffin pit detail at 6 in. from the east face (Photo 96-587-3-11) .....	185
72. Paraffin pit detail at 12 in. from the east face (Photo 96-587-3-15) .....	187
73. Detail of paper from paraffin pit (Photo 96-584-2-5) .....	189
74. Paraffin pit 18 in. from the east face (Photo 96-587-3-17) .....	191
75. Paraffin pit 30 in. from the east face (Photo 96-584-1-3) .....	195
76. Detail of wood in paraffin face (Photo 96-584-2-9) .....	197
77. Drum of canola oil in south wall of paraffin pit (Photo 96-584-2-11) .....	199
78. Sample of the sludge with inclusion of clay soil (soaked with paraffin) (Photo 96-584-1-10) .....	201
79. Sample of metal encased in paraffin (Photo 96-584-2-18) .....	203
80. Sample of wood encased in paraffin (Photo 96-584-1-6) .....	205
81. Type-H cement pit showing plugged injectors (Photo 96-743-1-9) .....	207
82. Detail of region with clogged injectors (Photo 96-743-1-11) .....	209
83. Region of porous soil outside Type-H pit (Photo 96-743-1-13) .....	211
84. Schematic of packer system showing individual packer and a dual packer used in tandem to seal core holes that had penetrated the bottom of the grouted region (Graphic M96 0443) .....	215

85. Schematic showing single packer with sealed adjacent core hole (Graphic M96 0444) .....	216
86. Core hole 2 in Type-H cement pit with water emanating from the top surface during packer testing (Photo 96-716-1-18) .....	221
87. Completed ungrouted field-scale permeameter with lid tie-downs; worker shown introducing water to the head pipe (Photo 96-658-1-30) .....	227
88. Details of ungrouted baseline field-scale permeameter collection system (Photo 96-658-1-27) .....	231
89. Completed grouted field-scale permeameter showing lid tie-downs and bucket collection system for grouted field-scale permeameter (Photo 96-658-1-24) .....	233
90. Relative position of drill grout hole and bottom layer of soil (Graphic M96 0448) .....	239
91. Plan-view and 3-D map of Pit D (Graphic M96 0453) .....	241
92. Moisture content profiles for NAT-51 (Graphic M96 0454) .....	244

## TABLES

1. Containerized waste in pits .....	9
2. Field-scale permeameter waste forms .....	41
3. Operational parameters for jet-gravity Type-H count in grouted field-scale permeameter (see Figure 28 for order) .....	73
4. Operational parameters for TECT pit (Pit A) .....	86
5. Operational parameters for paraffin pit (Pit B) .....	107
6. Operational parameters for Type-H cement ([1:1 by mass] 14 sacks/yd) pit (Pit D) .....	133
7. Log of core holes for grouted field-scale permeameter .....	139
8. Log of core holes for TECT pit .....	146
9. Log of core holes for paraffin pit .....	152
10. Log of core holes for Type-H pit .....	155
11. Summary of packer test for the TECT pit .....	218

12. Summary of packer testing for paraffin pit .....	219
13. Summary of packer testing for Type-H cement .....	220
14. Summary of packer test data for grouted field-scale permeameter .....	224
15. UngROUTed field-scale permeameter hydraulic conductivity data .....	235
16. Grouted field-scale permeameter hydraulic conductivity data .....	236
17. Estimated water increases and decreases resulting from moisture changes in sediments at NAT sites following grouting and drilling/packer testing .....	243
18. Estimated costs of full-scale implementation for an acre-sized pit .....	248

# Innovative Subsurface Stabilization Project—Final Report

## 1. INTRODUCTION

The Innovative Subsurface Stabilization Project is a series of applied research tests involving stabilizing simulated buried waste sites with grouting agents using jet-grouting techniques. The purpose of these tests is to provide necessary background information to validate the technology for application in hot buried waste sites.

The basic jet-grouting technique is to make the waste into a solid monolith, which is the same effect as simultaneous horizontal and vertical barriers, while also providing stabilization against subsidence. The monolith is created by jet grouting adjacent columns with the grouting material such that the soil-and-waste matrix forms a solid monolith. The jet grouting has been demonstrated for both single<sup>1</sup> and two-component materials<sup>2</sup> but has not been demonstrated for several new innovative materials in the subject study.

In FY-94, the Subsurface Stabilization Project first examined the proof of concept of stabilizing the waste by jet grouting then retrieving the resultant monolith. In this innovative retrieval concept, the grouted matrix agglomerated the waste into a matrix that reduced dust spread during retrieval. During this demonstration, it was shown that simple Type-1 Portland cement was jet groutable, the resultant monolith was free of voids, and there was a reduction in dust spread during retrieval compared with using conventional mining techniques to control dust. Next, in FY-95, the technology examined jet grouting a two-component acrylic polymer grout with two different formulations. One formulation resulted in a hard durable monolith for long-term confinement, and the other formulation resulted in a rubber-like monolith that was easily retrieved with little dust spread. Finally, the subject study was designed to expand the list of grouts that are jet groutable and to examine the use of a thrust block for controlling secondary waste. All of these studies are used as background information to support demonstrations or treatability studies for stabilizing contaminated buried waste sites.

A variety of grouting materials can be utilized for stabilizing and encapsulating buried waste sites for either in situ disposal or interim in situ storage and eventual retrieval. Buried radioactive waste sites need to avoid subsidence from void collapse within the waste to ensure cap integrity. In addition, encapsulating materials provide long-term containment of migrating contaminants. Finally, the waste may be stabilized for an interim period prior to retrieval.

Variables in grouting materials are chemical composition, chemical compatibility with the waste and surrounding environment, curing properties, compressive strength, retrievability of the matrix, hydraulic conductivity of the resultant grouted soil-and-waste mix, and how the various compositions are injected into the buried waste.

The focus of this investigation is evaluation of (1) the implementability of the various grouting agents by examining jet groutability, (2) the extent of encapsulation and the monolithic nature of the grouted pit by both destructive examination and coring, and (3) the hydraulic

conductivity (in full scale) of the grouted buried waste and comparison of this to the ungrouted value. The program is funded by the DOE Office of Technology Development Landfill Subsurface Contaminants Focus Group for Arid Sites. Data obtained will provide proof-of-concept information that could eventually be used to develop remedial investigation/feasibility study data on the technology as part of the Record of Decision for final deposition of transuranic pits and trenches at the Idaho National Engineering Laboratory (INEL) Radioactive Waste Management Complex (RWMC). These tasks represent a coordination of Office of Technology Development activities involving MSE Inc., Brookhaven National Laboratory, and the INEL.

At the INEL, there is 2 million ft<sup>3</sup> of transuranic waste commingled with 6–8 million ft<sup>3</sup> of soils. Options being assessed for this buried waste by the Environmental Restoration Program involve both retrieval and improving the confinement and leaving the waste in place. This testing program addresses both of these options by evaluating the retrievability of grouted monoliths during destructive examinations.

The testing program involved (1) construction of cold simulated buried test pits and field-scale permeameters specially prepared for controlled mass balance hydraulic conductivity testing, (2) grouting of the field-scale permeameter, (3) coring and destructive examination of treated pits, and (4) hydraulic conductivity testing of the field-scale permeameters and pits.

Phase 1 involved constructing four identical cold test pits (6 x 6 x 6 ft), and three field-scale permeameters (10 ft in diameter/10 ft deep). The pits and field-scale permeameters simulate the transuranic pits and trenches at the RWMC. Waste in the RWMC transuranic pits and trenches is containerized sludge, cloth, paper, wood, concrete, asphalt, metal, and glass from the Rocky Flats plant. Containers in the actual pits were 2 x 2 x 3-ft cardboard boxes, 55-gal steel drums and 4 x 4 x 8-ft plywood boxes. Because the four 6 x 6 x 6-ft pits are relatively small compared with the size of the actual waste containers, 30-gal drums were used to simulate both boxes and drums. However, the ratio of waste types was correctly simulated. The 10-ft-diameter concrete field-scale permeameters were large enough to use the 55-gal drums in a random drum orientation.

The field-scale permeameters were specially designed to facilitate hydraulic conductivity testing following jet grouting by using a specially designed head pipe attached to a top lid, which provided a head of water on the top surface of either grouted or ungrouted field-scale permeameters to accelerate the relatively low hydraulic conductivities expected (10<sup>-3</sup> to 10<sup>-7</sup> cm/s). All of the pits simulated the 2 x 3 x 2-ft cardboard boxes by using 0.004-in. polyethylene bagged combustible waste consisting of cloth and blotter paper. The rare earth tracer cerium oxide was used in each of the containers for the field-scale permeameter pits. In the 55-gal drums placed in the field-scale permeameters, the tracer was loaded at 200 g per drum. No tracer was placed in the bagged waste or in the 30-gal drums used in the pits. The drums were 90% cardboard and 10% metal drums.

Phase 2 involved jet grouting four 6 x 6 x 6-ft pits and one of the three field-scale permeameters. One of the field-scale permeameters was jet grouted with Type-H Portland cement, and a second permeameter was ungrouted for use as an ungrouted hydraulic conductivity measurement system. The third permeameter was planned to be grouted with an innovative

grouting material. However, budget issues only allowed construction of the field-scale permeameter (with no soil or waste). Therefore, this permeameter is in reserve for future testing. Materials used for grouting in this study include for the pits: low melting temperature paraffin, INEL-developed iron oxide solutions to form hematite, a proprietary iron oxide cement called TECT, Type-H cement mixed 1:1 by mass water and cement (14-sack mix), and organic water-based epoxy. The grouted field-scale permeameter used Type-H Portland cement mixed 1:1 by volume (18-sack mix).

Phase 3 involved coring of the cured grouted field-scale permeameter and the pits and a destructive examination of the 6 x 6 x 6-ft pits. The coring was done in four positions in the field-scale permeameter and in at least two positions in each of the pits. The destructive examination was performed by a standard backhoe making 6-in. slices of the pits.

Phase 4 involved performing hydraulic conductivity testing on both the ungrouted field-scale permeameter and the grouted field-scale permeameter using the falling head method and the specially designed head pipes. To determine the local hydraulic conductivity, packer tests were performed for all of the core holes in both field-scale permeameters and pits.

Programmatic issues such as deviations from the test plan, health, safety, and quality are given in Appendix A.

## 2. TEST OBJECTIVES

The objective of the test was to (1) determine the implementability of using jet grouting of innovative grouting materials to form monoliths out of buried waste material, and (2) establish basic hydraulic conductivity data of both grouted and ungrouted buried waste sites.

Determining the implementability of forming monoliths is resolved by examining a variety of issues including (1) emplacement efficacy (whether single- or two-component or heated material), (2) cure time and temperature, (3) mixing and curing of the grouting material with salts and sludges commonly found in the Rocky Flats waste, (4) pumpability of the grout materials, (5) grout returns and resultant secondary waste, and (6) penetration of grout into soil-and-waste matrix (presence of voids).

In evaluating these implementability issues, the following guidelines have been established: (1) emplacement efficacy was evaluated by measuring the time to perform the grouting operation, (2) the cure time was evaluated by measuring the temperature of the interior of the pit with a thermocouple data logger for up to 2 weeks after grouting, (3) mixing and curing of the grouting material with salts and sludges were evaluated by examining cores of the monoliths and during a destructive examination, (4) pumpability of the grout material was evaluated by recording the ease with which the grouting subcontractor could pump the materials (including observations of downtime caused by pumpability issues such as filter caking), (5) grout returns were evaluated by estimating the returns for each of the grout holes, and (6) penetration of grout into the soil-and-waste matrix was evaluated by examining the cores for voids and, during the destructive examination, examining the inclusions of pure soil within the soil grout matrix and looking for voids.

The objective of the permeability tests was to determine the hydraulic conductivity of both grouted and ungrouted buried waste matrices. The objective was met by employing two basic hydraulic conductivity measurement techniques, including packer tests and falling head method. The main issue was resolving the differences from the packer testing method, which gives a local isotropic conductivity, and the falling head method. The packer method was employed on both pits and field-scale permeameter, and the falling head method was applied only on the field-scale permeameter. Therefore, by comparing the results for the two methods on the field-scale permeameter sites, the packer test results can be related to a vertical hydraulic conductivity.

The data quality objectives were mainly qualitative data in the form of notebook observations and photographs. However, there were some quantitative results as well. For evaluating the efficacy of jet grouting the various grouting materials, jet-grouting data included time to grout a particular hole, amount of grout material injected, and an estimate of the grout returns. Destructive examination data included the amount of voids present in the matrix, the amount of soil inclusions in the soilcrete matrix, and the retrievability of the resulting monolith (the general monolithic nature of the soil-and-waste matrix). During grouting, the total grout injected in each hole was measured to +/- 5 gal, and the grout returns were estimated for each hole at +/- 5 gal. In addition, general operations, including timing of grouting, were measured to +/- 1 minute. The temperature of the cure in the pits was measured with a continuous thermocouple data logger, and data are taken every 10 minutes at +/- 1°F accuracy. During the hydraulic conductivity tests, the data were quantitative. The packer tests involved positioning the

packer to +/- 1 ft of the desired depth below the top of the field-scale permeameter. The flow totalizer for the packer was measured to +/- 0.02 gal, and the injection pressure was measured to +/- 0.5 psi, which equates to a lower sensitivity for a zero reading of  $10^{-7}$  cm/s hydraulic conductivity. During the falling head method, the change in volume of the riser pipe and the calibration pipe was measured at +/- 0.25 gal. Pressure measurements were made at various azimuthal and axial positions in the field-scale permeameters to help track the water front in the field-scale permeameters.

### 3. PROCEDURES AND SEQUENCE OF EVENTS

This section describes the exact procedures and sequence of events for all phases of the project. The test plan<sup>3</sup> described in detail all phases of the testing. This section includes details of the procedures and sequence of events for the following phases: pit and field-scale permeameter construction, grouting of the pits and field-scale permeameter, destructive examination and coring, and hydraulic conductivity testing. All testing was performed at the INEL Cold Test Pit area administered by the RWMC. Figure 1 shows a general layout of the Cold Test Pit area during subject testing. The Cold Test Pit area is sponsored by the DOE Office of Technology Development.

#### 3.1 Pit and Field-Scale Permeameter Construction

Both pits and field-scale permeameters were constructed as a preliminary to jet grouting and hydraulic conductivity testing. Four 6 x 6 x 6-ft simulated buried waste pits and three 10 x 10-ft field-scale permeameters were constructed at the INEL Cold Test Pit as shown in Figure 2. The figure shows the relative position of the subsurface stabilization testing area relative to the rest of the Cold Test Pit.

##### 3.1.1 Implementation Pits

Four identical 6 x 6 x 6-ft pits were constructed at the INEL Cold Test Pit area. These pits provided a test bed for evaluating the implementability of four different grouting agents. Each pit contained simulated waste packaged in 30-gal drums and plastic (polyethylene) 2 x 2 x 3-ft sacks. Table 1 gives a summary of the waste placed in each pit. Each of the pits contained 22-24 drums and two sacks with at least two of the drums metal sided and the other 20-22 cardboard sided to simulate the natural aging process of interred drums. Table 1 gives a summary of the simulated waste material in each drum and the disposition of where the drum was in the pit. Nominally, 40% of the drums contained combustible material including cloth, blotter paper, laboratory chemical wiping paper, and wood. Nominally 33% of the drums contained nitrate salt simulants and sludge material. At least two of the sludge drums contained a nitrate salt simulator (sodium sulfate) (see Figure 3), three of the drums contained an inorganic sludge stimulant (INEL soil), and three of the drums contained an organic sludge stimulant (3/5 canola oil, 2/5 absorbants). The two 2 x 2 x 3-ft sacks contained blotter paper and cloth. The remaining 27% of the drums contained concrete and metal materials as shown in Figure 4 and Figure 5, respectively.

Construction of these pits used a buildup method and berms. Basically, each pit was made up of three layers, and the exact position of the drums in any layer was surveyed (see Appendix B for details of pit construction). From an elevation approximately 9 ft below the existing west plain of the testing area, a berm defining the 6 x 6-ft boundaries of the pit was placed on relatively level ground, and the first layer of waste was placed within the confines of the berm as shown in Figure 6. Next, the region was backfilled to the approximate height of the drums as shown in Figure 7, and the interstitial positions between the drums were filled with soil as shown in Figure 8. Once filled, a new berm was formed and another layer added until finally, the top overburden layer was added. The overburden consisted of approximately 3 ft of compacted soil resulting in a pit that was nominally 6 ft thick with 3 ft of overburden. At each point, the exact

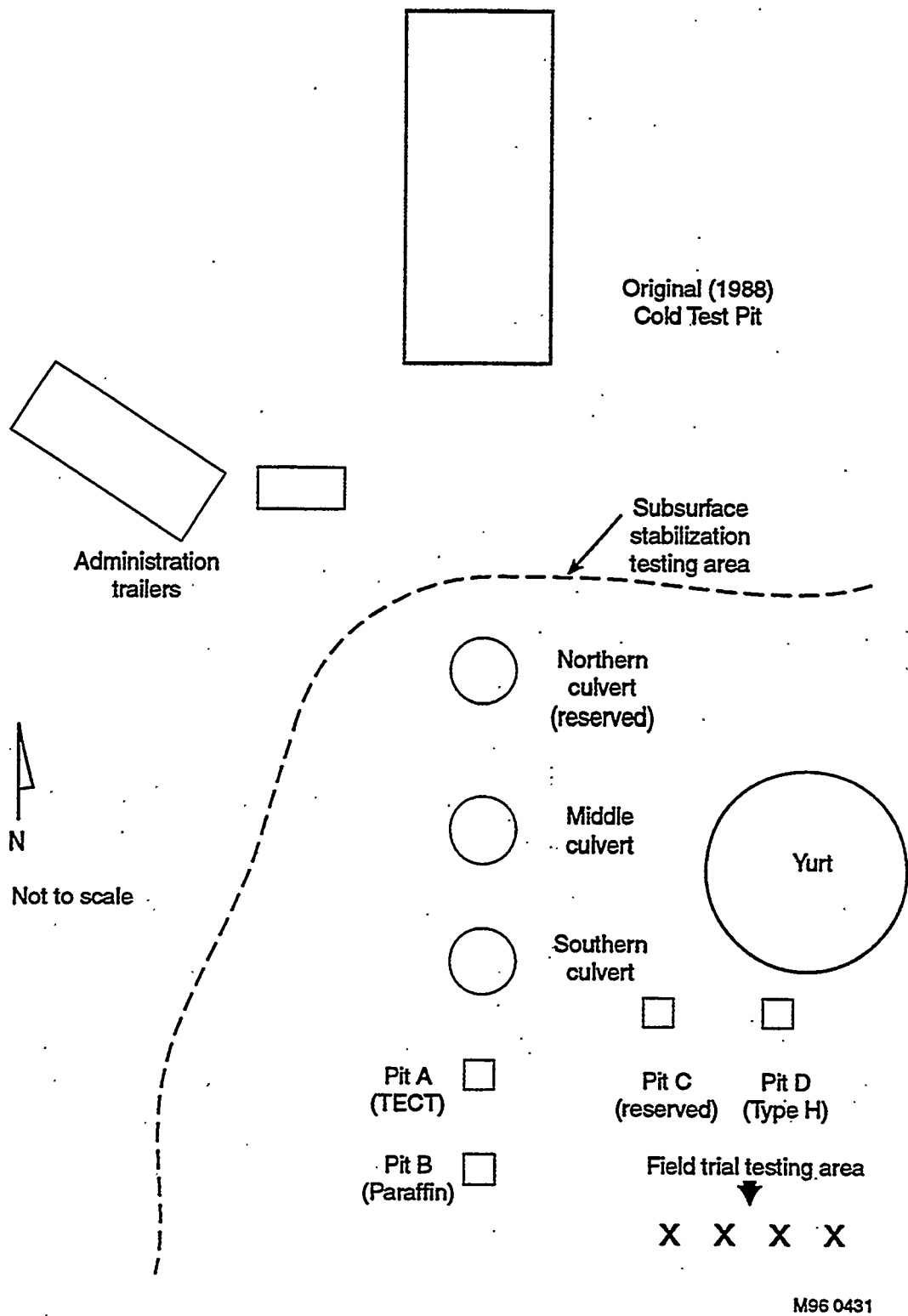
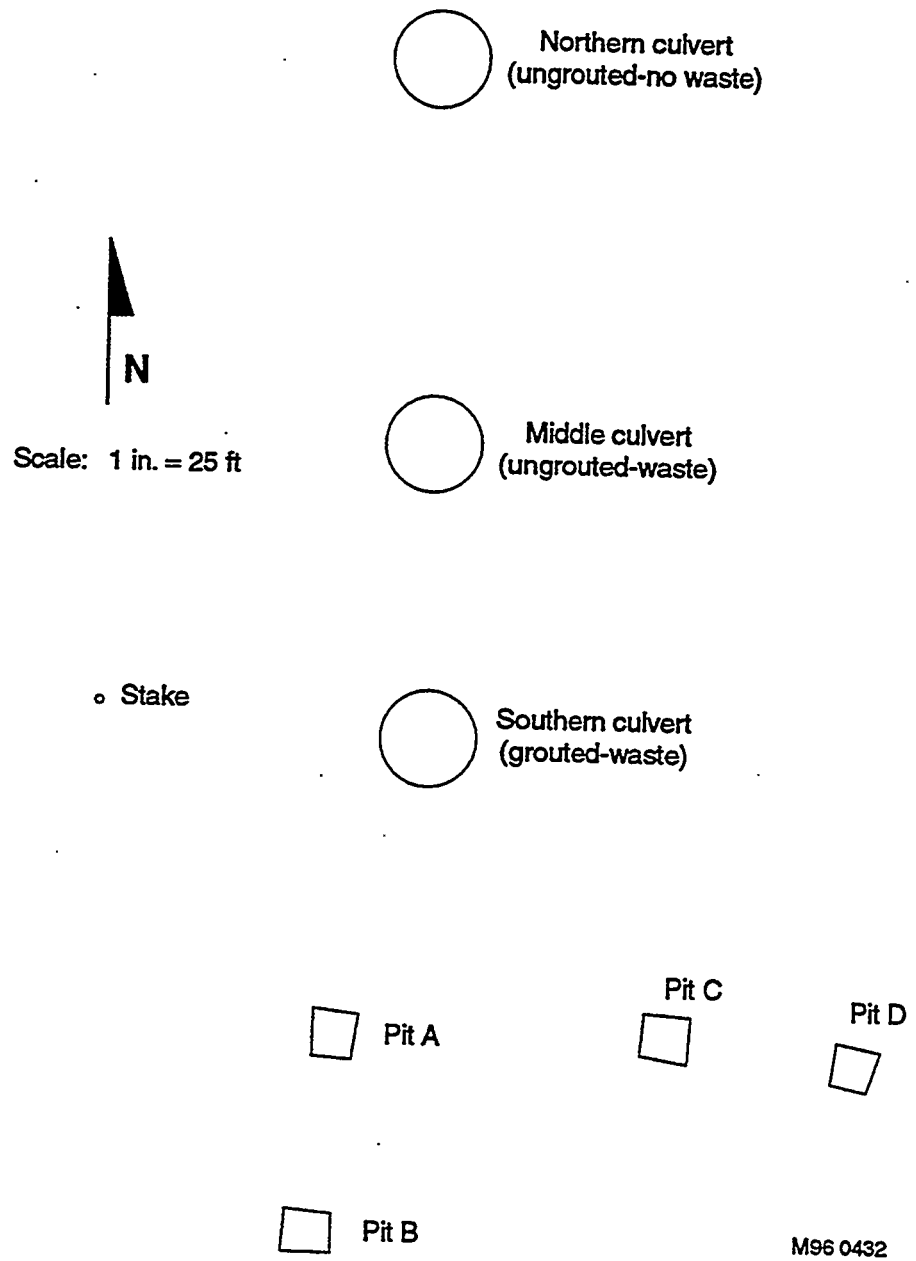


Figure 1. Subsurface stabilization testing area (Graphic M96 0431).



**Figure 2.** Relative position of field-scale permeameters and pits in FY-97 testing (Graphic M96 0432).

**Table 1.** Containerized waste in pits.

Pit A (TECT Pit)	Total Drums (24)	
	Total Bags (2)	
Drum Number	Type (30 gal)	Weight (lbm)
<b>Layer 1 (bottom)</b>		
59	Soil	276
121	Metal	121
65	Soil	274
58	Soil	260
57	Sodium sulfate	314
125	Metal	49
19	Paper	40
48	Wood	59
25	Paper	31
50	Wood	62
<b>Layer 2 (middle)</b>		
23	Paper	36
160	Metal/concrete	75
118	Sodium sulfate	314
173	Concrete	184
17	Paper	38
151	Sludge	228
150	Sludge	215
<b>Layer 3 (top)</b>		
168	Metal/concrete	109
28	Paper	35
197	Sludge	423
152	Sludge	226
12	Wood	73
26	Paper	34
17	Paper	38
2 bags	Paper/plastic	Did not weigh
Pit B (Paraffin Pit)	Total Drums (22)	
	Total Bags (2)	
<b>Layer 1 (bottom)</b>		
62	Soil	256
61	Soil	288
112	Sodium sulfate	315
147	Sludge	229
54	Wood	71
21	Paper	45
56	Wood	67
18	Paper	43

**Table 1.** (continued).

Drum	Type (30 gal)	Weight (lbm)
<b>Layer 2 (middle)</b>		
114	Sodium sulfate	314
153	Sludge	218
161	Metal/concrete	73
174	Concrete	179
162	Metal/concrete	91
51	Wood	52
68	Soil	276
<b>Layer 3 (top)</b>		
175	Metal (pipes)	173
164	Metal concrete	82
30	Paper	32
35	Paper	30
49	Wood	57
157	Sludge	246
29	Paper	50
2 bags	Paper/plastic	Did not weigh
<b>Pit C (Reserved)</b>		<b>Total Drums (22)</b>
		<b>Total Bags (2)</b>
<b>Layer 1 (bottom)</b>		
64	Soil	280
158	Metal/concrete	60
15	Wood	77
27	Paper	36
159	Metal/concrete	103
22	Paper	39
148	Sludge	215
53	Wood	61
113	Sodium sulfate	314
<b>Layer 2 (middle)</b>		
13	Wood	82
117	Sodium sulfate	315
32	Paper	32
156	Sludge	205
34	Paper	35
72	Soil	325
31	Paper	16

**Table 1. (continued).**

Drum	Type (30 gal)	Weight (lbm)
<b>Layer 3 (top)</b>		
155	Sludge	216
8	Concrete	150
122	Metal	166
46	Paper	31
69	Soil	275
169	Metal/concrete	125
<b>Pit D (Type-H Cement)</b>		<b>Total Drums (22)</b>
<b>Layer 1 (bottom)</b>		
63	Soil	279
124	Metal	197
		(metal drum)
60	Soil	287
52	Wood	82
20	Paper	25
47	Wood	69
120	Sodium sulfate	315
146	Sludge	245
<b>Layer 2 (middle)</b>		
149	Sludge	208
154	Sludge	236
14	Wood	78
165	Metal/concrete	93
123	Metal	154
6	Concrete	156
116	Sodium sulfate	313
163	Metal/concrete	122
		(metal drum)
<b>Layer 3 (top)</b>		
170	Metal/concrete	156
166	Metal/concrete	129
41	Paper	37
42	Paper	36
16	Wood	58
55	Wood	61





**Figure 3.** Sodium sulfate in drum (simulates nitrate salts) (Photo 96-417-2-1).





Figure 4. Concrete (cinder blocks) in drums (Photo 96-417-2-2).





Figure 5. Metal material in a drum (Photo 96-417-2-10).





Figure 6. Pit construction showing bottom layer (Photo 96-417-1-8).





Figure 7. Backfilling for second layer in a pit (Photo 96-417-1-20).





**Figure 8.** Handfilling interstitial soil in a pit (Photo 96-373-1-7).



cell dimensions and elevations were surveyed for later use during grouting and coring (see Appendix B). When the final overburden was added resulting in 3 ft of overburden and a 6-ft-thick seam of soil-and-waste matrix, marker flags for grouting holes were added on either a 20-in. or 18-in. triangular pitch matrix, depending upon whether the intended injected grout was single component or two component.

### 3.1.2 Hydraulic Conductivity Field-Scale Permeameters

The hydraulic conductivity field-scale permeameters were located on a line running approximately north and south as shown in Figure 2. The field-scale permeameters are concrete culverts commonly used for ditch bridge construction in irrigation systems. The permeameters consist of three rings and a lid totaling 11 ft high and have an inside diameter of 10 ft. The permeameters were constructed on top of 8-in. x 12 x 12-ft slabs of concrete with rebar for stability (Figure 9). Field-scale permeameters consist of three sections, the bottom two of which are 4 ft high, and the top section is 3 ft high as shown in Figure 10. Figure 11 shows a water-deflection ring placed between the sections to divert water flowing down the sides of the permeameter during hydraulic conductivity testing. In addition, Figure 11 shows the tar sealant that was placed below and above the ring for each section of the permeameter to provide a water-tight seal. Figure 11 shows an inside view of a water access hole, and Figure 12 shows an outside view of several access holes used to ascertain the mass balance of water into and out of the field-scale permeameter during hydraulic conductivity testing. These access holes are located at eight symmetrical locations on the bottom ring of the field-scale permeameter and at multiple other positions as discussed in the section on hydraulic conductivity testing. Each field-scale permeameter has a solid bottom (refer back to Figure 12), and the interior of the permeameter is painted with a concrete-compatible marine epoxy or equivalent to avoid soaking up excess water. The bottom of the permeameter has a convex shape with the center of the bottom raised about 6-8 in. above the inside diameter to focus water to the inside bottom diameter. The top of the permeameter is a sealable cap that can hold a 10-ft head of water. In the top of the cap are three access ports and a forth access port to place a head pipe to contain a column of water as shown in Figure 13 and Figure 14. Figure 15 shows a completed field-scale permeameter with safety railing and ladders to reach the top of the head pipe installed.

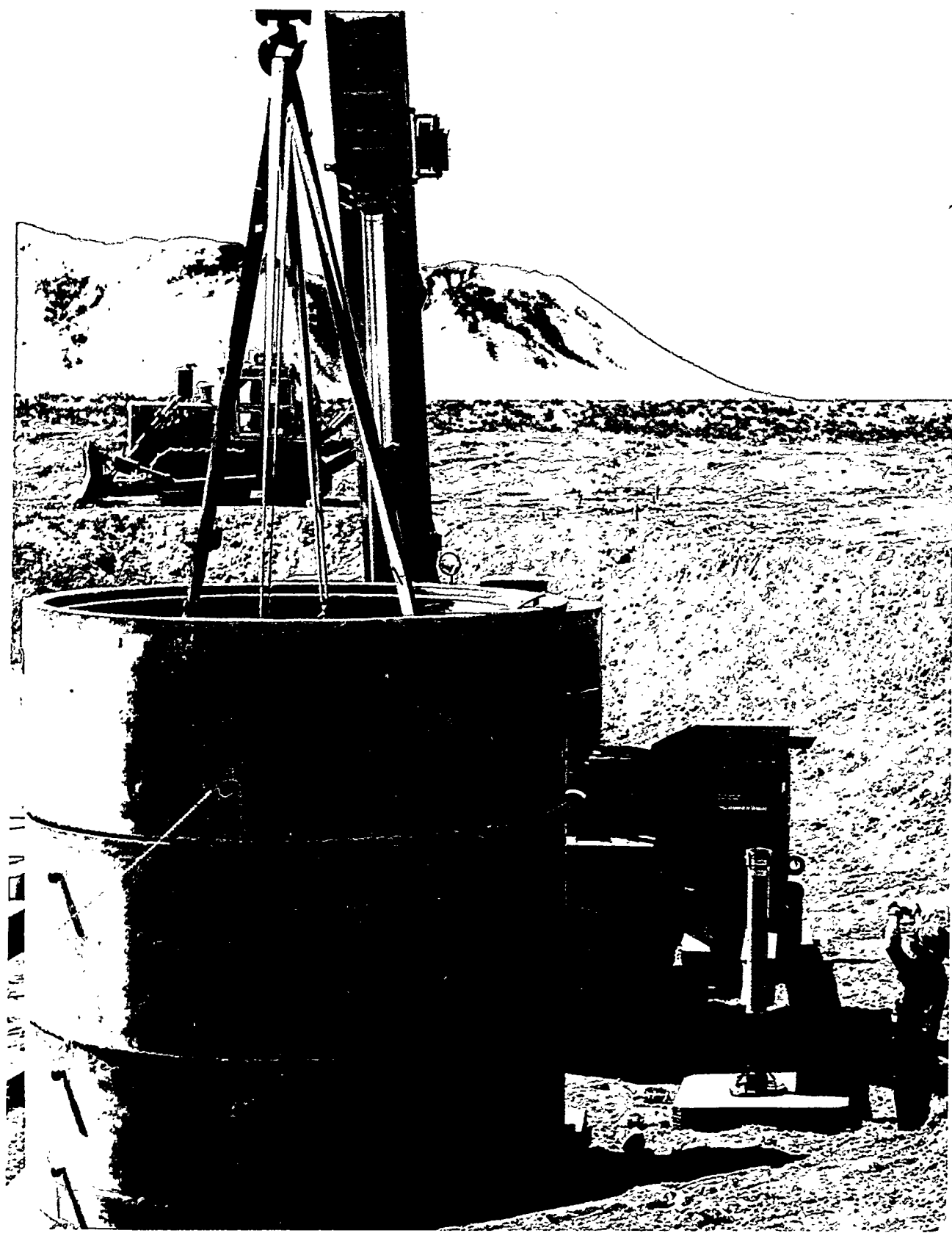
Each field-scale permeameter contains nominally thirty-three 55-gal drums intermingled with soil, with approximately 40% simulated waste and 60% soil as shown in Table 2. Approximately 1/3 of these drums is in each of the three sections. The simulated waste is contained in 55-gal drums and 2 x 2 x 3-ft polyethylene sacks. There are thirty-three 55-gal drums, four of which are metal and 29 of which are cardboard, all with polyethylene liners. Thirteen of the drums contain combustible materials, including a mixture of wood, blotter paper, and cloth. Twelve of the drums contain sludge material as follows: three drums with a mixture of NaNO<sub>3</sub> and KNO<sub>3</sub> (granular), four drums with INEL soil to simulate inorganic sludges, and five sludge drums with a mixture of vegetable oil and absorbants (3/5 canola oil, 2/5 absorbants-calcium silicate [micro cell E] and kitty litter). Eight of the drums contain metal, concrete, and asphalt. Each of the drums contained 200 g of nonsoluable cerium oxide powder (a stand-in for plutonium oxide in the actual waste). The five 2 x 2 x 3-ft sacks of simulated waste consist of combustibles, including cloth and paper. The above mix of simulated waste correctly approximates the volumes and contents of Subsurface Disposal Area buried waste.





Figure 9. Concrete rebar-reinforced pad for field-scale permeameter with first ring being placed (Photo 96-428-1-13).





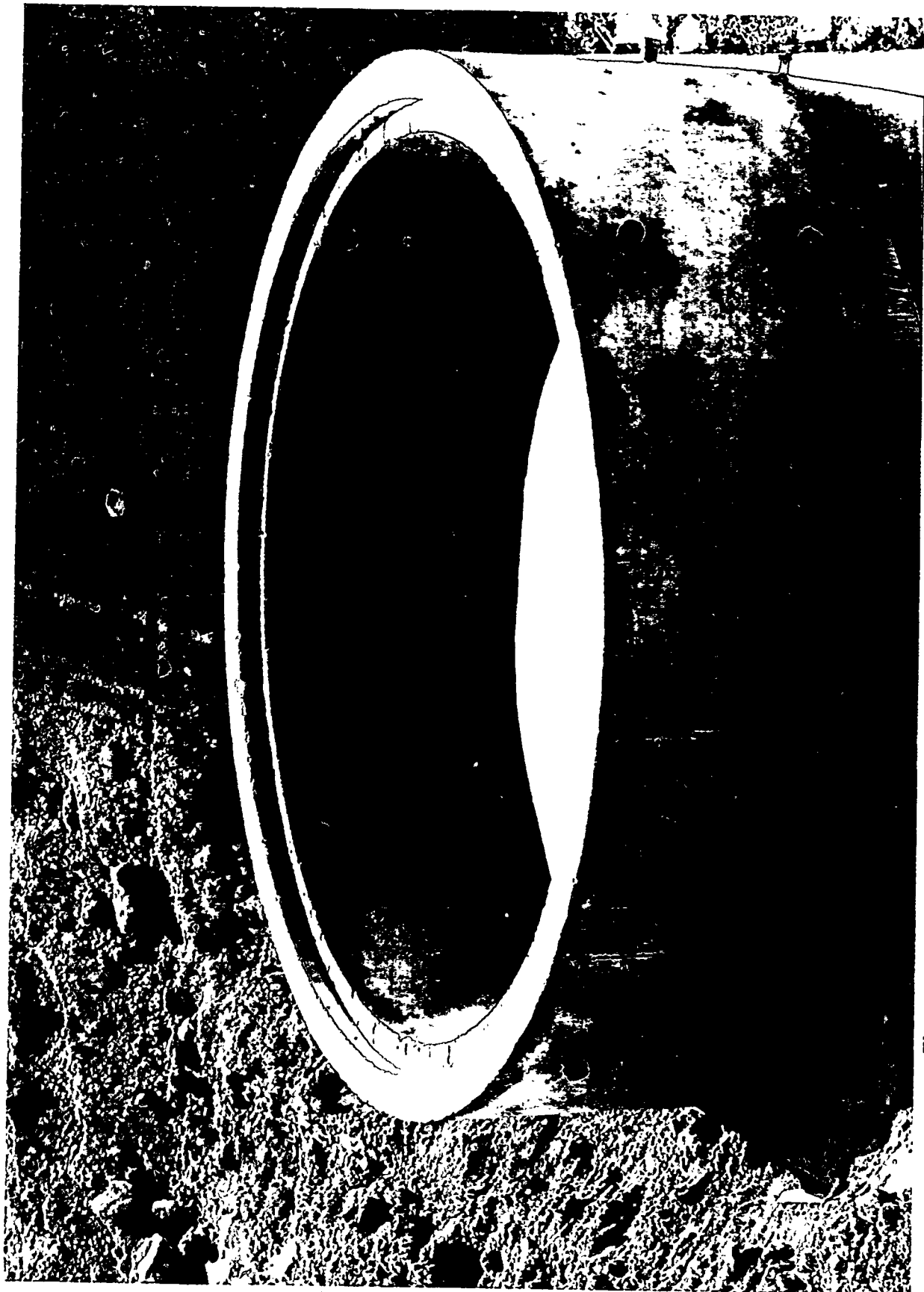
**Figure 10.** Field-scale permeameter with third ring being installed (Photo 96-471-1-16).





Figure 11. Metal water deflection ring with "tar" sealant and over water access hole inside view (Photo '96-450-1-17).





**Figure 12.** Outside view of water access ports in bottom ring (Photo 96-428-1-17).



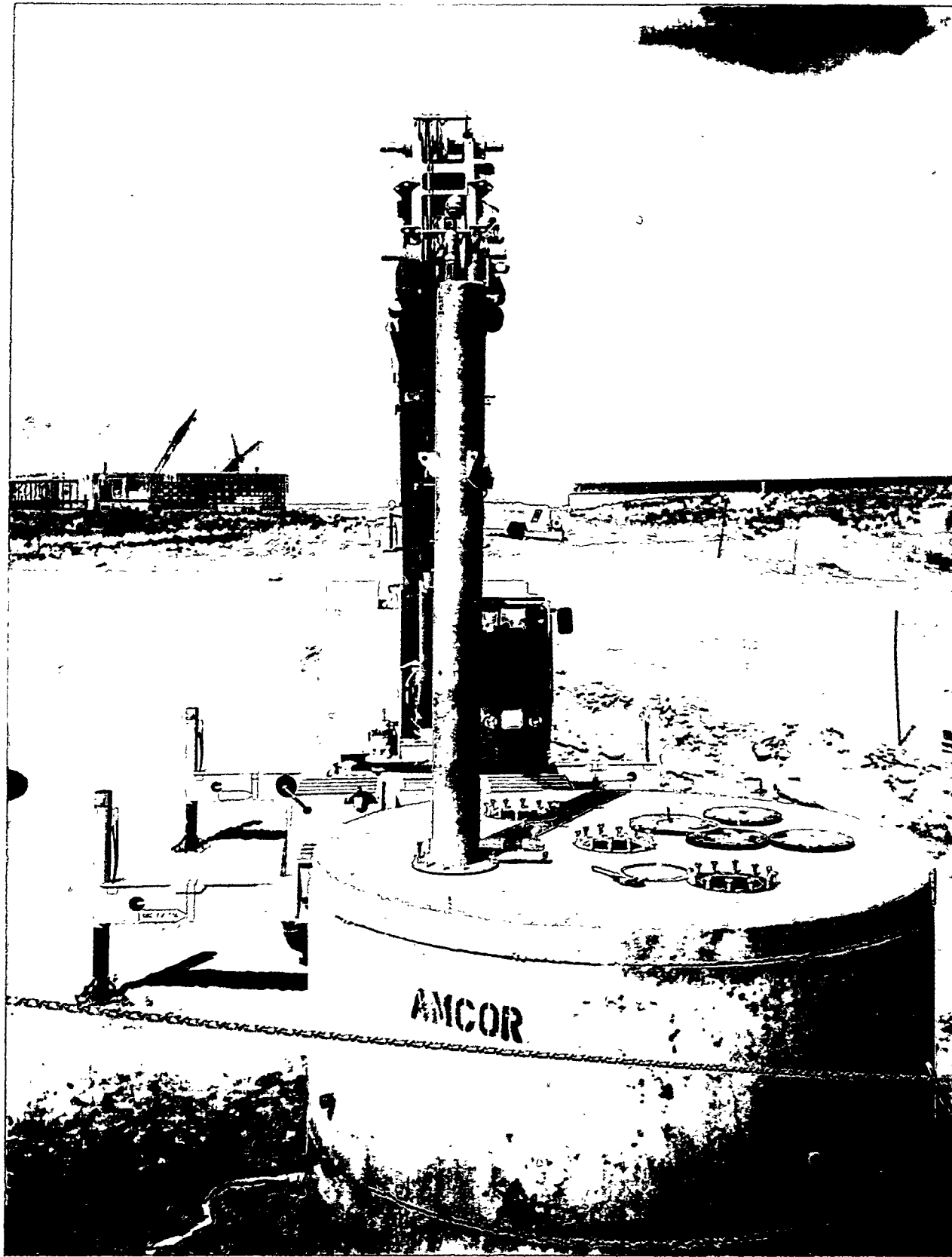


Figure 13. Top of field-scale permeameter showing three access ports and head pipe port (Photo 96-511-1-4).





**Figure 14.** Workers installing seals on access ports (Photo 96-498-1-10).



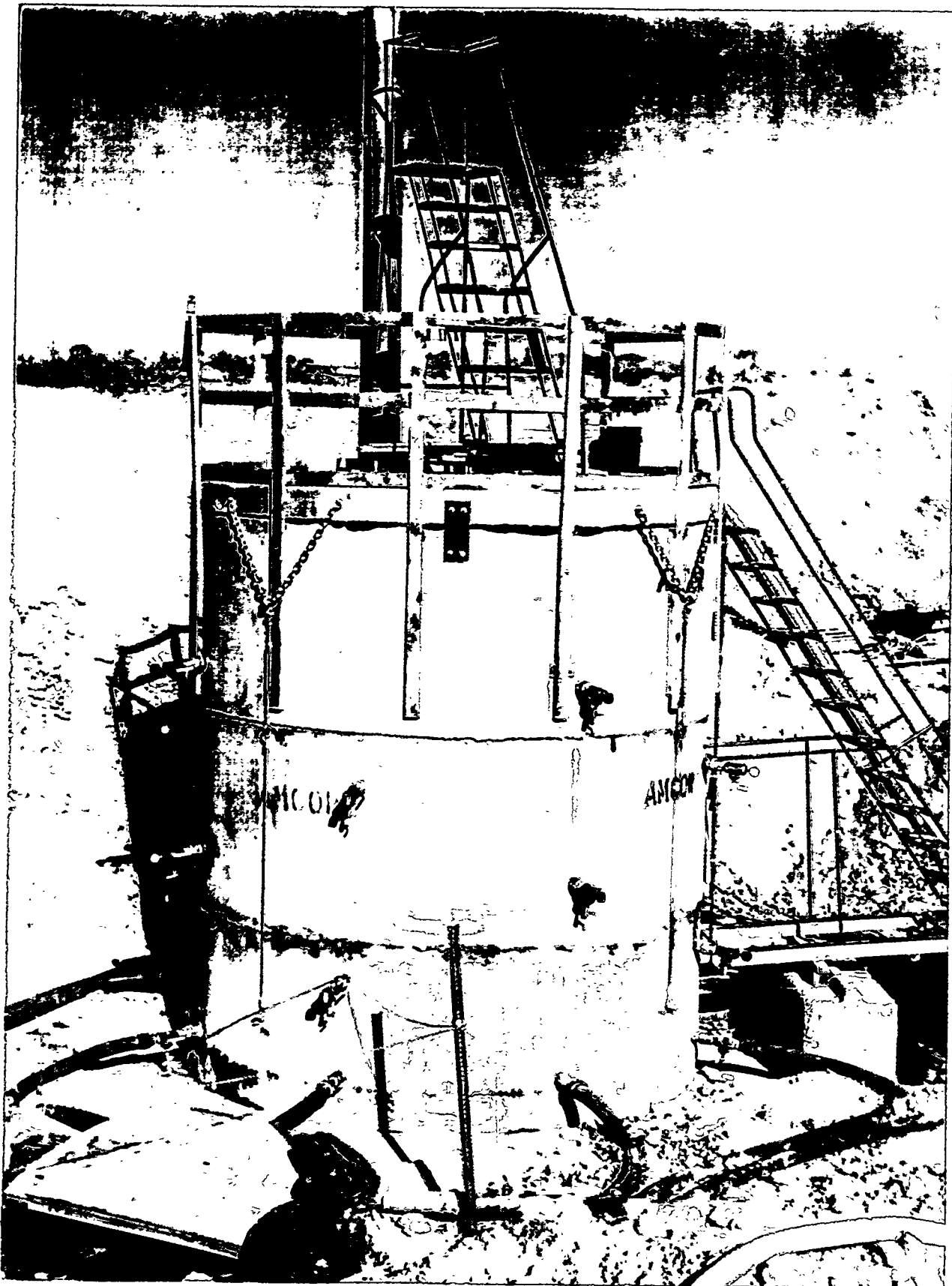


**Figure 15.** Field-scale permeameter with head pipe installed, including safety ladders and railing (Photo 96-658-2-26).



**Table 2. Culvert waste forms.**

Middle Culvert (ungROUTed)	Total Drums <sup>3</sup>	Type (55 gal)	Weight (lbm)
Drum			
Bottom layer			
181		Metal/concrete	193
1		Concrete	170
182		Metal	247
179		Sludge	415
178		Soil	635
11		Wood	87
180		Metal/concrete	212
83		Paper	43
140		Nitrates	511
79		Paper	50
98		Paper	57
Middle layer			
141		Nitrates	486
126		Metal/concrete	224
128		Metal/concrete	224
84		Paper	44
86		Paper	66
95		Paper	45
82		Paper	43
Top layer			
110		Wood	70
75		Paper	51
88		Paper	56
Unnumbered soil		Soil	—
Unnumbered soil		Soil	—
Unnumbered wood		Wood	—
Unnumbered sludge		Sludge	—
Unnumbered nitrates (143 or 144)		Nitrate	—
Unnumbered metal drum with soil		Soil	—
Unnumbered metal/concrete 5 sacks		Metal/concrete	—

**Table 2. (continued).**

South Culvert (grouted)

(Total Drums 33)<sup>a</sup>

5 Sacks

Drum	Type (55 gal)	Weight (lbm)
<b>Bottom layer</b>		
139	Nitrates	529
2	Concrete	269
85	Paper	46
80	Paper	41
176	Metal concrete	309
78	Paper	46
177	Sludge	435
9	Wood	102
10	Wood	102
<b>Middle layer</b>		
78	Paper	46
135	Nitrates	221
136	Nitrates	175
137	Nitrates	226
132	Metal/concrete	183
142	Nitrates	467
185	Sludge	434
183	Sludge	445
105	Wood	61
101	Paper	49
94	Paper	42
93	Paper	43
82	Paper	44
184	Metal	193
<b>Top layer</b>		
190	Metal	173
192	Soil	608
104	Wood	74
191	Soil	529
129	Metal/concrete	146
145	Nitrate	470
96	Paper	53
138	Metal/concrete	153
193	Soil	502
<b>Unknown</b>		
<b>5 sacks</b>		

<sup>a</sup> 200 g of C<sub>2</sub>O<sub>2</sub> placed in each drum.

The waste was approximately divided into thirds and randomly placed in each of the rings of the field-scale permeameter as shown in Figure 16. Once placed, the drums were backfilled with INEL soil using a hand-held compactor following general backhoe filling. In addition, approximately 1 ft of soil was placed in the bottom of the field-scale permeameter prior to placing waste in the first ring. For the third and final ring of the ungrouted field-scale permeameter, the soil was compacted to the point where there was a 1-ft space between the top of the field-scale permeameter and the soil as shown in Figure 17. During construction of each of the rings of the field-scale permeameter, water was randomly added to aid the backfilling of soil. For the ungrouted baseline field-scale permeameter, a total of approximately 650 gal of water was added. For the grouted field-scale permeameter, only about 400 gal of water was added. For the grouted field-scale permeameter, 3 ft of overburden over the top of the waste was added resulting in a top surface 2 ft above the top rim of the field-scale permeameter with 1 foot of soil inside the field-scale permeameter. Prior to complete covering of the grouted field-scale permeameter, the inside diameter of the field-scale permeameter was surveyed, and this survey was used once overburden was placed on top of the field-scale permeameter. Once the survey marks were recreated, flags were placed on a 2-ft triangular pitch matrix for jet grouting the single-phase Type-H (sulfate-resistant) Portland cement into the contents of the field-scale permeameter.

Field trials for grouting the various grouting materials were performed using a specially designed "contamination control" block. This block allowed near-surface grouting of columns in the INEL soil using the block to simultaneously contain the grout returns if any and provide a thrust block against heaving of the soil around the drill stem during jet grouting. A typical field trial involved jet grouting two columns varying the jet-grouting parameters of step size, drill stem rotation, duration on a step, and system pressure. To accomplish this goal, two 5-in. holes were placed through the thrust block to accommodate the 4-9/16 in. drill stem. The thrust block was supported by four 8-in.-high concrete blocks around the periphery of the thrust block and the edge backfilled with soil as shown in Figure 18. The thrust block was reusable and had lifting rings allowing crane moving following each injection of new material. Figure 19 shows a schematic of how the thrust block is used in actual practice.

### 3.2 Grouting Phase

The grouting phase involved performing grouting on field-scale permeameters, implementation pits, and field trials. The grouted field-scale permeameter was grouted with Type-H Portland cement mixed 1:1 by volume with water (the baseline field-scale permeameter was left ungrouted).

Pit A was grouted with the proprietary TECT1 or simply TECT grout. TECT is a high-performance cementitious grout designed for block encapsulation of buried waste by the jet-grouting process. The low-viscosity grout has been formulated to allow mixing and delivery in ordinary concrete mixer trucks. TECT grout remains liquid longer than Portland cement slurries but eventually hardens into a very dense, very low-permeability solid resembling a kiln-fired ceramic. The grout has a low heat of hydration and is formulated to tolerate and stabilize small amounts of organic contamination. Heavy metals contacted by the grout are stabilized during the curing process by pH, which first rises to 12 then falls below 9. The product hardens on the order of 1 day when mixed with soil. However, after approximately 12 months of curing, the grout





Figure 16. Placement of simulated waste in field-scale permeameter's bottom ring (Photo 96-450-1-4).



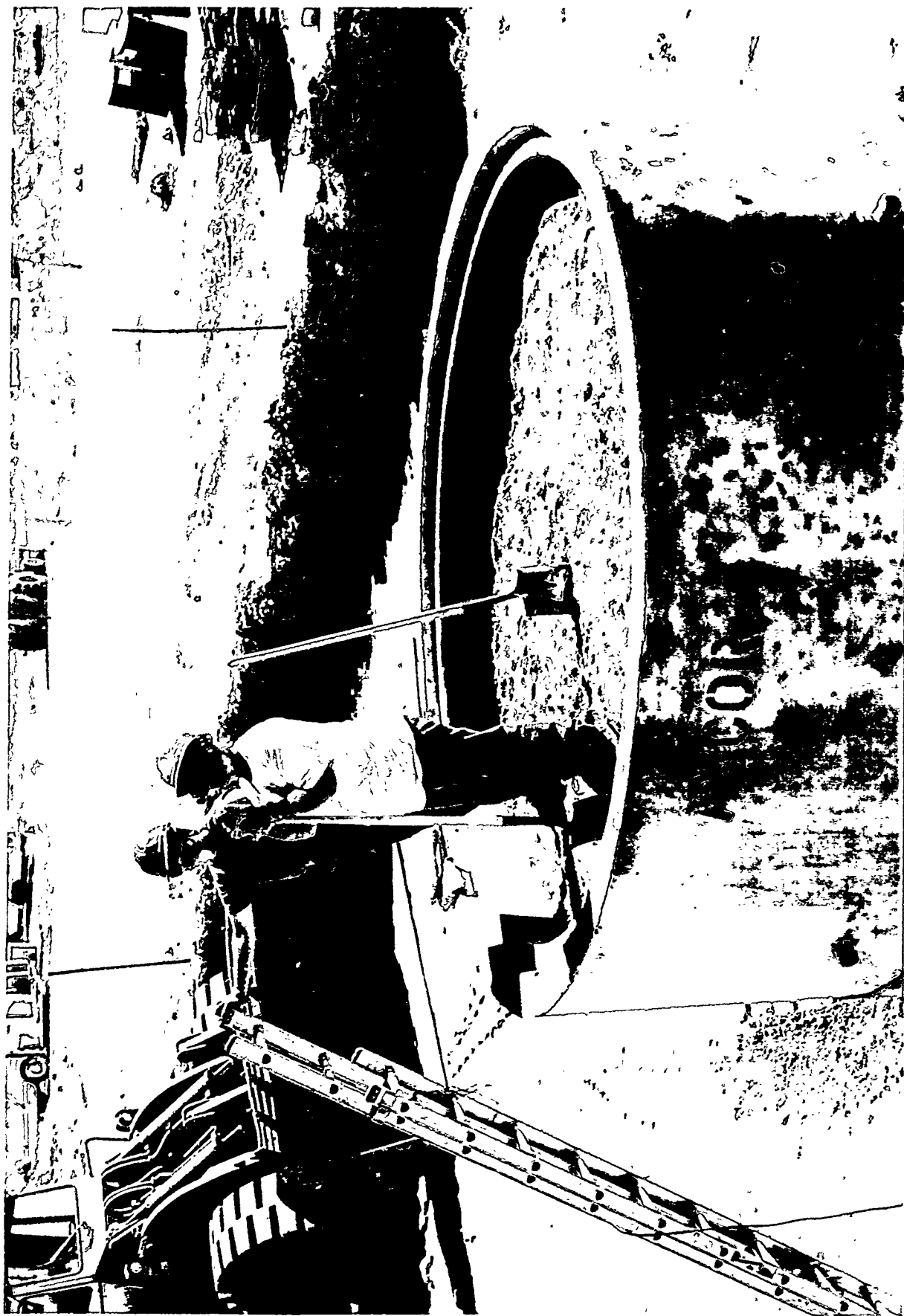


Figure 17. Final compaction of ungrouted baseline field-scale permeameter (Photo 96-503-1-8).





**Figure 18.** Thrust block backfilled with soil ready for field trials (Photo 96-503-1-13).



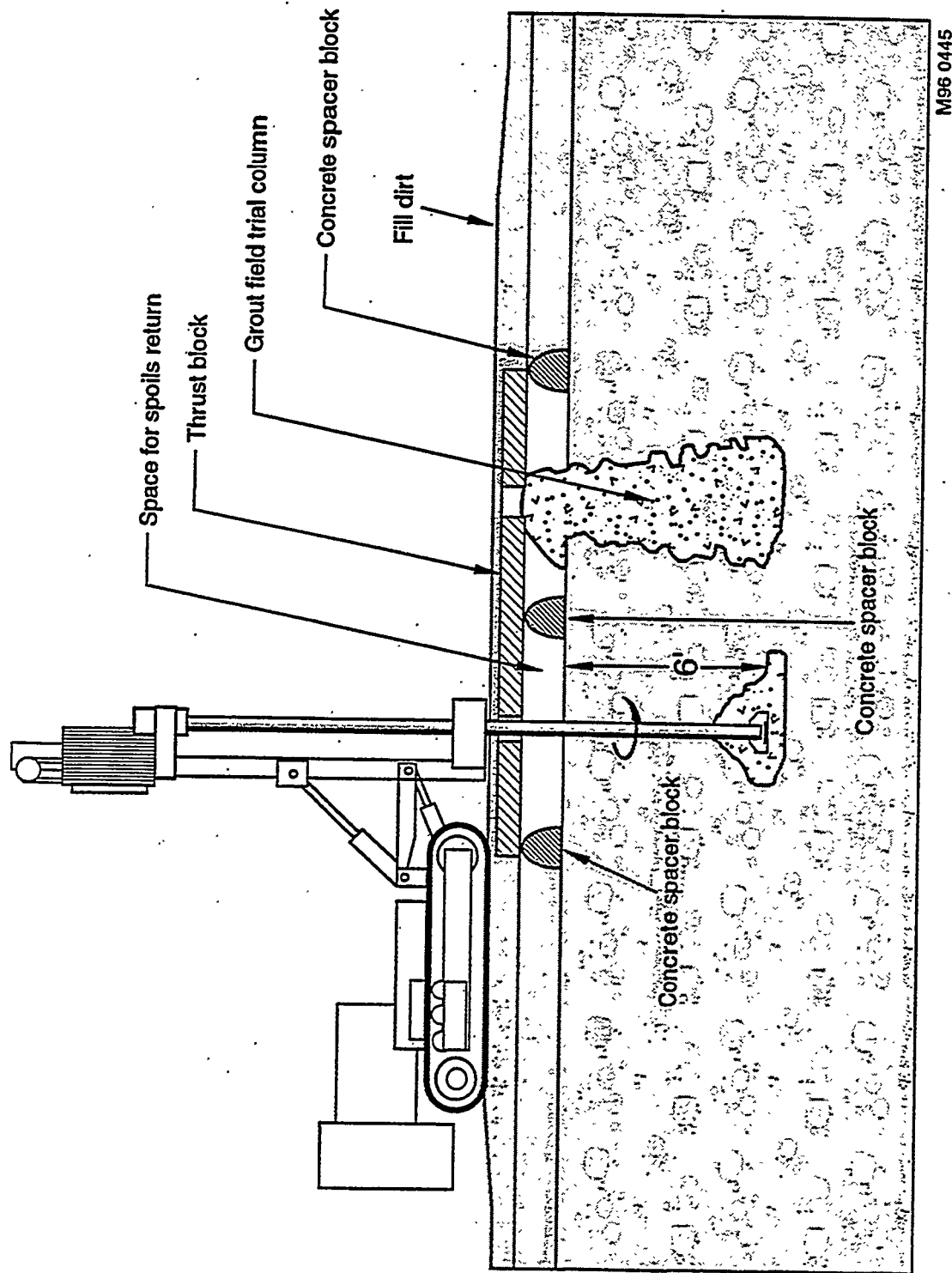


**Figure 19.** Schematic of field-trial grouting, showing thrust block with spacer blocks (Graphic M96 0445).



approaches its final matrix condition, which is thermodynamically stable and highly resistant to chemical attack.

Pit B was grouted with a low melting temperature paraffin mixture called WAXFIT 12. WAXFIT 12 is a low-temperature natural paraffin wax-based grout originally developed for jet grouting leakage of hydrofluoric acid from surface impoundments. The WAXFIT 12 additives allow the molten wax to blend with and even permeate soils regardless of their moisture content. The additives are multiple surfactants that also cause the grout to bond to water, oil, wet surfaces, and buried debris. WAXFIT 12 (referred to as paraffin for the remainder of the report) is designed to fully encapsulate buried waste and to isolate it from environmental waters. The grouted area will self-heal any fractures and will greatly minimize the potential for airborne dust if the material is excavated later. Paraffin is totally combustible and contains no toxic materials.

Pit C was reserved for the proprietary water-based epoxy material called CARBRAY 100. CARBRAY 100 is a two-component water-miscible elastomeric epoxy grout. The final product in the laboratory is a rubbery material that remains tacky indefinitely. The grout can be mixed with a little water such as when grouting wet soil and still form a solid product. This grout can use water and soap cleanup. As discussed in the results section, Pit C was never grouted because of operational difficulties with CARBRAY 100, and Pit C is currently held in reserve (ungROUTed).

Pit D was reserved for an INEL-developed grout called Artificial Hematite, which is formed by reacting an iron-sulfate solution with lime slurry. This forms a putty-like compound that has a characteristic rust color. The material slowly (up to a year) hardens into a clay-like mineral that may eventually become hematite rock. The two slurries are injected through separate nozzles into the soil where they are blended with each other and the soil. As discussed in the results section, Pit D was eventually grouted with Type-H cement mixed 1:1 by mass. This was a substitute grout for the artificial hematites that could not be grouted due to operational difficulties.

The above materials met the criteria set forth in an earlier INEL report.<sup>4</sup>

### **3.3 Coring/Hydraulic Conductivity Testing**

Coring was completed on the grouted field-scale permeameter and all grouted pits.

#### **3.3.1 Grouted Field-Scale Permeameter**

Once grouted, coring of the grouted field-scale permeameter was performed with the top 2 ft of overburden intact. In this coring, four 2.4-in.-diameter cores were obtained to 11 ft as shown in Figure 20. Coring involved using a water flow. In obtaining the 2.4-in. core, a nominally 3.6-in. hole was created. In this manner, the coring equipment never penetrated the sides or bottom of the field-scale permeameter. The coring was facilitated by adding a (polyvinylchloride [plastic]) PVC casing to the top 3 ft of overburden to prevent slumping of material into the core hole. Each core was placed in core boxes, photographed and described in the logbook. At a later date, the cores were placed in sequence with wooden spacers to represent unrecovered material and photographs taken. Once the coring operation was complete, residual water was removed from the core hole with compressed air and each hole was surveyed with a downhole camera. An

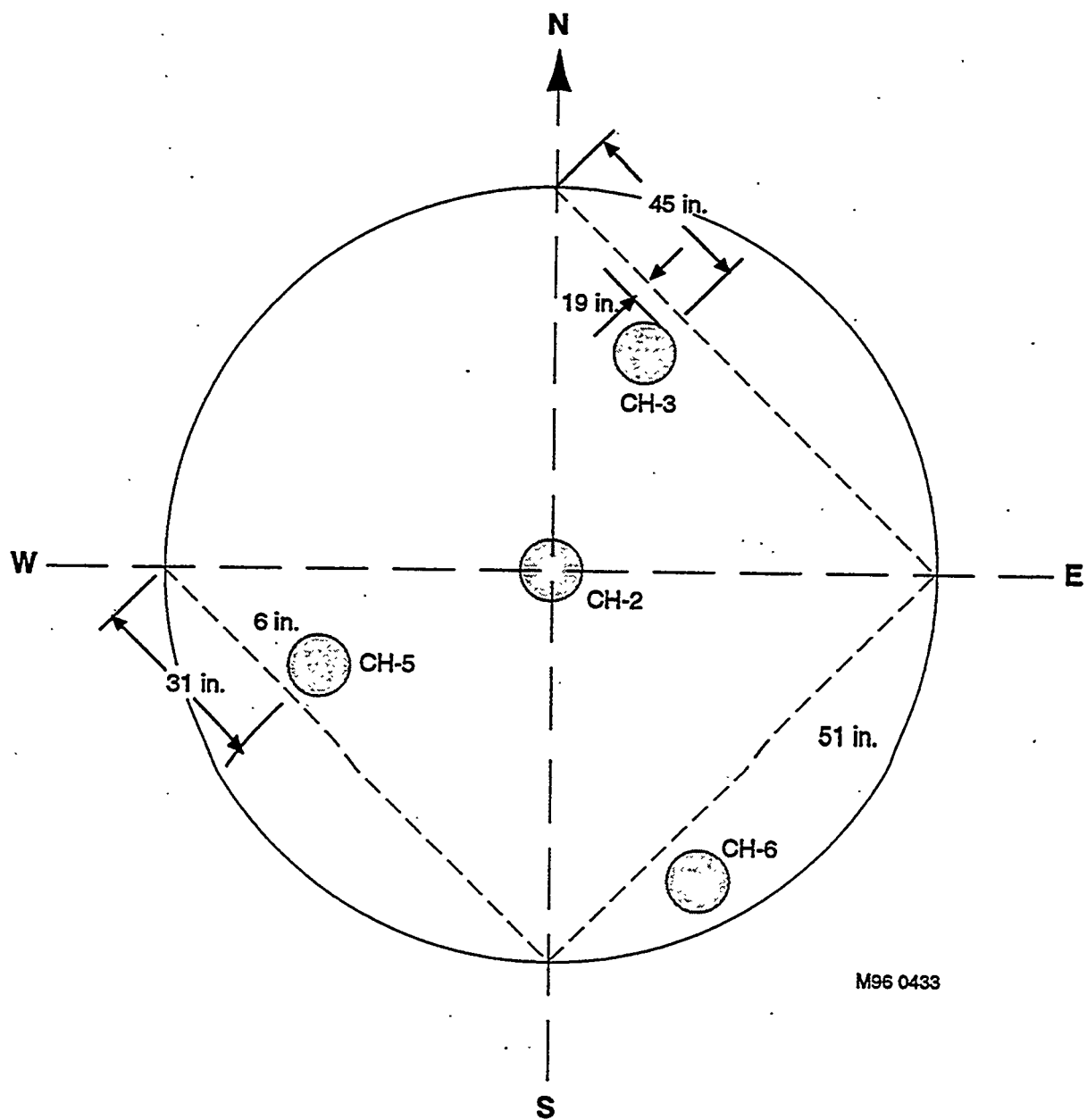


**Figure 20.** Relative position of four core holes for grouted field-scale permeameter (Graphic M96 0433).

RCS-1600 color television camera with built-in lighting was lowered into the core hole. This camera provided continuous video display of the core hole. The survey was monitored using a television and simultaneously recorded on video cassette tape. Following the TV video survey, packer hydraulic conductivity testing was performed in each of the four core holes.

The packer tests were conducted using both single- and dual-bellows packer systems. Figure 21 shows the packer apparatus on top of the grouted field-scale permeameter during testing. The packer test was performed according to standard practice. The packer was first placed into the core hole at the desired depth, the packer bellows were inflated, and water under pressure was introduced. Once water was introduced, the resultant flow of water into the packed off core hole for a variety of pressures (0-22 psi) was noted. The flow of water was recorded for both ascending and descending back pressure values using the U.S. Bureau of Reclamation Groundwater Manual 1977.

Figure 21 shows the apparatus used to perform the packer tests, including water supply tank, nitrogen pressure supply tank, flow meter, packer assembly, and associated equipment. If there was no flow for 10 minutes at a pressure of 20 psi, the local hydraulic conductivity was less than  $10^{-7}$  cm/s. To obtain a meaningful number, the error in reading the flow totalizer or 0.02 gal was used as the total flow in the equation in Appendix C. Using this 0.02 gal for a flow, resulted in a calculated hydraulic conductivity of  $10^{-7}$  cm/s or less. Once finished with the packer tests, the core holes were filled with Portland cement, and the overburden material was removed including the 1-ft section inside the top of the field-scale permeameter. Next, the top lid was sealed in place, and the head pipe was installed for the falling head hydraulic conductivity testing. The head pipe was designed to supply a head of water on the top surface of the field-scale permeameter to stimulate water flow through the matrix in a timely enough manner to collect recognizable amounts of water over a 90-day period. Once the lid and head pipe were emplaced, lids for the three access ports were emplaced, and top safety railing and industrial ladders were installed for access to the head pipe. A simple calibrated site glass was used to indicate the fall in water volume with time.

### 3.3.2 Packer Testing on Pits

Once the grouted field-scale permeameter was completed, coring of the pits was performed. Only the grouted Pits (A, B, and D) were cored, and Pit C was held in reserve. At least two cores were taken in each pit as shown in Figure 22, having at least one hole bisect the organic sludge simulant, the nitrate simulant, and paper, metal, and concrete. This was done by examining the waste configuration in Appendix B. The identical packer apparatus and procedures used for the grouted field-scale permeameter were used for the pits.

### 3.3.3 Falling Head Hydraulic Conductivity Testing on Permeameters

Hydraulic conductivity testing using the falling head method was performed on both the grouted field-scale permeameter and the ungrouted baseline field-scale permeameter. The soil surrounding the south and middle field-scale permeameters was removed and valves were placed on all access ports. Once installed, the bottom eight valves were attached to a water collection system, which allowed comparing the mass of water into and out of the matrix. Once emplaced, water was introduced into the head pipe and the system was allowed to saturate. Saturation was



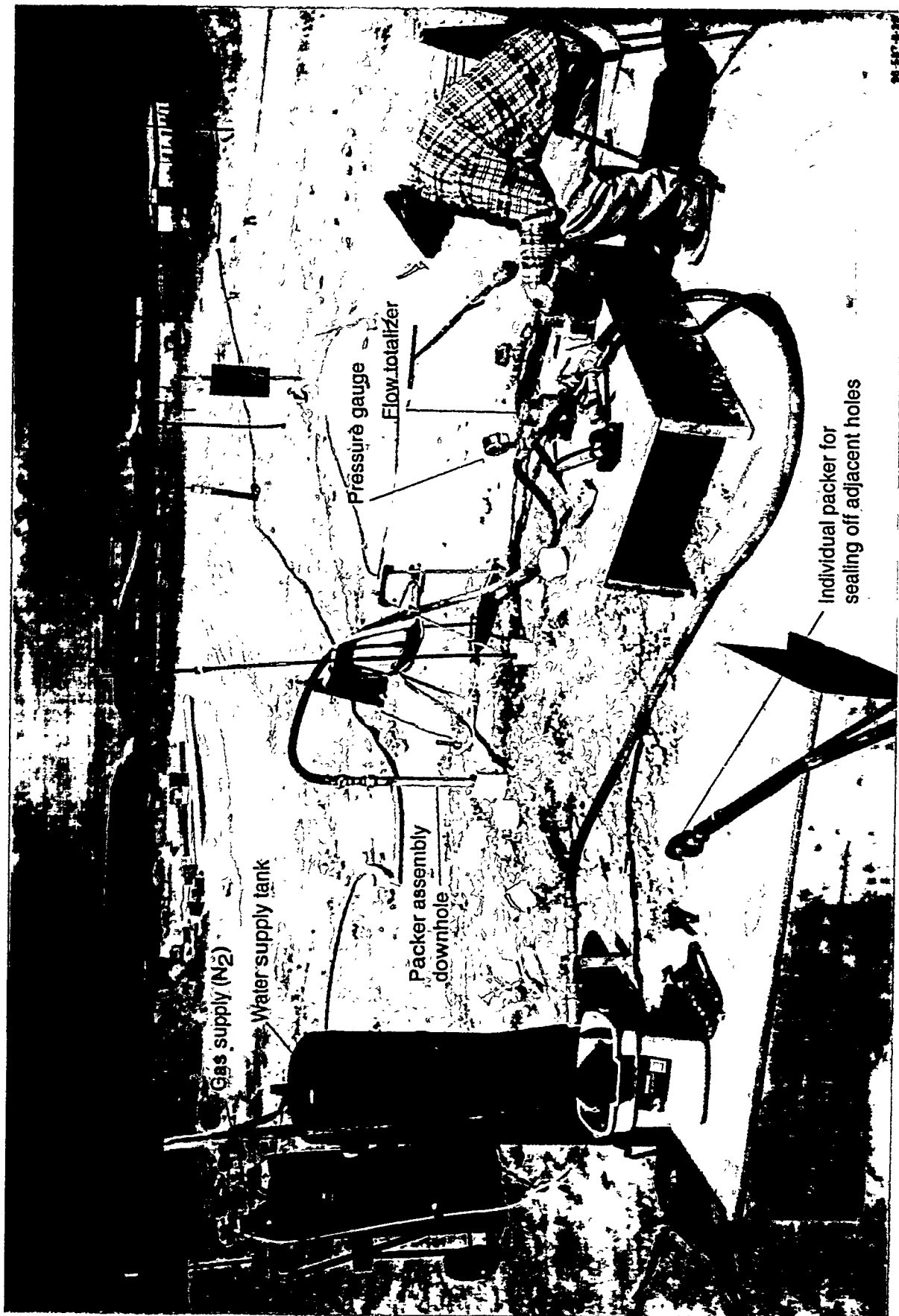
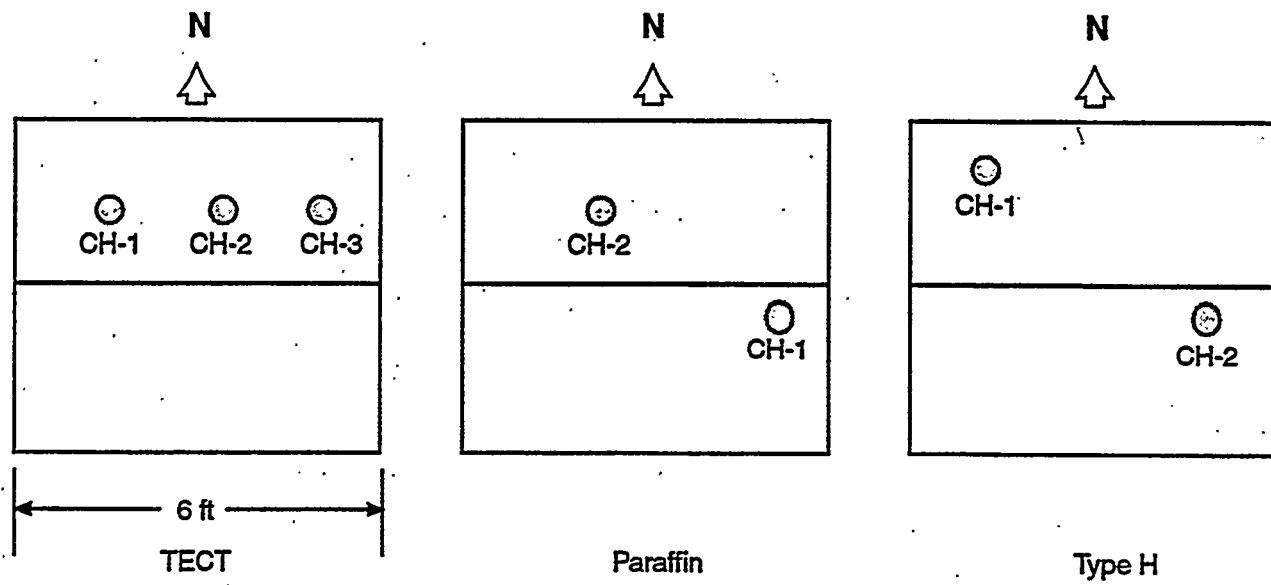


Figure 21. Packer testing of grouted field-scale permeameter (Graphic M96 0452).





M96 0434

**Figure 22.** Packer test hole location in Pits A, B, and D (Graphic M96 0434).



achieved when added water did not flow into the system from the head pipe at the top of the field-scale permeameter with the bottom valves closed. Once saturated, the falling head method was employed. This involved filling the head pipe and noting how much volume drop in water occurred over 8-24 hour intervals. A calibration head pipe with a semiclosed system (top vent but no bottom drain) was used to adjust the head pipes for changes in atmospheric conditions.

The increase in water in the collection system was checked daily (except weekends) and recorded, and the amount of water added to the top to maintain a falling head was performed daily and recorded. In addition to measuring the mass balance in the system, pressure cells were added to the access ports; and the relative heads of water in the system were tracked during the hydraulic conductivity testing.

### **3.4 Destructive Examination of Pits**

Pits A, B, and D were destructively examined by using a backhoe to slice 6-in. sections of the material off the monolith. For this procedure, the first step was to isolate the monolith and note whether the monolith can be freestanding. At each interval, notes were recorded in a logbook and the face photographed. Figure 23 shows the backhoe in operation on Pit A, the TECT pit.





**Figure 23.** Backhoe during destructive examination (Photo 96-587-9-17).



## 4. TEST RESULTS

The discussion of test results includes a discussion of the grouting of pits and field-scale permeameters, temperature measurements of the pits during curing, coring of pits and field-scale permeameter, hydraulic conductivity tests using packers for the pits, both packer and falling head tests on the field-scale permeameters, and a discussion of the destructive examination of the pits.

### 4.1 Grouting the Field-Scale Permeameter and Pits

This section discusses the grouting of the field-scale permeameter with Type-H cement mixed 1:1 by volume followed by grouting of Pit A with TECT, Pit B with Paraffin, Pit C with hematite, and Pit D with water-based epoxy (and subsequently Type-H cement mixed 1:1 by mass). Pit C was eventually held in reserve (ungROUTed).

#### 4.1.1 Grouted Field-Scale Permeameter

Twenty-seven holes were successfully jet grouted in a 2-day period into the grouted field-scale permeameter using Type-H cement mixed 1:1 by volume (or commonly referred to as an 18-sack per 1-yd<sup>3</sup> mix). The field-scale permeameter was grouted using the CASA GRANDE Jet 5 pump and C6S drill system shown in Figure 24 and Figure 25. The basic procedure was to first drive the drill stem into the soil-and-waste matrix in the field-scale permeameter and then withdraw the rotating drill stem while injecting grout through the nozzles in precise increments with a specified time of duration on any step.

The Type-H cement was delivered in a series of local Ready Mix trucks about 6 yd<sup>3</sup> at a time. The drill stem was driven 11 ft 8 in. into the top of the field-scale permeameter, which had a nominal 3 ft of overburden over the soil-and-waste matrix, and the bottom 9 ft 3 in. was grouted. The end of the drill stem with nozzles is shown in Figure 26. Two nozzles were located 180 degrees and 5 cm apart on the drill stem, nominally 4 in. from the bottom driving point with a 2.2-mm opening. All grouting was performed at 400 bars (nominally 6,000 psi), 2 revolutions per step, 5 cm per step, and a variation on dwell time or the time spent at a step depending upon grout returns and the desire to fill all the accessible voids in the pit with grout and/or grout soil mixture.

The nominal parameters used in the operation are shown on Table 3. A total of 27 holes were grouted with a slight variation in the amount of time spent on any discrete step. For most of the holes, a dwell time of 6 seconds per step was used. However, when excessive grout returns were observed (greater than 2 gal per hole), the dwell time was reduced to 4 seconds per step for holes 9 and 10 and then increased to 5 seconds per step for the remainder of the grouting phase. A total of 3,021 gal of grout was injected into the field-scale permeameter via the 27 holes for an average grout take of 116 gal per hole. The total estimated returns of grout was nominally 113 gal (on the outside, this would fill a spoils collection pit 2 x 2.5 x 4 ft).

Figure 27 shows the final grouting stages of the grouted field-scale permeameter with the spoils collection pit filling with spoils returns. Figure 27 also shows a heave in the top surface of



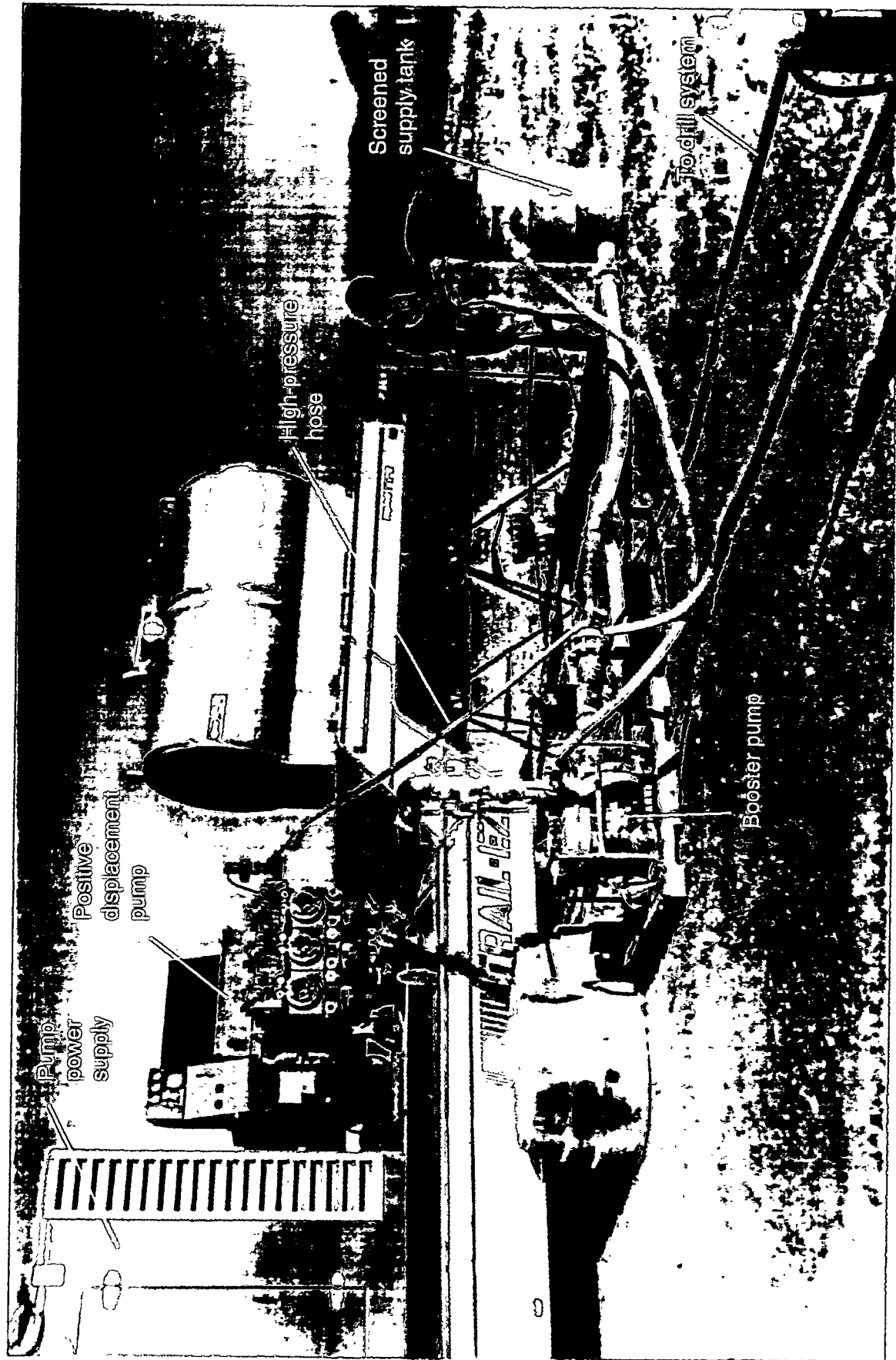


Figure 24. CASA GRANDE Jet 5 pump (Graphic M95 0469).

M95 0469



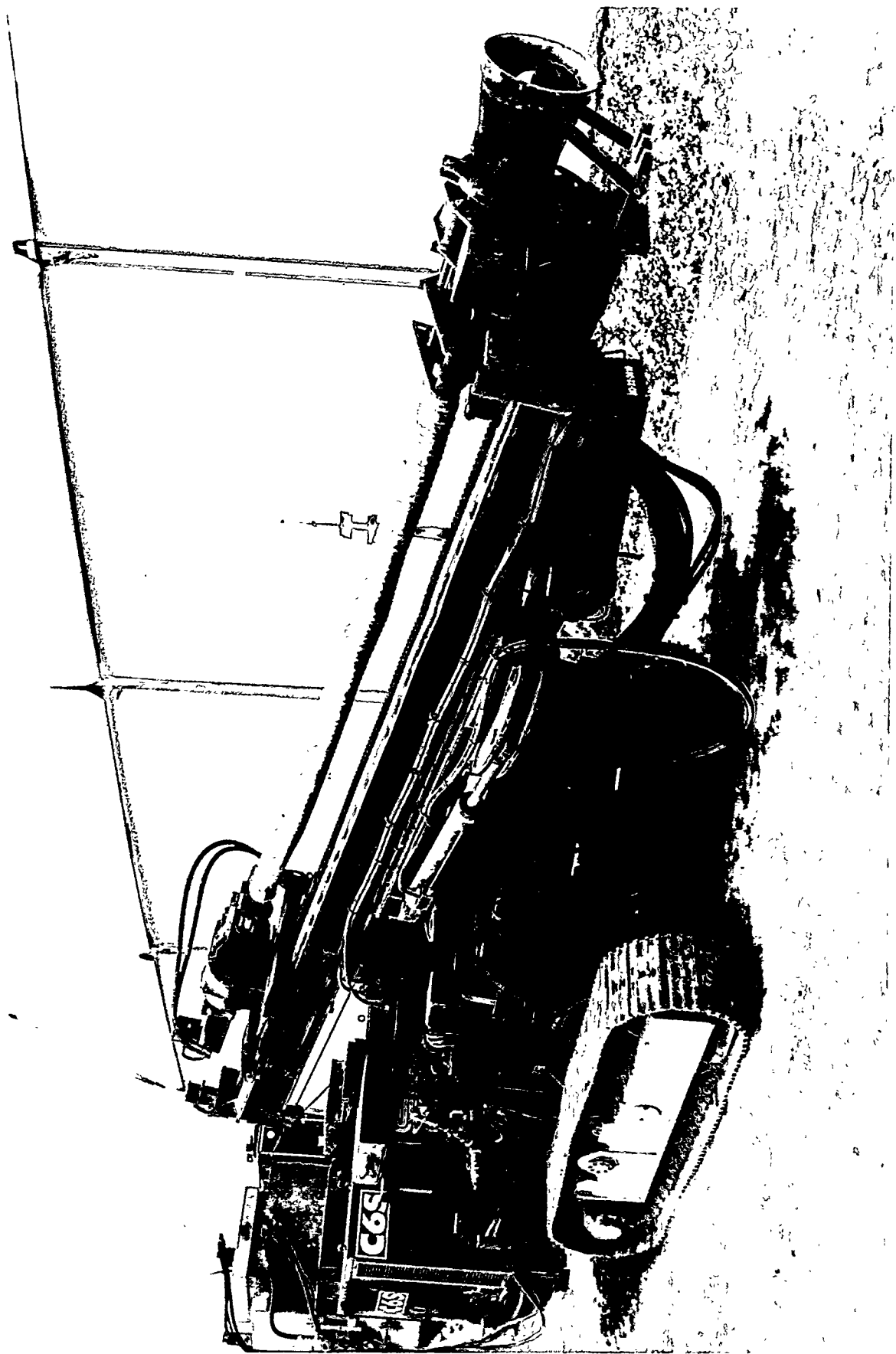


Figure 25. CASA GRANDE C65 drill system (Photo 94-715-1-12).





**Figure 26.** Drill stem used for Type-H cement, TECT, and paraffin (Photo 96-503-1-1).



**Table 3.** Operational parameters for jet-gravity Type-H count in southern culvert (see Figure 28 for order).<sup>a</sup>

2.2-mm Jets			
Hole	Date	Grout Take (gal)	Comments
1	7/23	50 (flow meter plugged) freed after core hole 1 assume 130 gal nominal	5 cm/step; 6 s per step; 2 rev/step; 6,000 psi No spoils return
2	7/23	130	5 cm/step; 6 s per step; 2 rev/step; 6,000 psi No spoils return
3	7/23	132	5 cm/step; 6 s per step; 2 rev/step; 6,000 psi No spoils return
4	7/23	129	5 cm/step; 6 s per step; 2 rev/step 6,000 psi No spoils return
5	7/23	137	5 cm/step; 6 s per step; 2 rev/step; 6,000 psi No spoils return
6	7/23	134	5 cm/step; 6 s per step; 2 rev/step; 6,000 psi No spoils return
7	7/23	127	5 cm/step; 6 s per step; 2 rev/step; 6,000 psi No spoils return
8	7/23	No data, assume 130 gal	2 gal spoils
9	7/23	124	Changed to 4 s/step flow up adjacent grouted hole ~1 gal
10	7/23	92	Changed to 4 s/step flow up adjacent grouted hole ~1 gal
11	7/23	Did not complete	Changed to 5 s/step. Jets plugged, shut down for day
11	7/24	110	5 cm/step 5 s per step; 2 rev/step; 6,000 psi 10 gal of water came out hole as lines cleared (note this is not a return of grout)
12	7/24	132	No spoils return
13	7/24	114	5 s/step; 5 cm/step; 2 rev/step; 6,000 psi No spoils return
14	7/24	60	5 s/step; 5 cm/step; 2 rev/step; 6,000 psi Hit major resistance at 6 ft down, grouted only top 3 ft of waste
15	7/24	62	Refused at 5 ft, only grouted 2 ft of waste
16	7/24	Did not grout	Hit resistance at 3 ft down
17	7/24	132	Major flow of returns, 20 gal of returns
18	7/24	109	5 gal of returns

**Table 3. (continued).**

2.2-mm Jets		Grout Take (gal)	Comments
Hole	Date		
20	7/24	128	5 gal of returns
21	7/24	119	10 gal of returns, hit obstruction (boulder) at 2 ft down, moved and redrilled
22	7/24	126	15 gal of returns
23	7/24	121	15 gal of returns
24	7/24	120	No grout returns
25	7/24	119	3-ft-high geyser out adjacent hole, 15 gal total return
27	7/24	97	Area between holes 23-27 showed heave of 1-2 ft; total return 15 gal
26	7/24	129	10 gal of returns
19	—	78	Area around hole 19 heaved 2 ft

**Summary:****For southern culvert**

Total holes: 27  
 Total grout tube: 3,021 gal  
 Total estimated returns: 113 gal  $\pm$  50 gal  
 Net amount in culvert: 2,908 gal  
 Average grout/hole: 116 gal  
 1:1 by volume = 18 sacks/yd<sup>3</sup>

**Elapsed time:**

Holes 1-11	Start	11:37 a.m.	Total elapsed time:	8 hr 29 min
	Stop	5:14 p.m.	Time/hole:	19 min
Holes 11-27	Start	12:17 p.m.		
	Stop	4:09 p.m.		

a. Field trial hole also grouted on 7/24  
 100 gal grouted interval 2.5 to 9.8 ft  
 No grout returns used  
 5 s/step; 5-cm step; 400 bars

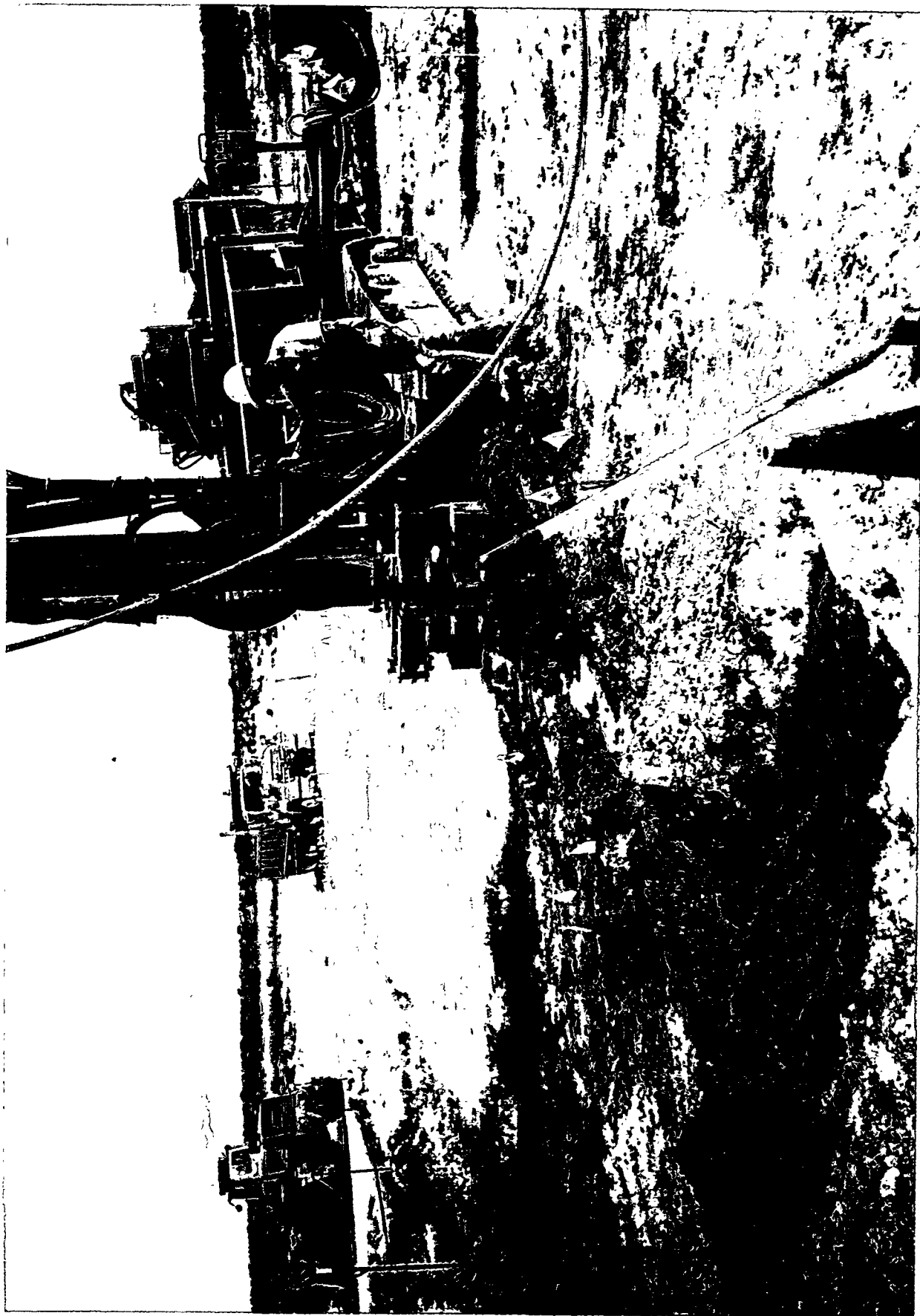


Figure 27. Heave of top surface of field-scale permeameter during grouting of Type-H cement (Photo 96-511-1-8).



the grouted field-scale permeameter caused by the grouting action. In previous grouting of pits, there was no heave of the top surface observed. However, this was a confined field-scale permeameter, and it is suspected that the field-scale permeameter was generally free of voids and that additional grout tended to thrust the top cured surface upward.

The net amount of grout left in the field-scale permeameter after accounting for returns was 2,908 gal, which accounts for 53% of the volume of the field-scale permeameter without waste or soil (assuming only the 9-ft 3-in. height of the grouting). Figure 28 shows the order of grouting, which was designed to minimize the amount of time spent repositioning the drill rig when moving from hole to hole. It is a modified "Z" pattern, which greatly reduced the setup time for grouting. Grouting of the 27 holes was performed in a 2-day period, with several periods of downtime each day.

Common problems with the Type-H cement included several delays due to "filter caking" of the cementitious material in the Jet 5 pump and in the bottom of the drill stem. The first day's operation was shut down after a Jet 5 failure to pump after only 11 holes in 5.5 hours of operation, which included a 3-hour delay to weld a new bracket on the drill stem. During the second day's operation, holes 11-27 were completed in 4.5 hours, with a total delay of 1 hour to "clean out a cured grout-like consistency plug in the bottom of the drill stem. This plugging is thought to be caused by the use of the 1:1 mixture of Type-H cement and water by volume (18-sack mix), which has a much higher viscosity and more particulate to filter cake per volume than the desired 14-sack mix (1:1 mixture of Type-H cement and water by mass).

Examination of the spoils return pit 12 hours after completion of grouting showed a prominent white residue on the surface of the collection pit as shown in Figure 29. It is speculated that sodium and potassium nitrate dissolved in the Portland/soil mixture in the field-scale permeameter during grouting and that some of this material came to the surface with the spoils. As the grout cured, the nitrate-salt rich solution migrated to the free surface and evaporated, leaving the white residue on the surface. In previous grouting experiments with Type-1 Portland cement,<sup>1,2</sup> there was a tendency for a slight film of white residue (presumably calcium hydroxide or calcium carbonate) on grout returns. However, the residue observed in the subject spoils returns was considerably more pronounced, suggesting the possible presence of nitrate salts (not supported by sampling, however).

#### **4.1.2 TECT Pit (Pit A)**

Successful jet grouting of the TECT grout was performed in a 1-day period for two field trials and a pit involving 11 holes. For this TECT grouting demonstration, the identical equipment used for the grouted field-scale permeameter was used, except that the nozzle size was changed to 3 mm to accommodate the higher viscosity TECT material. The proprietary TECT grout was premixed in a local Ready Mix plant and delivered to the site of testing in the truck.

An INEL-designed thrust block was used to perform the field trials. The thrust block consisted of an 8-in.-thick reinforced concrete block placed on 8-in. concrete blocks to allow near-surface jet grouting and containment of the spoils returns. The thrust block was found to adequately perform the function of containing the returns with near-surface grouting. Two holes 5 in. in diameter penetrate the block as shown in Figure 30, which shows the 4-9/16-in. drill stem



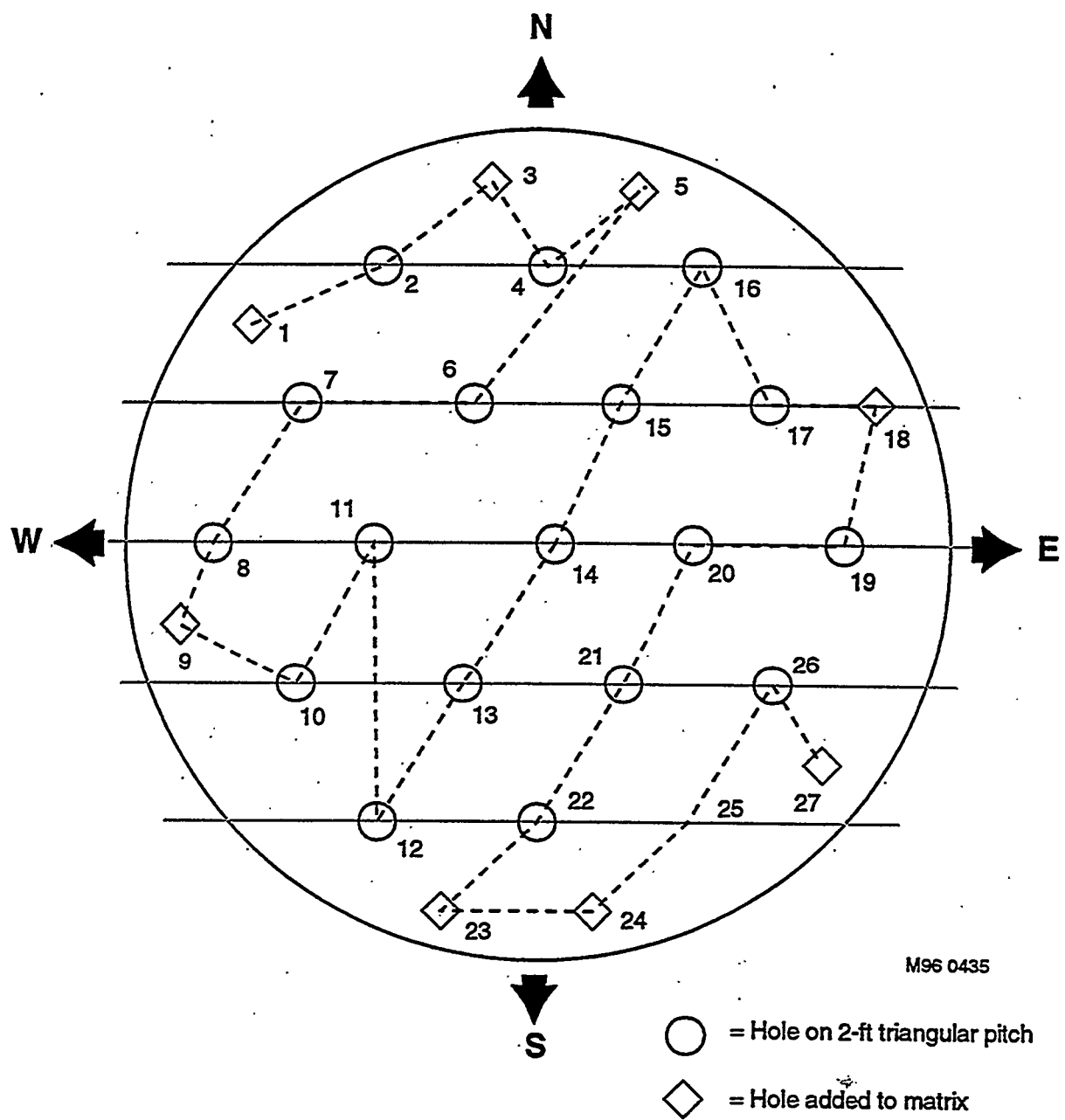


**Figure 28.** Orientation of grout holes for grouted field-scale permeameter (order of grouting) (Graphic M96 0435).





**Figure 29.** White film on spoils collection pit for grouted field-scale permeameter (Photo 96-512-2-3).



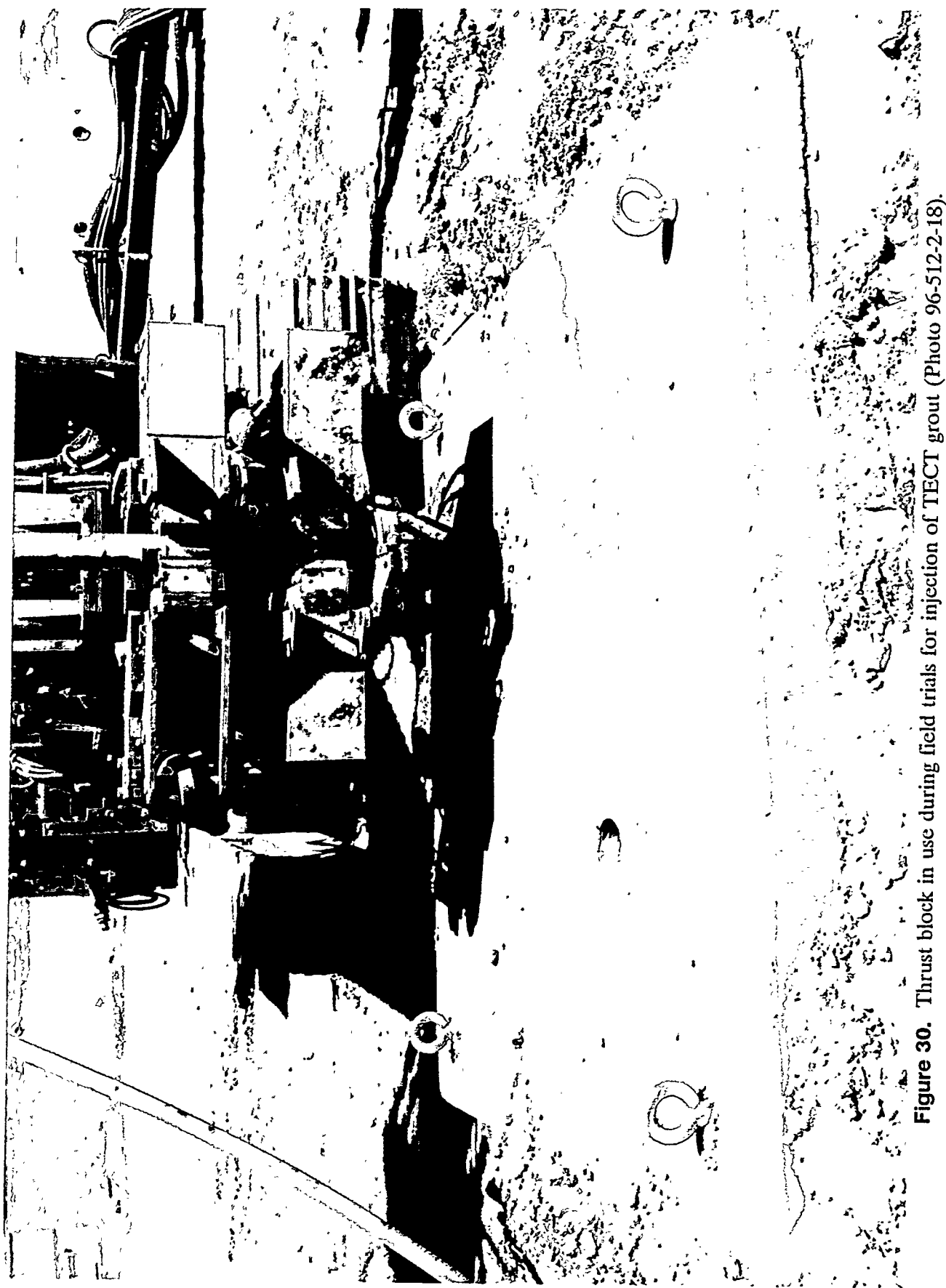


**Figure 30.** Thrust block in use during field trials for injection of TECT grout (Photo 96-512-2-18).



penetrating the thrust block during the first field trial. During the field trial, the drill stem was inserted 6.5 ft and the bottom 6 ft was grouted (within 6 in. of the surface). The four lifting rings on the thrust block were used to reposition the block for the next set of field trials using a crane.

During the field trials, no TECT grout escaped the confines of the thrust block. Two field trials were performed to set the injection parameters with the dwell time on a step being the variable between the two field trials (the 5-cm step and 2 revolutions per step were kept constant). The first field trial used 4 seconds per step and resulted in 124 gal of grout being injected in the 6-ft section. The second field trial used 6 seconds per step and resulted in only 102 gal injected. It is speculated that the larger volumetric flow for the 4-second dwell time was the result of long delays prior to grouting the first field trial hole. Since the grouting operation includes a trickle flow to keep lines from curing, any delay adds to the total amount shown on the flow meters. This explanation is speculation because, in general, a longer dwell time should result in more total volume recorded. The 6-second dwell time was picked, based on a destructive examination of the field trial hole, immediately following the test. The thrust block was removed, and it was found that the 4-second dwell time produced a jet-grouted column of soil and grout with a 17-in. diameter. For the 6-second dwell time, the column was 24 in.

A total of eleven 6-ft-deep holes were jet grouted in Pit A in only 1 hour and 20 minutes. The reason only 11 of the expected 18 holes were grouted is that the field trials used more grout than expected, and there was not enough to complete the entire pit. Table 4 gives details of the grouting parameters, and Figure 31 shows the general order of TECT pit grouting. The total injected amount of TECT grout was 1,167 gal, for an average of 106 gal per 6-ft hole. The total estimated amount of grout returns was only 50 gal, resulting in 1,117 gal of grout left in the pit. The amount of estimated grout left in the pit represents 69% of the total volume of the pit, even though only 11/18 or 61% of the pit had been grouted.<sup>a</sup> This represents a much higher percentage of total volume compared to that injected into the grouted field-scale permeameter (53%). The TECT grout seemed to assess the available void space more easily than the Type-H Portland grout. Another contributing factor is that the field-scale permeameter had an impervious barrier on the exterior positions of the waste, whereas, in the TECT pit, the exterior positions were compacted soil. Therefore, the Tect grout may have extended into adjacent positions more readily than the Type-H grout and not come up the drill stem hole.

An antifoaming agent (1 pt of liquid silicon mixed with 1.5 gal of water) was sprayed into the 1,400 gal of TECT grout in the Ready Mix truck prior to grouting operations to prevent foaming caused by mixing calcium lignosulfonate with other proprietary ingredients of TECT. During grouting, the average flow for a 6-ft column was 106 gal (Table 4) compared to the 116 gal for a 9.25-ft column in the grouted field-scale permeameter (Table 3). This is attributed to the fact that the 3-mm nozzle allowed a higher flow for the same relative grouting parameters than the 2.3-mm nozzle used for the Type-H cement. However, the Type-H cement mixed 1:1 on volume (18-sack mix) was visibly less viscous than the TECT grout, which had the consistency of hot maple syrup. To avoid solid particulate in the grouting system, a fine mesh screen (simple nylon door screen) was used to filter the TECT grout prior to feeding the grout to the Jet 5 pump. This operation is shown in Figure 32. There were minimal grout returns for the TECT grout (nominally 50 gal total).

---

a. It is noted here that the total estimated void of the pit was only 50%. Therefore, 69% filling guarantees that the voids are filled. The additional grout left in the pit must fill voids in the surrounding soils due to the jet-grouting action extending away from the pit boundary.

**Table 4. Operational parameters for TECT pit (Pit A).**

3-mm Jets		Grout Take (gal)	Comments
Hole	Date		
1	7/25	102	5 cm/step; 6 s/step; 2 rev/step; no spoils
2	7/25	112	5 cm/step; 6 s/step; 2 rev/step; no spoils
3	7/25	113	Small eruptions on surface, no major grout returns
4	7/25	127	Cross communication out hole #3 1-2 gal
5	7/25	121	2 gal spoils out hole #4
6	7/25	27	Drilled 3 different positions around #6 position only grouted 2 ft
7	7/25	115	Copious returns up hole #6, estimate 40 gal of material came up hole #6
8	7/25	120	No grout returns
9	7/25	115	5 gal grout returns up hole #8
10	7/25	106	Used gravity feed to feed Jet 5 pump; supply pump failed
11	7/25	109	No grout returns
12	7/25	Did not grout	Ran out of grout
Field Trial Hole			
Field Trial Number 1			
Parameters		4 s/step	
		5 cm/step	
		2 rev/step	
Drilled in 6.5 ft			
Grouted out 6.0 ft			
Grout take 124 gal			
Field Trial Number 2			
Parameters		6 s/step	
		5 cm/step	
		2 rev/step	
Drilled in 6.5 ft			
Grouted out 6.0 ft			
Grout take 102 gal			
Column size	4 s/step = 17 in.		
Column size	6 s/step = 24 in.		
Summary:			
Total holes grouted:		11	
Total grout take:		1,167 gal	
Average/hole:		106 gal	
Total estimated returns:		50 gal	
Total grout in pit:		1,117 gal	
Total elapsed time:		81 min	
Time/hole:		7.3 min	

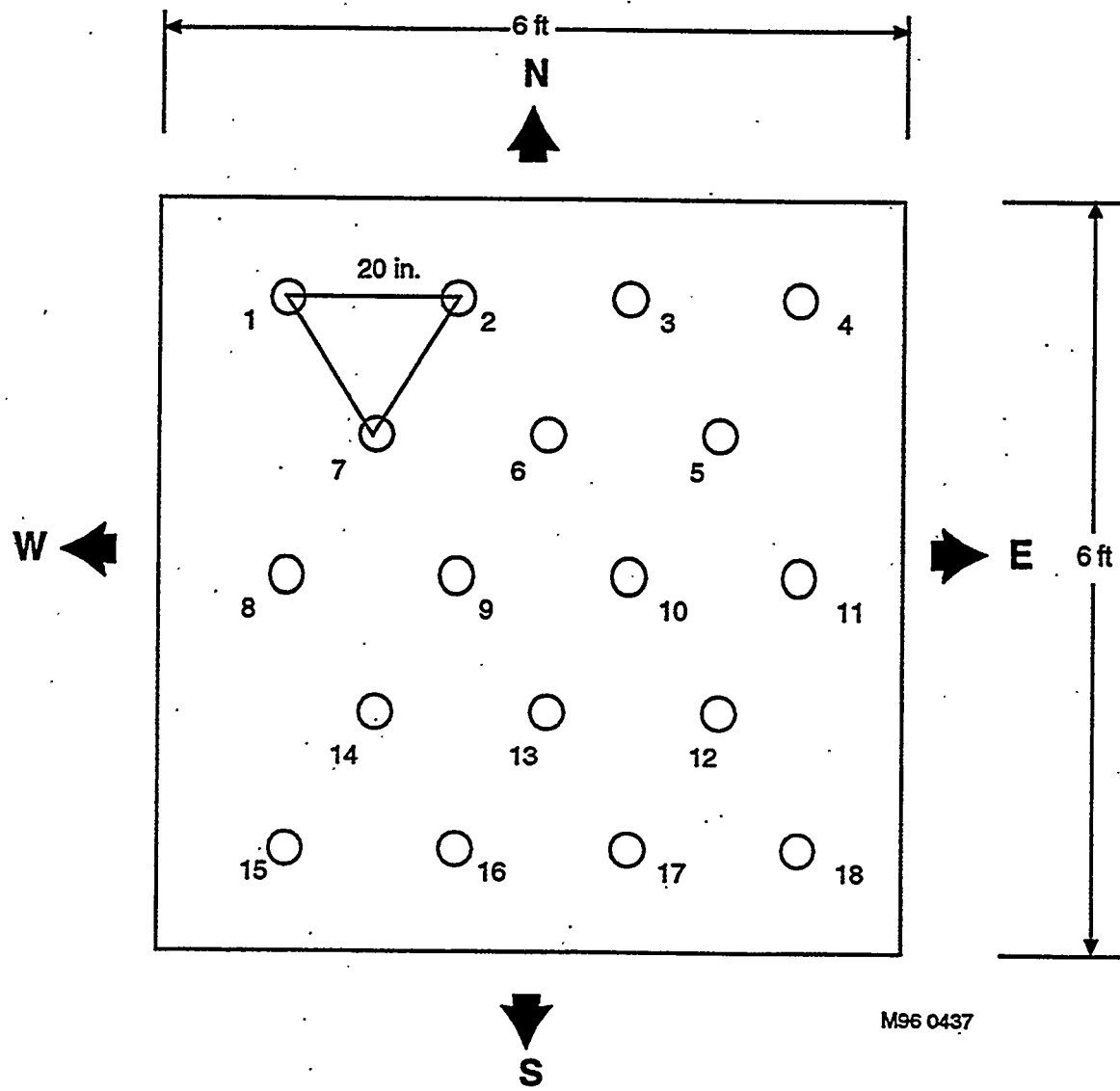


**Figure 31.** Hole orientation of TECT Pit A (Graphic M96 0437).



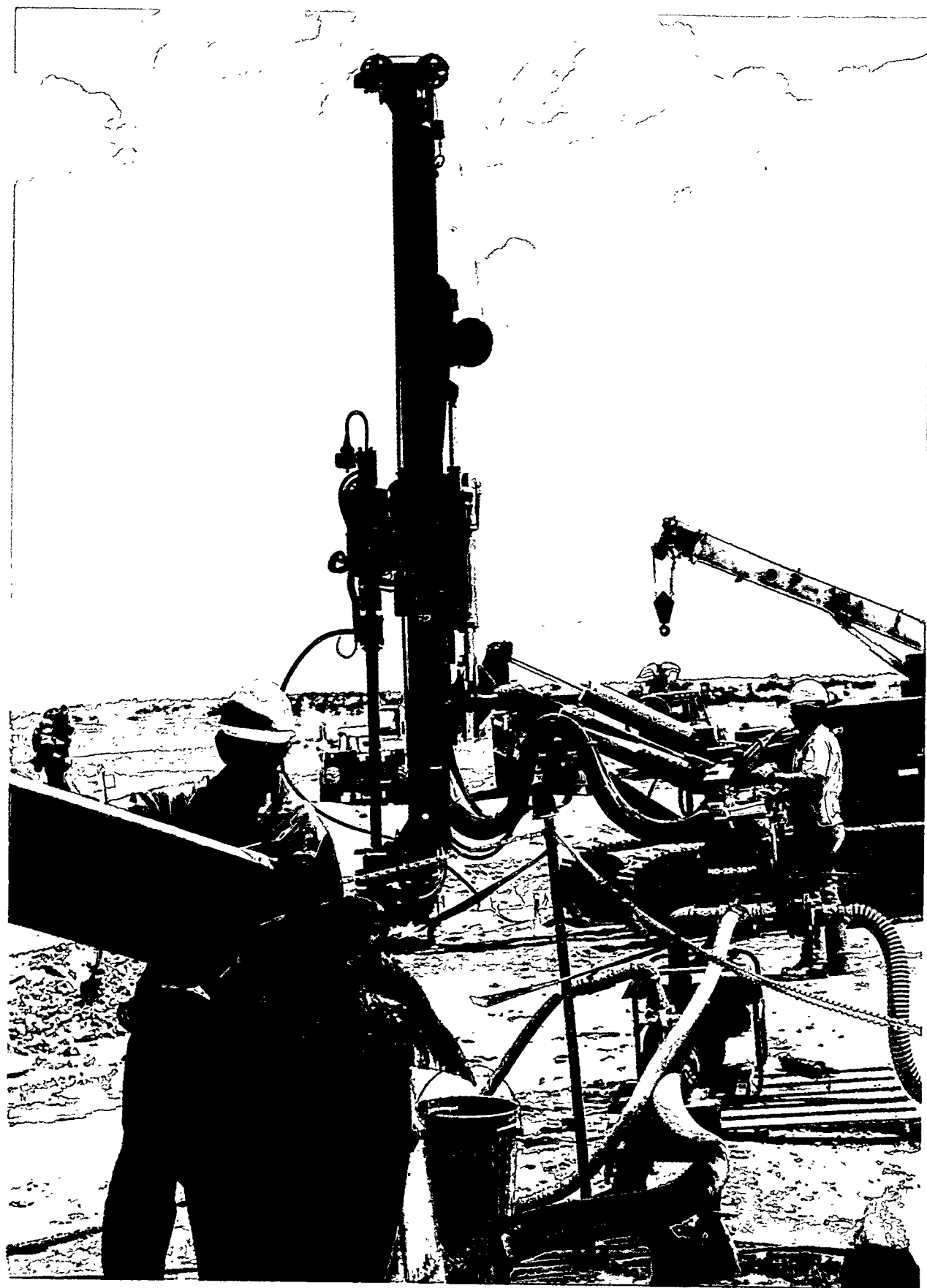


Figure 32. Grouting operation for TECT Pit A (Photo 96-512-1-2).



Figure 33 shows about 5 gal of soil/grout mixture that emanated out of a just-grouted hole. After grouting hole 9 (see Figure 31), a 0.5-in. diameter, 9.5-ft-long copper rod with a sealed end was placed into the just-grouted hole as a well for recording the curing temperature of the pit. A later section will discuss the results of the curing temperature of both the TECT pit and the paraffin pit for which this same technique for recording the curing temperature was employed.

#### 4.1.3 Paraffin Pit (Pit B)

Pit B was successfully grouted with the WAXFIX (paraffin-based grout) in 1 day of grouting, including two field trial holes using the thrust block. The grouting was performed with virtually no major problems, and 15 holes were grouted in 1 hour and 30 minutes. However, considerable modifications of the feed system were made prior to grouting. These modifications were made to counteract the solidification of the paraffin caused by cooling. These modifications involved using heater tape and insulation on all high-pressure hoses, Jet 5 pump, and low-pressure feed system. Figure 34 shows the heater tape being applied to the high-pressure supply lines. Figure 35 shows the insulation being applied over the heater tape on the high-pressure system. Figure 36 shows the system during the grouting operation. Figure 37 shows details of the entire supply system, including the relative position of the flow totalizer used to track the amount of injected grout material.

The paraffin was delivered to the Cold Test Pit in a large tanker truck in a molten form at 140°F. The tanker truck contained 1,400 gal of molten paraffin and 1,400 gal of 180°F water for use as cleanup of the system and for keeping the paraffin hot during transport. In the transport from Pocatello, Idaho, to the Cold Test Pit (approximately 1.5 hours transit time), there was no drop in temperature of either the paraffin system nor the water system due to high volume and adequate insulation in the tanker truck. Figure 38 shows the tanker truck with the supply line connected to the paraffin feed. A gravity feed system was employed, and neither the paraffin nor the cleanout hot water required pumping for feed to the high-pressure Jet 5 pump.

Two field trial holes were jet grouted using the thrust-block system. The first field trial hole used parameters of 6-second dwell time, 5-cm step, and 2 revolutions per step, and the second field trial hole used a 4-second dwell time. On the south side of the thrust block, the low-viscosity paraffin material ran out a crack in the block system that had not been covered with dirt as shown in Figure 39. No paraffin escaped out either the top hole or the three sides that had been covered with soil, emphasizing the need to properly seal the thrust block prior to grouting. After removing the thrust block, it was discovered that the first field trial column had not solidified, which was attributed to the presence of about 32 gal of water in the high-pressure lines prior to grouting, which mixed with the paraffin in the hole and resulted in a soft "putty-like" column of soil, paraffin, and water. The second field trial hole employed pure paraffin grout and resulted in a cured column with a diameter of 24 in. The first field trial hole resulted in an injection of 131 gal of paraffin/water with the 6-second dwell time, and the second field trial hole took 121 gal with a 4-second dwell time. It was desired to grout 80–100 gal per hole, so it was decided, based on the field trials, to grout the first hole in Pit B at a 2-second dwell time.

The actual grouting of the pit proved to be an easy operation with observed grout returns similar to those observed for the acrylic polymer in FY-95.<sup>2</sup> A total of 15 holes were grouted in 1.5 hours, and details of the grouting operation are given in Table 5. Figure 31 shows the hole





**Figure 33.** Grout returns during grouting of TECT pit (trickle flow of grout shown emanating from nozzles) (Photo 96-512-1-10).





Figure 34. Heater tape applied to high-pressure hose (Photo 96-512-2-8).





**Figure 35.** Insulation applied over heater tape on high-pressure hose (Photo 96-512-2-10).



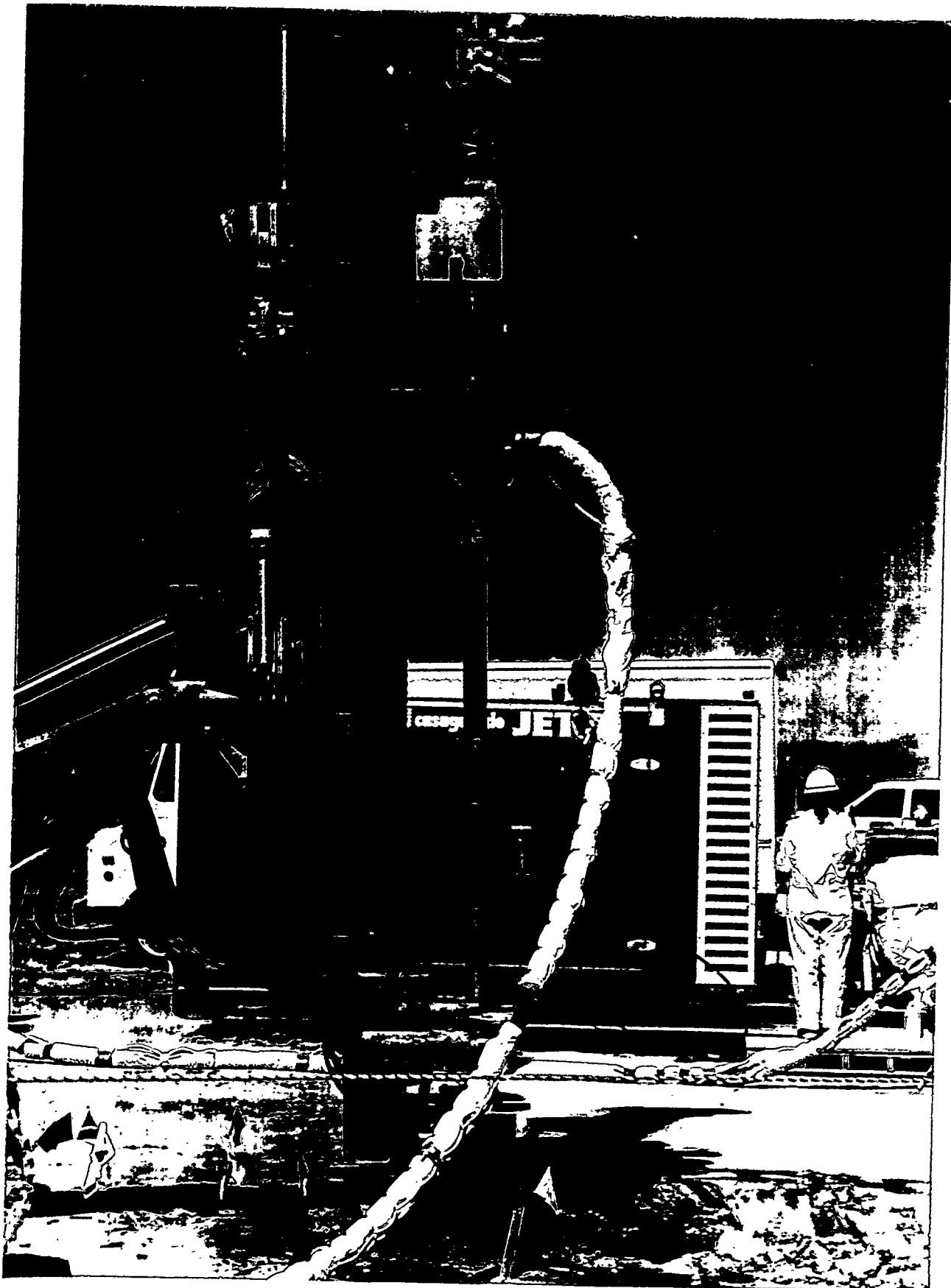


**Figure 36.** System in operation during injection of paraffin grout (Photo 96-517-3-4).



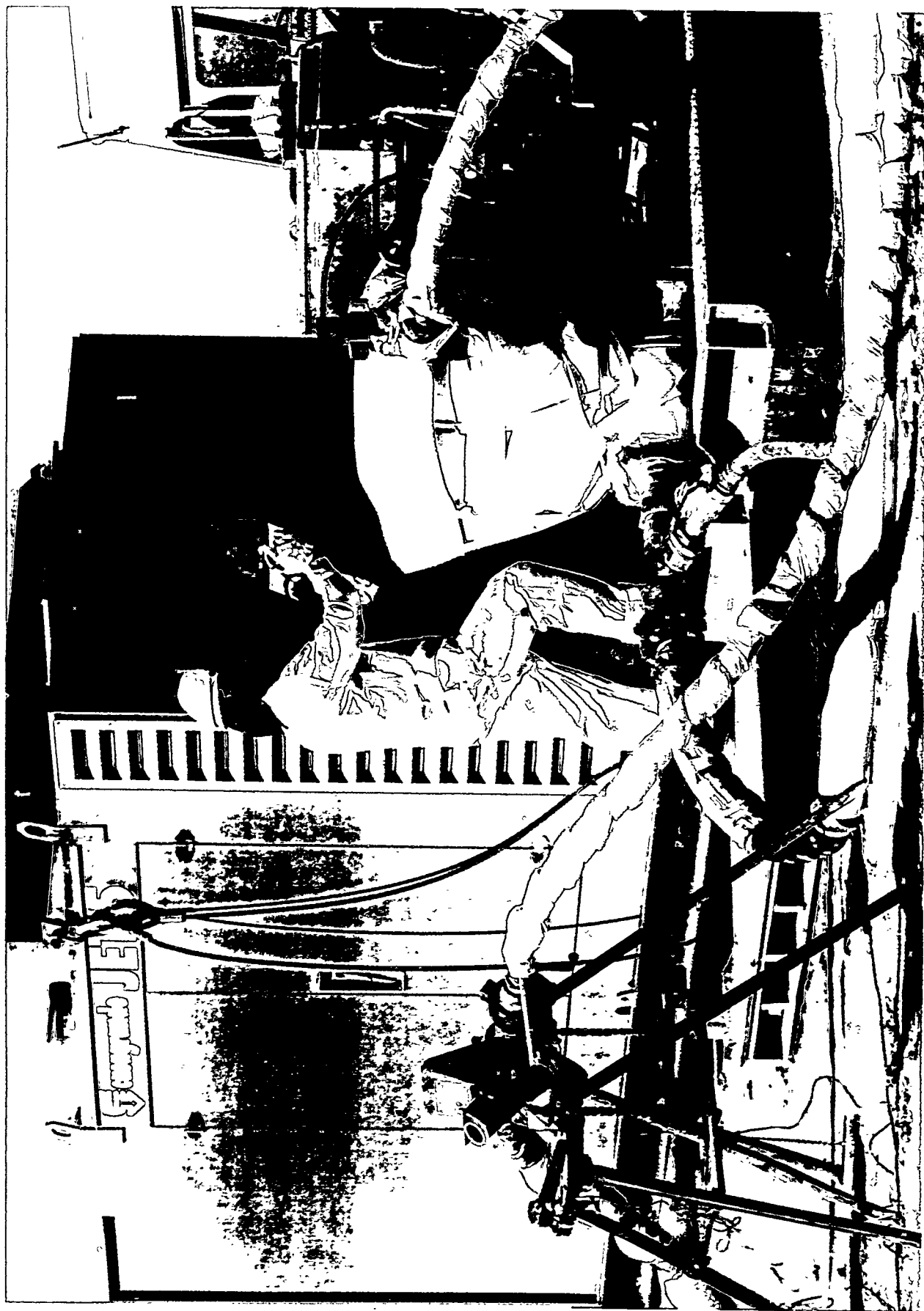


Figure 37. Detail of supply lines during grouting of paraffin (Photo 96-517-2-13).



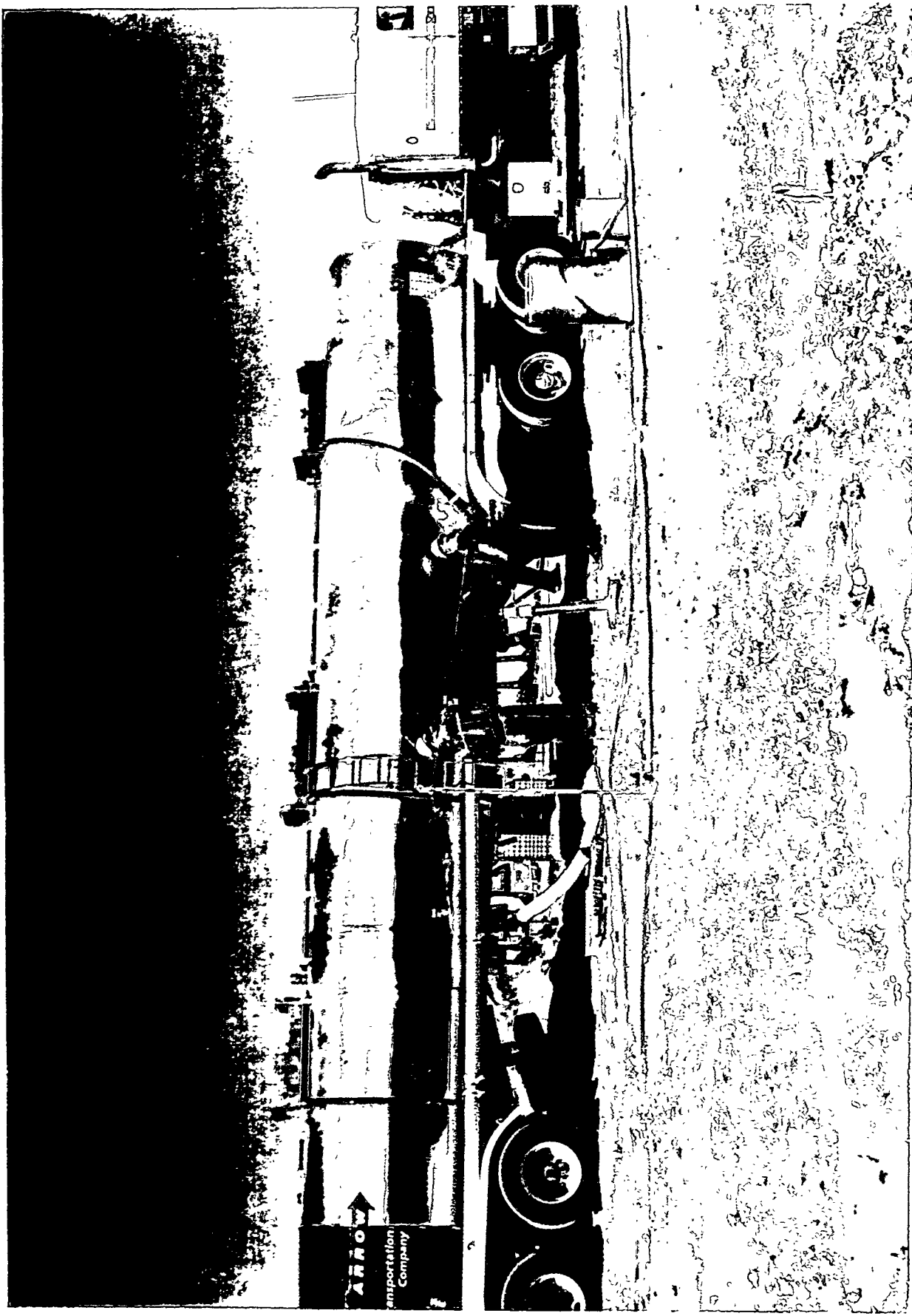


Figure 38. Tanker truck containing hot paraffin (140°F) and hot water for cleanout (180°F) (Photo 96-517-2-11).





**Figure 39.** Paraffin grout emanating from an uncovered crack in the thrust block during the paraffin field trials (Photo 96-517-2-18).



**Table 5. Operational parameters for paraffin pit (Pit B).**

2.3-mm Jets		Grout Take (gal)	Comments
Hole	Date		
1	7/30	62	2 s/step 2 rev/step 5 cm/step No grout returns
2	7/30	89	3 s/step 2 rev/step 5 cm/step No grout return
3	7/30	77	Cross communication with #2
4	7/30	79	Large flow up hole #1, difficult to estimate flow
5	7/30	No data (80 assumed)	No data, TC placed in hole
6	7/30	80	Significant geyser out hole #1
7	7/30	88	Copious returns
8 <sup>a,b</sup>	7/30	87	Cross communication in 1, 2
9 <sup>a</sup>	7/30	89	Cross communication with 5, 6, 7, 8
10 <sup>a</sup>	7/30	86	Copious flow out 5, 6, 7
11 <sup>a</sup>	7/30	83	Attempted to plug hole #2 with dirt, did not work, copious returns
12	7/30	95	Copious returns out all holes
13	7/30	91	Copious returns out all holes
14	7/30	89	Geyser out hole #6
15	7/30	52	Truck empty at 20 gal; grouted an additional 32 gal (line volume) and stopped
Summary			
Truck Temp:		Paraffin Water	140°F 180°F
Total holes:			15
Total grout take:			1,227 gal
Total estimated returns:			392 gal (see Figure 40)
Net amount left in pit:			835 gal
Average grout/hole:			81 gal
Total elapsed time:			99 minutes
Time/hole:			6.6 minutes

a. Core hole 9 was grouted 20 minutes after core hole 8 in an attempt to reduce cross communication.

b. Order of grouting was core hole 11, 10, 8, and 9.

layout. The total grout take was 1,227 gal, and the average grout per hole was 81 gal. The first hole was grouted with a 2-second dwell time, and only 62 gal of grout went into the hole. It was decided to increase the dwell time to 3 seconds for subsequent holes. After grouting the second hole at a 3-second dwell time and achieving 89 gal total flow, it was decided to stay with that dwell time. There were considerable grout returns (approximately 26 gal per hole) of what appeared to be neat liquid paraffin grout for every hole, starting with hole 3. Starting with hole 3, the grout returns were qualitatively described as "copious" in the logbook, and at times, as the various holes in the pit were grouted, pure paraffin emanated from both adjacent and nonadjacent grout holes.

Figure 40 shows the layout of the spoils collection pit. Even though the grout returns were copious, management of these spoils or returns was easy. The returns were managed by digging shallow canals from the top surface of the pit to the spoils collection pit. Figure 41 shows the grouting operation in progress with flow emanating from both adjacent and nonadjacent holes. An attempt was made to allow a 20-minute set between the grouting of holes 8 and 9 in the hope that the copious returns would diminish because of thermal mixing and setting of the soil/paraffin mixture. However, the same copious returns resulted. Therefore, the remainder of the pit was grouted in sequence without delay.

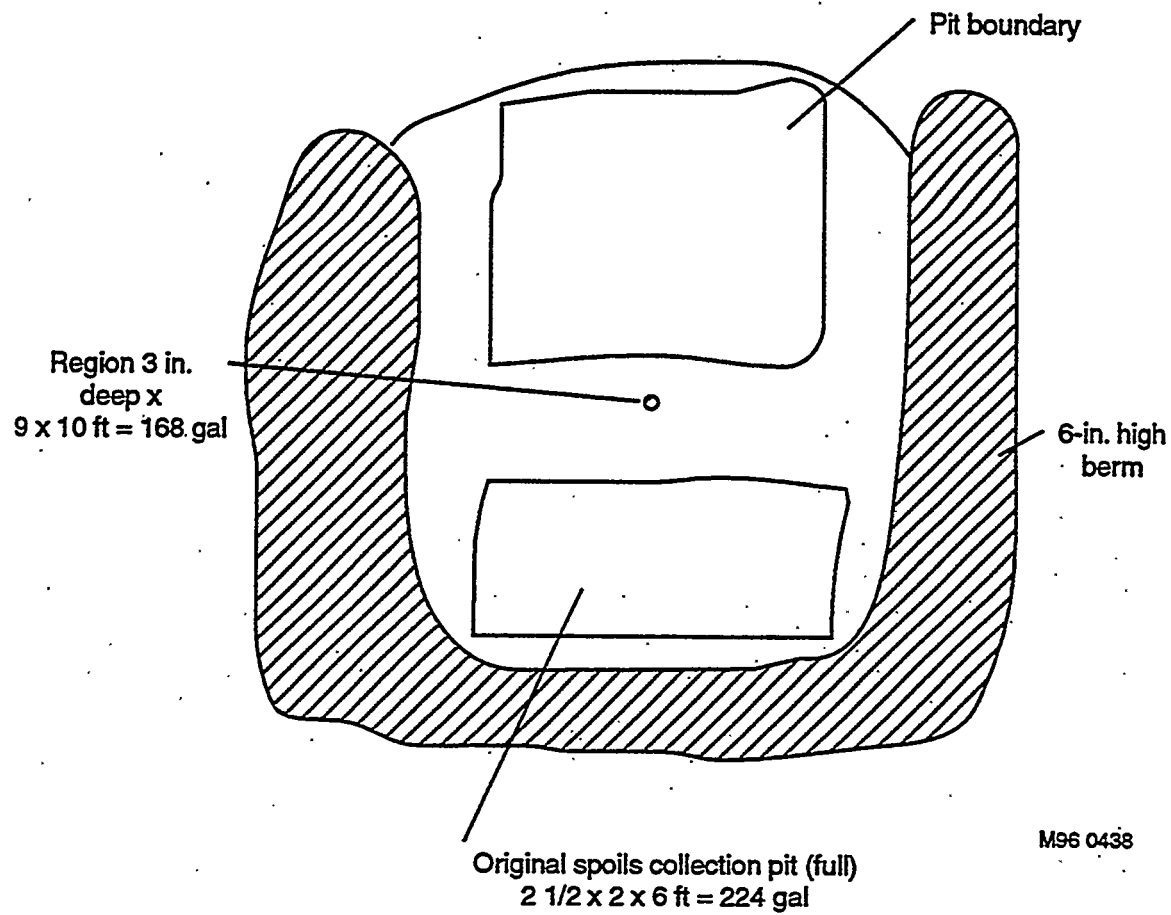
The 0.5-in. copper tube was placed in hole 5 and, following the completion of grouting, the thermocouple was moved from the TECT pit to the hole 5 paraffin pit to track the cooling of the pit. Figure 40 shows that a total estimated amount of grout returns was 392 gal, which means a total of 835 gal was injected into the pit. This represents (on a total pitwide volume) 52% of the volume of the pit, which is sufficient grout to fill the estimated void volume of 50%. It appears that in the TECT pit with a 6-second dwell time, more of the soil surrounding the pit was filled with grout than the paraffin pit with a nominal 3-second dwell time. Another difference about this pit from the TECT pit is that a standing head of still molten grout of about 3 in. was left over the top surface of the pit due to overflow of the spoils collection pit. This volume was available to fill void spaces by gravity feed down the grout holes for up to 8 hours following grouting because the top surface remained liquid. In fact, the interior of the actual spoils collection pit (see Figure 40) remained liquid for 3 days following grouting.

Following the grouting phase, cleanup of the apparatus was easier than anticipated. It was anticipated that solidification of paraffin due to heat loss would build up in the Jet 5 pump and associated hoses. However, by switching the supply line in the tanker truck from the paraffin feed to the hot (180°F) water supply, 300 gal of water completely cleaned the system. As a precaution, a portable hot water cleaning system was used to clean the flow meter and pump assembly.

#### 4.1.4 Hematite Pit (Pit C)

Grouting of the INEL-developed hematite grout was attempted but was found not to be jet groutable using the CASA GRANDE Jet 5 pump and the Schwing pump and associated delivery systems described previously. No positions in the pit were grouted. However, an attempt to grout two field trial holes is described below.

The hematite grout was a two-component material, and the system was arranged such that the Jet 5 pump was used for the A side and the Schwing pump for the B side (identical to that used for the acrylic polymer grouting described in reference 2). The A side grout material was a mixture of ferrous sulfate fertilizer and water mixed as follows: A Ready Mix truck was preheated



Total spoils returns for paraffin pit =  $224 + 168 = 392 \text{ gal}$

**Figure 40.** Spoils collection pit for paraffin (Graphic M96 0438).





Figure 41. Grout returns during grouting of the paraffin pit (Photo 96-517-3-32).



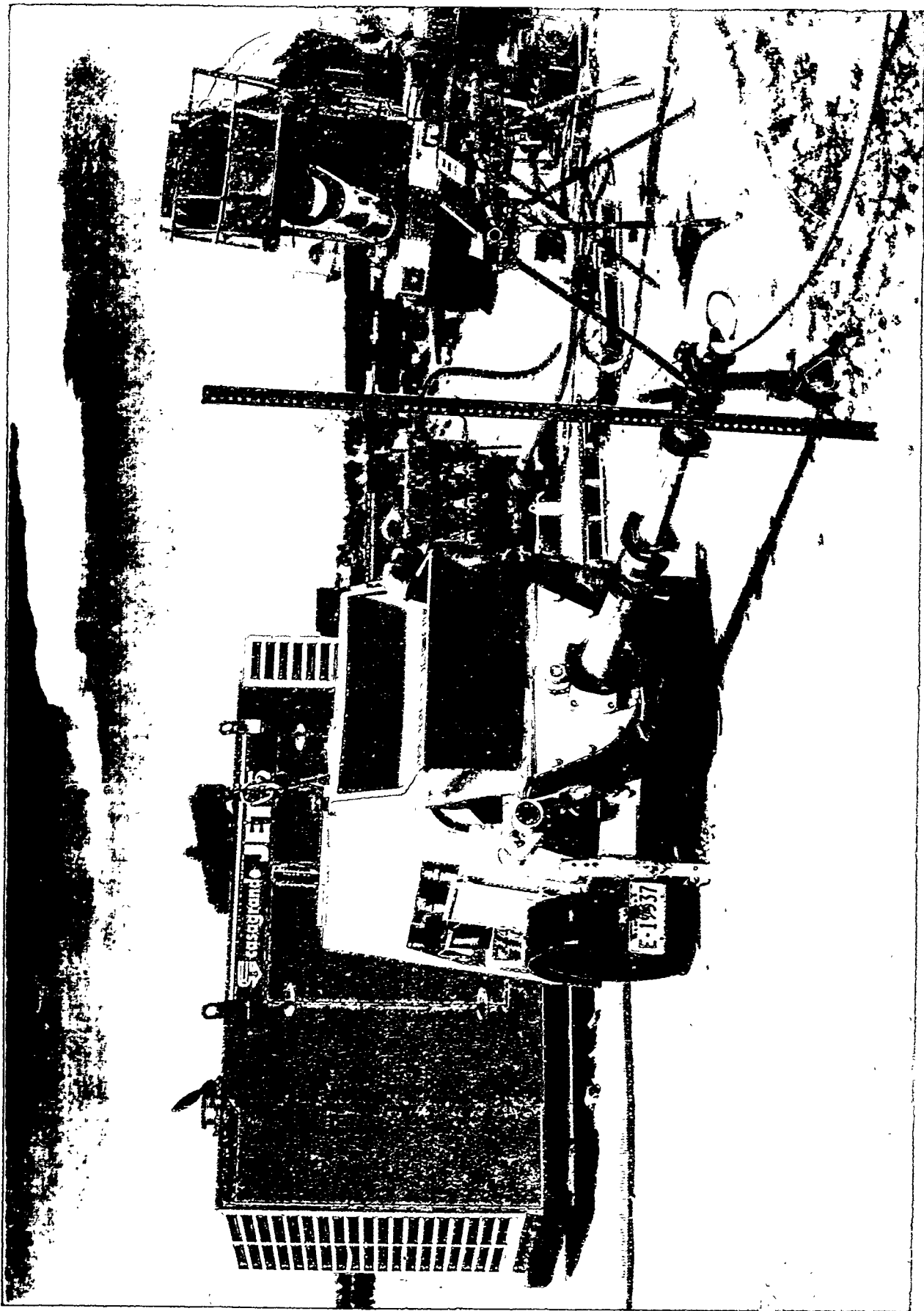
with 180°F water, and the water was dumped. The A-side truck was then filled with 558 gal of 180°F water and 2,000 lb of iron sulfate (bulk bag) and 4,210 lb of Ironsil (iron sulfate fertilizers) to make a total of 930 gal of solution. In addition, because of a pH of between 1 and 2, 4 lbm of plain food grade gelatin was added to inhibit corrosion. In the second truck for the B side mixture of slaked lime (calcium hydroxide), 408 gal of water was mixed with 1,700 lbm of hydrated lime. This formed an estimated 473 gal of lime slurry. The plan was to mix 2 parts iron sulfate solution to 1 part lime solution by volume. All mixing of the materials occurred in Idaho Falls at a Ready Mix plant, and the A and B materials were brought to the site in separate Ready Mix trucks.

Figure 42 shows the relative position of the two pumps with associated flow meters and lines, and Figure 43 and Figure 44 show the Ready Mix trucks feeding the ferrous sulfate and lime slurries respectively. The CASA GRANDE drill system was positioned for the first field trial, and multiple attempts at grouting occurred. The system was oriented for two-phase injection with the same annular nozzle used for the acrylic polymer cited in reference 2. This nozzle has a center flow of the A part at 6,000 psi, and around this flow path the B part is injected at 1,000 psi. Mixing occurs in the ground as the two parts violently mix with the soil-and-waste material. Figure 45 shows the drill bit and nozzle arrangement.

Trouble with establishing a flow through the B (lime slurry) was immediate. Flow would start at a lower than desired rate and decrease to zero. Following cleanout of the nozzle system, the same plugging of the B side of the nozzle would occur. A side flow (ferrous sulfate slurry) worked as expected throughout the test. Figure 46 shows the flow of the ferrous sulfate side of the nozzle alone without the lime slurry. Figure 47 shows the low B side lime slurry flow prior to plugging, and Figure 48 shows a completely plugged flow of the B side. Several attempts were made to reduce this "filter caking" problem, including diluting the original 408 gal of lime slurry mix in the Ready Mix truck first with 100 gal of water and finally adding 80 gal of calcium lignosulfonate.

Basically, all of these attempts failed to allow a reasonable flow of the B side slurry, and the test was stopped. The problem was that the slaked lime slurry mixture too readily plated out or filter caked on surfaces. A good example of this is the solid residue on the coarse filter screen on the B pump intake shown in Figure 49. It was concluded that the slurry mix required adjustment and that a new nozzle design for two-phase injection was needed. It is not clear at this time whether the lime slurry mix used for this test would filter cake any injection system and nozzle design. It is speculated that there was a potential for injecting the B part lime slurry through the A side of the nozzle (or simply use the CASA GRANDE system in the single-phase orientation) into the waste, followed by total cleanout and immediate injection of the A side or ferrous sulfate solution into the just-grouted pit. This technique would double the amount of drilling and grouting time, and there is no guarantee that the nozzle would not plug in situ because of premature curing of the mixture. It was deemed impossible to mix the A and B component prior to grouting because of the lack of control of the cure time resulting in a "frozen" system. Other formulation of A and B or a combination with slower cure times may be possible.





**Figure 42.** Schwing, Jet 5 pump, and two Ready Mix trucks with slaked lime slurry and ferrous sulfate slurry during hematite pit injection (Photo 96-529-1-14).



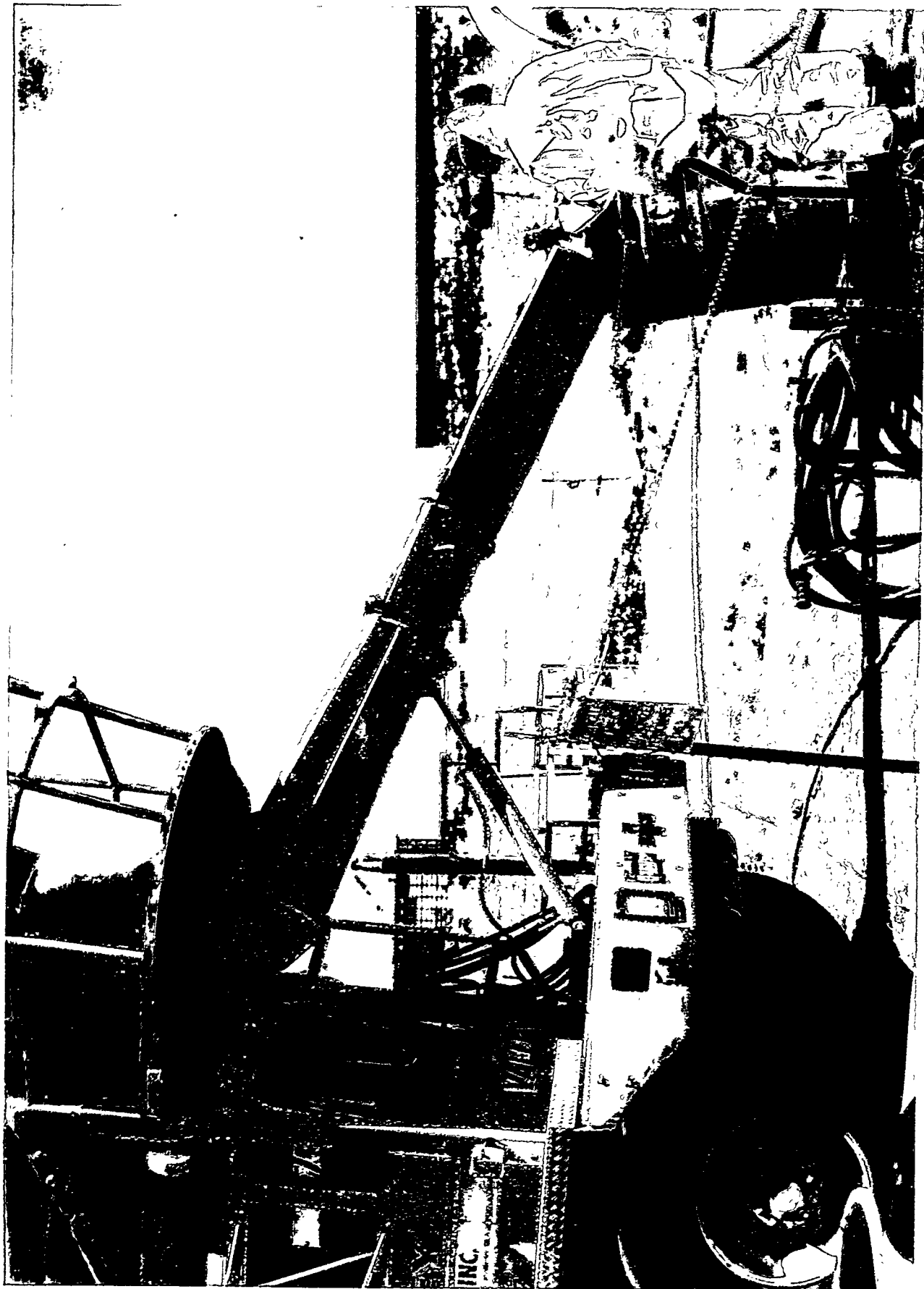
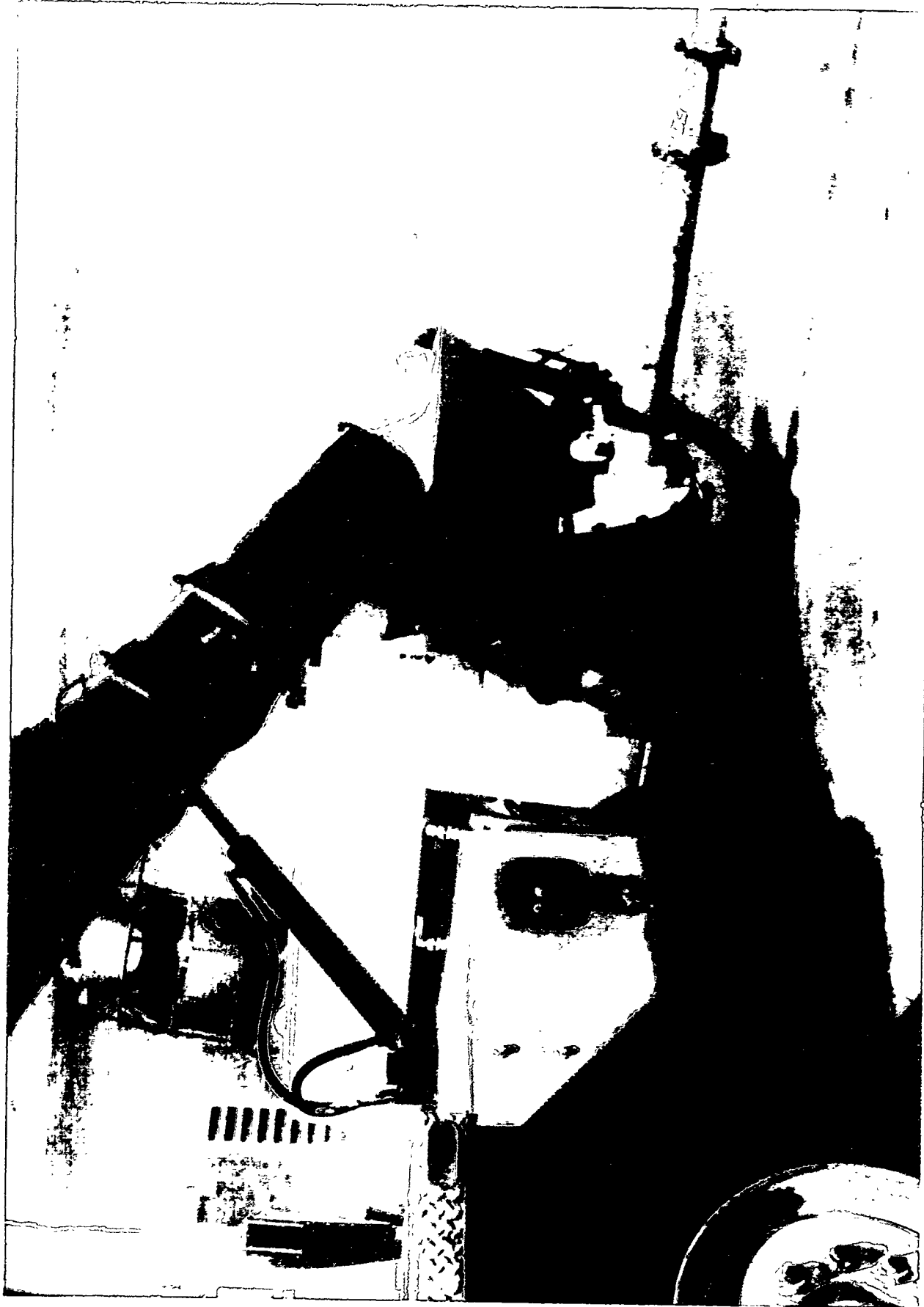


Figure 43. Feed from Ready Mix truck on the ferrous sulfate side (Photo 96-529-1-25).





**Figure 44.** Feed from Ready Mix truck on the ferrous sulfate side (Photo 96-529-1-27).



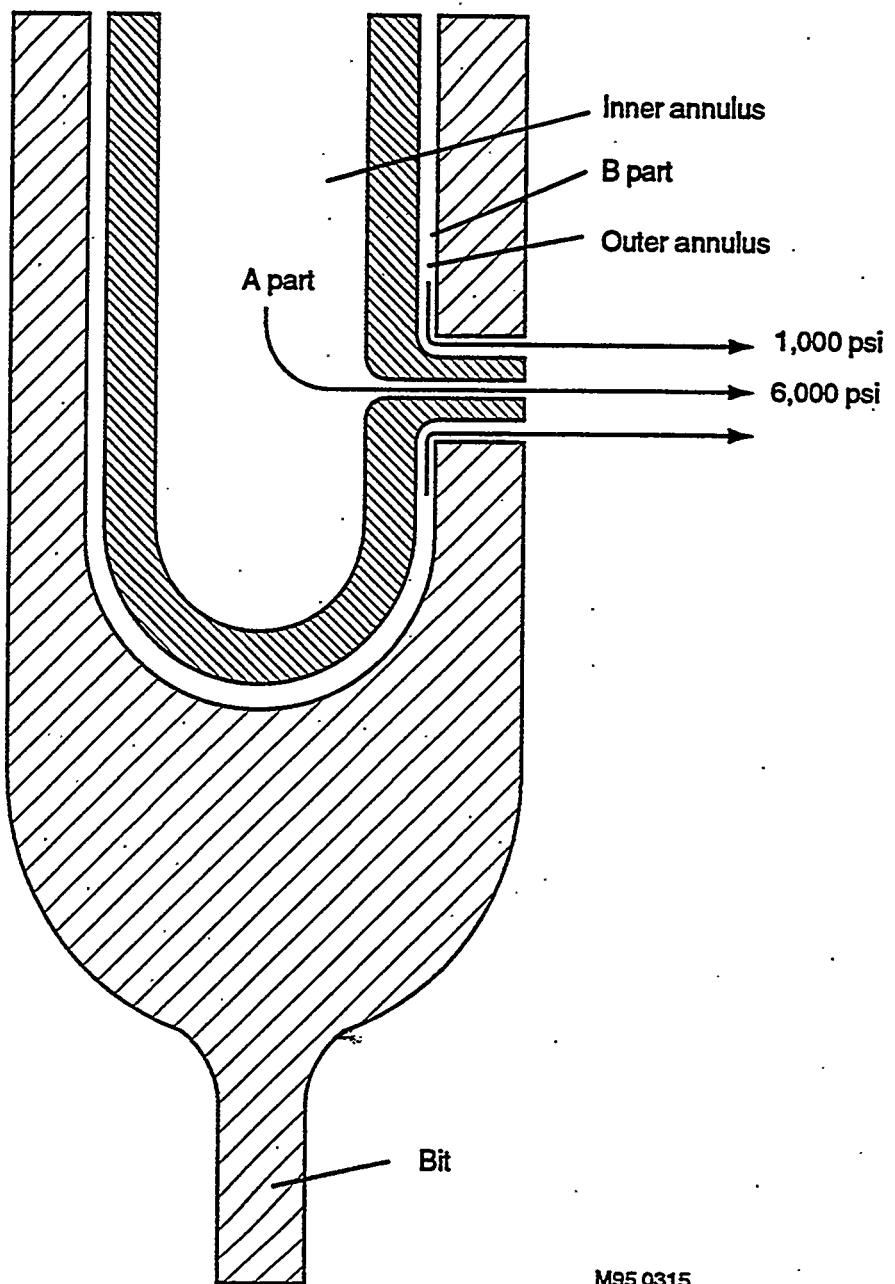


**Figure 45.** Dual concentric annulus drill stem (Graphic M95 0315).



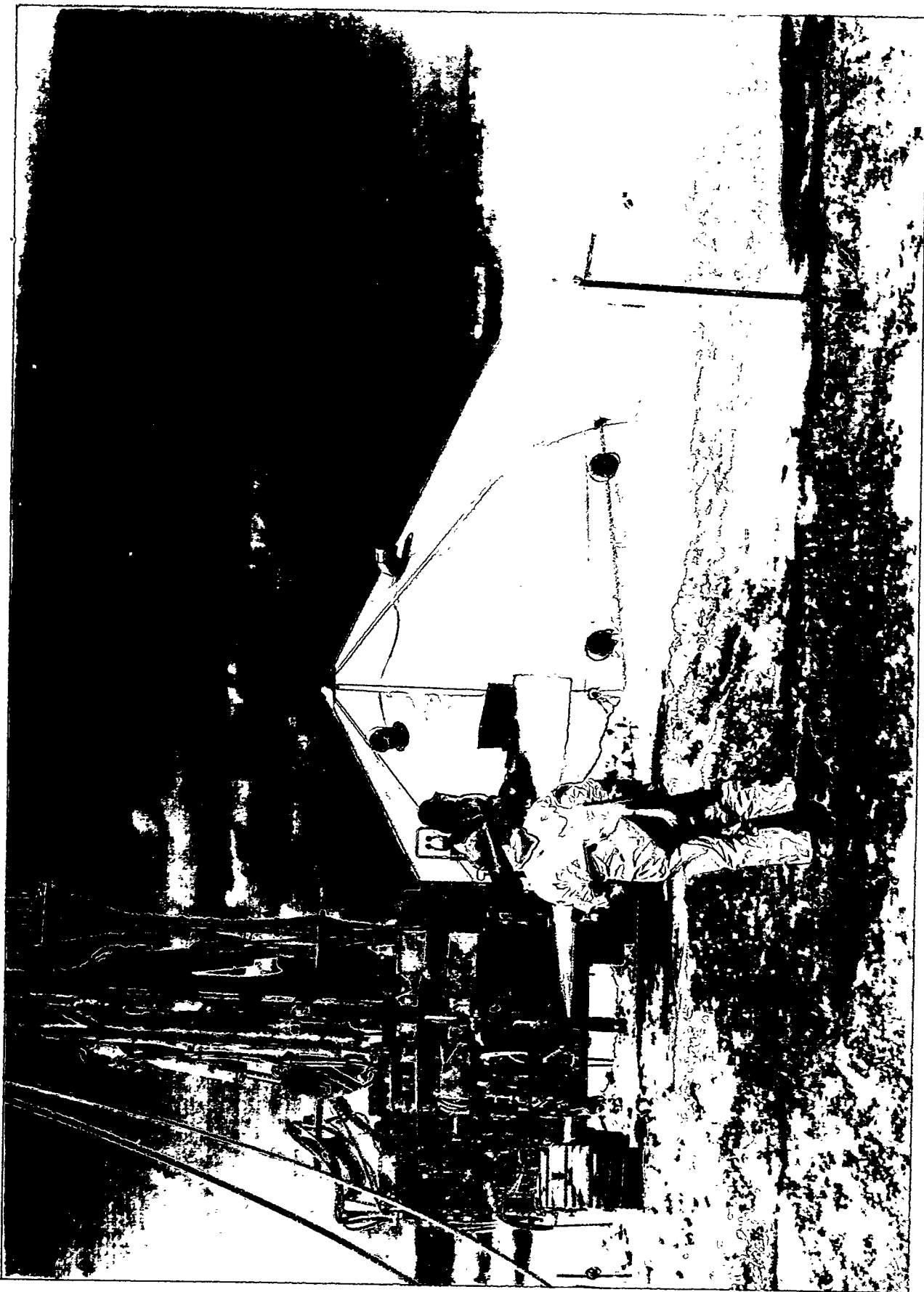


**Figure 46.** Ferrous sulfate flow above ground (in position to attempt field trial) (Photo 96-529-2-5).



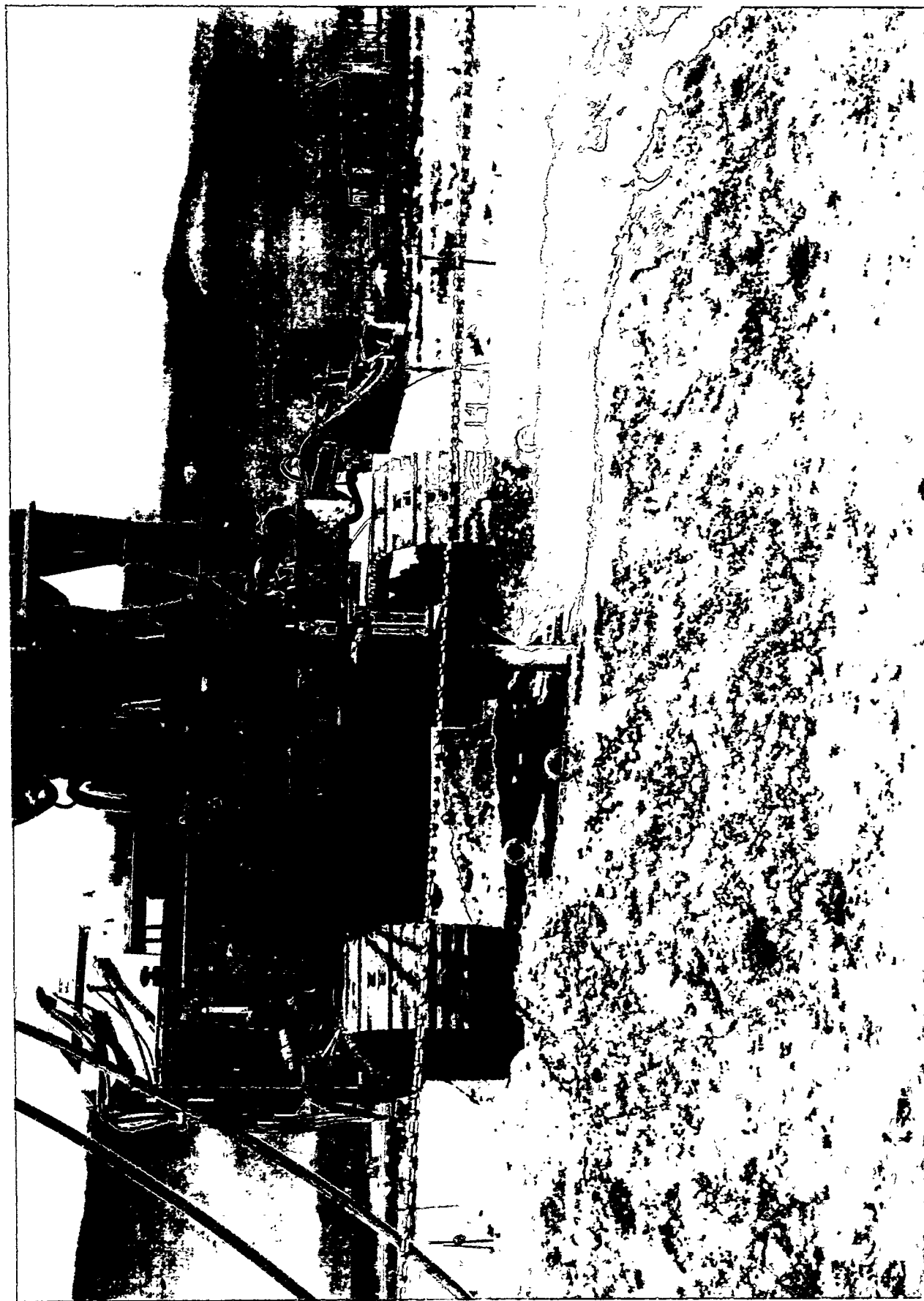


**Figure 47.** Line slurry flow just prior to plugging (Photo 96-529-2-3).



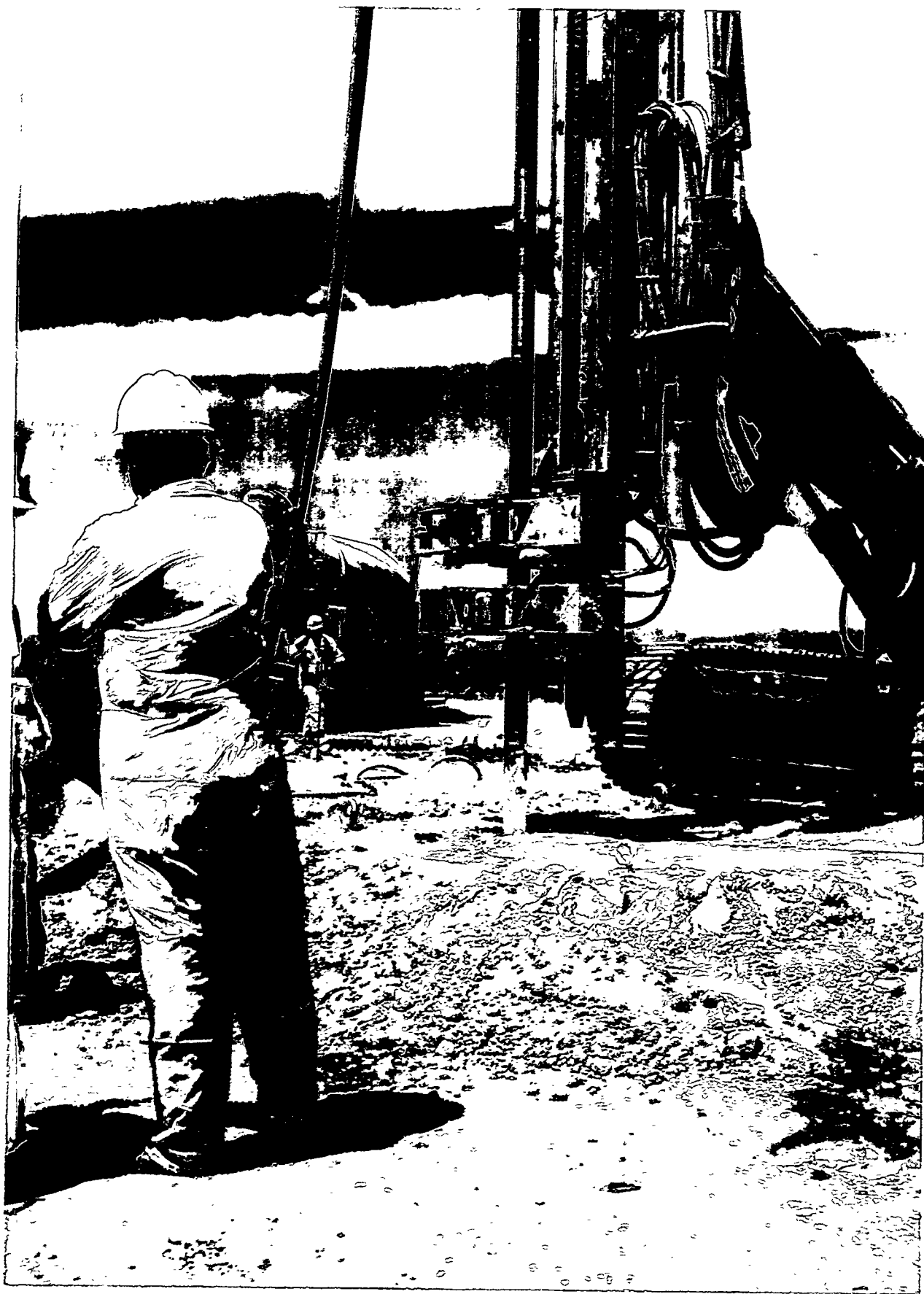


**Figure 48.** Line slurry flow completely plugged (Photo 96-529-2-1).





Figure 49. Filter caking of line slurry on B pump intake screen (Photo 96-5292-6).



#### 4.1.5 Epoxy Pit (Pit D)

An unsuccessful attempt was made to grout the two-component water-based epoxy into Pit D. The epoxy consisted of an A part and B part. The test setup was identical to that used during injection of the acrylic polymer (FY-95, reference 2), including the identical supply tanks. However, the feed material was pumped to the high-pressure pump rather than gravity feed. A total of 1,400 gal of material was to be used (440 gal of B part, 960 gal of A part [220 gal of the A part diluted with 740 gal of sodium lignosulfonate]). The sodium lignosulfonate was premixed in intermediate drums, with the A part material prior to transfer to the supply tank. The injection ratio was to be 3.36:1 A part to B part by volume.

Figure 50 shows the experimental setup. Basically, the B part material proved too viscous to pump through the B side of the system, and no injection could occur. An attempt was made to reduce the viscosity of the B part fluid by diluting the supply tank for the B part side, which contained 275 gal of B part with an additional 137 gal of water. This action actually exacerbated the problem, as the fluid viscosity seemed to increase to the point of solidification throughout the system, and the grouting vendor initiated system cleanout immediately upon noticing the rapid increase in viscosity.

The A part material proved pumpable with the 6,000 psi pump though the nozzle assembly shown in Figure 45. It is not clear whether the B part material could have been pumped through the A side system at 6,000 psi. Reformulation of the material to be more easily handled in the field is needed for this product. The idea of injecting the material via a 6,000 psi pump as a single component fluid might be possible if the cure time were correctly controlled.

Two technical difficulties have to be overcome for this to work. First, the material cure time needs to be 6–10 hours once mixed, with certainty of that interval. Second, the mixed material viscosity must be reduced enough to be pumpable by the 6,000 psi CASA GRANDE pump. There is other speculation that simply using a higher pressure B side pump may have solved the pumpability problem. The relatively high cost of the epoxy material and the field difficulties that were encountered in this experiment will have to be weighed against the high-quality soil-and-waste matrix that results from epoxy injection.

Laboratory samples involving a 67% soil/33% epoxy mixture result in a solid matrix with a flex like a "hard rubber" eraser. This relatively soft forgiving property is desirable when considering future cracking of the matrix and potential leaching of contaminants as well as retrievability of a buried waste matrix with improved confinement. If this property is mandatory, then the epoxy material should be considered for further study.

#### 4.1.6 Type-H Cement Pit (Pit D)

The Type-H cement pit was successfully jet grouted with essentially no grout returns. This was accomplished by adjusting the operational parameters to just fill the void space. The nominal desired grout injection per hole was 70 gal, which was achieved as shown in Table 6. A total grout injection of 1,436 gal (for 19 holes) (see Figure 51) results in an average grout take per hole of about 75 gal. The total estimated grout returns were only 21 gal, which left a net amount of grout in the pit of 1,415 gal or 87% of the total volume of the pit. This means that all the theoretical voids in the pit were filled, and the surrounding soils also received grout.

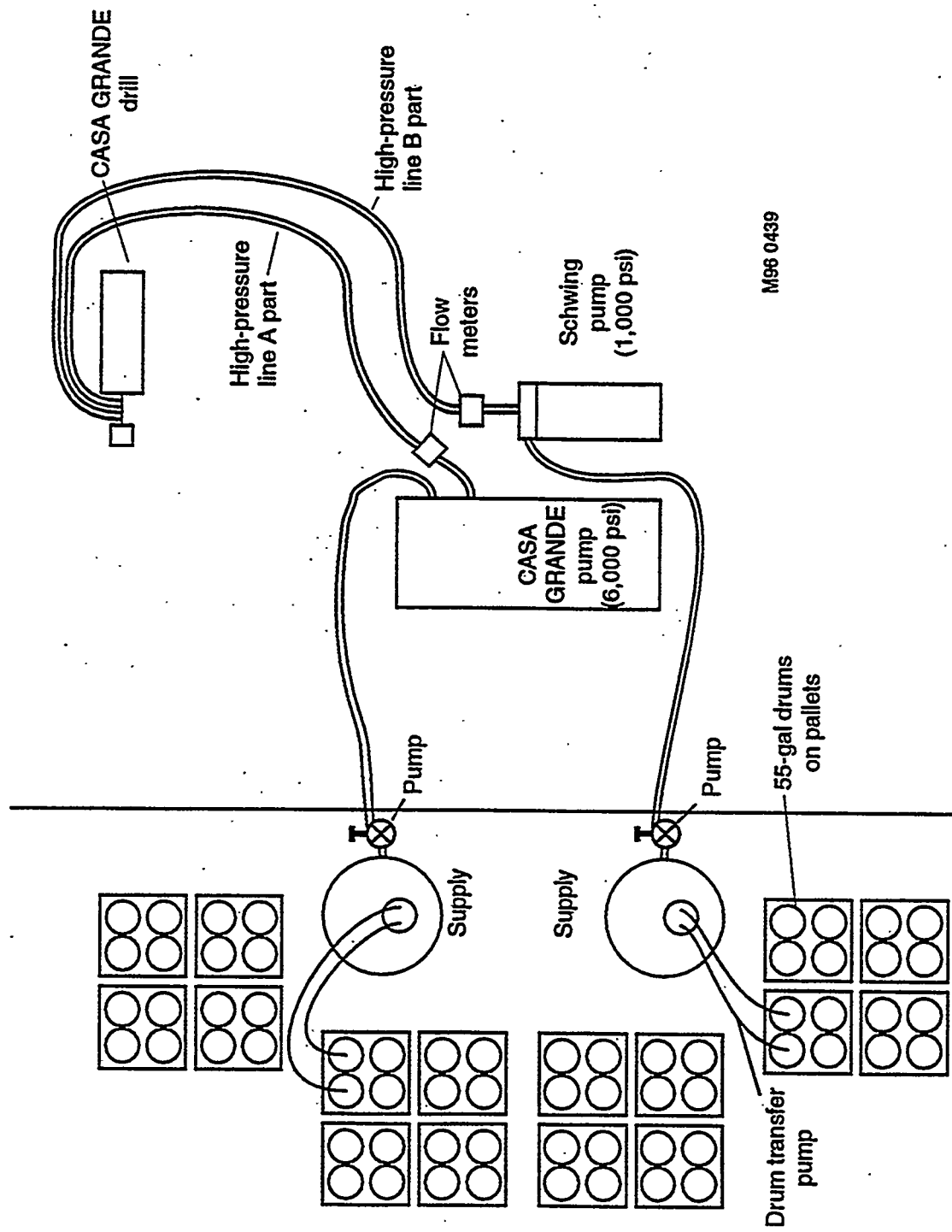


Figure 50. Schematic of two-component setup for epoxy jet grouting (Graphic M95 0447).

**Table 6. Operational parameters for Type-H cement ([1:1 by mass] 14 sacks/yd) pit (Pit D).**

2.3-mm Jets		Grout Take (gal)	Comments
Hole	Date		
1	8/8/96	104	6 s/step; 5 cm/step; 2 rev/step
2	8/8/96	90	Changed to 5 s/step
3	8/8/96	89	9 gal used during insertion
4	8/8/96	76	Changed to 4 s/step, no spoils
5	8/8/96	80	Changed to 4 s/step, no spoils
6	8/8/96	72	Changed to 4 s/step, no spoils
7	8/8/96	70	Changed to 4 s/step, no spoils
8	8/8/96	71	Changed to 4 s/step, no spoils
9	8/8/96	74	No spoils
10	8/8/96	92	Small amount of spoils (<1 gal)
11	8/8/96	75	Changed to 3.5 s/step small amount of spoils (<1 gal)
12	8/8/96	68	No spoils
13	8/8/96	69	1 gal returns
14	8/8/96	69	5 gal returns
15	8/8/96	66	5 gal returns
16	8/8/96	67	No spoils
17	8/8/96	65	10 gal returns
18	8/8/96	69	No spoils
19	8/8/96	70	No spoils
<b>Summary</b>			
Total holes:		19	
Total grout take:		1,436 gal	
Total estimated returns:		21 gal	
Net amount in pit:		1,415 gal	
Average grout/hole:		75.57 gal	
Start time:		12:27 p.m.	
Stop time:		2:26 p.m.	
Total elapsed time:		1 hr 59 min	
Average/hole		6.3 min	

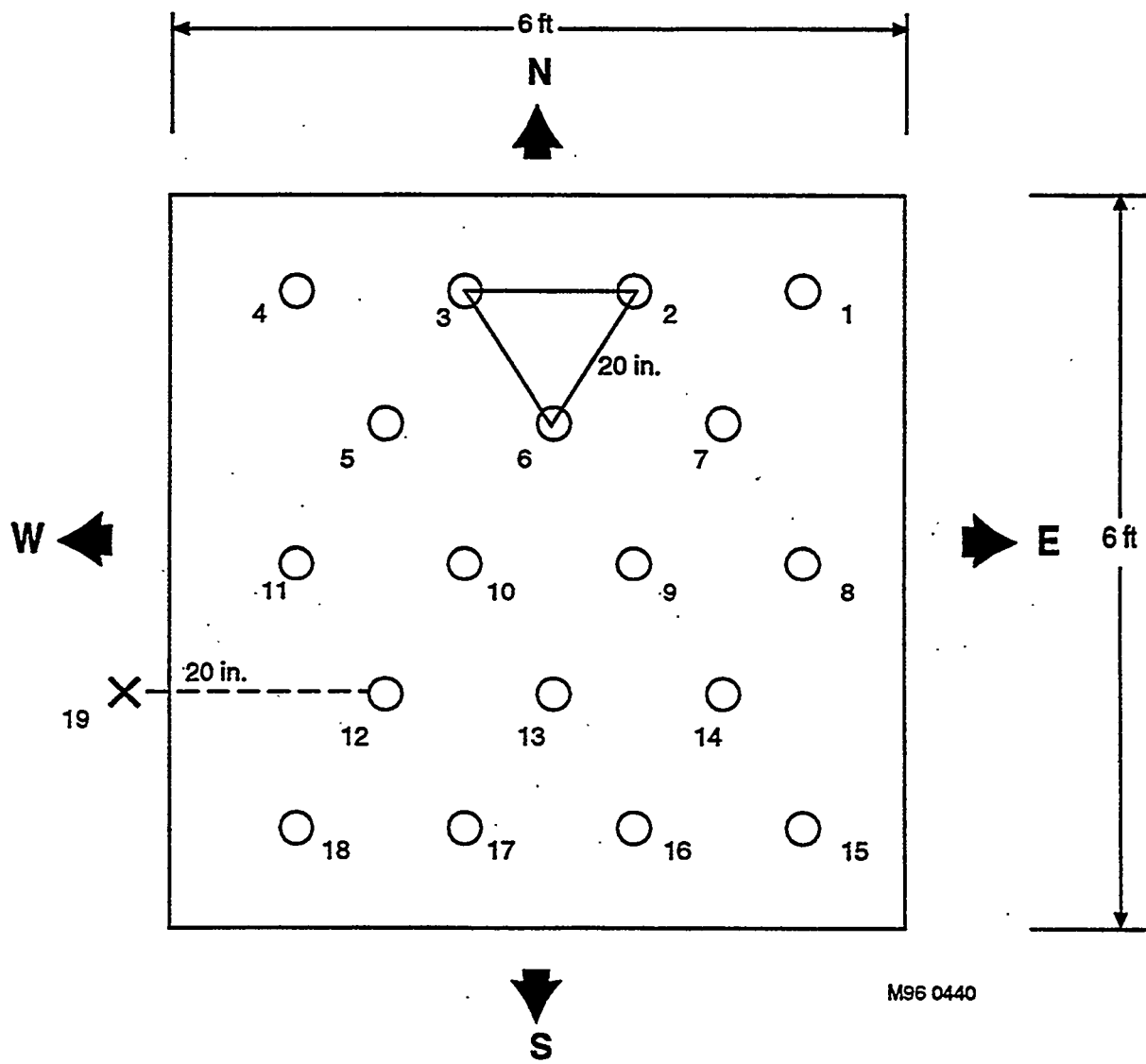


Figure 51. Grouting hole orientation for Type-H cement (Pit D) (Graphic M96 0440).

Since the grout columns extend beyond the original boundaries of the pit, comparison with the original volume is not valid. At a 7 x 7 x 6-ft grouted region, the 1,415 gal is only 64% of that volume. The grout was a Type-H cement with a 14-sack per cubic yard mix of material, meaning a 1:1 mixture of dry grout and water by mass. This mixture is considerably less viscous than that used for the grouted field-scale permeameter, which was mixed at 18 sacks per cubic yard of material or 1:1 by volume. The total elapsed time for grouting was 1 hour 59 minutes or 6.3 minutes per hole. This compares well with the TECT pit at 7.3 minutes per hole and the paraffin pit at 6.6 minutes per hole and contrasts with the Type-H cement injection into the field-scale permeameter at 19 minutes a hole. The more viscous fluid in the 18-sack mix led to more operational difficulties. Even though the TECT grout had a higher visual viscosity than the Type-H 18-sack mix, the amount of suspended particulate must have caused the tendency for more filter caking. The paraffin behaved as a low-viscosity pure fluid with no particulate, and there was no possibility of filter caking.

## 4.2 Temperature Time History of TECT and Paraffin Pits

A copper tube was placed in the middle of the grouted portion of both the TECT and the paraffin pit to track the temperature history during curing. Tracking the temperature time history gives insight into cure times. The TECT pit cured (solidified into a monolith) on the order of days and the paraffin pit on the order of a week. The copper tubes were 0.5-in. 9.5-ft-long tubes with an end cap sealed with duct tape on the downhole end. The tube was placed in a just-grouted hole (hole 9 for the TECT pit and hole 5 for the paraffin pit) during grouting of the respective pits. The thermocouple was a T type and was connected to a Campbell Scientific 21X (no. 9889) system. The system was programmed to take data every 10 minutes.

Figure 52 gives a temperature/time history of the TECT and paraffin pit and additionally the field trial hole for the hematite grout. Figure 52 shows that the TECT pit had a peak cure temperature of 55°C (131°F) and had decayed to 45°C (113°F) in 5 days. This is consistent with the Portland Type-1 cement data obtained in reference 1. The paraffin material does not cure. However, it solidifies as the soil/paraffin matrix cools. The peak recorded temperature was 64°C immediately upon insertion of the thermocouple, and cooling in the relative center of the pit at the bottom was 42°C (107°F) after 5 days and 36°C (97°F) after 14 days. This compares with the theoretical melting point of 49°C (120°F). There was minor evidence of curing in the hematite field trial hole, as the temperature (25°C [77°F]) elevated only a few degrees above the ambient temperature of 15°C (59°F).

## 4.3 Evaluation of Cores Taken in the Pits and Field-Scale Permeameter

Cores and video logs of the grouted field-scale permeameter, the TECT, paraffin, and Type-H cement pits were obtained to determine the extent of grout pervasiveness and structural integrity of the monoliths. The core holes were also the access holes for the hydraulic conductivity tests discussed in a later section. Generally, the core hole data showed relatively solid matrix for the TECT and paraffin pit. However, the grouted field-scale permeameter with Type-H cement (18-sack mix) and the Type-H pit (14-sack mix) showed less integrity. This general observation is in agreement with hydraulic conductivity data discussed in a later section.

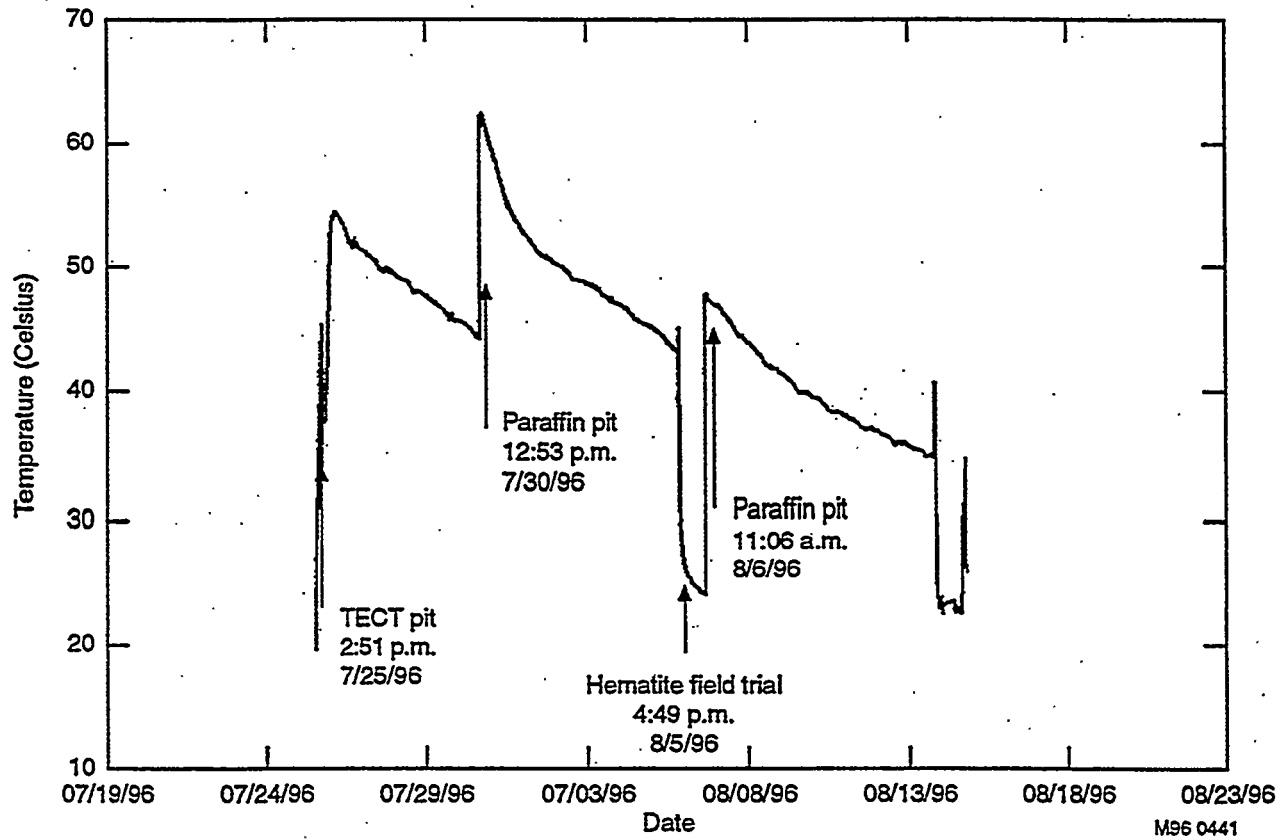


**Figure 52.** Temperature/time history of TECT/paraffin pit (Graphic M96 0441).

Four core holes were obtained in the grouted field-scale permeameter, three core holes in the TECT pit, and two core holes each in the paraffin and Type-H cement pit as shown in Figure 53. The cores were laid out for visual inspection and photographed with wooden dowel spacers for regions where there was no recovery. By examining the percentage of core recovery and the consistency of the recovered core, the solid nature of the pit can be determined without a destructive examination. Things that can cause a poor recovery are voids in the monolith, incompletely grouted material, or partly cured grout. The coring action using cooling water at the core bit tends to wash out loose debris like loose soil. The coring process involved water flow, and there is a potential in any core to have blocking in the bit such that the material is simply ground up and washed away. The problem is that there is no way to determine this potential phenomenon.

#### 4.3.1 Grouted Field-Scale Permeameter

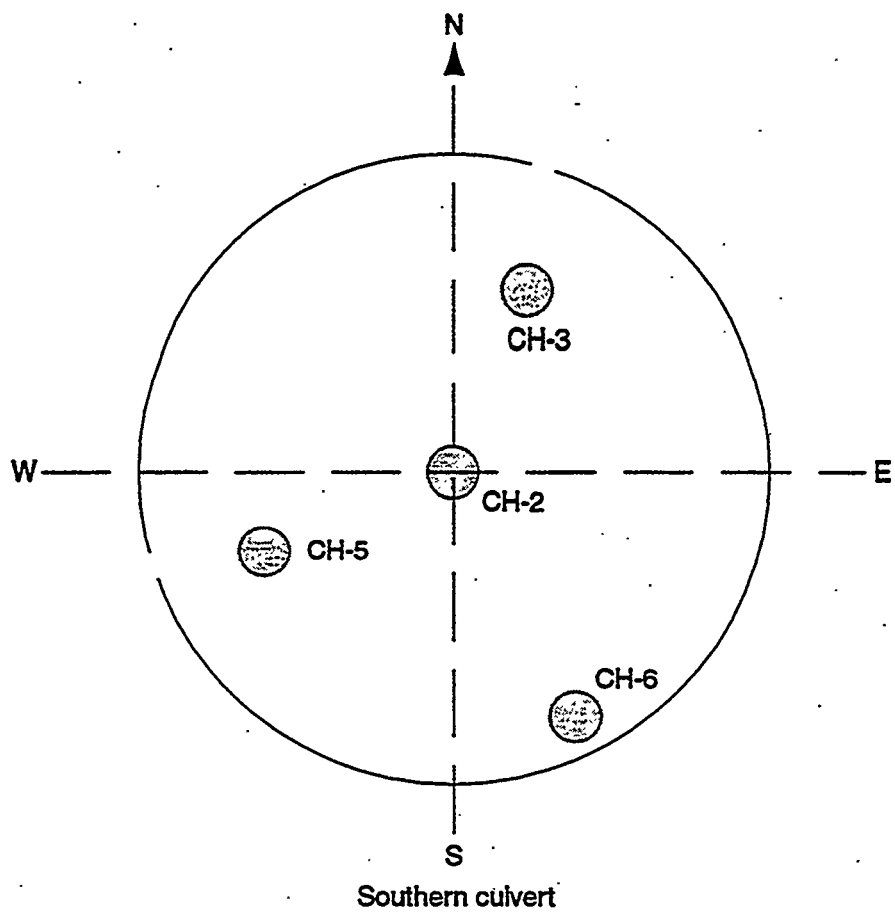
Recovery in the cores for the grouted field-scale permeameter was relatively poor, with two of the four cores with less than 50% recovery and the other two ranging from 75–78% recovery. Table 7 summarizes the core log for the grouted field-scale permeameter, and Figure 54 and Figure 55 show composite photographs of the entire cores.

**4.3.1.1 Core Hole-2.** Core hole 2 (Figure 54) was located in the exact center of the grouted field-scale permeameter and showed very poor recovery (about 48 in. out of 119 in. total core or only 40%). One possible explanation for this poor core recovery is that grout hole 14 (see Figure 28 and Table 3) had a refusal due to the presence of metal debris in a drum container, and only 60 gal of grout was grouted, whereas normally 116 gal were emplaced in an average hole.

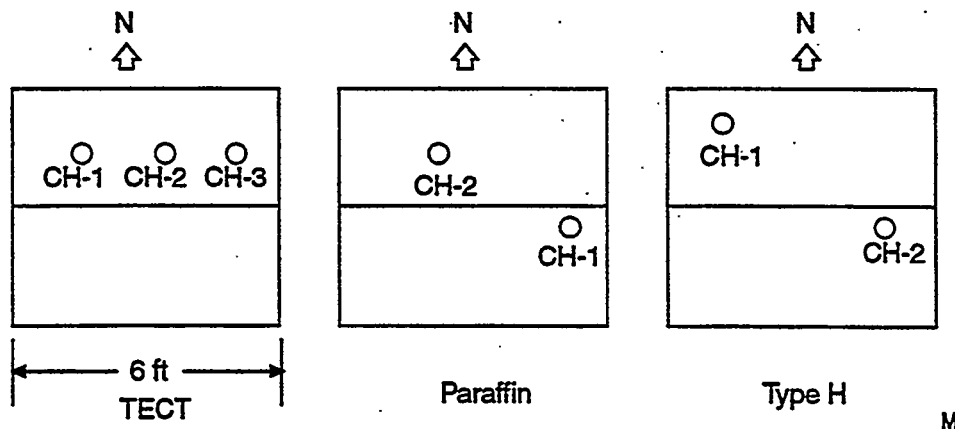
**4.3.1.2 Core Hole-3.** Core hole 3 was in the vicinity of a general area that experienced refusal of the drill stem, which stopped penetrating further during the grouting phase (see discussion on grouting holes 14, 15, 16, and Figure 28 and Table 3). Even though this core hole was in a region of drill refusal, there was fairly high recovery. Core hole 3 had a 77% recovery with 79 in. of recovery out of 101 in. of core as shown in Figure 54.

**4.3.1.3 Core Hole 5.** Core hole 5 showed only a 40% recovery or 43 in. out of a grouted region of 109 in. as shown in Figure 55. Core hole 5 was in the vicinity of a hole that experienced difficulty in grouting (grout hole 11—see grouting section and Figure 28 for location), and grouting was suspended for the day. The next day, grouting started in grout hole 11, and the entire hole may not have been grouted. When there is no recovery, it is assumed that the region was either poorly cured grout that was dissolved in the water flow used to reduce friction during coring or was ungrouted soil that simply washed out with the water flow. Additionally, poor recovery can indicate regions of high voids. The ungrouted soil could have been caused by temporarily blocked nozzles as discussed later.

**4.3.1.4 Core Hole 6.** Core hole 6 had a 75% recovery (83 in. of recovery out of 111 in. of core), and the relatively good recovery is related to excellent grout take in that region as shown in Figure 55. Around grout holes 25, 26, and 27, there was considerable heave of the whole southwestern portion of the pit indicating that the area underneath was completely filled with grout; therefore, the 75% recovery was not unexpected.



Southern culvert



M96 0442

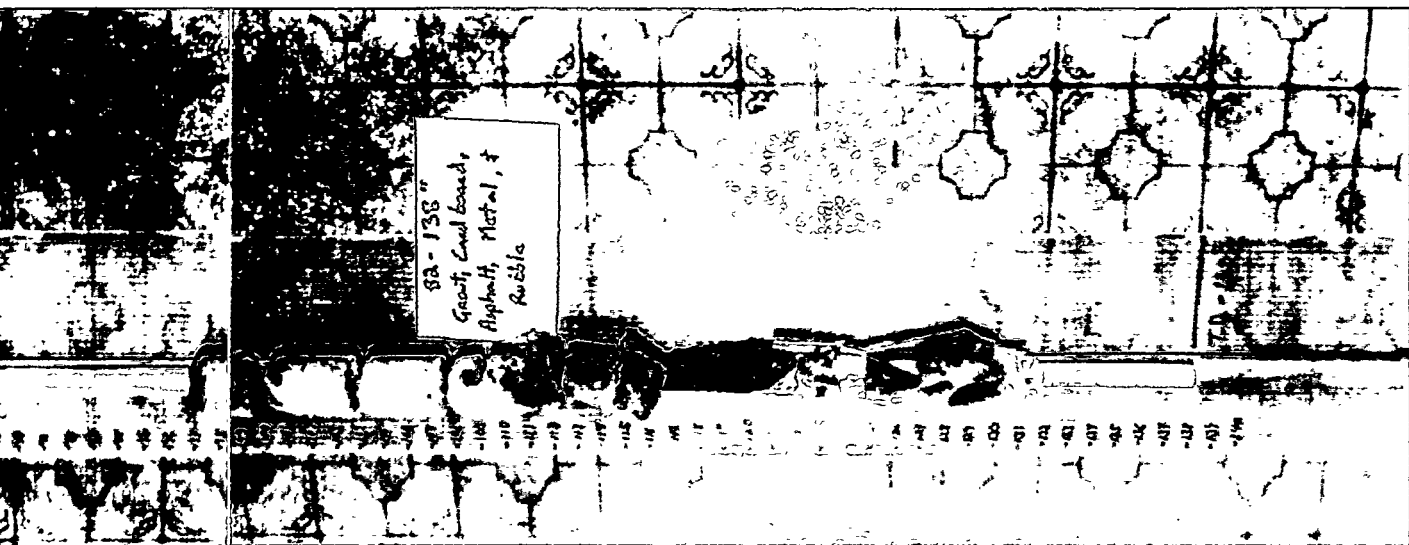
**Figure 53.** Relative position of core holes for the grouted field-scale permeameter, Type-H, TECT, paraffin grout (Graphic M96 0442).

**Table 7. Log of core holes for southern culvert.**

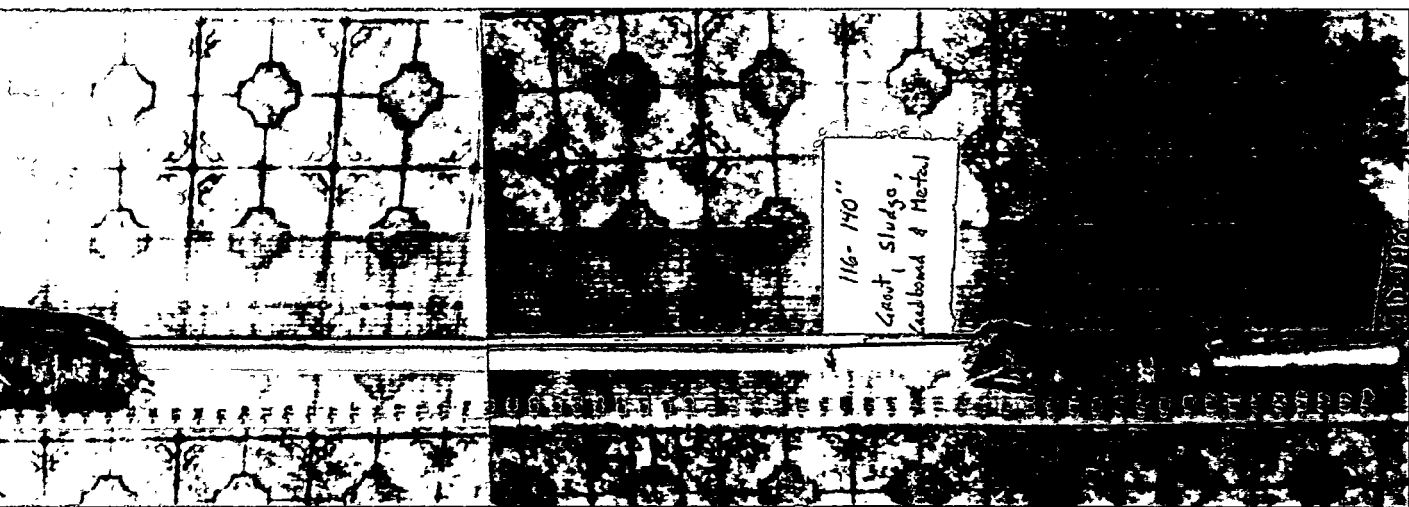
Hole	Elevation	Description	Recovery (in.)
CH-2	0-21	Surface casing in overburden	0
	21-56	Soilcrete rubble/metal	15
	56-116	Metal, soil, cardboard, grout	15
	116-140	Grout, sludge, cardboard, metal	18
		Total	48 (40%) <sup>a</sup>
CH-3	0-36	Surface casing in overburden	0
	37-55	Grout rubble	18
	55-60	Grout/cardboard	5
	60-75	Kitty litter, cardboard, grout	15
	75-82	Plastic, cardboard, grout	7
	82-138	Grout, cardboard, asphalt, metal	37
		Total	79 (77%) <sup>a</sup>
CH-5	0-36	Overburden	0
	36-59	Grout rubble	5
	59-118	Grout rubble, metal, plastic, cardboard	14
	118-121	Cardboard	3
	121-125	Grout	4
	125-142	Cardboard, grout, soil, metal	17
		Total	43 (40%) <sup>a</sup>
CH-6	0-28	Surface casing	0
	28-50	Grout rubble and soil	11
	50-60	Grout, paper, cardboard	10
	60-77	Grout, cardboard, paper, plastic, metal	17
	77-81	Kitty litter, grout	4
	81-92	Grout, metal, and cardboard	11
	92-117	Metal	8
	117-124	Metal, grout, plastic, cardboard	7
	124-129	Grout	5
	129-139	Cardboard, metal, grout	10
		Total	83 (75%) <sup>a</sup>

a. Only considers grouted region (not overburden).



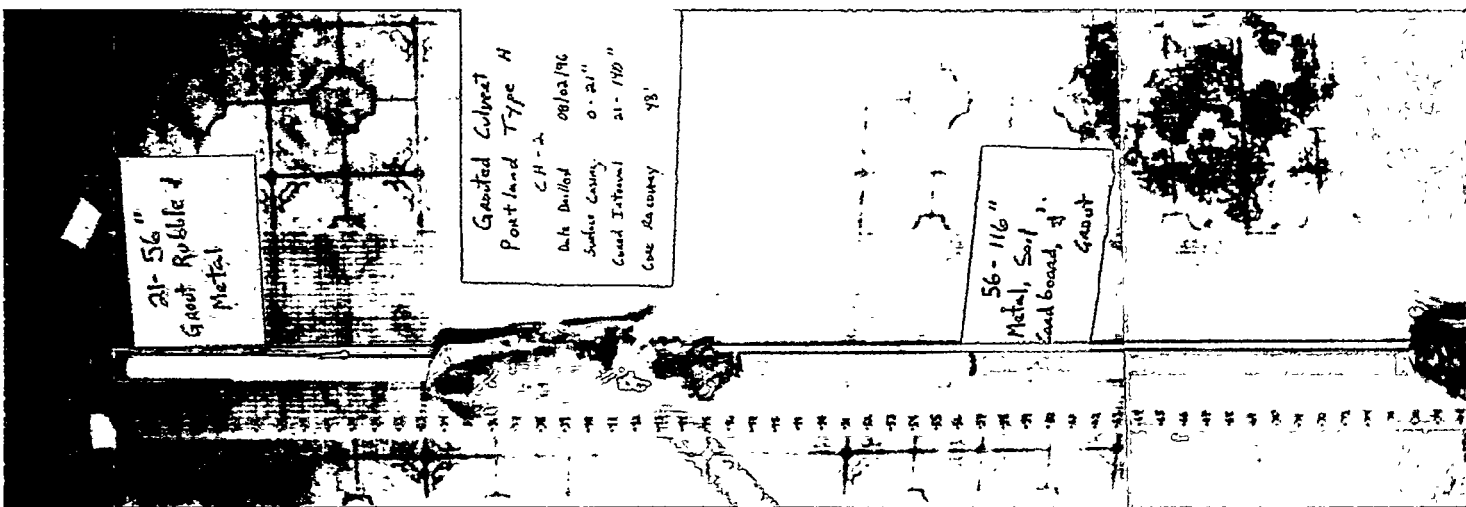
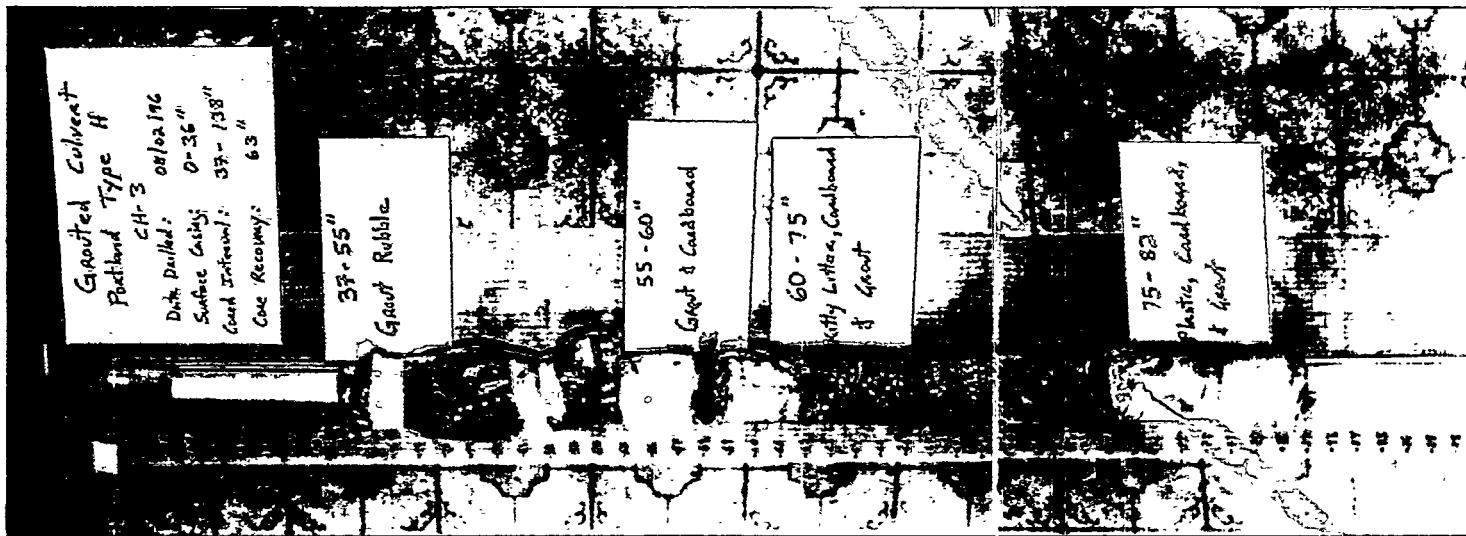


M96 0457



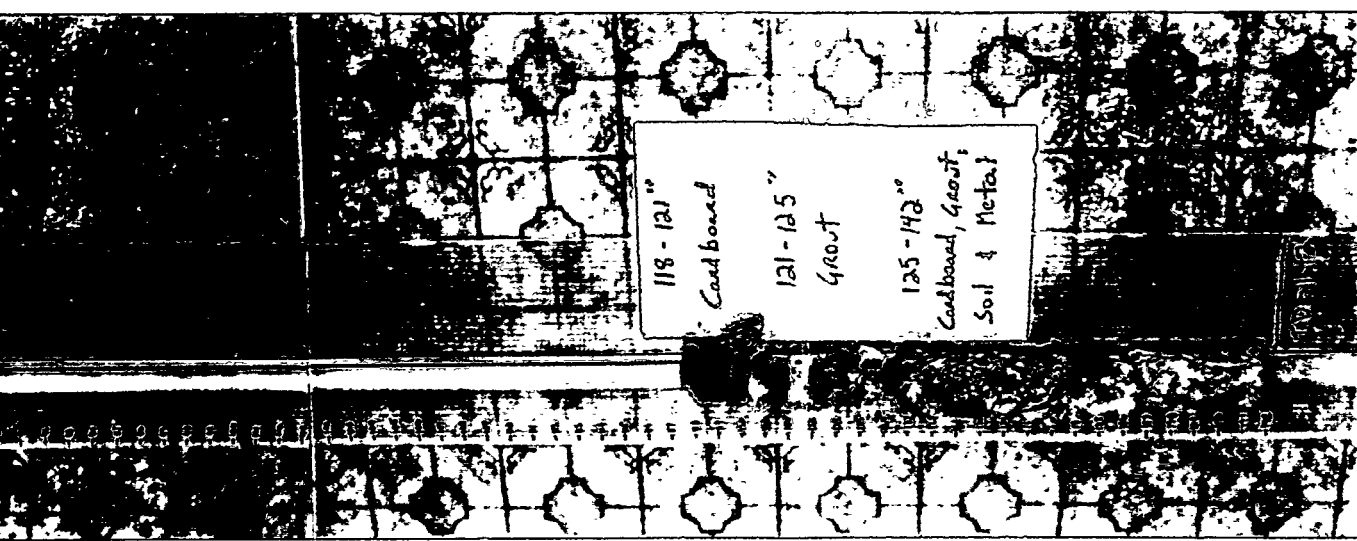
M96 0456

Figure 54. Core holes 2 and 3, grouted field-scale permeameter (Graphics M96 0456 and M96 0457).



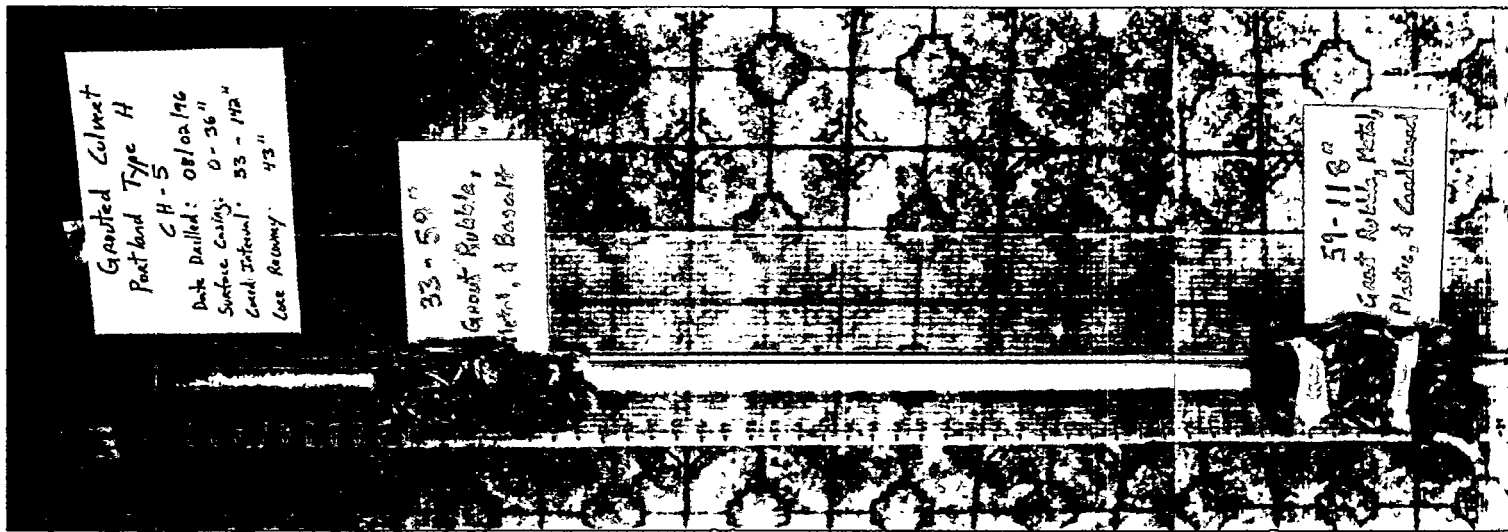
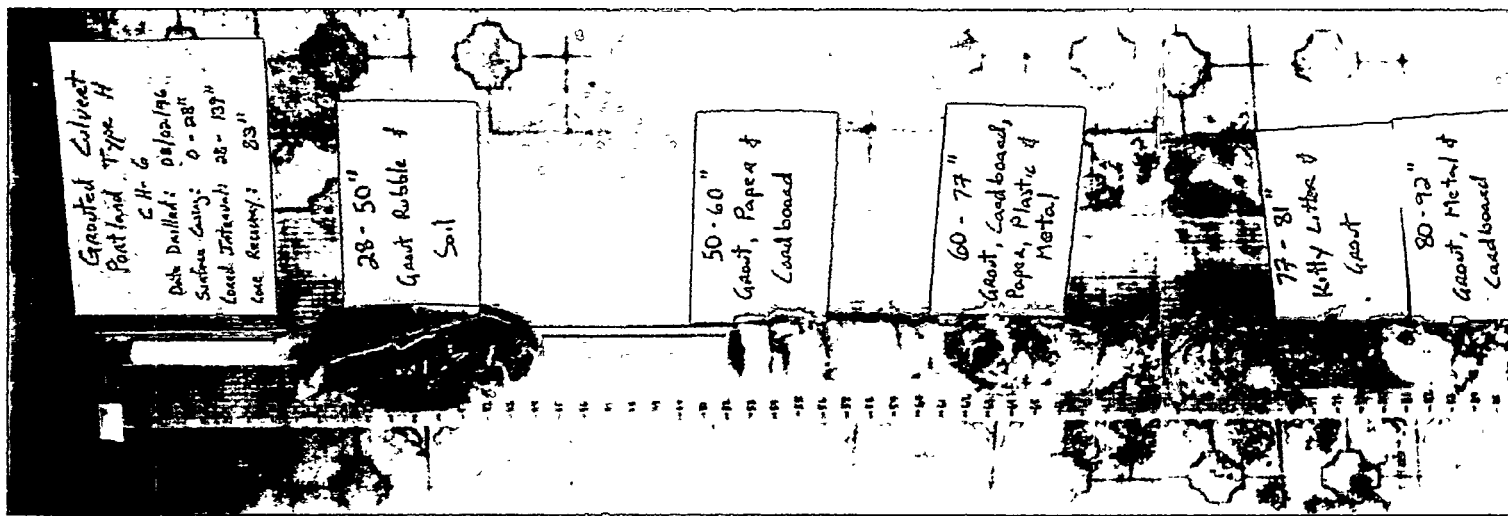


M96 0459



M96 0458

Figure 55. Core holes 5 and 6, grouted field-scale permeameter (Graphics M96 0458 and M96 0459).



Overall, the only explanation from the grouting data that accounts for the generally poor recovery of cores in the field-scale permeameter is this: In those regions where a drill stem refusal occurred (due to large metal objects in the pit), positions below the refusal do not receive as much grout. In addition, the coring process using water for cooling of the bit causes washout of the material—whether ungrouted soil or poorly cured grout—resulting in incomplete cores.

#### 4.3.2 TECT Pit

Examination of the cores in the TECT pit showed much better recoveries than those found in the grouted field-scale permeameter. Table 8 shows three core holes with recoveries for many positions ranging to 100%. Figure 56 shows photographs of the core with excellent solid cores of soilcrete, waste, and neat TECT grout.

**4.3.2.1 Core Hole 1.** Core hole 1 had an 82% recovery of the zone covering the theoretical position of the grouted portion of the pit (36–108 in. or 6 ft of pit). For this zone, much of the core is in solid pieces as shown in Figure 56. The region between 67 in. below the surface and 104 in. below the surface showed excellent 100% recovery. However, between 29–67 in., only a 47% recovery was observed. Referring back to Figure 31 for the grout hole location and to Table 4, a description of the grouting operation, it is noted that grout hole 7, which is in the vicinity of core hole 1, had copious grout returns up to 40 gal out of a total of 115 gal injected. It is not clear why the excessive grout returns occurred nor at which axial position the drill stem was when the maximum returns occurred. However, it is possible that the regions between 29–67 in. did not receive as much grout and that this accounts for the only 47% recovery in that region.

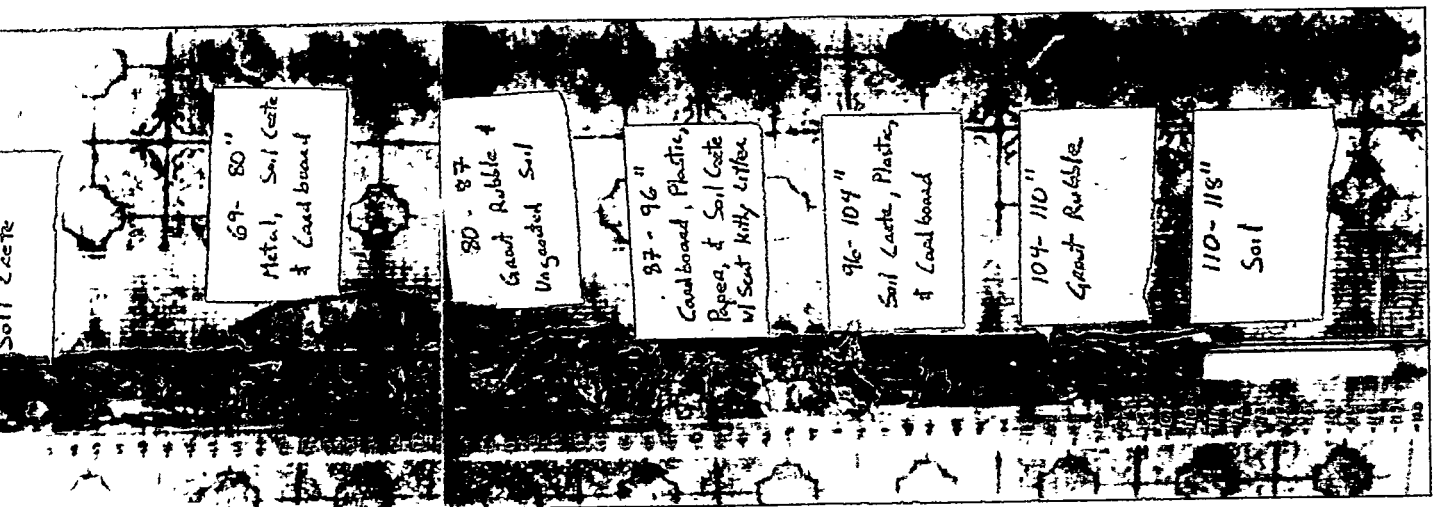
**4.3.2.2 Core Hole 2.** Core hole 2 had a 93% recovery in the theoretical region between 36 and 108 in. The zone between 43 and 77 in. showed fairly rubblized grout, which also may have been caused by partially blocked nozzles. The phenomena of blocked nozzles and the resulting effect on grouting performance was examined in prior INEL jet grouting. In prior jet-grouting experiments involving Portland cement mixed 1:1 by mass,<sup>1</sup> a field trial column in soil only was performed, which, when upon excavation, showed the effects of plugging of one of the two nozzles. Figure 57 shows the resultant field trial from that test with bands of soilcrete and of ungrouted soil. This is caused by the offset in the nozzle spacing on the drill stem. A plugged nozzle is not necessarily manifested in any feedback to the operators during the grouting phase, especially if the nozzle plugs and unplugs as it is withdrawn. Even though this phenomena causes localized incomplete mixing of soil and grout, it is a minimal impact on the overall pit because it does not occur frequently. Between 73 to 99 in., there was evidence of cured grout with the kitty litter found in the organic sludge simulant. Prior jet-grouting experiments<sup>1</sup> with Type-1 Portland showed that the canola oil/kitty litter mixture did not mix well with the grout and did not form a cured product. Therefore, the TECT grout is an improvement over the Type-1 Portland in the curing of mixtures of grout and organic sludges. It is assumed here that REGAL motor oil in the actual waste may behave similarly to the canola oil.

**4.3.2.3 Core Hole 3.** Core hole 3 showed excellent 100% recovery in the zone of the grouted pit. The core was mostly solid material with very little evidence of fractured soilcrete attributed to potentially blocked nozzles. Core hole 3 also correlates to a very solid monolith discussed later in the section on destructive examination. Examining the grouting log (Table 4), it

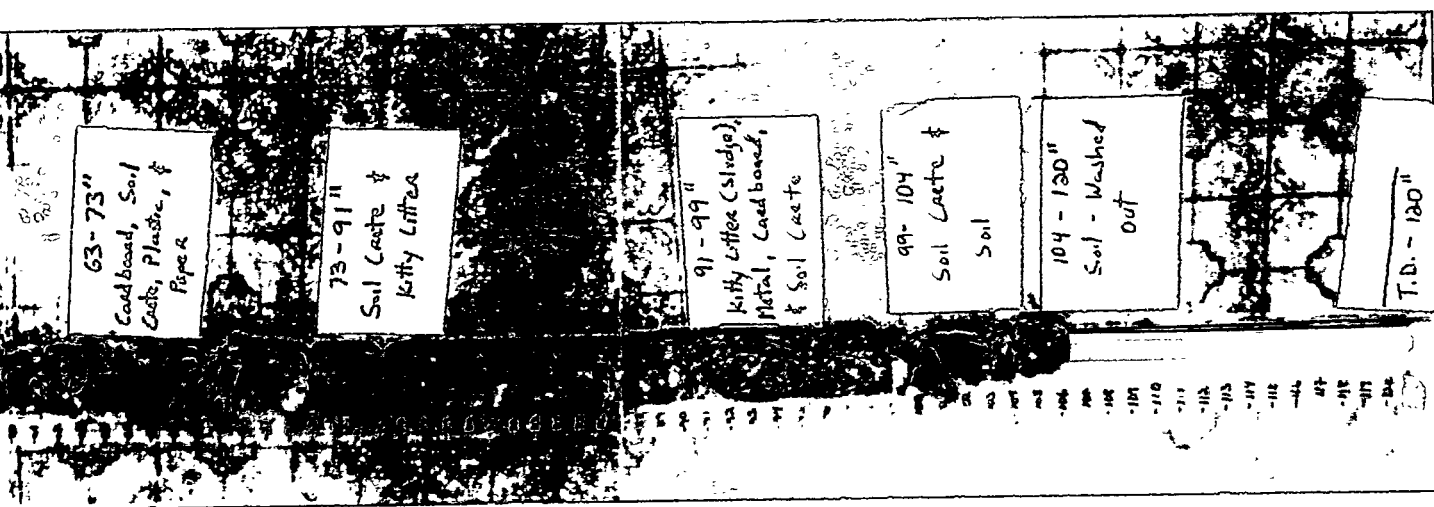
**Table 8.** Log of core holes for TECT pit.

Hole	Elevation	Description	Recovery (in.)
CH-1	0-36	Surface casing	0
	36-67	Cardboard, soilcrete	18
	67-80	Cardboard, plastic, metal, kitty litter, soilcrete	13
	80-87	Soilcrete	7
	87-92	Soil, cardboard	5
	92-95	Soil	3
	95-101	Cardboard, soil, soilcrete, kitty litter	6
	101-104	Soil/soilcrete	3
	104-117	Soil/soilcrete	<u>13</u>
	Total recovery in grouted region		59 (82%)
CH-2	0-43	Soil only	23
	43-49	Soilcrete rubble	6
	49-63	Soilcrete, metal, plastic	14
	63-73	Cardboard, soilcrete, plastic, paper	10
	73-91	Soilcrete, kitty litter	18
	91-99	Kitty litter, metal, cardboard, soilcrete	8
	99-104	Soilcrete and soil	5
	104-120	Empty	<u>0</u>
	Total recovery in grouted region		67 (93%)
CH-3	0-44	Soil only	16
	44-50	Soil, soilcrete, rubble	6
	50-55	Soilcrete	5
	55-69	Wood, plastic, soilcrete	14
	69-80	Metal, soilcrete, cardboard	11
	80-87	Grout rubble, soil	7
	87-96	Cardboard, plastic, paper, soilcrete, kitty litter	9
	96-104	Soilcrete, plastic, cardboard	8
	104-110	Grout rubble	6
	110-118	Empty	<u>1</u>
	Total recovery in grouted region		72 (100%)

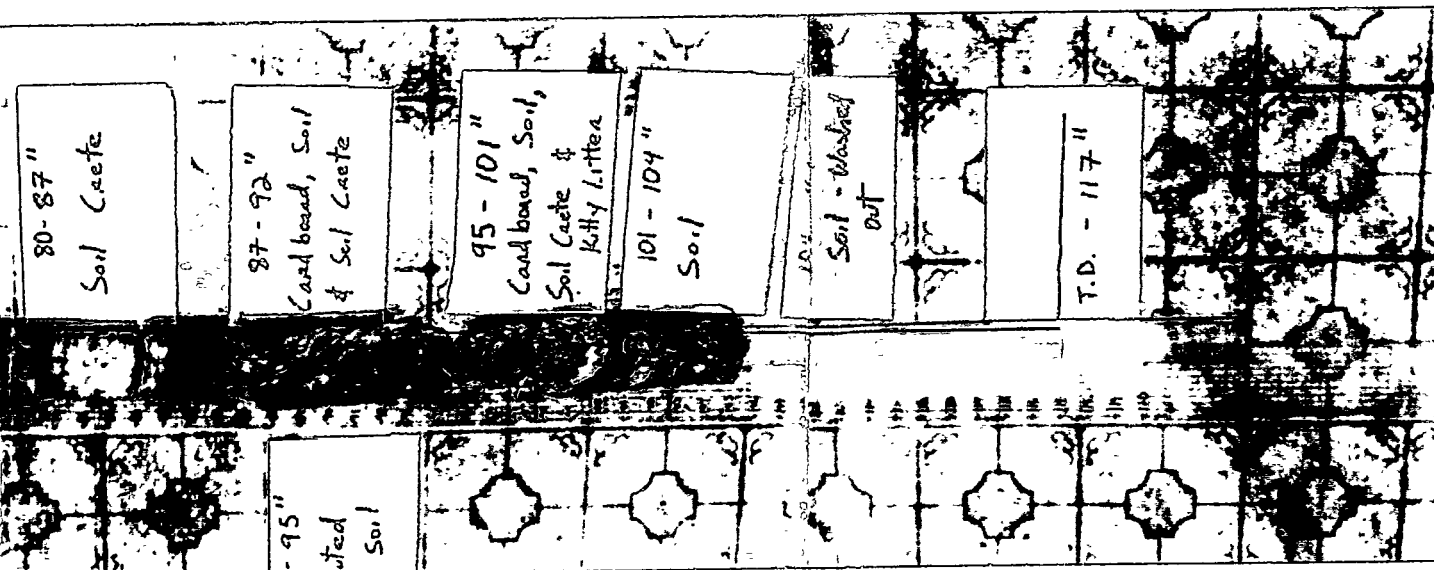
a. Grouted region is 36-108 in.



M96 0466



M96 0465



M96 0464

Figure 56. Core holes 1, 2, and 3, TECT pit (Graphics M96 0464, M96 0465, and M96 0466).

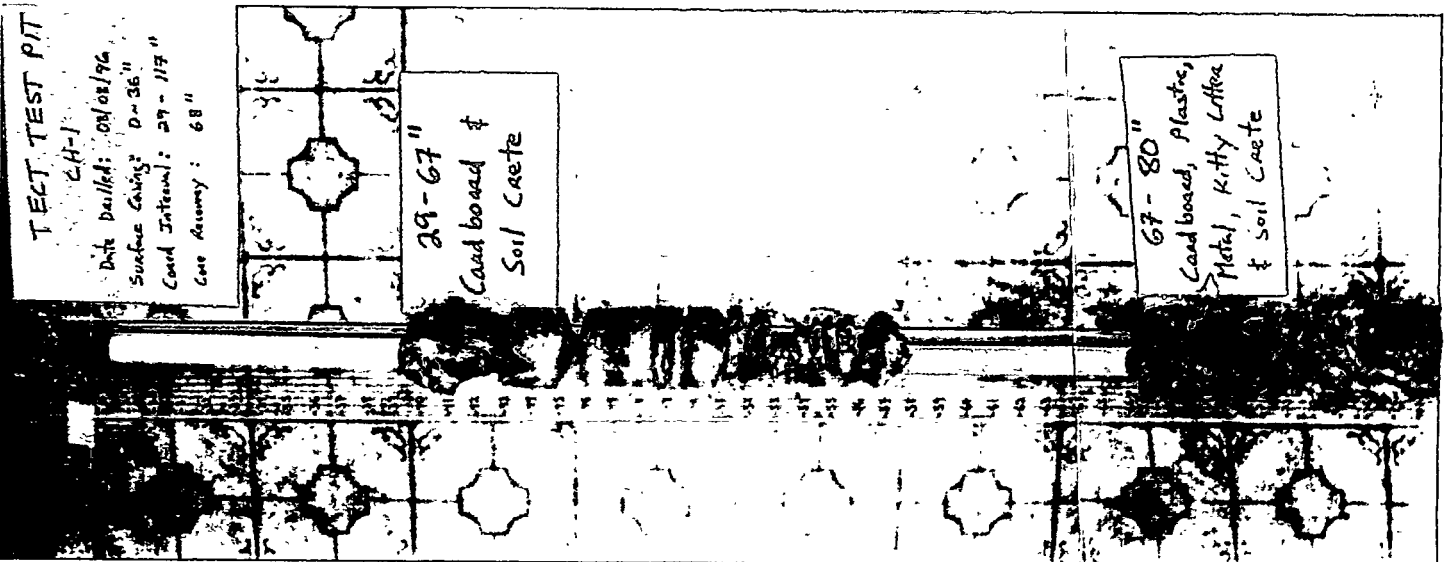
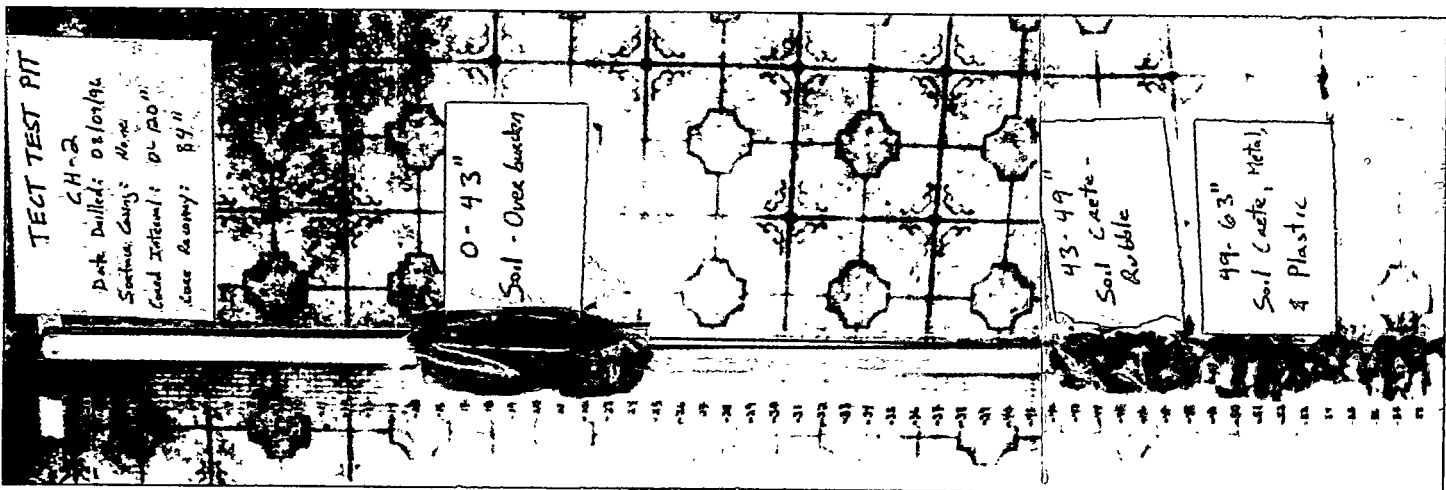
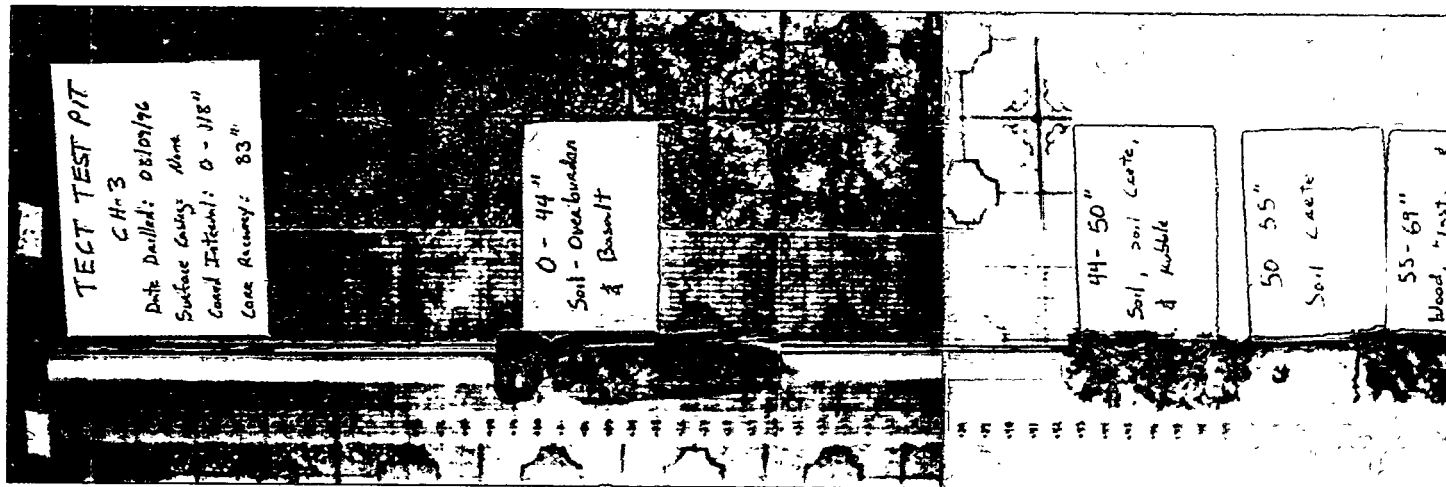




Figure 57. Drill stem hole 3 with blocked injector during field trials (Photo 94-715-2-1).



is noted that the grout holes nearest the core hole 3 displayed above-average grout take and minimum grout returns with no refusal of the drill bit.

### 4.3.3 Paraffin Pit

The paraffin pit had the best recoveries of all cores in either the field-scale permeameters or pits. Recoveries ranged to 100%, and the top overburden soil layer had enough permeation of paraffin from the top such that the resultant soil/paraffin matrix was cohesive enough to withstand the effects of the water stream used during coring. Table 9 gives a summary of the core hole recoveries, and Figure 58 contains photographs of the complete paraffin cores. For the paraffin pit, the cores did not extend through the bottom of the pit as was the case with the TECT pit (see previous section). This was done to eliminate unwanted cross communication during the packer hydraulic conductivity testing discussed in an upcoming section.

**4.3.3.1 Core Hole 1.** Core hole 1 is an example of perfect 100% recovery in a coring operation. In the grouted region, the core is cohesive and the grout appeared to completely encapsulate all materials in the pit, including organic sludges and sodium sulfate used as a stand-in for nitrate salts. The wood materials appear completely soaked in paraffin as did the plastic, paper, and soil. Referring to Figure 58, at the 76 to 84-in. elevation, the sodium sulfate residue region (a white zone) appears cohesive, indicating good mixing and encapsulation of the granular powder.

**4.3.3.2 Core Hole 2.** Core hole 2 had 100% recovery in the region of the core. However, what recovery there was displayed a similar paraffin penetration as shown in Figure 58. There was a section of metal debris from 54 to 69 in. that was apparently unrecovered. There is nothing in the grouting log to explain the absence of at least neat paraffin in the region from 54 to 69 in., unless that region contained paraffin loosely attached to the metal, and the water flow used in the coring operation washed out the interstitial paraffin. This idea will be expanded upon in the discussion on destructive examination of the paraffin pit. In general, the cores for paraffin were complete and solid. In an upcoming section on destructive examination, it will be noted that the paraffin had permeated the entire matrix, and even soil inclusions that were not grouted in the TECT pit were permeated with paraffin in the paraffin pit.

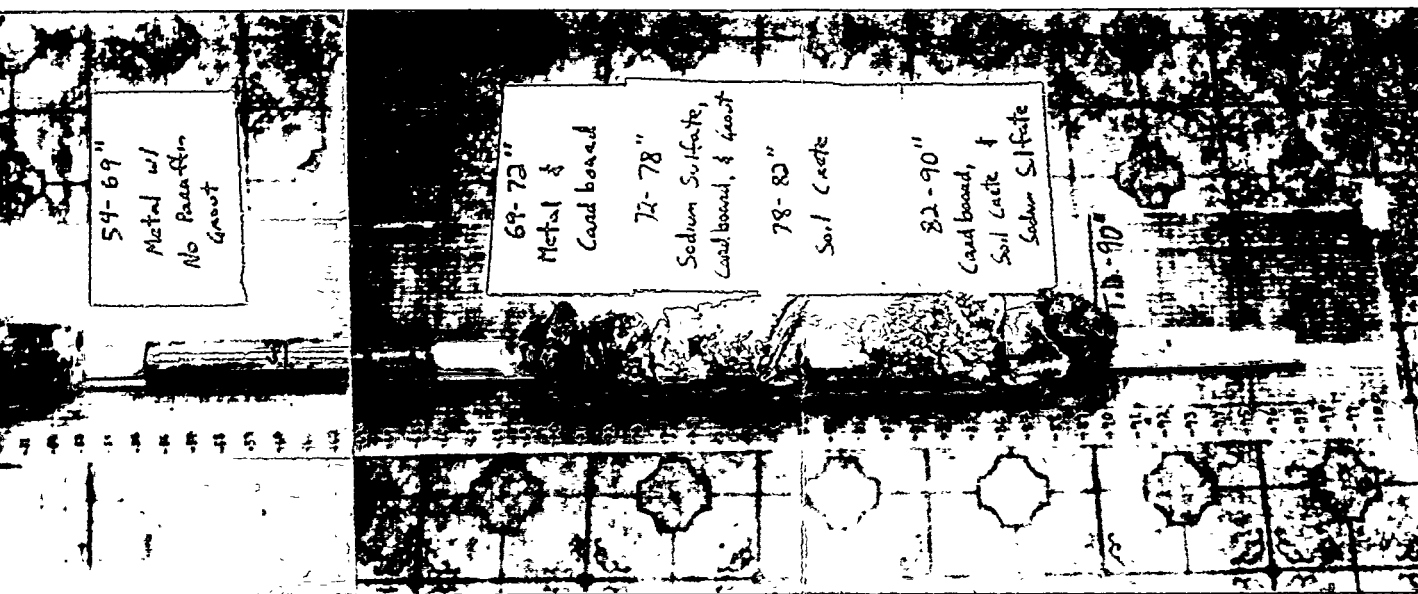
### 4.3.4 Type-H Cement Pit

The Type-H cement pit displayed poor recoveries in the cores (55-64%). Table 10 gives details of the recoveries, and Figure 59 contains photographs of the cores.

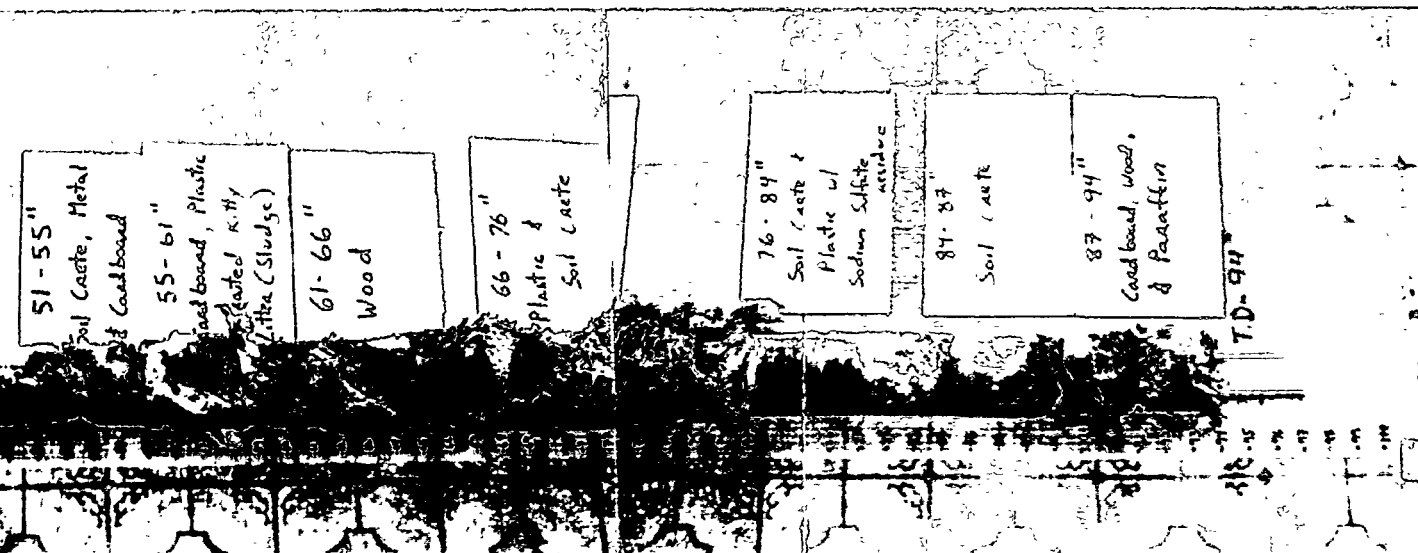
**4.3.4.1 Core Hole 1.** In core hole 1 shown in Figure 59, there was no recovery for the top 20 in. One explanation for the poor recovery in the cores is that the Type-H cement is prone to filter caking, and the nozzles could have intermittently become plugged and unplugged as observed previously in other grouting tests.<sup>1</sup> In this previous testing, a field trial of jet grouting Type-1 cement in soil displayed a similar pattern as shown in Figure 57. Examining Figure 59, there are regions where several fragments of solid grout about 5 cm in length are similar to the pattern seen in Figure 57. The coring process simply washed out the soil between the grouted layers.

**Table 9.** Log of core holes for paraffin pit.

Hole	Elevation	Description	Recovery (in.)
CH-1	0-10	Soil (impregnated with paraffin)	5
	10-36	Soil (impregnated with paraffin)	26
	36-51	Soilcrete	15
	51-55	Soilcrete, metal, cardboard	4
	55-61	Cardboard, plastic, kitty litter	6
	61-66	Wood	5
	66-76	Plastic, soilcrete	10
	76-84	Soilcrete, plastic (sodium sulfate)	10
	84-87	Soilcrete	3
	87-94	Cardboard, wood, paraffin	7
Total recovery grouted section 36-97 in.			58 (100%)
CH-2	0-10	Soil (impregnated with paraffin)	2
	10-34	Soil (impregnated with paraffin)	24
	34-54	Soilcrete	20
	54-69	Metal trace	15
	69-72	Metal/cardboard	3
	72-78	Sodium sulfate, cardboard	6
	78-82	Soilcrete	4
	82-90	Cardboard, soilcrete, sodium sulfate	8
Total recovery grouted section 36-90 in.			54 (100%)



M96 0461



M96 0460

Figure 58. Core holes 1 and 2, paraffin pit (Graphics M96 0460 and M96 0461).

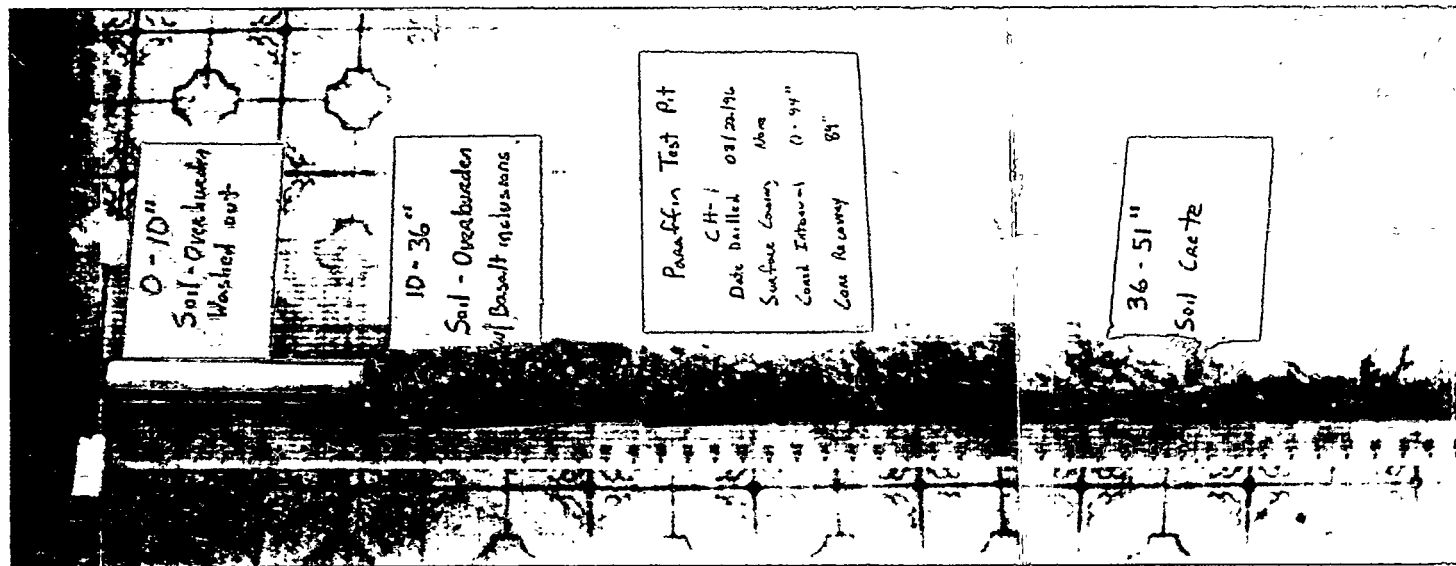
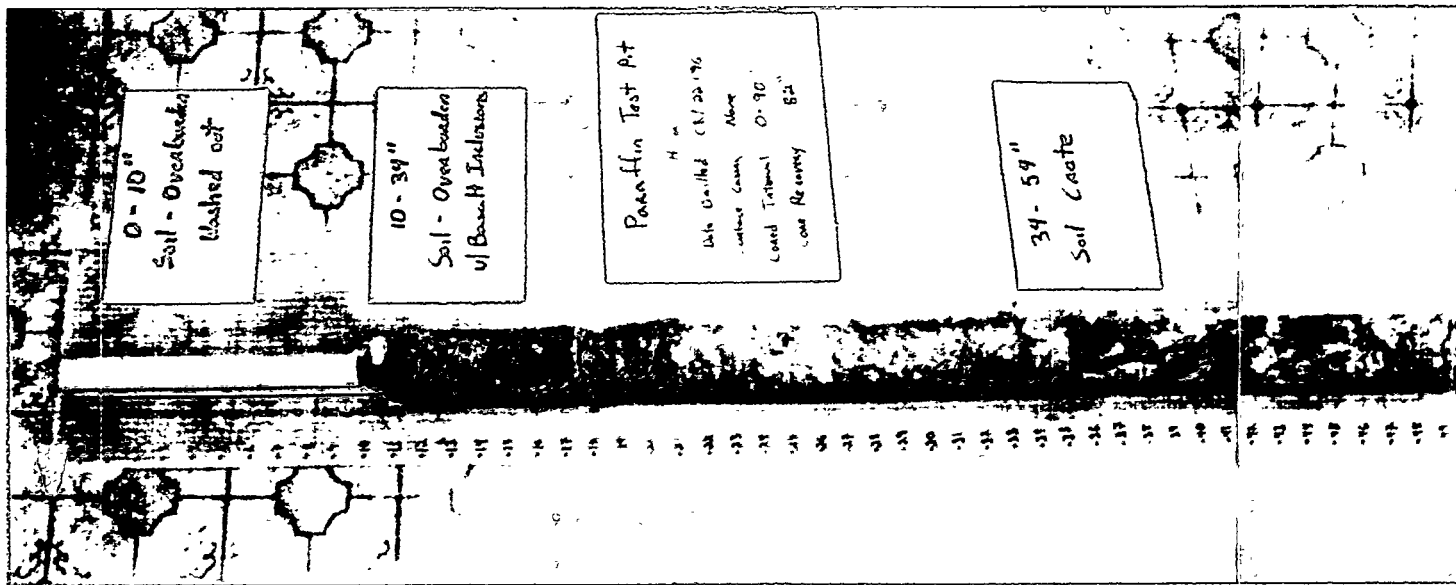
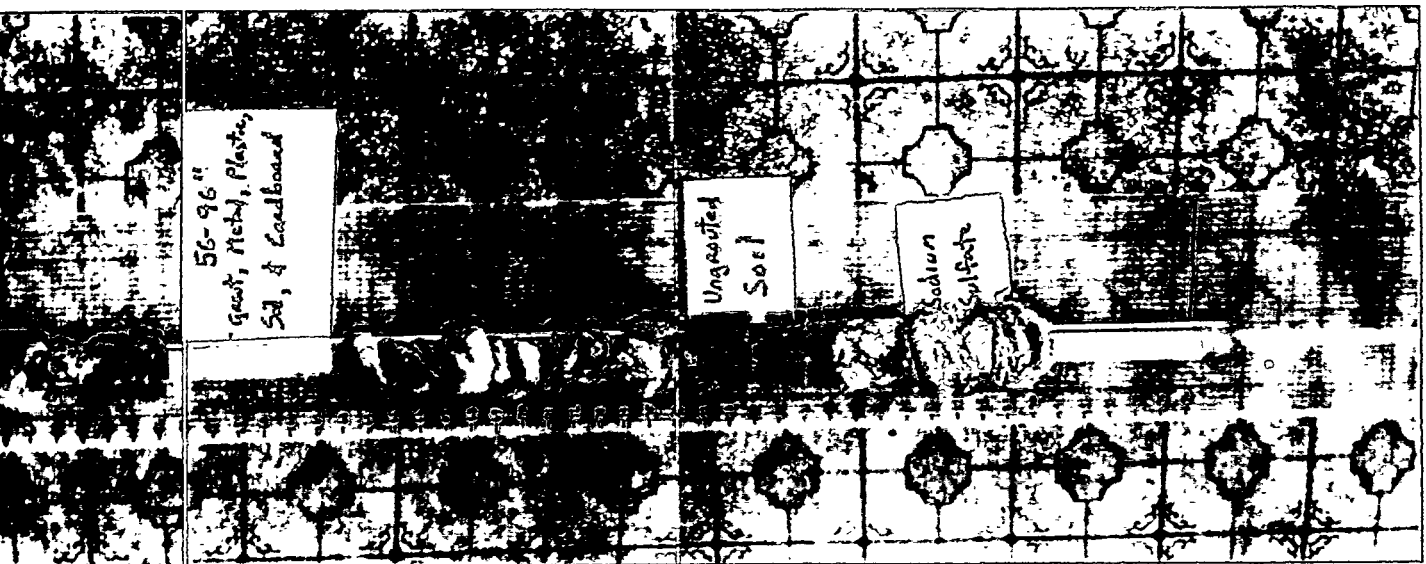


**Table 10. Log of core holes for Type-H pit.**

Hole	Elevation	Description	Recovery (in.)
CH-1	0-56	Soil, basalt rubble	17
	56-62	Basalt floaters, grout, plastic, cardboard	6
	62-71	Grout-encapsulated kitty litter	9
	71-78	Cardboard, metal, plastic, grout	7
	78-92	Grout	14
	Total recovery grouted section 36 in.		36 (64%)
CH-2	0-44	Soil	5
	44-56	Grout with basalt inclusions	12
	56-96	Grout, metal, plastic, soil (75-84) ungrouted soil (84-89) sodium sulfate solidified	22
			Total
			40 (55%)



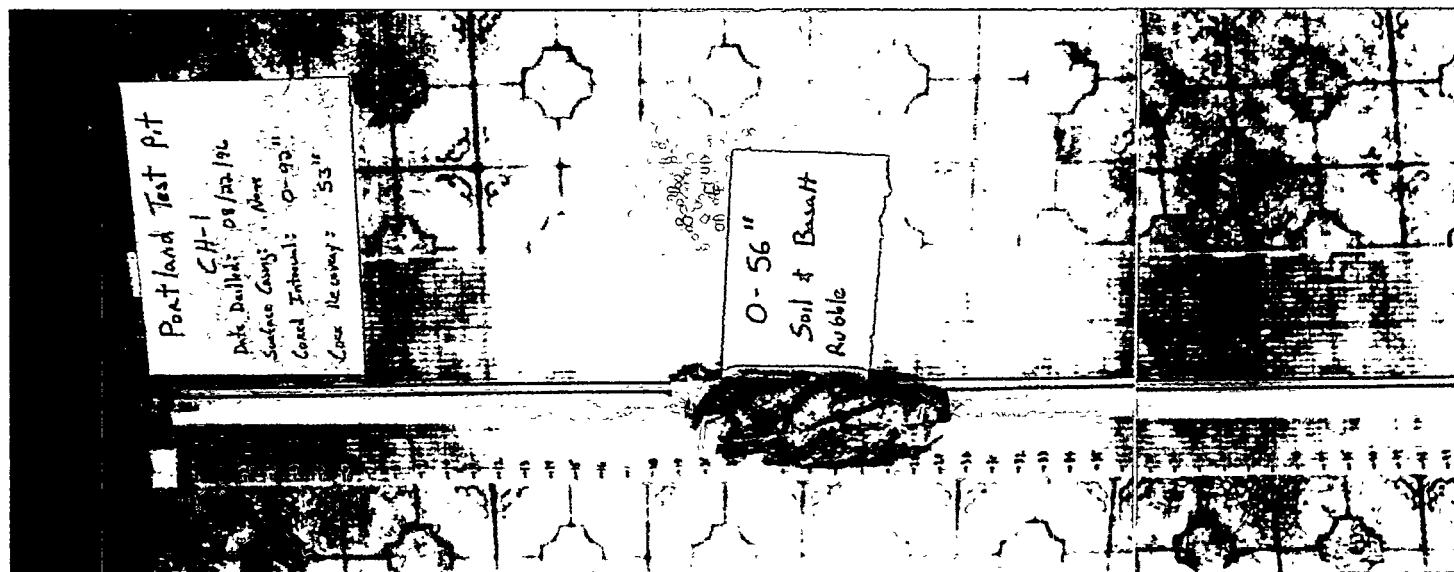
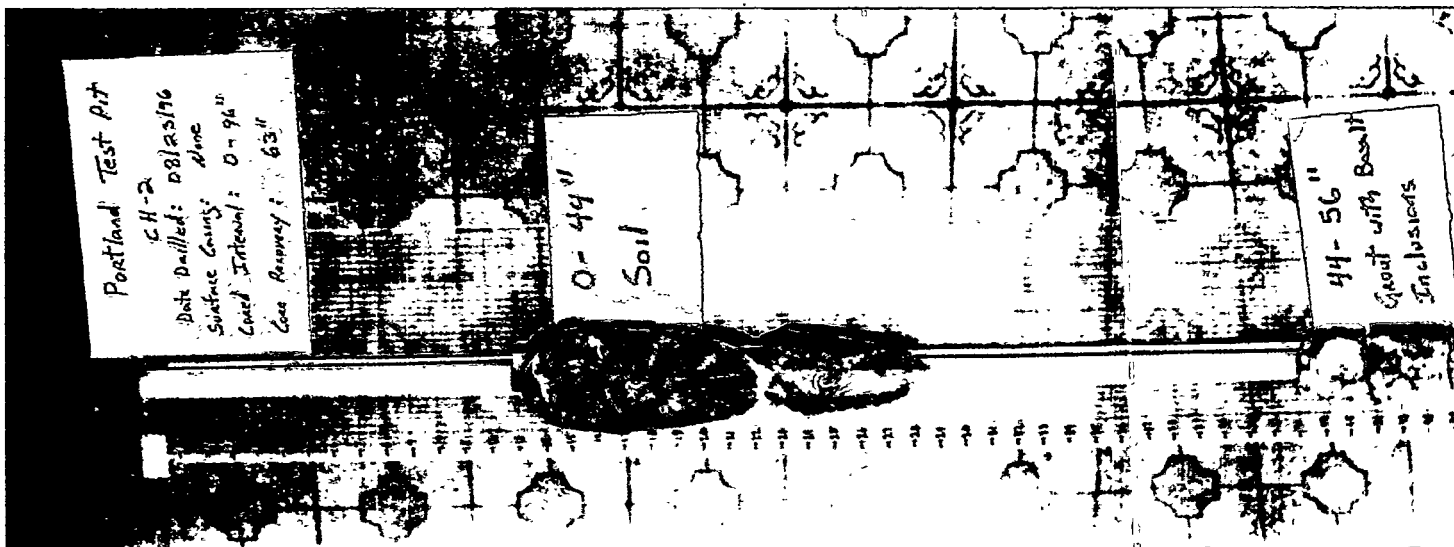


M96 0462



M96 0463

Figure 59. Core holes 1 and 2, Type-H pit (Graphics M96 0463 and M96 0462).



Since filter caking was common in the pump, nozzle, and lines during the Type-H grouting operations, it is possible that for both the field-scale permeameter and the Type-H pit that the nozzles alternated between plugged and unplugged conditions, resulting in many regions of ungrouted soil. These core data will be correlated with hydraulic conductivity testing using packer systems in a later section of this report. Also shown in Figure 59 (CH-1) is a region between 62 and 71 in. that is a solid cured mixture of kitty litter and Type-H cement, indicating that Type-H cement has the capability to incorporate and encapsulate organic sludges.

**4.3.4.2 Core Hole 2.** In core hole 2, the recovery was only 55% in the region of the grouted pit. There were sections of no recovery in the top, middle, and bottom of the grouted section (36-108 in.) (see Figure 59 [CH-2]). Between 75-84 in., there were regions of completely ungrouted soil, again indicating a completely plugged nozzle that became unplugged as the drill stem was withdrawn. The soil in this region was cohesive enough not to have been washed out by the coring water and therefore must consist of tightly packed clay. What recoveries were observed in core hole 2, displayed fragmented cores again potentially attributable to plugged or partially plugged nozzles. To graphically display the difference between a core that is solid and cohesive and one that is fragmented (both having full recovery), compare in the Type-H pit Figure 59 section 63 to 75 in. (highly fractured) to the paraffin core hole 1 Figure 58 (very little fracturing).

#### 4.3.5 Discussion of the TV Video Log of the Core Holes

A color video log was taken of each of the core holes, and virtually in all cases the log showed a cohesive monolith and solid core hole, whether for the TECT, paraffin, or Type-H pit or for the grouted field-scale permeameter. In no cases were large caverns or voids observed in the sides of the core hole. These video logs are available for general viewing by contacting the authors of this report. (Reference 5 gives a complete description of the video logs.)

### 4.4 Destructive Examination of Pits

A destructive examination of the TECT, paraffin, and Type-H pits was performed approximately 25 days after grouting using a standard backhoe. The examination was accomplished by first isolating the pit from the surrounding overburden material and then removing 6-in. increments taking field notes, collecting samples, and obtaining detailed photographs. In general, the core data and the destructive examination data are in agreement. Approximately one-half of each pit was destroyed in the examination, and the other half was left buried for future studies.

### 4.5 TECT Pit

Destructive examination of the TECT pit revealed that the injected TECT grout cured creating a solid monolith out of the original soil-and-waste matrix. The cured pit was difficult to dismantle because of the cohesive and solid nature of the monolith. The overburden soil was first removed and the general outline of the pit was isolated on three sides using the backhoe. Once roughly isolated, the backhoe removed 6-in. slices of side burden soil until the TECT soilcrete appeared. At this point, note taking and photography were initiated.

Figure 23 shows the backhoe taking 6-in. slices of the isolated TECT pit. Once the destructive examination had uncovered the first 18 in. of the pit, it became apparent that the pit was now a cohesive monolith of waste, soil, and grout with no voids. Figure 60 shows the difference between an ungrouted portion of the pit and the actual monolith (recall that only 12 holes were grouted, and the back two rows of holes were ungrouted—see Figure 31 and Table 4). In this figure, loose ungrouted soil is in contact with a hard soilcrete part of the monolith. Measurement of the actual width of the monolith was 58 in. for the three rows of holes grouted. The hole spacing from the first row to the third row spanned only 34 in. Therefore, the grout extended a cumulative total of 24 in. beyond the hole spacing.

Retrieval of the pit was extremely difficult with the standard backhoe. The backhoe had to be extended 4-5 ft above the pit and dropped to create enough force to break off a 6-in. slice. As the face was further exposed, it was obvious that all containers that had been exposed to the grout injection via puncturing and jet grouting had filled with grout and that interstitial soil had formed a solid soilcrete mix. The soilcrete mix contained inclusions of unmixed clay soil as shown in Figure 61. Positions that had cured as neat TECT inside containers and drums showed no inclusions of soil. These inclusions of soil in the general soilcrete found in the monolith are estimated at 15% of the volume. Even though inclusion of clay is common in the soilcrete mix, the encapsulating nature of the mix eliminates the possibility of one clay layer connecting to another. In addition, the clay material is inherently low-permeability material.

At the 30-in. mark from the edge of the pit (eastern edge), a drum full of general office trash representing paper and combustibles was exposed in the face. Figure 62 shows the embedded drum at the 30-in. mark as well as a small (1.5-2 gal) cavity toward the north side of the monolith. When removing the drum of office trash, the paper in the drum separated from the surrounding grout material and came out of the face as dry paper. If this paper had been contaminated with transuranic material, it could have contacted soil and spread contaminants.

Also shown in Figure 62 is the imprint of core hole 3 (discussed under coring) and a cavity of moist soil to the right of the core hole. It is speculated that the moisture in the soil was due to the water used in the core hole drilling process and water injected during packer testing. Also at the 30-in. layer, a drum of completely encapsulated organic sludge was uncovered. Figure 63 shows the outline of the drum with the absorbent kitty litter sprinkled throughout the matrix.

Figure 64 shows a detailed photograph of the encapsulated sludge material. The odor of the material was unmistakably of the canola oil used as an organic oil simulant. In prior grouting experiments,<sup>1,2</sup> with either Portland Type-1 or two-component acrylic polymer, the canola oil-based sludge simulant and the grout never mixed and the material came out viscous (flowable). Figure 65 shows an example of a sludge drum that was in the southern ungrouted region of the TECT pit. This is the original condition of the sludge/absorbent mixture and has low enough viscosity to run off a tilted shovel. At the 36-in. section, the cavity and core hole 3 became more pronounced. The cavity was up to 5 gal in volume and contained totally saturated soil (mud).

Figure 66 shows an overview showing that the drum containing office trash in Figure 62 was partially removed and the contents of the drum were still embedded in the face. This means that the TECT grout completely filled all interstitial positions in the drum and essentially glued the material together. However, when removing the material, the grout easily falls away from the



**Figure 60.** Interface between ungrouted soil and the TECT monolith (Photo 96-587-9-30).





**Figure 61.** Inclusions of clay soil in TECT monolith (Photo 96-584-2-23).





**Figure 62.** TECT monolith 30 in. from east face showing drums of office trash embedded in the face (Photo 96-587-9-4).





Figure 63. Outline of encapsulated oil sludge drum in TECT pit at 30 in. from east face (Photo 96-587-9-13).





**Figure 64.** Detail of encapsulated sludge showing kitty litter inclusion (Photo 96-587-9-15).





**Figure 65.** Ungrouted canola oil-based sludge simulant in southern end of TECT pit (ungrouted portion) (Photo 96-587-4-3).





Figure 66. Overview of TECT pit at 36 in. from east face (Photo 96-587-9-22).



paper, leaving dry paper as discussed before. Figure 67 shows more detail of the cavity and core hole showing that there is standing water in the cavity and that the cavity is completely isolated from positions below. The cavity was obviously connected to core hole 3, and the saturated condition was caused by the water used during either packer testing and/or drilling of the core hole. The origins of the pocket of soil in an otherwise completely grouted region is unknown except for the potential for a partially blocked nozzle during grouting or the presence of a large pocket of tightly packed solid clay.

At the 42-in. level from the east face, a drum containing wood completely impregnated with TECT grout was uncovered as shown in Figure 68. Also shown in Figure 68 is a completely ungrouted region underneath the drum. This region corresponds to a grout hole refusal area in which the drill stem was inserted and only the top portion of the pit was grouted in that area (refer to Table 4, hole 6). Figure 69 shows a detailed photograph of a region that was ungrouted due to the refusal of penetration by the drill stem. In this region, a drum containing ungrouted sodium sulfate (simulating nitrate salts) was observed and shown as punctured with the dry powder running out (see Figure 69). It is noted that there may be regions like this in the actual pit that have been jet grouted. However, these regions are a small percentage of the total volume of a pit and most likely are completely encapsulated on the top and sides. In this case, there is no possibility of migration of water from above causing movement of the contaminant.

#### 4.6 Paraffin Pit

Destructive examination of the paraffin pit was performed 21 days following the paraffin injection, and enough time had elapsed that the paraffin formed a completed monolith out of the soil-and-waste matrix with no ungrouted positions. The low viscosity of the molten paraffin and the slow cure time allowed visually total hydraulic conductivity of clay inclusions in the general soil-and-waste matrix. In general, the destructive examination using the backhoe showed that the paraffin material is easily retrieved and should result in minimum dust generation during retrieval.

The paraffin pit was examined the same as the TECT pit in that 6-in. slabs of the pits were removed following isolation of the pit from the overburden and side burden soils. Prior to the destructive examination, the top surface of the pit had a film of paraffin 3 in. thick. This top surface was penetrated as shown in Figure 70, and it was found that the top 3.5 in. of soil on the pit had been permeated with paraffin. Figure 70 shows a pocket knife at the bottom of the small excavation on the dry unpermeated soil, the 3.5-in. layer of permeated paraffin, and the top surface of pure paraffin. The blue color is a food grade dye used to distinguish paraffin from the surrounding soil.

Figure 71 shows the face of the paraffin pit at 6 in. from the east face. The inclusions of clay soil are in the paraffin soilcrete matrix. However, the inclusions had soaked through with paraffin leaving no positions in the face of the pit with dry soil. As a result, there is virtually no dust spread during the retrieval activities. Figure 72 shows the face 12 in. from the east side, with a drum containing paper in the face. The paper in the drum was completely soaked in paraffin, and any contaminant on the drum would have been encapsulated.

An example of the paper from the pit is shown in detail in Figure 73 with a completely encapsulated piece. Figure 74 shows the face 18 in. from the east face, with the total monolithic



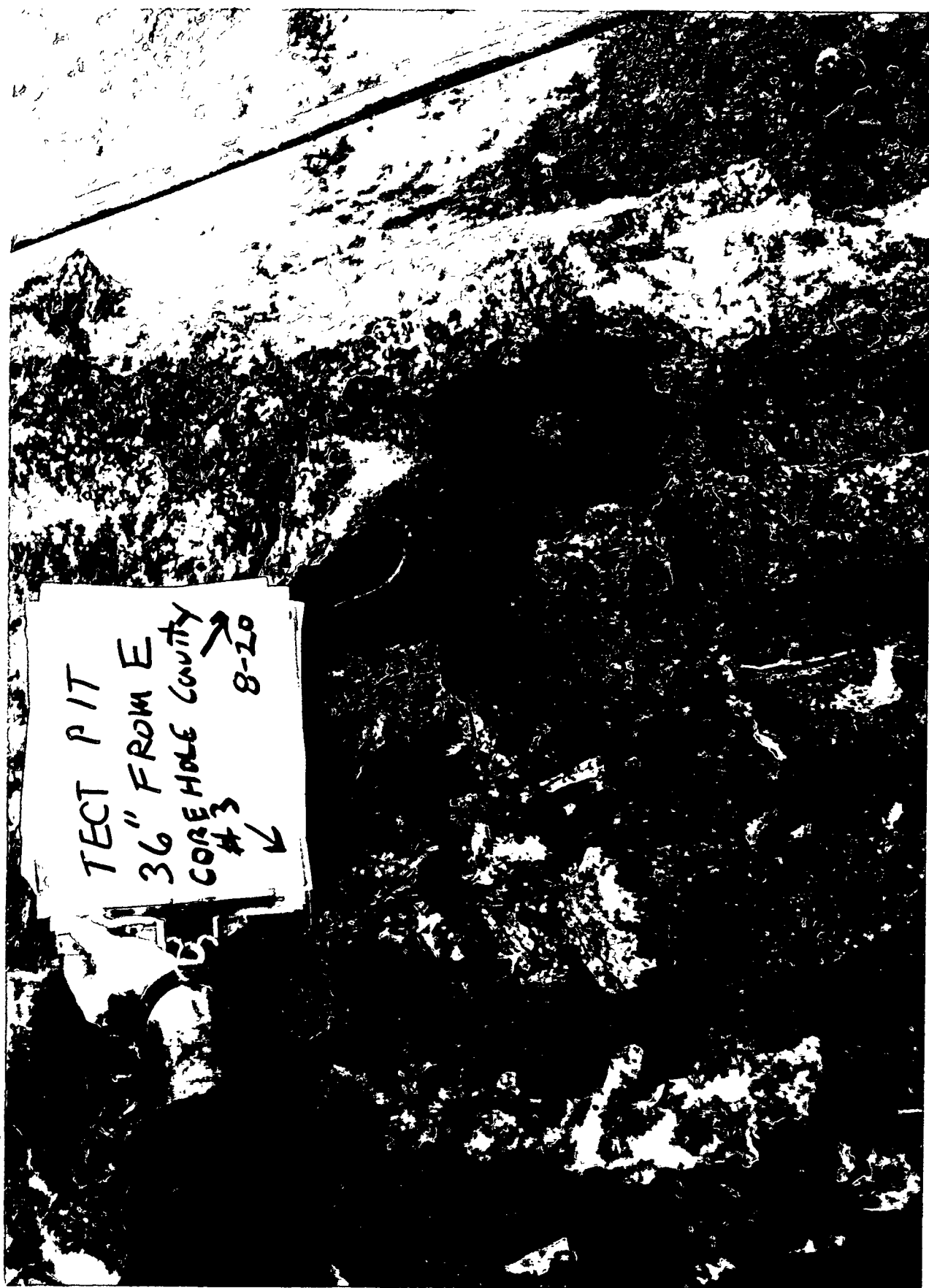


Figure 67. Detail of core hole 3 and soil cavity in TECT pit at 36 in. from east face (Photo 96-587-9-24).





**Figure 68.** Drum of wood at the 42-in. level from the east face of the TECT pit (Photo 96-584-2-28).





**Figure 69.** Sodium sulfate in ungrouted drum at the 42-in. level from the east face for the TECT pit (Photo 96-587-10-35).



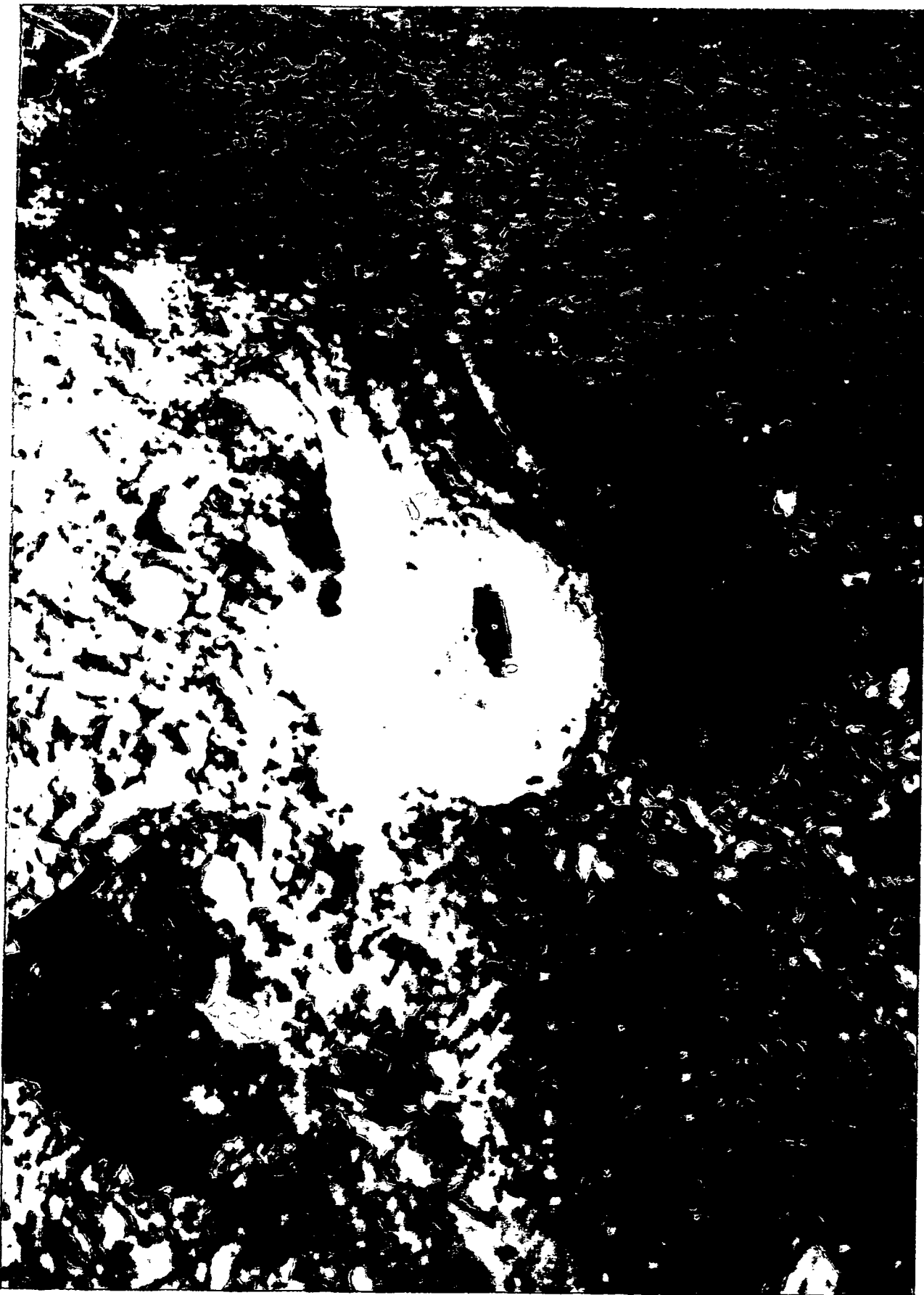


**Figure 70.** Top of paraffin pit prior to destructive examination (Photo 96-587-2-10).





Figure 71. Paraffin pit detail at 6 in. from the east face (Photo 96-587-3-11).





Figure 72. Paraffin pit detail at 12 in. from the east face (Photo 96-587-3-15).





Figure 73. Detail of paper from paraffin pit (Photo 96-584-2-5).





Figure 74. Paraffin pit 18 in. from the east face (Photo 96-587-3-17).



nature of the pit evident. The paraffin even encapsulated the plastic liners of the drum as shown in the figure. At 30 in. from the east face, a drum of wood encapsulated in paraffin is shown in Figure 75, and Figure 76 shows the detail of how pervasive the molten paraffin had penetrated the wood. It was evident that the molten paraffin had low enough viscosity to literally soak all waste forms prior to curing.

The temperature history of the pit during curing showed that the pit remained above the melting temperature of 120°F for at least 3 days. Therefore, during this period, the molten paraffin could penetrate most voids. Figure 77 shows a drum of canola oil sludge penetrated with paraffin. The consistency is like lard but will not run off of a shovel as with the acrylic polymer or cement.<sup>12</sup> Figure 78 shows a sample of the sludge material with some soil inclusions, and again the soil inclusions are soaked with paraffin. The sample of the sludge can stand alone at room temperature.

Figure 79 and Figure 80 are samples of metal and wood encased in paraffin. The wood sample was soaked 0.25 in. into the wood. The metal sample had neat paraffin inside the container that was ruptured during digging. In short, all positions in the paraffin pit had been encapsulated with paraffin, and there were no observed voids. In addition, excavation of the pit was essentially dust free and easy to perform with the backhoe.

#### 4.7 Type-H Cement Pit

A destructive examination of the Type-H cement pit showed that the Type-H cement mixed at 1:1 by mass (14 sacks per cubic yard of fluid) and jet grouted at nominally 70 gal per hole resulted in a solid monolith. For this pit, however, compared to the TECT pit, there was evidence of plugged injectors, which is consistent with the discussion of the cores for the Type-H pit. Figure 81 shows the Type-H pit after excavating approximately 2.5 ft from the south wall. In the figure, the general solid monolithic nature of the pit is shown. However, near the bottom of the pit in at least two locations is the evidence of a plugged injector, which is similar to previous data<sup>1</sup> shown in Figure 57.

Figure 82 shows detail of evidence of a plugged injector in the Type-H pit, which is exactly comparable to that shown in Figure 57 from the previous experiment.<sup>1</sup> In the soil immediately east of the grouted portion near the bottom of the pit extending 3–4 ft to the southeast was a zone about 2.5 ft in diameter of highly porous light-colored soil/grout/potentially sodium sulfate. It is unlikely that Type-H cement can form hard monoliths when encountering 100% nitrate materials. Figure 83 shows the southeast corner of the pit with the region of porous light-colored soil extending to the east away from the pit. The bent metal pipe in this photograph is a neutron probe access pipe used for assessing migration of water away from the pit (to be discussed in a later section).

This pipe was located about 1 ft from the eastern edge of the pit. This soil was observed to be more brittle and drier than the general soil surrounding the pit and appeared to be a mixture of soil/poorly cured Type-H cement and sodium sulfate. Analysis of a sample of this material showed 323 mg/L of sulfates in a one-to-one water extract of 50 g of soil, indicating poor mixing of cement and sodium sulfate in that region of the pit. One possible explanation for this relatively brittle porous region of soil is that a hydrofracture line extending to the southeast from





**Figure 75.** Paraffin pit 30 in. from the east face (Photo 96-584-1-3).



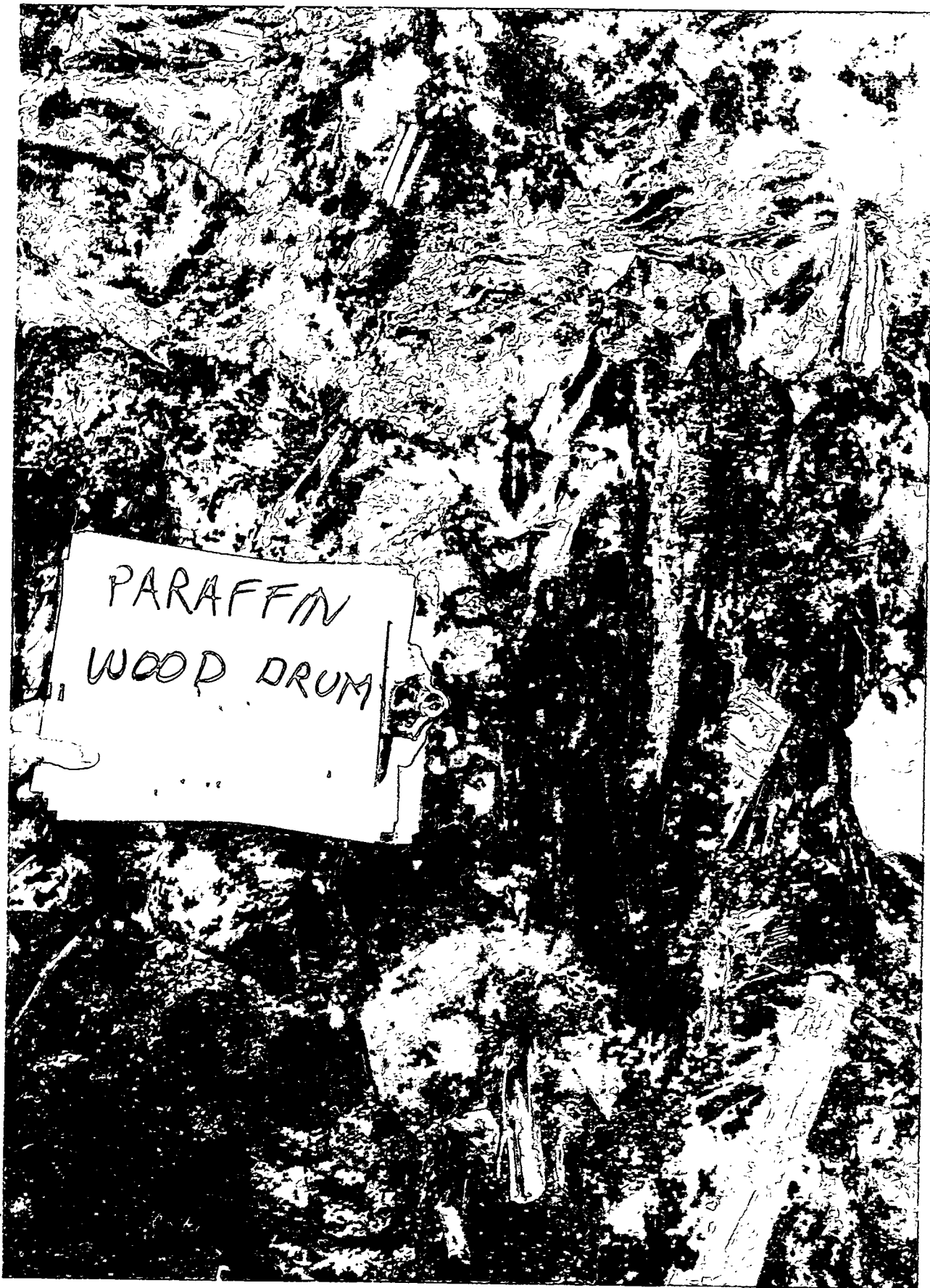


**Figure 76.** Detail of wood in paraffin face (Photo 96-584-2-9).



SLUDGE  
DRUM  
SOUTH  
WALL

8/26

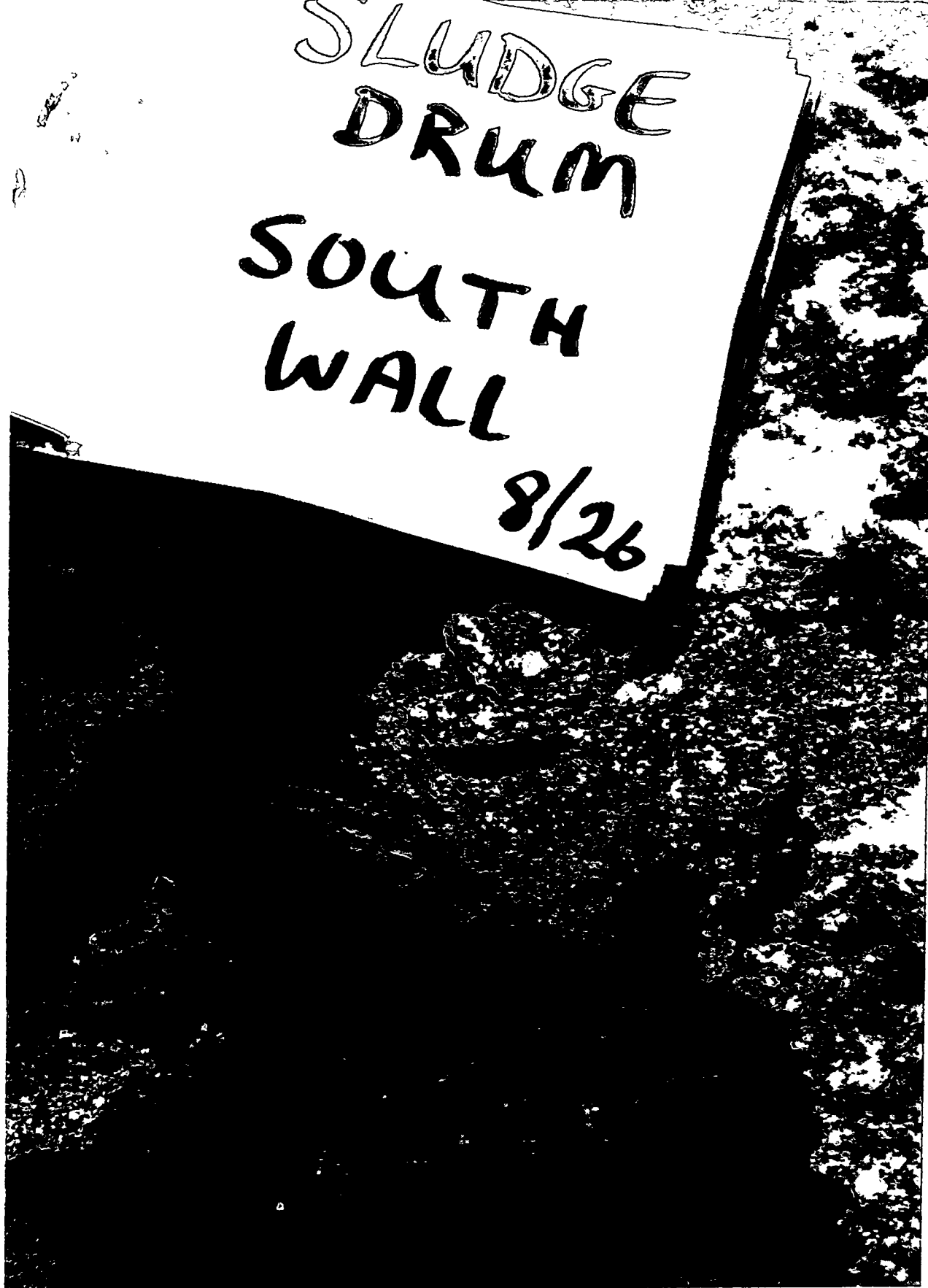


Figure 77. Drum of canola oil in south wall of paraffin pit (Photo 96-584-2-11).





**Figure 78.** Sample of the sludge with inclusion of clay soil (soaked with paraffin) (Photo 96-584-1-10).





**Figure 79.** Sample of metal encased in paraffin (Photo 96-584-2-18).



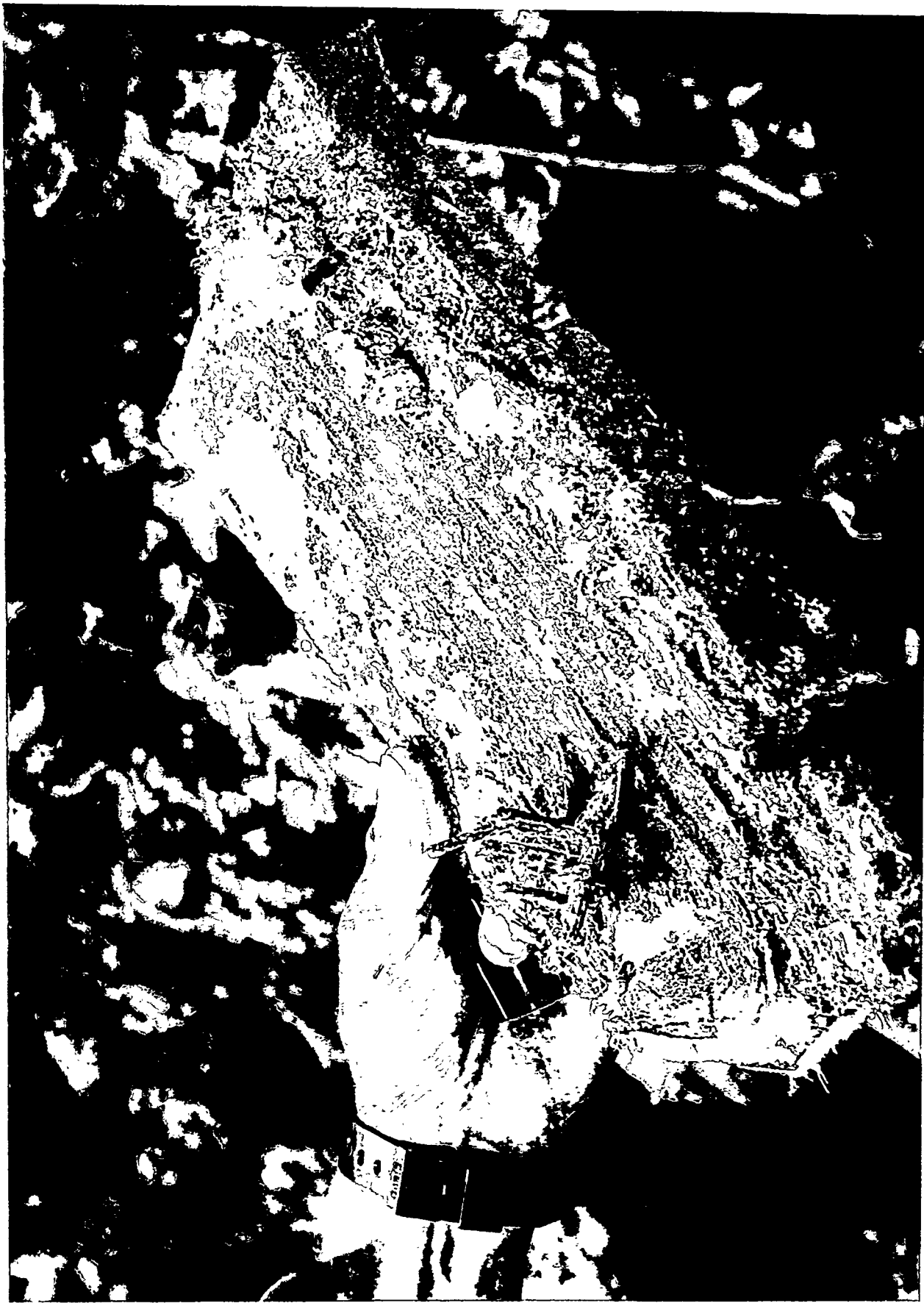


**Figure 80.** Sample of wood encased in paraffin (Photo 96-584-1-6).





Figure 81. Type-H cement pit showing plugged injectors (Photo 96-743-1-9).





**Figure 82.** Detail of region with clogged injectors (Photo 96-743-1-11).





**Figure 83.** Region of porous soil outside Type-H pit (Photo 96-743-1-13).



the southeastern corner focused a preferred path for water flow during drilling of core hole 2 and subsequent packer testing.

In a following section on hydraulic conductivity packer testing, it will be discussed that water actually flowed from core hole 2 to the surface about 3 ft southeast of the pit. This flow of water through a relatively low hydraulic resistance pathway is possibly due to a sodium sulfate drum located in the exact corner of the pit being poorly mixed with the Type-H cement during the grouting operation as discussed above. When water was added in the core hole drilling process and during packer testing for core hole 2, fluid flowed through a relatively weak soil/grout structure and was focused to the surface by a lens of dry soil. The soil in that area surrounding the pit must have been relatively dry (less than 10% moisture by mass) and only loosely packed. A sodium sulfate drum (number 120—see Appendix B Pit D data) was located in the bottom layer in the exact southeast corner of the pit. Therefore, the interaction of the grout with the sodium sulfate must have left a poorly cured region (porous material) that, when penetrated with core hole 2, allowed coring/packer water to flow away from the pit.

The important observations from the destructive examination are that the Type-H cement forms a solid monolith with minimal grout injection, is prone to plugged injectors, and appears to form a porous mixture of grout and sodium sulfate when drums of pure sodium sulfate are encountered.

## 4.8 Hydraulic Conductivity Testing Results

Hydraulic conductivity data were obtained for all grouted pits and the grouted field-scale permeameter. Data were obtained using the packer technique for the field-scale permeameter and all the grouted pits and in addition, the full-scale falling head method was also used in the grouted field-scale permeameter and the ungrouted field-scale permeameter. The packer testing was performed using the core holes described in a previously discussed section of this report. Appendix C contains details of how the packer data and falling head data translate to hydraulic conductivity. In addition, Appendix C contains raw data from the permeation testing.

### 4.8.1 Packer Testing in Pits and Grouted Field-Scale Permeameter

Packer testing for the pits showed that positions in the TECT and paraffin pit displayed less than  $10^{-7}$  cm/s hydraulic conductivity. However, the Type-H cement pit was so porous that the pit would take the entire flow of the packer for any pressure, indicating hydraulic conductivity of  $10^{-3}$  to  $10^{-4}$  cm/s. Packer testing in the core holes of the grouted field-scale permeameter revealed considerable cross communication. However, in several of the holes, a packer test with  $10^{-7}$  cm/s results was observed for several positions.

In performing the packer tests using the core holes, several special procedures were required to obtain packer data with an adequate seal. It was necessary in some cases to isolate one hole from another using individual packers and in some cases cement sealant because many of the holes were hydraulically interconnected for water pressures of 2-22 psi in the packer. It became clear that the coring process affected the matrix, especially at the bottom of the pits if the core hole penetrated below the region of the grout. Also, in some cases, to obtain good packer data, one hole required sealing with cement from another. Good packer data are defined here as a test

in which a nonmeasurable flow is detected in the packed-off area for a period of nominally 10 minutes under a water pressure of nominally 22 psi. This equates to a local isotropic hydraulic conductivity of  $10^{-7}$  cm/s or less (see Appendix C).

The hydraulic conductivity is calculated from the equation:

$$K = \frac{Q}{CrH}$$

where

$K$  = hydraulic conductivity (length/time)

$Q$  = flow rate into the test section (volume/time)

$C$  = coefficient (dimensionless) based on a ratio of  $r/H$

$r$  = radius of test hole (length)

$H$  = effective head (length) of water column (distance between pressure gauge and bottom of hole plus applied pressure at gauge)

This equation stems from the Bureau of Reclamation procedure.<sup>6</sup> The only modification from the procedure stated in reference 6 is that 10-minute rather than 20-minute intervals were used to hold the pressure. This was done because the packed off section was relatively short (on the order of several feet). Obviously at zero flow, it is impossible to have a measurable hydraulic conductivity. Therefore, using the reading error of the flow totalizer (0.02 gal) as a flow in the above equation allowed calculating the hydraulic conductivity. Using this flow nominally results in a hydraulic conductivity of  $10^{-7}$  cm/s or less.

Both double and single packer systems were employed. If a single packer system failed to work because of a suspected leak out the bottom of the pit, a double packer system was employed. In some cases, the bottom section of the hole was filled with cement grout and allowed to cure to provide a seal so that the single packer system could be used. In other cases, adjacent holes once tested were sealed with bentonite or cement to isolate one hole from another. Through trial and error, successful tests were performed on the grouted field-scale permeameter, TECT pit, and paraffin pit. However, packer data could not be obtained in the Type-H cement pit because of the relatively porous nature of the pit in the vicinity of the sodium sulfate drums.

Figure 21 shows the overall layout of equipment used for the packer testing, including nitrogen supply tanks to supply back pressure for both the packer and the water, a water supply tank, associated hoses, a flow totalizer, pressure gauge, and packer assembly downhole. Figure 84 is a schematic showing the dual packer system packing off the bottom of the grouted region with an individual packer used to isolate the bottom of the pit in an adjacent core hole. Figure 85 is a schematic showing a single packer system in use where the core holes penetrated the bottom of the grouted region. In this scenario, the bottom of the hole has been filled with cement and allowed to cure to isolate the system. What follows is a discussion of the individual packer data for the TECT pit, paraffin pit, Type-H pit, and grouted field-scale permeameter.

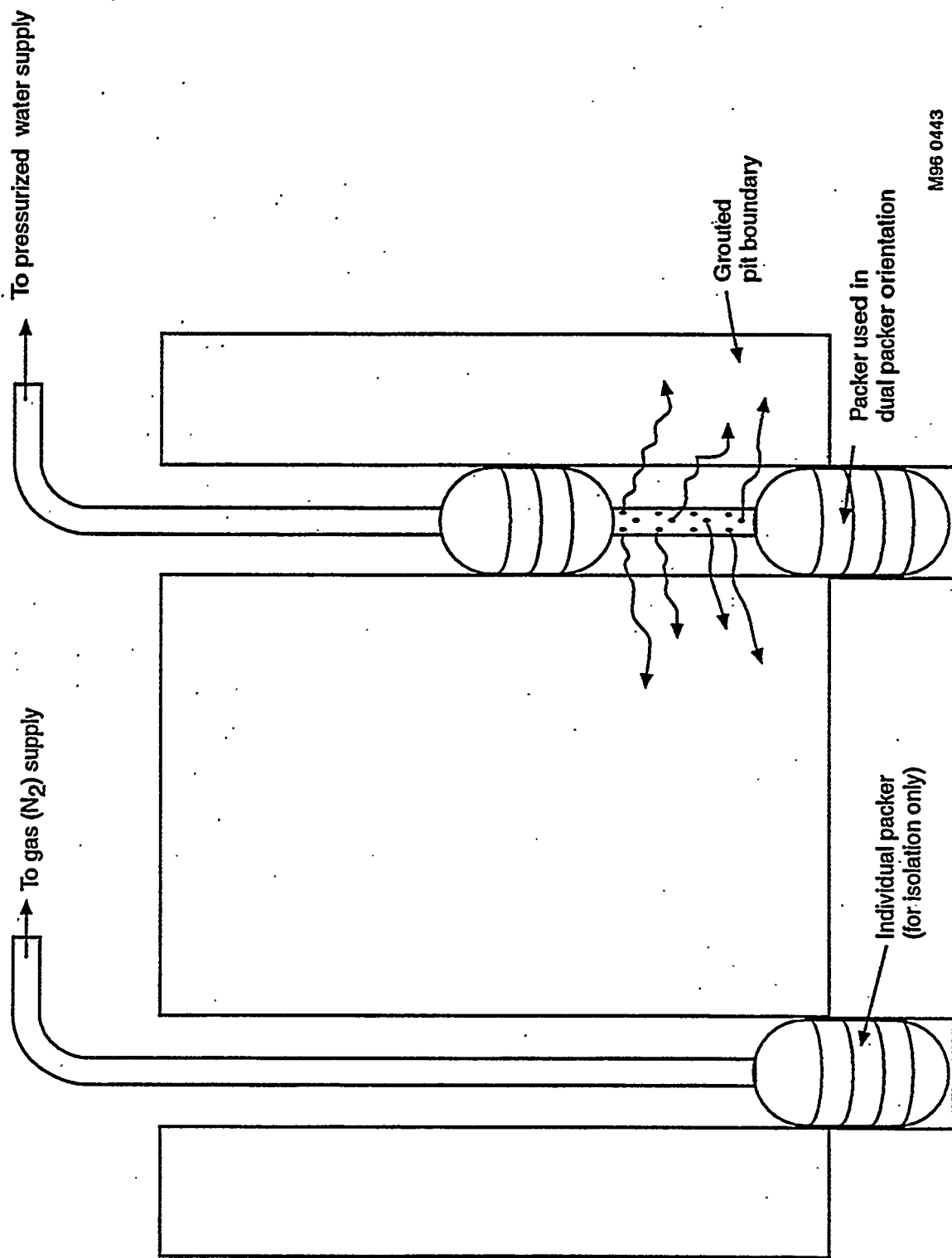


**Figure 84.** Schematic of packer system showing individual packer and a dual packer used in tandem to seal core holes that had penetrated the bottom of the grouted region (Graphic M96 0443).

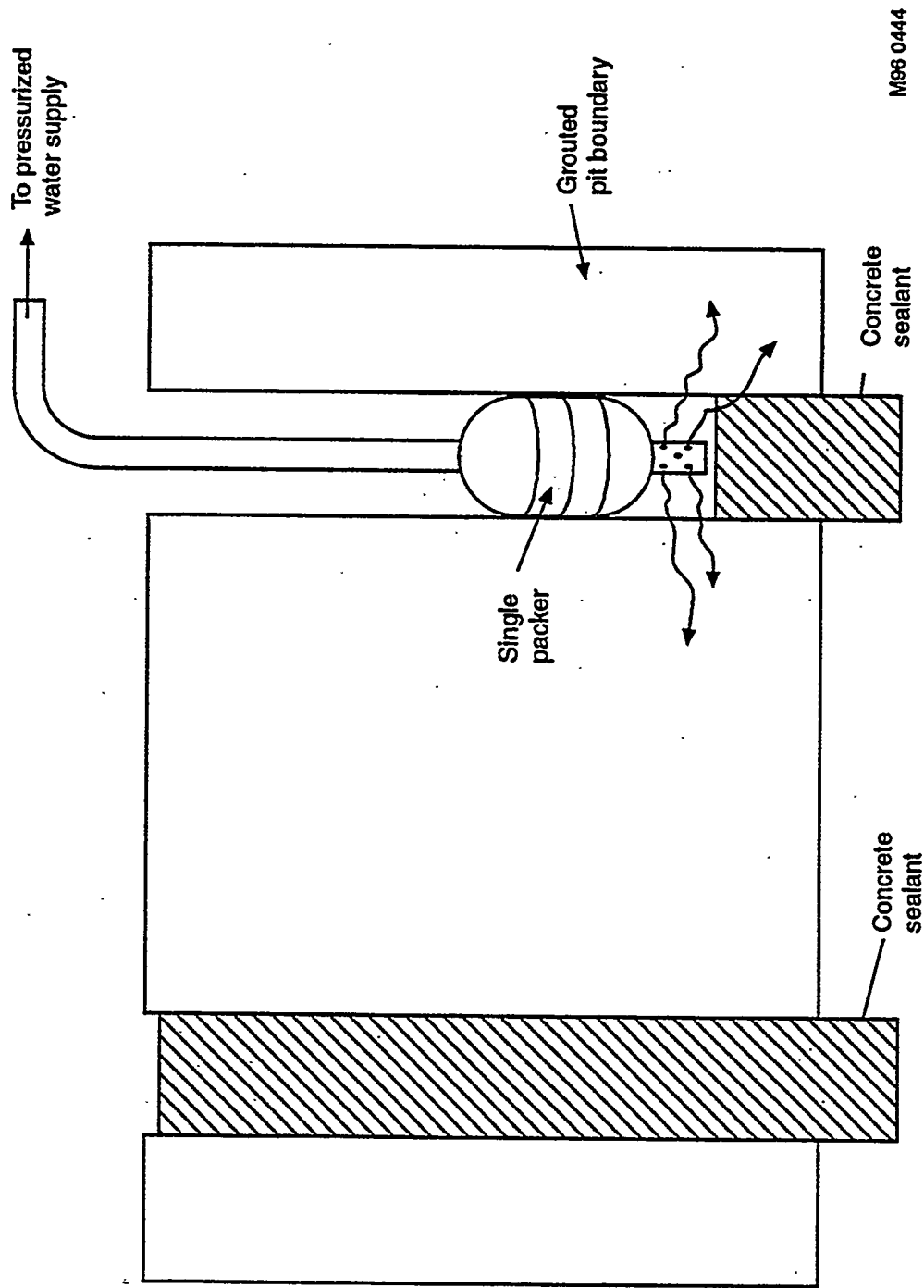


Figure 85. Schematic showing single packer with sealed adjacent core hole (Graphic M96 0444).

**4.8.1.1 TECT Pit.** For the TECT pit, three core holes were packer tested with only one of the three holes exhibiting a tight seal. A tight seal is defined here as a nominal 10-minute time with no flow at nominally 20 psi water pressure. Using the equation from reference 6, and further using the reading error on the flow totalizer (0.02 gal) when, in fact, zero flow was measured results in calculated hydraulic conductivities of less than  $10^{-7}$  cm/s. Table 11 summarizes the packer data for the TECT pit showing that core hole 1 (refer to Figure 53 for the orientation of the holes).

Core holes 2 and 3 could not be sealed, even with using the double packer technique and the individual packer arrangement shown in Figure 84. For these core holes, the original core hole extended through the bottom of the grouted region; and it is possible that water flowed out the bottom of either core hole 2 or 3 to adjacent positions and cross communicated with the adjacent holes by flowing water under pressure in the ungrouted soil matrix under the pit. In addition, as discussed in the destructive examination section, core hole 3 displayed a large cavity possibly extending to core hole 2. After the bottom of the hole was sealed with cement, the packer test was successfully run in core hole 1 with less than  $10^{-7}$  cm/s results. Figure 85 is the test arrangement for this case.

**4.8.1.2 Paraffin Pit.** A packer test was successfully run on core hole 1 in the paraffin pit with less than  $10^{-7}$  cm/s hydraulic conductivity. However, attempts at performing a packer test in core hole 2 was not performed because a video log of the hole showed irregular pieces of metal that could have punctured the packer system. This positive result for core hole 1 is consistent with the discussion on the cores and destructive examination of the paraffin pit. Table 12 shows the data for core hole 1 (see Figure 53 for the location of the core hole). For this core hole, the hole did not extend below the grouted region, as the lessons learned from the packer testing in the TECT pit were utilized.

**4.8.1.3 Type-H Cement Pit.** An attempt was made to perform packer tests on the Type-H cement pit with poor results. Tight packer data could not be obtained on either core hole 1 or 2 (see Figure 53 for the location of the core hole), even using individual packer systems. In fact, both of these core holes displayed a strong flow of water under only a few psi out of the pit to ungrouted regions. Table 13 summarizes the packer data for the Type-H cement pit. Core hole 1 would not pressurize under packer testing, and flow was observed coming out the side of the spoils collection pit located approximately 3 ft north of the pit. For this core hole, approximately 30 gal of water was injected into the hole before terminating the test. For this pit, as well as the paraffin pit, this high-conductivity packer data persisted even though the core holes did not extend through the bottom of the grouted section.

For core hole 2, the same high hydraulic conductivity phenomena was observed. Water was injected at 2-8 psi, with copious flow coming out of the top surface of the ground approximately 3 ft from the southeast corner of the pit in a southeasterly direction (see Figure 86 showing a pool of water emanating from the top surface under the vehicle). Referring back to the section on destructive examination, it was speculated that the 14-sack mix (1:1 by mass concrete/water ratio) did not mix well with a drum of sodium sulfate in the southeastern portion and at the bottom of the pit near where core hole 2 was located. This poor mixing combined with a relatively porous soil in the southeastern region and a hydrofractured lens of cured grout to focus the flow caused the flow of water to the surface.

**Table 11.** Summary of packer test for the TECT pit.

Core Hole	Time (min)	Q (ft <sup>3</sup> /s)	C	Pressure (psi)	R (cm/s)
CH-1 <sup>a</sup> (5.3–7.0-ft interval)	0–5	$3.7 \times 10^{-5}$	50	2	$1 \times 10^{-5}$ <sup>b</sup>
	5–16	$8.4 \times 10^{-6}$	51	7	$1.2 \times 10^{-6}$
	16–26	$4.6 \times 10^{-6}$	80	14	$2.6 \times 10^{-7}$
	26–36	$2.3 \times 10^{-5}$	100	21	$7.6 \times 10^{-7}$
	36–48	$4.6 \times 10^{-6}$	80	15	$2.5 \times 10^{-7}$
	48–58	$4.6 \times 10^{-6}$	56	8	$5.6 \times 10^{-7}$

a. CH-2, CH-3 could not seal even with double packer. Holes were filled with bentonite. Bottom of core hole 1 was refilled with Portland cement to seal the bottom because it was suspected that the original core drill extended below the grouted section in core hole 1.

b. Suspected lines filling.

**Table 12. Summary of packer testing for paraffin pit.**

Core Hole	Time (min)	Q (ft <sup>3</sup> /s)	C	Pressure (psi)	K (cm/s)
CH-1 <sup>a</sup> (6.3-7.8-ft interval)	0-2	$1.3 \times 10^{-3}$	42	3	$3.6 \times 10^{-4}$ <sup>b</sup>
	2-13	$4.2 \times 10^{-6}$	55	8	$5.24 \times 10^{-7}$
	13-26	$3.8 \times 10^{-6}$	85	16.5	$1.8 \times 10^{-7}$
	26-36	$4.6 \times 10^{-6}$	100	23	$1.4 \times 10^{-7}$
	36-46	$4.6 \times 10^{-6}$	85	16	$2.23 \times 10^{-7}$
	46-56	$4.6 \times 10^{-6}$	55	8.5	$5.5 \times 10^{-7}$

a. For core hole 2, a good seal could not be achieved with the packer.

b. Suspected lines filling.

**Table 13. Summary of packer testing for Type-H cement.**

Hole	Time Duration (min)	Pressure (psi)	Flow (gal)
CH-1	NA	Would not pressurize	30
CH-2	NA	2-8	Copious flow; flow came up 3 ft to the SE of the SE corner of the pit



**Figure 86.** Core hole 2 in Type-H cement pit with water emanating from the top surface during packer testing (Photo 96-716-1-18).



**4.8.1.4 Grouted Permeameter—Packer Testing in the Grouted Permeameter.** Results of packer testing in the grouted field-scale permeameter showed that two of four core holes showed  $10^{-7}$  cm/s flow. One packer test could not be run because of the presence of metal debris that could have ruptured the packer, and a forth hole showed copious flow at all pressures. Table 14 summarizes selective packer data for the grouted field-scale permeameter. Core hole 2 located in the center of the permeameter showed  $10^{-7}$  cm/s hydraulic conductivity or less.

During examination of the video log, core hole 5 displayed a ragged edge of metal in the hole. Therefore, no packer testing was performed because of the potential for packer rupture. For core hole 3, a packer test showed copious flow into the matrix at all pressures and the packer test could not be performed. It is expected that this hole showed poor packer performance due to possibly ungrouted regions caused by drill refusal in that region during grouting and further that, during the coring operation, water flow washed out loose soil in this region.

For core hole 6, however, a tight packer test was performed indicating  $10^{-7}$  cm/s or less hydraulic conductivity as shown in Table 14. This was accomplished only after all the other core holes had been filled with Portland Type-1 cement and allowed to cure. Filling the other core holes with grout was required to seal communication pathways at the bottom of the field-scale permeameter. This good packer data for core hole 6 agrees with the good recovery (75%) observed for this hole. The good recovery and subsequent good packer test was attributed to excellent grout filling in this area of the pit as evidenced by a general heave of the region during grouting. Following packer testing, the excess water in the hole was removed and replaced with Type-1 Portland cement mixed with water for later large-scale hydraulic conductivity testing.

Valves on the outside of the permeameter were periodically opened during the packer testing, and no flow of water was observed. This indicates a tight matrix, which is in agreement with the calculated hydraulic conductivity of "less than  $10^{-7}$  cm/s."

#### 4.8.2 Hydraulic Conductivity Testing on the Grouted and Ungrounded Permeameters

Measurements of the hydraulic conductivity in specially prepared field-scale permeameters showed that buried waste has a hydraulic conductivity on the order of  $10^{-5}$  cm/s, which is lower by two orders of magnitude than previous data performed without field-scale permeameters.<sup>7</sup> In the jet-grouted system, the measured hydraulic conductivity was only on the order of  $10^{-6}$  cm/s or only a one-order-of-magnitude decrease from the ungrouted case. It was expected that a hydraulic conductivity of  $10^{-7}$  cm/s or less would have been achieved in the jet-grouted case based on laboratory testing of soil/grout mixtures.

There are three possible explanations for this unexpectedly high hydraulic conductivity performance for the grouted field-scale permeameter. One explanation is that nitrate salts within the permeameter cause poor curing of the Type-H cement, resulting in regions where there are a preferred pathway for water flow. A second explanation is that water preferentially runs down the sides of the permeameter because the grouted soil-and-waste matrix may shrink away from the walls when cured, also resulting in a measured too high hydraulic conductivity for the matrix. Finally, a third possibility is a combination of the above two explanations.

Full-scale controlled mass balance hydraulic conductivity testing was performed on both the ungrouted field-scale permeameter containing typical buried simulated waste and a field-scale

**Table 14.** Summary of packer test data for southern culvert.

Core Hole <sup>a</sup>	Time (min)	Q (ft <sup>3</sup> /s)	C	Pressure (psi)	Hydraulic Conductivity k(cm/s)
CH-2 (5.8-7.0-ft interval)	0-10	$4.6 \times 10^{-6}$	52	7	$6.8 \times 10^{-7}$
	10-20	$4.6 \times 10^{-6}$	75	12	$3.2 \times 10^{-7}$
	20-28	$4.6 \times 10^{-6}$	90	18	$2.4 \times 10^{-7}$
	28-38	$4.6 \times 10^{-6}$	100	20	$1.6 \times 10^{-7}$
	38-50	$4.6 \times 10^{-6}$	78	13	$2.9 \times 10^{-7}$
	50-65	$4.6 \times 10^{-6}$	52	7	$6.6 \times 10^{-7}$
CH-6 (4.6-6.8-ft interval)	0-5	$2.3 \times 10^{-4}$	48	4	period of saturating $5 \times 10^{-5}$
	1-5	$1.2 \times 10^{-5}$	48	4	$2.7 \times 10^{-6}$
	5-15	$1.4 \times 10^{-4}$	51	6	period of saturating $2.4 \times 10^{-5}$
	15-30	$3.7 \times 10^{-4}$	70	12	period of saturating $2.8 \times 10^{-5}$
	30-40	$4.6 \times 10^{-6}$	80	15	$2.5 \times 10^{-6}$
	40-62	$2.1 \times 10^{-6}$	100	21	$7.0 \times 10^{-8}$
	62-73	$4.2 \times 10^{-6}$	80	14.5	$2.4 \times 10^{-7}$
	73-84	$4.2 \times 10^{-6}$	55	8	$5.4 \times 10^{-7}$

a. Core hole 3 did not have a tight hole; core hole 5 had metal pieces extending into the core hole, which would have ruptured the packer. Portland cement was placed in core holes 2, 3, and 5 before using core hole 6.

permeameter containing buried waste that had been jet grouted with Type-H cement. By using a field-scale permeameter to focus water flow through the matrix much like small-scale laboratory hydraulic conductivity testing, a controlled mass balance could be realized without water running horizontally into surrounding matrix. For both the ungrouted and the grouted field-scale permeameter, the falling head method (ASTM-2434) was utilized.<sup>8</sup> To accelerate the flow of water through both the grouted and ungrouted matrix, a 10-ft-high head pipe was utilized above the top of the field-scale permeameter much like the pressurization systems used in laboratory permeameter apparatus only at lower pressures. In this method, the hydraulic conductivity (K) was determined by measuring the drop in head of a head pipe and equating this to a volumetric flow through the field-scale permeameter and using the following equation:

$$K = LQ/ATH$$

where

K = hydraulic conductivity (length/time)

L = length of column

Q = total volume of fluid added to the head pipe in time T

A = cross-sectional area of field-scale permeameter

T = time

H = head of water in head pipe (length)

In the actual performance of the hydraulic conductivity tests, operational difficulties allowed a net head of water above the field-scale permeameter top of 4 ft. Only being able to achieve a 4-ft total driving head was the direct result of a top lid that was not heavy enough to withstand the upward force of the head of water in the head pipe, resulting in copious leakage out the seal between the lid of the field-scale permeameters and the top ring of the field-scale permeameter. Prior to emplacement of the lids, the systems were saturated with a standing head of water of about 1 ft inside the top ring as previously described. This was accomplished with the bottom valves first closed and then opened to ensure a flow of water through the system. Once saturation conditions occurred (evidenced by a head check with no change in level for a period of approximately 48 hours in the top pool surface of the field-scale permeameter), the lids were emplaced and the head pipes and associated safety ladders were installed. Water was introduced to the head pipes, and it was immediately obvious that a 10-ft head of water could not be obtained because of leakage between the lids and the top ring of the field-scale permeameter.

After several attempts at sealing from the outside, it was discovered that the leakage was caused by the lid actually lifting at the exact pound force exerted by the water head (about 4 in. of head up the head pipe) applied over the entire surface area of the lid. The decision was made to apply a new seal of the tar-like material and tie the lid to the field-scale permeameter rings using both steel plate and a turnbuckle system. These systems are shown in Figure 87. Once tied



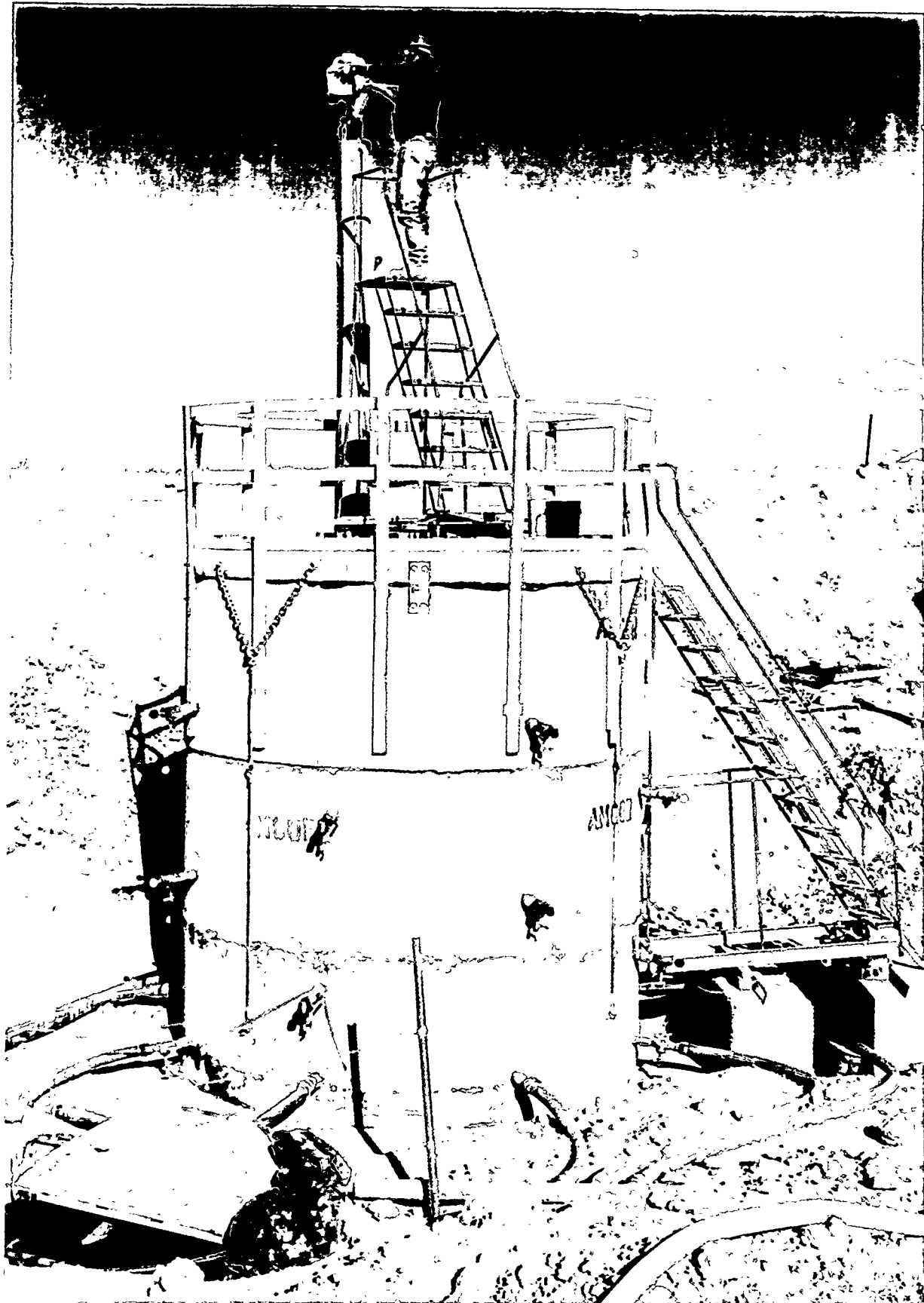


**Figure 87.** Completed ungrouted field-scale permeameter with lid tie-downs; worker shown introducing water to the head pipe (Photo 96-658-1-30).



down, it was discovered that a seal on the top lid could be maintained only if the water head in the head pipe was 22 in. or less. At 22 in. of water in the head pipe, there was a total head above the top surface of the grouted matrix in the grouted field-scale permeameter or ungrouted waste in the ungrouted field-scale permeameter of about 4 ft.

After sealing all visible leaks (basically just visible stains on the side of the field-scale permeameters) with mortar mix, the hydraulic conductivity testing was started. The hydraulic conductivity testing involved, in the ungrouted baseline field-scale permeameter, attaching hoses to the eight collection ports and fitting them to manifolds connected to collection tanks (Figure 87). In addition, Figure 87 shows a worker filling the head pipe to the 22-in. mark. Figure 88 shows details of the collection system, including manifolds and access ports, for the ungrouted baseline field-scale permeameter. Figure 89 shows the grouted field-scale permeameter fitted with buckets to collect outflow from the permeameter.

Table 15 summarizes the collected data from the hydraulic conductivity testing for the ungrouted field-scale permeameter, and Table 16 summarizes the data for the grouted field-scale permeameter. For each table, the hydraulic conductivity is listed for calculations that used for a volume of fluid the water placed into the system as well as the amount of water collected in either the holding tanks for the ungrouted field-scale permeameter or in the buckets for the grouted field-scale permeameter. In calculating these hydraulic conductivities, a head of water equal to 4 ft was used for each calculation, even though the actual head varied between periods of filling the head pipe. Using a constant 4 ft for head is a good approximation in that only a few gallons of water needed to be added on a any given day to get the head back up to 4 ft, indicating that the average head was between 2 and 4 ft at all times.

**4.8.2.1 Ungrouted Field-Scale Permeameter.** For the ungrouted field-scale permeameter, the total amount collected as outflow was 387.4 gal, and the amount placed in the field-scale permeameter was 413.6 gal over a period of nominally  $2.4 \times 10^6$  seconds, which nearly equals a perfect mass balance (a difference of only 26 gal out of nominally 400 gal). The hydraulic conductivity either calculated from the inflow or outflow was about  $2 \times 10^{-5}$  cm/s, which is two orders of magnitude less than that reported in reference 7. In reference 7, the surrounding soil may have preferentially absorbed water because a different test setup was used. In these tests, a battery of small (nominally 2-in.) tubes with a central supply tank were used. The tubes were placed into the ungrouted pit and gravity feed with water from the supply tank. The pit had been consolidated and saturated. However, it is possible that if the true hydraulic conductivity of the pit was on the order of  $10^{-5}$  cm/s, water introduced in the tubes may have run off the ungrouted but consolidated pit into looser packed surrounding soil resulting in an erroneously high reading of  $10^{-3}$  cm/s. In the subject test, the water is focused through the matrix, and the inflow and outflow agree lending credence to the data.

**4.8.2.2 Grouted Field-Scale Permeameter.** Examination of inflow and outflow data for the grouted permeameter shows that an unsteady condition prevailed throughout the test. There is a large discrepancy for the calculated hydraulic conductivity between using the amount of water added (inflow) and using the amount of water collected (outflow) as shown in Table 16. Both calculations reach an asymptote at the same  $10^6$  seconds. However, there is an order-of-magnitude difference in the two values. Based on the outflow data collected in the buckets, the hydraulic conductivity approaches  $10^{-6}$  cm/s, and for the inflow, the value approaches  $10^{-5}$  cm/s. It is expected that the outflow data are more accurate in this field-scale permeameter





Figure 88. Details of ungrouted baseline field-scale permeameter collection system (Photo 96-638-1-27).





**Figure 89.** Completed grouted field-scale permeameter showing lid tie-downs and bucket collection system for grouted field-scale permeameter (Photo 96-658-1-24).



**Table 15. Baseline culvert permeation data.**

Date	Collected Outflow (gal)	Added Inflow (gal)	Time Interval (s)	Hydraulic Conductivity Based on Outflow (cm/s)	Hydraulic Conductivity Based on Inflow (cm/s)
9/20/96	16.4	16.8	81,960	$2.6 \times 10^{-5}$	$2.6 \times 10^{-5}$
9/23/96	82.0	63.7	354,660	$3.0 \times 10^{-5}$	$2.3 \times 10^{-5}$
9/24/96	97.0	90.7	431,940	$2.9 \times 10^{-5}$	$2.7 \times 10^{-5}$
9/25/96	124.6	124.5	526,140	$3.0 \times 10^{-5}$	$3.0 \times 10^{-5}$
9/26/96	139.5	145.0	607,500	$2.9 \times 10^{-5}$	$3.1 \times 10^{-5}$
9/27/96	157.3	161.3	700,560	$2.9 \times 10^{-5}$	$2.9 \times 10^{-5}$
9/30/96	215.8	198.6	954,960	$2.9 \times 10^{-5}$	$2.7 \times 10^{-5}$
10/1/96	219.3	216.6	1,051,020	$2.7 \times 10^{-5}$	$2.7 \times 10^{-5}$
10/2/96	229.3	231.6	1,122,840	$2.6 \times 10^{-5}$	$2.6 \times 10^{-5}$
10/3/96	244.6	249.2	1,212,240	$2.6 \times 10^{-5}$	$2.6 \times 10^{-5}$
10/4/96	257.9	264.5	1,294,500	$2.6 \times 10^{-5}$	$2.6 \times 10^{-5}$
10/7/96	296.9	287.8	1,558,200	$2.4 \times 10^{-5}$	$2.4 \times 10^{-5}$
10/8/96	307.9	307.1	1,656,480	$2.4 \times 10^{-5}$	$2.4 \times 10^{-5}$
10/9/96	317.9	318.1	1,731,480	$2.3 \times 10^{-5}$	$2.3 \times 10^{-5}$
10/10/96	327.9	327.6	1,815,120	$2.3 \times 10^{-5}$	$2.3 \times 10^{-5}$
10/11/96	337.9	335.6	1,898,580	$2.3 \times 10^{-5}$	$2.3 \times 10^{-5}$
10/14/96	363.2	366.1	2,163,720	$2.2 \times 10^{-5}$	$2.2 \times 10^{-5}$
10/15/96	371.9	378.6	2,245,620	$2.1 \times 10^{-5}$	$2.2 \times 10^{-5}$
10/16/96	381.4	393.6	2,344,440	$2.1 \times 10^{-5}$	$2.2 \times 10^{-5}$
10/17/96	387.4	413.6	2,424,180	$2.1 \times 10^{-5}$	$2.2 \times 10^{-5}$

**Table 16.** Grouted culvert permeation data.

Date	Collected Outflow (gal)	Added Inflow (gal)	Time Interval (s)	Hydraulic Conductivity Based on Outflow (cm/s)	Hydraulic Conductivity Based on Inflow (cm/s)
9/20/96	6.2	9.1	75,000	$1.1 \times 10^{-5}$	$1.5 \times 10^{-5}$
9/23/96	14.5	24.9	348,300	$5.4 \times 10^{-6}$	$9.28 \times 10^{-6}$
9/24/96	16.3	39.4	422,160	$5.0 \times 10^{-6}$	$1.2 \times 10^{-5}$
9/25/96	18.5	48.4	512,880	$4.7 \times 10^{-6}$	$1.2 \times 10^{-5}$
9/26/96	20.7	50.0	594,900	$4.5 \times 10^{-6}$	$1.2 \times 10^{-5}$
9/27/96	22.7	64.8	688,500	$4.3 \times 10^{-6}$	$1.2 \times 10^{-5}$
9/30/96	28.6	79.8	940,500	$4.0 \times 10^{-6}$	$1.1 \times 10^{-5}$
10/1/96	30.7	87.8	1,040,100	$3.8 \times 10^{-6}$	$1.1 \times 10^{-5}$
10/2/96	32.3	92.6	1,111,080	$3.8 \times 10^{-6}$	$1.1 \times 10^{-5}$
10/3/96	34.1	100.9	1,199,100	$3.7 \times 10^{-6}$	$1.1 \times 10^{-5}$
10/4/96	36.3	107.8	1,283,400	$3.7 \times 10^{-6}$	$1.1 \times 10^{-5}$
10/7/96	41.7	120.8	1,545,660	$3.5 \times 10^{-6}$	$1.0 \times 10^{-5}$
10/8/96	43.9	129.1	1,644,900	$3.5 \times 10^{-6}$	$1.0 \times 10^{-5}$
10/9/96	45.6	134.7	1,720,140	$3.4 \times 10^{-6}$	$1.0 \times 10^{-5}$
10/10/96	47.7	140.5	1,803,900	$3.4 \times 10^{-6}$	$1.0 \times 10^{-5}$
10/11/96	50.0	146.0	1,891,080	$3.4 \times 10^{-6}$	$1.0 \times 10^{-5}$
10/14/96	54.5	163.8	2,150,940	$3.3 \times 10^{-6}$	$1.0 \times 10^{-5}$
10/15/96	55.8	170.3	2,233,560	$3.2 \times 10^{-6}$	$1.0 \times 10^{-5}$
10/16/96	52.0	181.8	2,332,380	$3.2 \times 10^{-6}$	$1.0 \times 10^{-5}$
10/17/96	58.3	192.1	2,412,360	$3.1 \times 10^{-6}$	$1.0 \times 10^{-5}$

because of the potential for collected leakage for this permeameter. The unknown collected leakage is part of the amount of water added. However, the amount of water collected presumably flowed through the matrix.

For the grouted field-scale permeameter, there existed a combination of small unmeasurable leaks that could be visually classified as "weeps." These collected weeps could have accounted for the fact that over the period of the testing, 54.9 gal of water was collected as outflow in the buckets and 193.1 gal was added in the head pipe meaning the total leakage was on the order of 138 gal in nominally  $2.4 \times 10^6$  seconds. Evaporative losses in the collection bucket during that timeframe only account for about 15 gal. Therefore, the true discrepancy between inflow and outflow is 123 gal.

Another possibility for the mass difference is that the cured Type-H cement absorbed the additional 123 gal. Both the concept of collected weeps and of Type-H cement absorbing the excess mass are speculative. The fact that the data settle to an asymptote suggests that a steady state had been achieved. However, the value of nominally  $10^{-6}$  cm/s was disappointingly high compared with the expected value of  $10^{-7}$  cm/s or less as indicated by the packer data discussed in the previous section and also observed for laboratory samples of Portland cement/soil mixtures. It is also possible that the excess water input to the field-scale permeameter compared with the outflow was occupying small regions that had not been saturated previously. There was no way to quantify the collected weeps, so this idea is only speculative.

One of the explanations for the relatively high hydraulic conductivity is that the matrix has a preferred migration path in connected zones involving the nitrate salts. A nitrate salt drum was located in each of the three rings, and incomplete mixing or poor curing of the Type-H grout could have created a zone with relatively high hydraulic conductivity. Recall that in the examination of the Type-H pit, most of the matrix appeared solid except in the region of a drum of sodium sulfate where the matrix appeared porous. In fact, packer testing could not be performed. In addition, when analyzed, the nitrate salt concentration in the collected effluent from the grouted field-scale permeameter was 5,360 ppm nitrates and 0.25 mg/L cerium (see Appendix D for completed analysis) from the nonsoluble cerium oxide tracer placed in each container. The nitrates were soluble in the flowing water, but the cerium was not. Cerium's presence in the collected water indicates a mechanical tracer movement through the medium.

Another explanation for the high hydraulic conductivity measurement is that the matrix shrunk away from the walls during curing, and a preferred pathway occurred in the annulus region. Metal rings (extending 3–4 in. into the matrix) were added to each of the rings to cause a damming effect for water flow down the walls. These rings focused water flowing down the walls back into the matrix. It is possible that shrinkage of the matrix upon curing caused a gap formation. On any given day, approximately 7 gal of fluid was added to the pool of fluid on top of the field-scale permeameter to maintain a level during the hydraulic conductivity testing shown in Table 16.

For the 10-ft-diameter 10-ft-high field-scale permeameter, 7 gal of fluid could fill a gap that was only .035 in. With this small a gap, it is not clear whether surface tension effects would have kept the water from falling. However, there is other evidence that supports the gap theory as follows. During packer testing, 12 of the valves in the system, including three of the bottom

valves, were opened. In that testing, no water flowed out the valves, suggesting that the interior system was impervious to flow or at least a very low permeability and that water could be flowing down the walls during the falling head hydraulic conductivity testing. It was also observed that water flow in the bottom valves started only after a head was established in the top of the field-scale permeameter, although this explanation could support either the relatively high preferred path idea in the interior of the matrix due to the nitrate salts or the gap idea.

For the water flowing down the gap idea, the presence of the nitrate salts in the effluent could be accounted for due to a drum of nitrates that was near the outer gap. The jet-grouting operation could have thrown poorly cured and poorly mixed nitrate salts to the edge of the field-scale permeameter, and water flowing down the gap could have dissolved nitrate salts collected in the bottom valves.

One puzzling problem with all of these ideas is the presence of up to 1 ft of INEL soil covering the bottom valves, which should act as both a filter to flow of any insoluble tracer (cerium oxide) and should also slow the general flow of water regardless of mechanism (see Figure 90 for a schematic of the drilling details). This layer of soil may cause another effect in the overall mass balance of water flow in that it might not have been totally saturated prior to the start of the hydraulic conductivity testing. If not totally saturated during the so-called saturation period (a period of 20 days with a 1-ft head on the top of the field-scale permeameter prior to actual testing), any water that gets down to the bottom of the field-scale permeameter could be saturating this soil.

For example, the volume occupied by this soil is 587 gal; and at 33% voids in this soil to absorb water, there was the potential to absorb up to 193 gal of water. Comparing the 193 gal of potential void space in this 1-ft layer to the 138-gal difference (123 gal accounting for evaporative loss in the collection buckets) between what was added and what was collected could account for the mass balance imbalance. The core holes did not penetrate to this lower level, so there is no way to actually determine if the jet-grouting operation actually grouted this region or if it remained intact. In destructive examinations of jet-grouted soil columns,<sup>1</sup> the soil column is usually limited to a fairly well-defined column up to 28 in. in diameter, with small areas of hydrofractured grout tendrils at random positions. There is no penetration of grout downward, only outward from the drill stem.

Also, based on past experiments,<sup>1,2</sup> a pool of Type-H cement grout in the bottom of the field-scale permeameter would not penetrate the fine INEL silty clay soil by permeation. Referring to Figure 90, the actual grouting started at approximately 16 in. from the bottom because the nozzles on the drill stem were 4 in. above the bottom of the terminal position of the drill and, when added to the approximately 12 in. of soil, equals 16 in. of potentially ungrouted matrix that could absorb migrating water.

Another idea about the soil layer in the bottom of the field-scale permeameter is that this layer is of relatively low permeability ( $10^{-6}$  cm/s) but thin compared to the entire height of the field-scale permeameter. Water introduced in the top may have readily run down any gaps formed between the grouted soil-and-waste matrix and the inside diameter of the field-scale permeameter and then encountered the soil layer. The net result is a measured hydraulic conductivity of  $10^{-6}$  cm/s, which could be a false indication of actual soil-and-waste matrix.

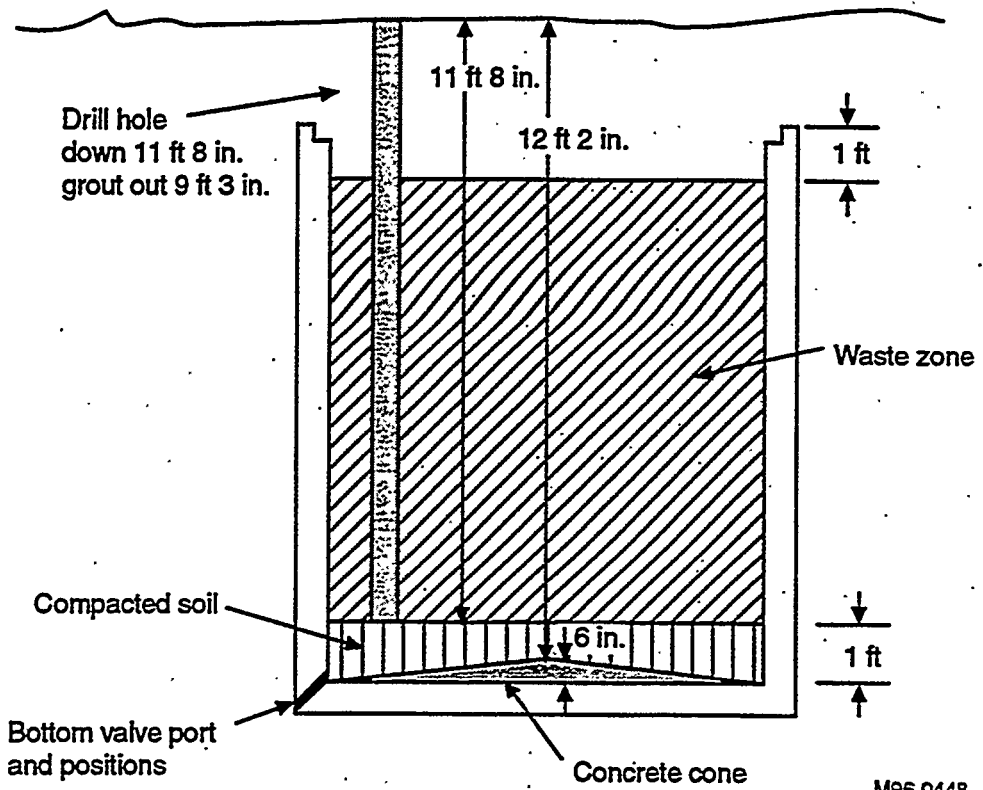


**Figure 90.** Relative position of drill grout hole and bottom layer of soil (Graphic M96 0448).

Referring back to the discussion on the ungrouted field-scale permeameter, the same 12 in. of soil existed in the ungrouted field-scale permeameter. In the discussion on the ungrouted field-scale permeameter, it was suggested that the  $10^{-5}$  cm/s conductivity was a proper measurement compared with the 1987 value of  $10^{-3}$  cm/s using a potentially inferior method.<sup>7</sup> The 12 in. of soil in the subject test could, in fact, have provided a relatively high resistance to water flow, when the actual soil-and-waste zone may have had considerably higher water hydraulic conductivity, perhaps  $10^{-3}$  cm/s. The combined effect of the 12 in. of soil at  $10^{-6}$  cm/s and the soil and waste at  $10^{-3}$  cm/s would then be measured as  $10^{-5}$  cm/s. This idea is also speculative.

In summary, the data are inconclusive for the true hydraulic conductivity of the Type-H cement monolith inside the field-scale permeameter. The packer tests suggest regions within the permeameter of less than  $10^{-7}$  cm/s. Yet, the overall falling head tests show  $10^{-6}$  cm/s. It is speculated that some combination of the gap between the field-scale permeameter wall and the matrix and poorly cured grout due to the presence of nitrate salts caused the unexpectedly high hydraulic conductivity. The only explanation for the presence of the tracer cerium oxide is that the nitrate drum in the bottom ring of the field-scale permeameter was in contact with the potential gap, and water flow entrained the micron-sized particles of cerium oxide out of the system through the bottom valves.

It is abundantly clear that in future experiments involving these field-scale permeameters, care must be given to the bottom layer of material and further that any gaps between the grouted soil-and-waste matrix and the inside diameter of the field-scale permeameter need to be sealed. This could have been accomplished by removing a key way around the top inside diameter between the soil-and-waste matrix and the culvert wall and filling it with epoxy. This would have forced water to flow through the matrix rather than through any gaps between the waste and the wall of the field-scale permeameter. It is recommended that the falling head hydraulic conductivity test be redone for both the ungrouted field-scale permeameter and the grouted field-scale permeameter. In the grouted permeameter, a key way should be cut around the edge of the grouted matrix and the space be filled with epoxy, thus bonding the wall of the permeameter to the matrix. In the ungrouted permeameter, the test should be redone utilizing more of the access ports as an indication of where the water is preferentially flowing.

## 4.9 Water Migration Study During Grouting

Movement of excess moisture away from Pit D following the Type-H cement grouting operation was investigated using the neutron probes. The objective of using neutron probes to monitor water movement was to assess the moisture contents in sediments near the pit and to determine if water in the grout mixture was sufficient to mobilize waste constituents. Data from the neutron probes indicate that water introduced to the pit and surrounding sediments as part of the grout mixture had little effect on moisture levels in ungrouted sediments outside the pit. Detailed analyses are in Appendix E.

Moisture was monitored using the neutron probe. Thirteen neutron-probe access tube (NAT) holes were drilled in and near the pit (Figure 91). A set of four holes was located on each of three sides of the pit (north, east, and south) at distances of 1, 2, 3.5, and 5 ft from the closest pit perimeter (as shown in Figure 91). In addition, one hole was drilled through the waste at the center of the pit. All holes were drilled to the basalt. NAT holes were monitored before

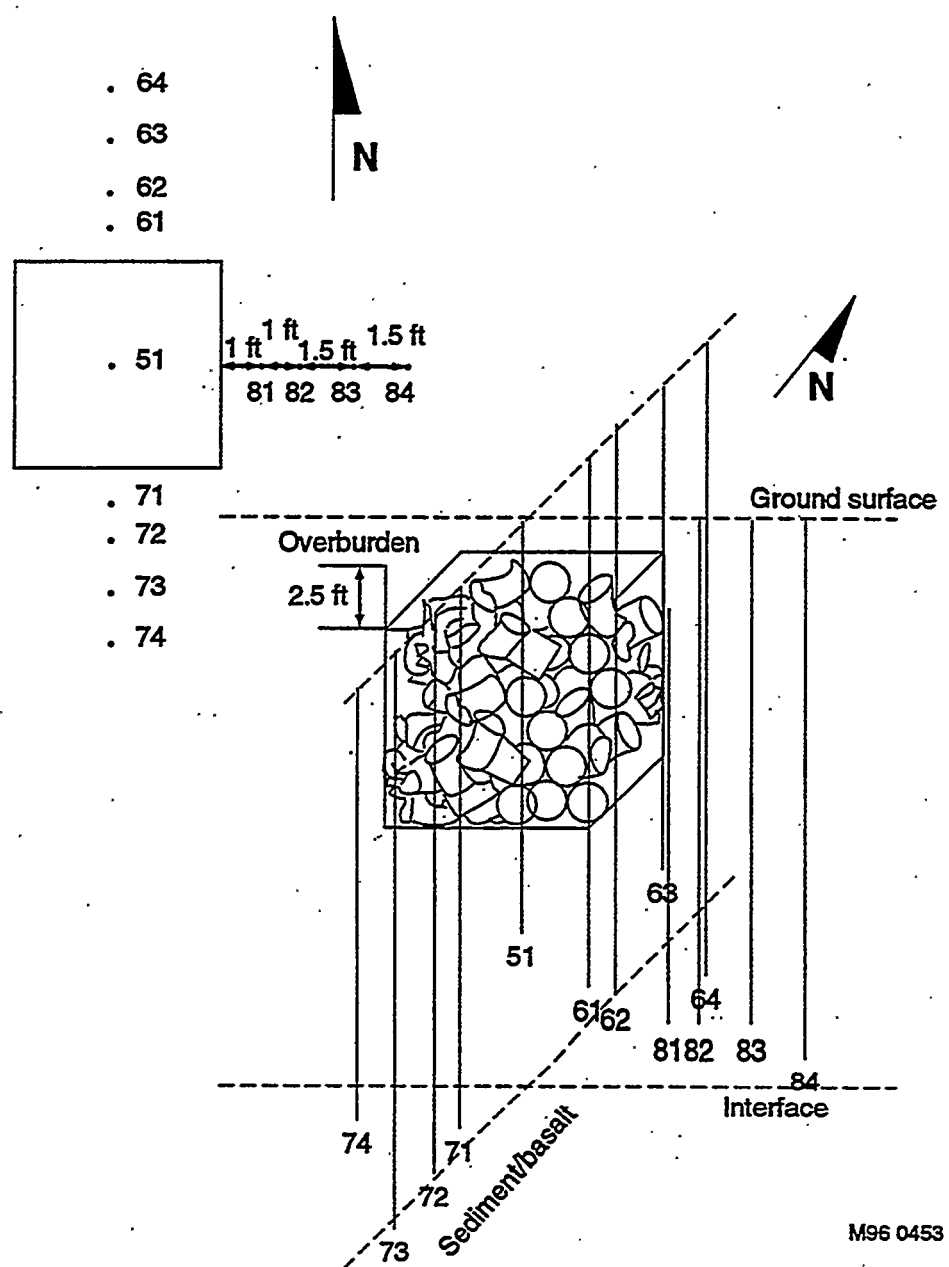


**Figure 91.** Plan-view and 3-D map of Pit D (Graphic M96 0453).

the August 8, 1996, grouting to establish ungrouted moisture contents for the sediments. After introduction of the grout, the holes were monitored twice before additional water was introduced into the pit and surrounding sediments by the drilling of core holes 1 and 2 into the Pit D monolith on August 22 and 23 and by packer testing, conducted on August 23. The test was concluded by monitoring most of the holes three additional times, with a final monitoring on October 11, 1996.

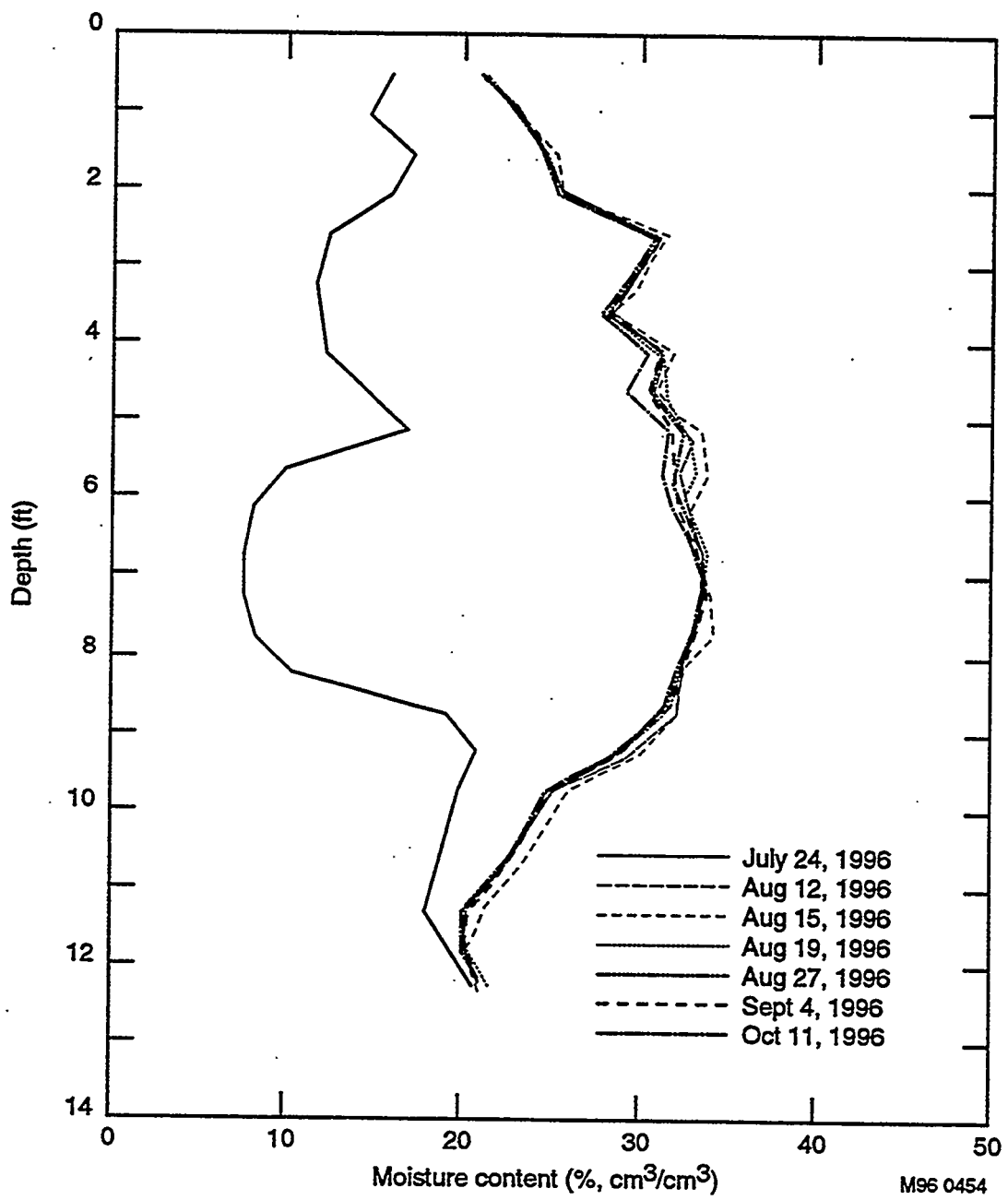
Table 17 lists estimated moisture increases (positive values) and decreases (negative values) derived from neutron-probe readings taken a few days after the August 8 grouting and the August 22-23 core drilling/packer testing. These estimates were obtained by integrating the differences between subsequent moisture content profiles over the length of the access tube. This technique results in an estimate for the amount of total moisture change in the vicinity of each NAT hole but does not reflect total amounts of moisture increases or decreases for the Pit D area.

Figure 92 shows the neutron moisture profiles for NAT-51, the hole drilled in the center of Pit D. The solid line shows moisture contents inside the pit before grouting. All other profiles follow grouting. Although the postgrouting profiles indicate that considerable moisture has been introduced to the pit, their relatively unchanging nature over time indicates that the moisture is bound in the cured grout. Some changes are noted (about 4 to 6.5 ft) in the postgrout profiles, suggesting that grouting in this area of the pit is probably not thorough. Grout may not have completely permeated materials at this depth interval.

Overall, the moisture data indicate that water introduced to the pit and surrounding sediments as part of the grout mixture had little effect on moisture levels in ungrouted sediments outside the pit. Because the water is bound in the cement monolith, it has not significantly affected the moisture contents in sediments outside the grouted sections. The results suggest that because there is little free water associated with the grout after it has cured, there is insufficient moisture for the possible mobilization of waste components.

**Table 17.** Estimated water increases and decreases resulting from moisture changes in sediments at NAT sites following grouting and drilling/packer testing.

NAT hole	Increases (-decreases) in moisture around each hole (inches of water)	
	Grouting (July 17/24–Aug 12)	Core drilling/packer test (Aug 19–27)
NAT-51	20.48	(-0.49)
NAT-61	5.02	(-0.113)
NAT-62	0.45	0.13
NAT-63	0.35	0.43
NAT-64	0.07	0.06
NAT-71	1.01	(-0.18)
NAT-72	0.43	0.06
NAT-73	0.11	0.13
NAT-74	(-0.02)	(-0.16)
NAT-81	0.58	0.14
NAT-82	0.27	(-0.02)
NAT-83	0.18	0.07
NAT-84	0.25	(-0.00)



**Figure 92.** Moisture content profiles for NAT-51 (Graphic M96 0454).

## 5. DISCUSSION OF RESULTS-RELEVANCE OF TECHNOLOGY

The technology of jet grouting buried waste sites to provide stabilization and containment has been shown to be practicable. Filling voids in the waste eliminates the potential for subsidence and for compromise of the integrity of any cap placed atop the waste. In the subject test, a variety of grouting materials have been demonstrated to be field implementable, including TECT, high-sulfate-resistant Portland cement, and paraffin. This adds to the body of knowledge from other related testing by Technology Development in FY-94 and FY-95, which included demonstrating jet groutability of Type-1 cement and two-phase injection of acrylic polymer. In addition, the FY-94 testing demonstrated that puncturing the buried waste containers as part of the jet-grouting process (driving the drill stem through the containers) could be accomplished with no release of tracer material from the containers to the air surrounding the drill rig.

The difficulty encountered when jet grouting the INEL-developed iron oxide solutions and the water-based epoxy material in the subject test underscores the need for pregrouting checkout of the materials rather than a failure of the materials. The iron oxide solutions are a potentially inexpensive method of providing stabilization and containment of buried waste for geological times because of the abundance of naturally occurring stable iron oxide (hematite) zones throughout the United States. Therefore, the difficulty encountered in the subject testing must be put into a long-term perspective. What is needed for the INEL iron oxide material to be implementable is a refinement in the slaked lime slurry, possible use of a higher pressure B side pump, and an investigation into nozzle design.

Other potential areas of investigation include the possibility of injecting each phase of the material as a single-phase material. The water-based epoxy requires a refinement in the B part component to reduce the overall viscosity of the material. Better quality control over the proprietary ingredients and pretesting of the materials in the high-pressure pumps would have uncovered the problems encountered, and possible solutions could have been overcome. In fact, the water-based epoxy was a late addition to the program, replacing another promising but expensive material called polysiloxane. Because of time constraints to meeting grout-schedule deadlines, the quality control factors were overlooked. The lesson learned is that all future materials should be field tested in the "hundreds of gallons" quantities using the full-scale jet-grouting equipment prior to committing to thousands of gallons of material in a field test.

Another important finding that makes the technology further valid for buried waste sites is that the control of secondary waste has been demonstrated. Use of a thrust block to contain any grout returns eliminates unwanted potentially contaminated material from cluttering the work area. The thrust block, in fact, becomes part of the cap material.

Evaluation of the permeability of the grouted buried waste in full-scale field testing had mixed results in that the grouted field-scale permeameter displayed only  $10^{-6}$  cm/s hydraulic conductivity compared with the desired result of  $10^{-7}$  cm/s. However, packer testing in the various grouted materials displayed less than  $10^{-7}$  cm/s of hydraulic conductivity. These packer testing results were actually based on no observable measurement in packer flow. Rather, only the reading error on the flow totalizer was used as a flow rate to calculate the hydraulic conductivity. The actual hydraulic conductivity was potentially orders of magnitude lower. Sealing the potential gap between the waste and the field-scale permeameter wall in the grouted field-scale

permeameter using an epoxy material should result in water being forced down through the matrix. This is expected to result in a hydraulic conductivity of  $10^{-7}$  cm/s or lower.

Overall, the technology is ready to advance to actual hot waste applications. Ideal candidate buried waste sites include the transuranic buried waste at the INEL's Subsurface Disposal Area. These sites have interstitial soil of tightly packed clay that makes permeation grouting impossible. To provide subsidence control at buried waste sites mandates that the voids have to be filled. In buried containerized waste, either each container requires puncturing and filling with a grout material or some mechanical consolidation process needs to be applied. Mechanical solidification involves dropping large ("tens" of tons) blocks of solid material onto the top of the waste and reducing the voids in the waste by compaction. This technique has never been examined for the INEL buried transuranic waste site. It is suggested that if puncturing the waste is impossible for regulatory reasons, then a research program involving dynamic compaction should be investigated. In either case, it is mandatory to control the subsidence of buried waste sites prior to final capping efforts.

## 6. FULL-SCALE IMPLEMENTATION

This section provides information with which to evaluate the technology for full-scale operation using either the TECT, paraffin, or Type-H cement grout. An acre-sized transuranic waste pit 8 ft deep jet grouted in 2 years at the INEL Subsurface Disposal Area is assumed for discussion purposes. In general, it is assumed that a single-component grout is jet grouted at a rate of 12.5 gal per vertical foot of hole, resulting in 100 gal per 8-ft hole injected. In addition, a 2-ft triangular pitch matrix results in 24,000 holes per acre. Also, it is assumed that there will be an engineered cap placed over the waste by another program. It is further assumed that this technology is either a Record of Decision or a treatability study. Permitting costs, including any interaction with state and local governments, are not included but are assumed to equal half the cost of the actual remediation. Estimates for grouting are based on operations by the same vendor that supplied grouting for this demonstration using government-supplied equipment, with some additional parts purchased as capital equipment. If another vendor is chosen for this technology, an additional \$2 million in capital costs should be added to all estimates. Table 18 summarizes the estimated costs of full-scale implementation for an acre-sized pit: \$22 million for TECT materials, \$13.5 million for paraffin, and \$10.7 million for Type-H cement. These numbers equate to \$1,704 per cubic yard for TECT, \$1,045 per cubic yard for paraffin, and \$829 per cubic yard for Type-H cement. These cost values are at least an order of magnitude less than current costs associated with treatability studies for buried transuranic waste pits currently undertaken at the INEL.

**Table 18. Estimated costs of full-scale implementation for an acre-sized pit.**

---

Equipment and Capital Cost

1. \$75K for spare parts for high-pressure injection pump and drill system and associated plumbing systems. This will allow instantaneous change out of contaminated or failed equipment such that the operation is not impeded.
2. \$200K for a poured-in-place reinforced concrete thrust block including holes with neoprene wiper assemblies.
3. \$150K weather shield/shroud.

Site Preparation

\$50K to level the site.

Grouting

\$6,000K—24,000 holes at \$250/hole

Secondary Waste Management/Health Physics

\$375K, 1 full-time health physics professional for 2 years and a half-time waste disposal expert for 2 years.

Grout Material

TECT - \$12,000K = \$5/gal x 100 gal/ hole x 24,000 holes

Paraffin - \$4,800K = \$2/gal x 100 gal/ hole x 24,000 holes

Type-H cement \$2,400K = \$1/gal x 100 gal/ hole x 24,000 holes

Total Operating and Capital

TECT- \$18,850K

Paraffin - \$11,650K

Type H - \$9,250K

Management (10% of total)

TECT- \$1,885K

Paraffin - \$1,165K

Type H - \$925K

Profit (6% of total)

TECT - \$1,131K

Paraffin - \$699K

Type H - \$555K

Grand Total for 2-Year Project

TECT - \$21,866K

Paraffin - \$13,514K

Type H - \$10,730K

## 7. CONCLUSIONS/RECOMMENDATIONS

One commercial grout and four innovative grouts have been field demonstrated in the application of creating monoliths out of buried waste sites using jet grouting. The commercial grout is high-sulfate-resistant Portland cement (Type-H cement) mixed both 1:1 on mass and on volume. The innovative materials include low melting temperature paraffin, proprietary TECT, INEL-developed hematite, and proprietary water-based epoxy. Only Type-H cement, paraffin, and TECT have been shown to be implementable in the field. Specific conclusions are as follows:

1. Grouting of the TECT material can be efficiently accomplished with minimal grout returns and still fill voids in the pit. The paraffin grouting operation results in copious grout returns (about 33% of injected volume). However, long-term (multiday) cooling of the molten interior of the grouted pit results in considerable permeation of ungrouted soils, paper, and other porous material like wood, leaving all contents of the pit—both soil and waste—virtually soaked in paraffin.
2. Use of both TECT and paraffin in jet grouting of buried waste sites results in a cohesive (stand-alone) monolith with essentially no voids. The TECT material is difficult to retrieve because the resultant soilcrete in the monolith cures to a hard high-compressive-strength (greater than 1,000 psi) material. The paraffin monolith, while freestanding, is easily retrieved with a standard backhoe, and the retrieval operation causes minimal dust spread. Both of these materials can be recommended for jet grouting buried transuranic waste sites or radioactive soil zones. It is recommended that the TECT grout be used in applications where the monolith is left in an undisturbed state and that the paraffin material be applied for interim storage followed by retrieval at a later date. It is recommended that a spoils return management strategy be refined for application of the molten paraffin grout.
3. The TECT grout readily mixed with the organic sludge simulant (canola oil/kitty litter) and formed a cured cohesive monolith. This is in contrast to poor results with the Type-1 cement and the acrylic polymer grouting performed in previous experiments.
4. Once cured, the TECT pit was uncovered to show a solid monolith with small inclusions of ungrouted soil completely surrounded by grout. These inclusions represent approximately 15% of the pit volume. Paper material is completely encapsulated. However, upon retrieval, the paper separates from the soilcrete and has the potential for contaminant spread. For the paraffin, however, the inclusions of soil were completely permeated with paraffin prior to solidification, and there were virtually no positions not encapsulated with paraffin.
5. The Type-H cement is jet groutable in field application and forms a cohesive monolith following jet grouting, except in regions of high concentrations of a nitrate salt simulator sodium sulfate. Jet grouting did not form a hard mixture in the vicinity of a sodium sulfate drum located on the edge of a pit. Although jet groutable, the Type-H cement has a tendency to build up on filters and intermittently plug nozzles during injection when mixed 1:1 by volume (18-sack mix). However, when mixed 1:1 by mass (14-sack mix), plugging was not observed. Chemical similarities of sodium sulfate and nitrate relative to grout curing require further study.

6. The INEL-developed hematite material could not be jet grouted because of "filter caking" of the slaked lime slurry mixture. Any further applications would require solving the physical properties of the lime slurry or nozzles, pumps, and injection strategies of different design.
7. The proprietary epoxy material could not be jet grouted because the mixture's B part was too viscous to jet grout with existing nozzles. Diluting the material with water exacerbates the problem. A complete redesign of the nozzles may be required to apply this material.
8. The thrust-block concept for secondary waste management works well for controlling grout returns for the TECT grout. However, applying this idea to paraffin may require some modification or expansion of the volume within the thrust block. In either case, the concept appears workable for field application.
9. It is recommended that future applications devise an online flow meter that alerts operators of potential plugging during jet grouting. In the event that a plugged nozzle is detected, the procedure should attempt to regROUT the hole. In addition, procedures for handling (accepting) positions that experience drill bit refusal during drilling need to be developed.
10. Use of core and TV video log data in drilled core holes is in general agreement with destructive examination data. The TV logs show the sides of the core holes to exhibit a solid walled monolith, indicating that coring and the use of TV video logs may be a replacement for destructive examination.
11. Hydraulic conductivity testing using a controlled mass balance has shown that the ungrouted condition in an INEL-simulated buried transuranic waste pit has a hydraulic conductivity of about  $10^{-5}$  cm/s, which does not agree with previous data. In the previous data, water was free to flow isotropically through the matrix as well as horizontally away from the matrix, possibly accounting for the difference.
12. Hydraulic conductivity testing of the field-scale permeameter grouted with Type-H cement is inconclusive due to unsteady data. Packer testing shows less than  $10^{-7}$  cm/s conductivity, while the falling head method shows  $10^{-6}$  cm/s. It is thought that the grouted permeameter has a hydraulic conductivity lower than  $10^{-7}$  cm/s based on the fact that no water flowed out the opened access ports of the permeameter when the packer tests were being performed.
13. Packer testing of select positions in both the TECT and paraffin pit showed evidence that the general matrix is less than  $10^{-7}$  cm/s hydraulic conductivity. In addition, packer testing in select core holes in the Type-H cement grouted field-scale permeameter also showed less than  $10^{-7}$  cm/s, indicating a cohesive soil-and-waste matrix.
14. Moisture migration data indicate that water introduced to the pit as part of the operating process had little effect on moisture levels in surrounding soils. Therefore, containment migration is not thought to be promoted from the grouting process.
15. Coring of grouted matrix using water has the potential of adding considerable water to the matrix, which is desirable for achieving saturation conditions. However, the water can wash out loose debris in the core-reducing recovery.

16. It is recommended that (a) more extensive testing be performed on the grouted and ungrouted field-scale permeameters, (b) the grouted field-scale permeameter have a positive seal placed between its wall and the grouted soil-and-waste matrix at the top surface of the permeameter, and the falling head tests be redone, and (c) the falling head test for the ungrouted field-scale permeameter be redone using a more extensive array of access ports to track water flow.
17. The cost estimate shows that this technology is not cost prohibitive compared with other interim retrieval actions for buried waste being conducted at the INEL. Depending on grout material, buried waste can be stabilized for nominally \$1,000 per cubic yard.

In summary, the technology is ready to advance to actual hot applications. Ideal candidate sites include the buried transuranic waste pits at the INEL's Subsurface Disposal Area. The technology can also be applied to regions of contaminated soil that require containment against migration of contaminants.

## REFERENCES

1. G. G. Loomis and D. N. Thompson, *Innovative Grout/Retrieval Demonstration*, INEL-94/001, January 1995.
2. G. G. Loomis, D. N. Thompson, and J. H. Heiser, *Innovative Subsurface Stabilization of Transuranic Pits and Trenches*, INEL-95/0632, December 1995.
3. G. G. Loomis, *Test Plan Innovative Subsurface Stabilization Project*, INEL-96/0132, April 1996.
4. P. G. Shaw and J. R. Weidner, *Laboratory Performance Criteria for In Situ Waste Stabilization Materials*, INEL-96/0069, March 1996.
5. A. P. Zdinak, *Core Evaluations and Hydraulic Conductivity Measurements in Support of the INEL Waste Stabilization Project*, HMP-18, January 1997.
6. U.S. Department of the Interior--Bureau of Reclamation, *Ground Water Manual*, Water Resources Publication, First Edition, p. 480, 1977.
7. G. G. Loomis and J. O. Low, "In Situ Grouting for Improved Confinement of Buried TRU Waste at the INEL," *Proceedings from SPECTRUM '88, Pasco, Washington, September 11-15, 1988*.
8. *Standard Test Method for Permeability of Granular Soils (Constant Head)*, ASTM-2434, 1984.

## **Appendix A**

### **Programmatic Issues**



## **Appendix A**

### **Programmatic Issues**

#### **Modifications from Test Plan**

The major modifications are listed below.

1. The test plan called for up to 7 pits grouted with 7 different grout materials and two grouted field-scale permeameters. Budget was decreased following the planning phase and only 5 materials were evaluated including TECT, Paraffin, Epoxy, hematite, and Type-H cement (1:1 by volume for the field-scale permeameter and 1:1 by mass for Pit D). Only two field-scale permeameters were built and only one field-scale permeameter was grouted; however, hydraulic conductivity testing was performed on all testing systems.
2. The location of the pits were modified to the location shown in Figure 2. This was caused by the presence of the YURT which would; not allow heavy equipment traffic in the area.
3. The hydraulic conductivity tests were attempted as per the test plan; however, the falling head method in the field-scale permeameters could not be performed as planned using the entire 10 ft of head in the head pipes because of the presence of leaks primarily in the lid. These leaks are attributed to a bad seal design as discussed in the results section.
4. The schedule in the test plan was dramatically changed due to late construction of the pits and field-scale permeameters.
5. The grouted field-scale permeameter was grouted with Type-H cement mixed for an 18 sack per cubic yard mix meaning 1:1 by volume rather than the 1:1 by mass called for in the test plan. This was a mistake made by the ready mix plant.
6. Pit D was grouted with Type-H cement mixed 1:1 by mass or a 14 sack per cubic yard mix. This was not mentioned in the test plan.
7. The water-based epoxy grout and the hematite grout proved ungroutable with the existing nozzles and pumping systems. Only field trials were attempted. This left Pit C in reserve for FY-97 studies if desired.

#### **Health and Safety**

The safety engineer worked closely with the principal investigator on all phases of the project. The following are specific safety items that were implemented during the field testing. All workers and visitors wore safety glasses with side shields and steel toes boots. When a new worker or visitor wanted access to the site, a special training occurred and a orange card issued acknowledging the health and safety plan for the Cold Test Pit. When constructing pits, operators were encouraged to wear their seatbelts and when constructing waste drums proper

ventilation and protective clothing and dust masks were utilized. When operating earth equipment, proper barriers were placed to ensure that the walls are sufficiently far from the workers. When excavating the monoliths, the side burdens were managed to allow examination without wall cave-in. The grouting vendor controlled an exclusion zone around all grouting equipment to control potential injury from high-pressure injection devices. For the all grout materials instructions on the MSDS were followed (see attached MSDS). Safety and industrial hygienist will also help in identifying potential storage, spill, and handling procedures associated with the four materials.

### **Environmental Overview/Residuals Management**

Care was taken to avoid spillage during the grouting operation. However, some spillage was unavoidable and any spills were allowed to cure and retrieved and placed on a spoils collection pile. In fact all retrieved waste during the construction phase as well as all dumped (and mixed) material was placed on the pile for disposal at a sanitary landfill. Only water was used to clean out systems and this fluid was allowed to run onto the ground.

### **Quality Assurance**

All testing was done within the approved test plan. Any major changes to that test plan were coordinated by the principal investigator and the project manager with input from the Landfill Focus Area management. Any agreed upon changes were redlined in a copy of the test plan that is left in the Landfill Focus Area Trailer.

During all phases of the operation either the principal investigator, project manager or the technical assistant was present to ensure that the test plan was followed and the proper photographic record is keep and that the logbook entries are recorded.

The principal investigator continuously audited the testing activities to ensure that the data quality was not jeopardized. The quality representative for the landfill focus group made at least weekly visits to observe the operations. During the excavations of the field-scale permeameters and implementation monoliths, the safety engineer was present daily to apply direct guidance. The grout materials was handled at the direction of subcontractors.

## **Appendix B**

### **Details of Pit and Field-Scale Permeameter Construction**





17 #59 39

#121

38

#65

37

16

#19

#48

36

35

#57  
42

#58

41

#125

40

#50

33

18

19

SCALE: 1" = 1'

PITT A

1  
LAYER

COLD TEST PIT - 1996  
PIT A

---

Positions determined with Topcon electronic total station on 6-20-96  
by K. V. Beard. (Re-calculated 6-24-96).

Horizontal Datum: NAD 83, Idaho East Zone, State Plane Coordinates, feet.

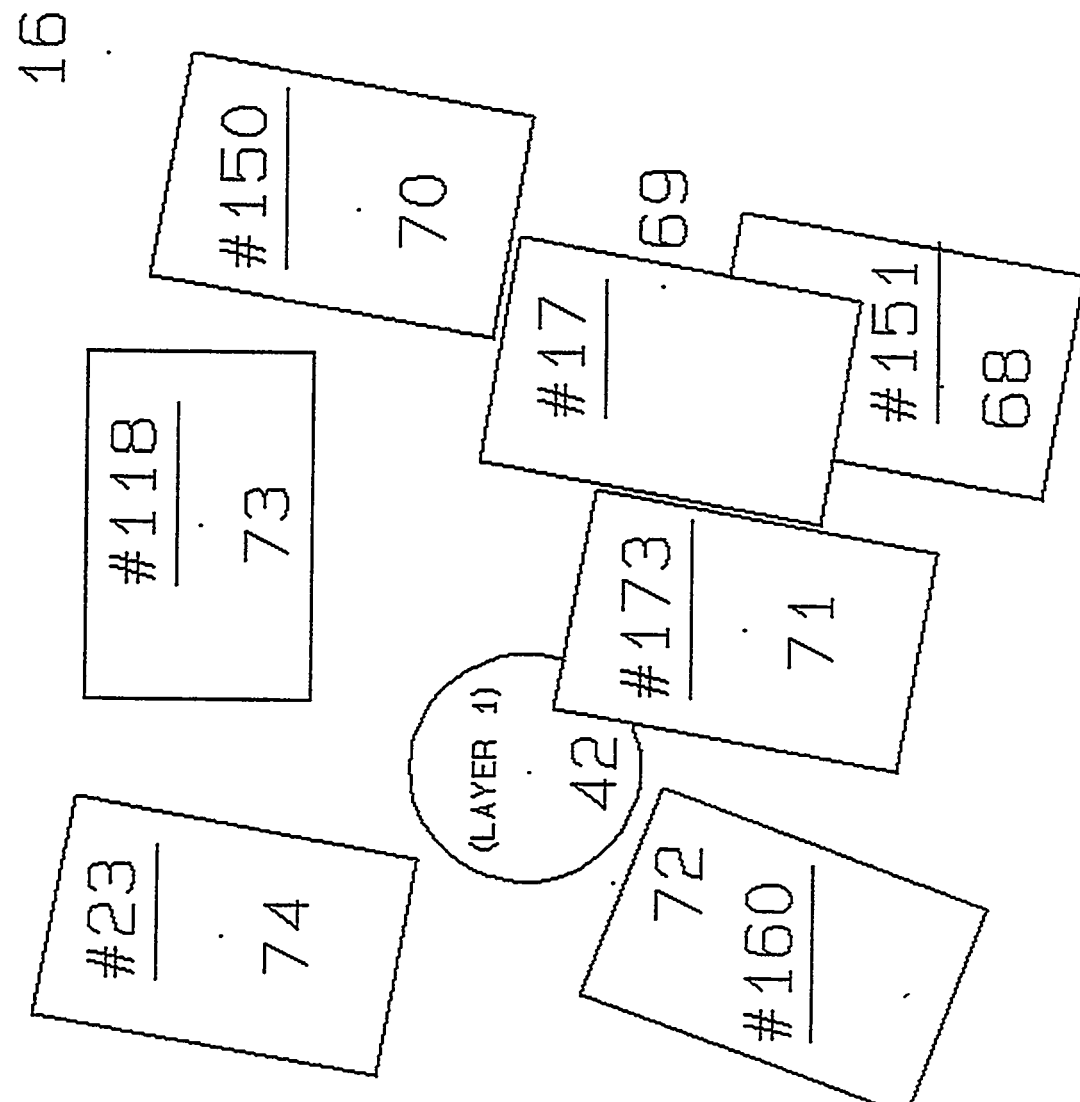
Vertical Datum: NAVD 88, feet.

PT#	North	East	Elevation
-----	-------	------	-----------

16	667477.6	422576.8	5014.0
17	667478.4	422570.8	5014.0
18	667472.5	422570.4	5014.3
19	667471.7	422575.6	5014.5
33	667472.2	422574.8	5016.1
34	667473.7	422575.0	5016.0
35	667475.6	422575.9	5015.7
36	667476.0	422574.4	5015.8
37	667477.6	422575.5	5015.6
38	667477.4	422573.2	5015.8
39	667477.3	422571.1	5015.9
40	667473.2	422572.3	5016.2
41	667474.3	422570.7	5016.0
42	667475.1	422572.7	5016.7

---

17



18



16

SCALE: 1 " = 1'

P T T

A

LAYER 2

19

COLD TEST PIT - 1996  
PIT A - LEVEL 2

---

Positions determined with Topcon electronic total station on 6-25-96  
by K. V. Beard.

Horizontal Datum: NAD 83, Idaho East Zone, State Plane Coordinates, feet.  
Vertical Datum: NAVD 88, feet.

PT# North East Elevation

---

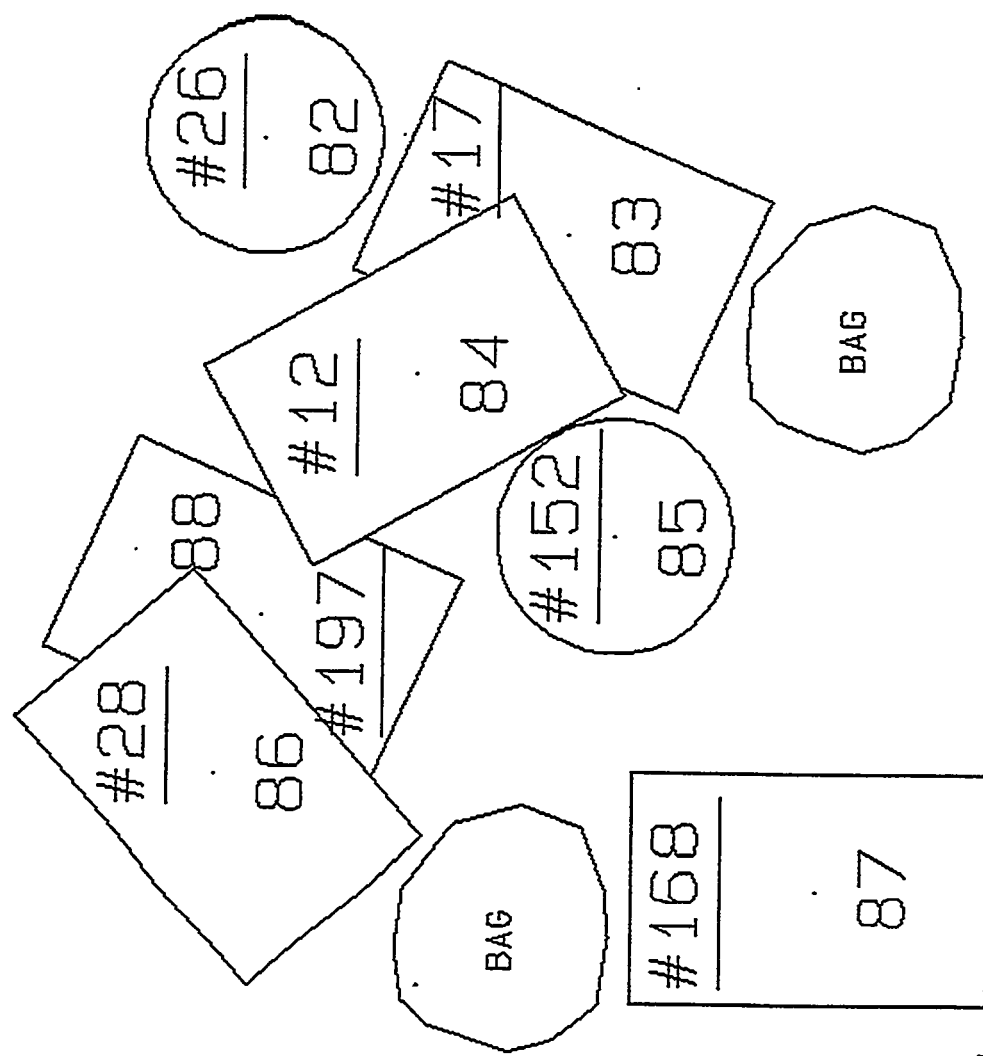
42	667475.1	422572.7	5016.7
68	667472.8	422575.0	5017.5
69	667474.4	422575.5	5018.4
70	667476.1	422575.9	5017.1
71	667473.9	422573.5	5017.5
72	667474.6	422572.1	5018.1
73	667477.0	422574.1	5017.1
74	667476.9	422571.7	5017.3

---

17

16

A N



18

19

COLD TEST PIT - 1996  
PIT A - LEVEL 3

---

Positions determined with Topcon electronic total station on 6-24-96  
by K. V. Beard.

Horizontal Datum: NAD 83, Idaho East Zone, State Plane Coordinates, feet.  
Vertical Datum: NAVD 88, feet.

PT# North East Elevation

---

16	667477.6	422576.8	5014.0
17	667478.4	422570.8	5014.0
18	667472.5	422570.4	5014.3
19	667471.7	422575.6	5014.5
82	667476.3	422575.8	5019.4
83	667474.6	422575.2	5018.4
84	667475.4	422574.4	5019.5
85	667474.3	422573.5	5019.7
86	667476.6	422572.2	5019.5
87	667473.2	422571.5	5019.4
88	667476.3	422573.1	5018.4

---

21

#62  
50

#1 1/2  
49

#147  
46

#61  
43

20

#21  
48

#56  
47

#18  
45

#54  
44

N

SCALE: 1" = 1'

PIT B

LAYER 1

23

22

COLD TEST PIT - 1996  
PIT B

---

Positions determined with Topcon electronic total station on 6-24-96  
by K. V. Beard.

Horizontal Datum: NAD 83, Idaho East Zone, State Plane Coordinates, feet.

Vertical Datum: NAVD 88, feet.

PT#	North	East	Elevation
-----	-------	------	-----------

20	667451.7	422573.7	5014.6
21	667452.3	422567.8	5014.7
22	667446.5	422567.2	5014.8
23	667446.1	422573.3	5014.5
43	667447.8	422568.0	5016.5
44	667446.9	422570.2	5016.4
45	667447.3	422572.5	5016.3
46	667448.7	422569.9	5016.4
47	667449.1	422572.5	5016.3
48	667450.7	422572.6	5016.4
49	667450.6	422570.2	5017.2
50	667450.7	422568.4	5016.4

---

## Pit #2 First Layer

N

Scale: 1" = 1'-0"

# 21  
Paper

# 56  
Wood

# 18  
Paper

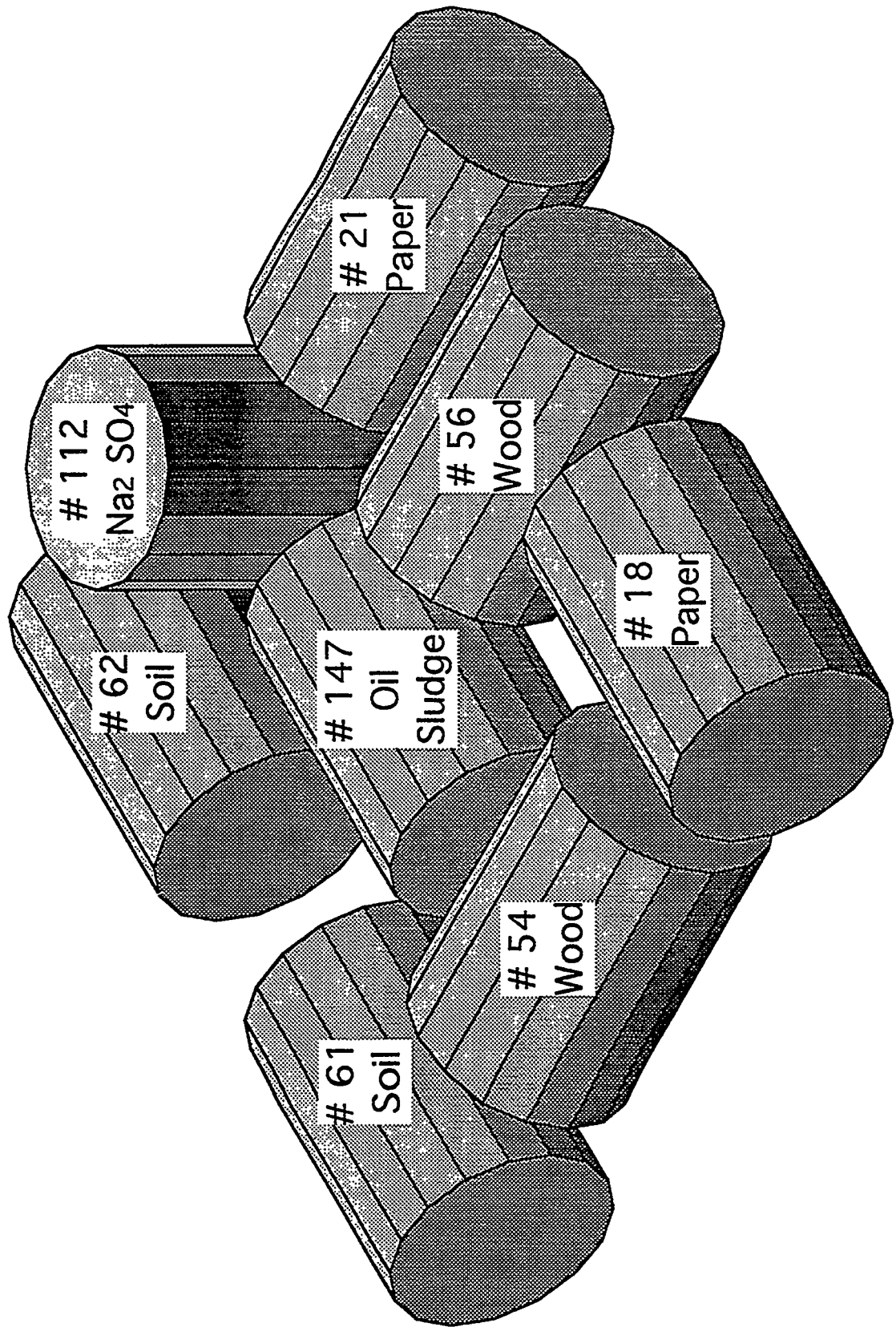
# 112  
Na<sub>2</sub>SO<sub>4</sub>

# 147  
Oil  
Sludge

# 54  
Wood

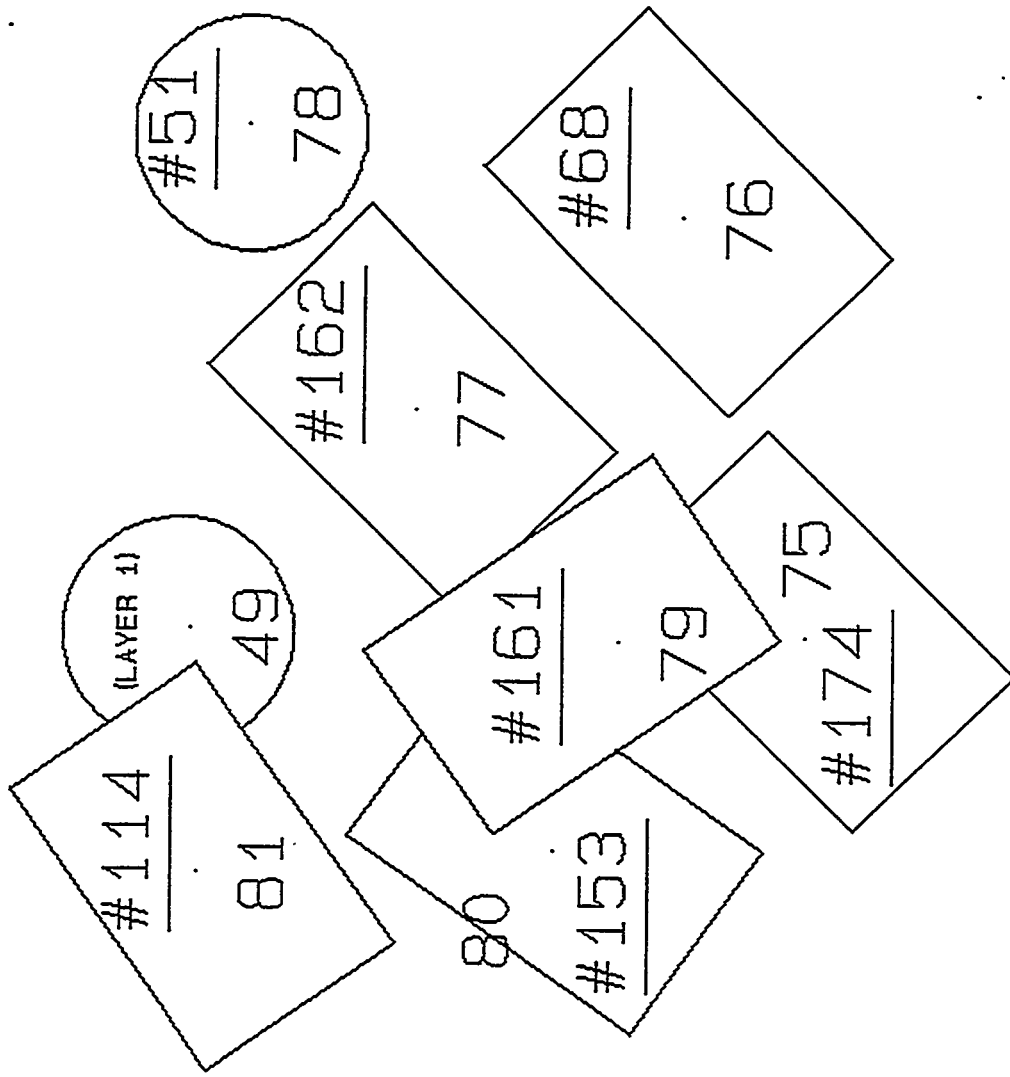
# 62  
Soil

# 61  
Soil



21

20



22

LAYER 2

23

SCALE: 1"=1'

COLD TEST PIT - 1996  
PIT B - LEVEL 2

---

Positions determined with Topcon electronic total station on 6-25-96  
by K. V. Beard.

Horizontal Datum: NAD 83, Idaho East Zone, State Plane Coordinates, feet.

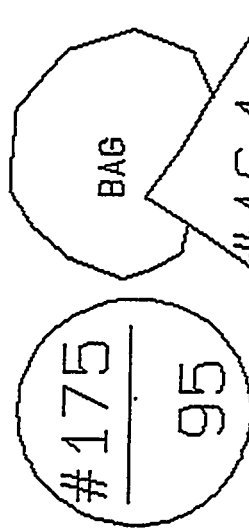
Vertical Datum: NAVD 88, feet.

PT#	North	East	Elevation
-----	-------	------	-----------

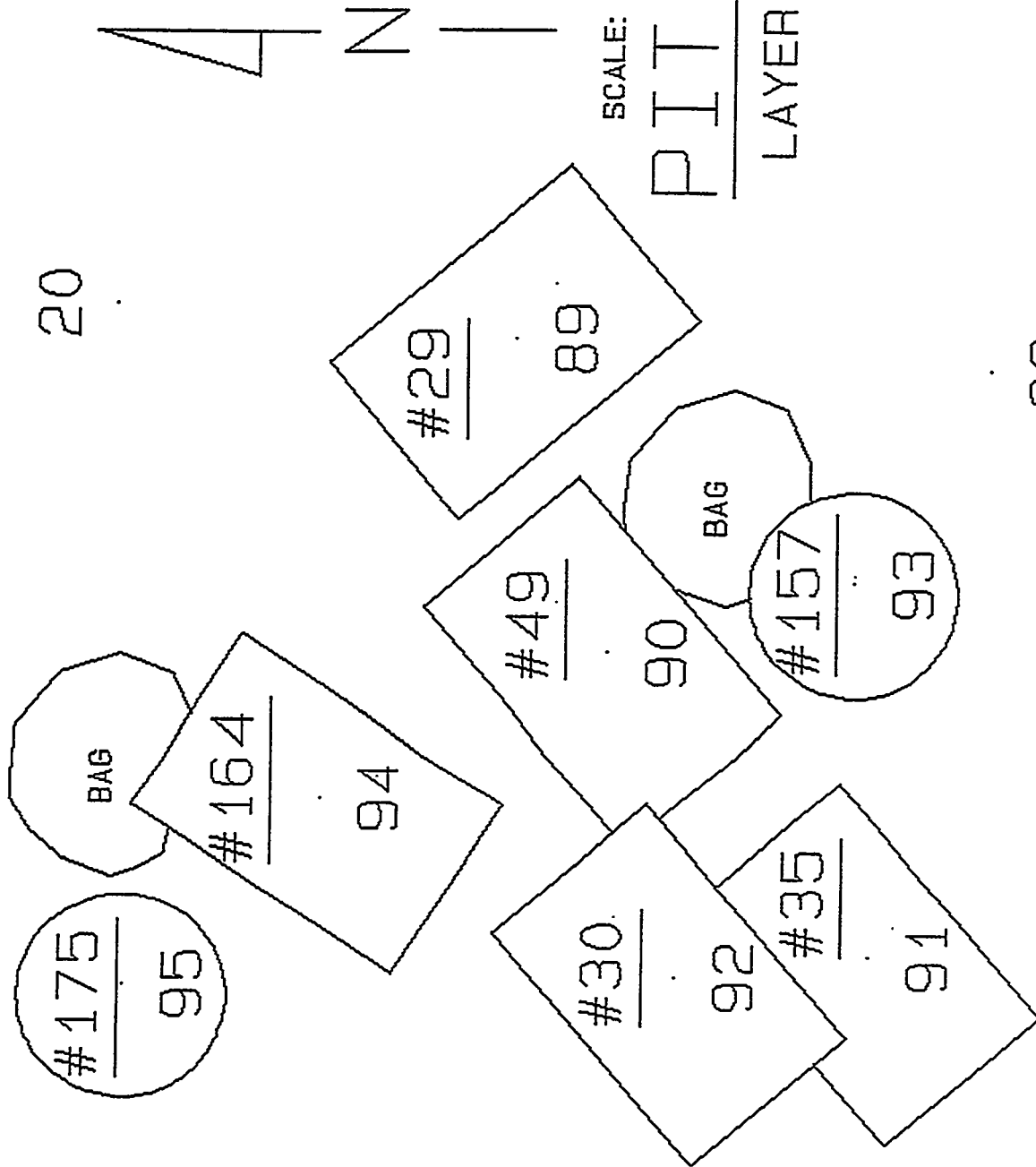
49	667450.6	422570.2	5017.2
75	667447.1	422570.2	5017.7
76	667447.8	422572.6	5017.6
77	667449.3	422571.5	5017.7
78	667450.3	422573.1	5018.5
79	667448.1	422570.1	5019.0
80	667448.5	422568.9	5017.9
81	667450.6	422568.8	5017.7

---

21



20



22

23

COLD TEST PIT - 1996  
PIT B - LEVEL 3

---

Positions determined with Topcon electronic total station on 6-24-96  
by K. V. Beard.

Horizontal Datum: NAD 83, Idaho East Zone, State Plane Coordinates, feet.  
Vertical Datum: NAVD 88, feet.

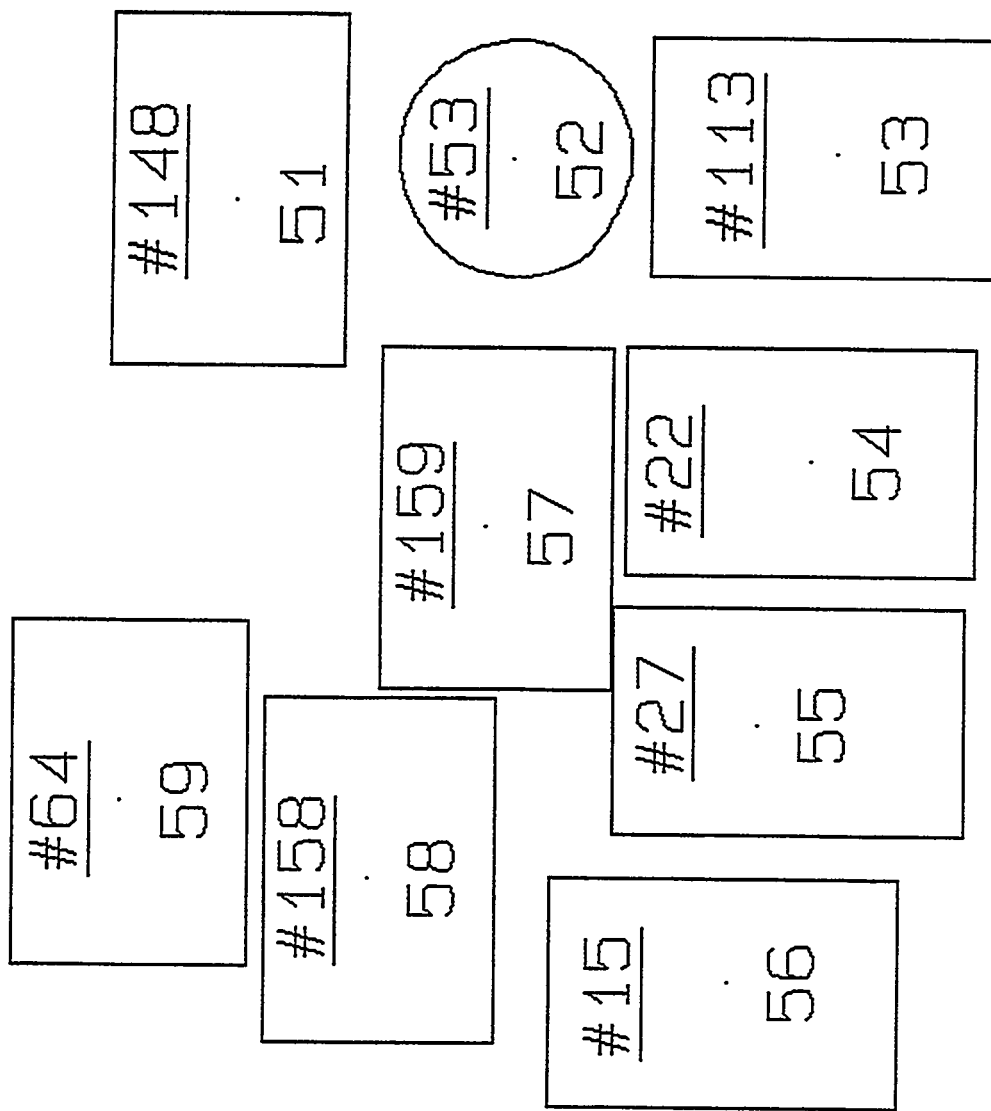
PT# North      East      Elevation

---

20	667451.7	422573.7	5014.6
21	667452.3	422567.8	5014.7
22	667446.5	422567.2	5014.8
23	667446.1	422573.3	5014.5
89	667449.1	422573.5	5020.2
90	667448.5	422571.5	5019.9
91	667446.9	422569.5	5019.8
92	667448.1	422569.4	5020.8
93	667447.0	422571.9	5019.8
94	667450.4	422570.5	5020.1
95	667451.6	422569.3	5019.5

---

24



25

SCALE: 1" = 1'

PIT C

1 LAYER

26

COLD TEST PIT - 1996  
PIT C

---

Positions determined with Topcon electronic total station on 6-24-96  
by K. V. Beard.

Horizontal Datum: NAD 83, Idaho East Zone, State Plane Coordinates, feet.

Vertical Datum: NAVD 88, feet.

PT# North      East      Elevation

24	667478.5	422614.7	5014.7
25	667473.1	422613.8	5014.9
26	667471.9	422620.1	5015.0
27	667477.6	422620.8	5014.0
51	667477.0	422619.4	5016.0
52	667475.4	422619.6	5016.7
53	667473.6	422619.7	5016.2
54	667473.7	422617.9	5016.3
55	667474.0	422616.4	5016.3
56	667474.2	422614.9	5016.3
57	667475.6	422617.5	5016.1
58	667476.3	422615.5	5016.2
59	667477.7	422615.9	5016.1

---

24

#13  
102

BAG  
#156  
99

27  
#31  
96

#117  
101

#34  
98

25

SCALE: 1" = 1'  
PIT C  
#72 97  
#32 100

LAYER 2

26

COLD TEST PIT - 1996  
PIT C - LEVEL 2

---

Positions determined with Topcon electronic total station on 6-26-96  
by K. V. Beard.

Horizontal Datum: NAD 83, Idaho East Zone, State Plane Coordinates, feet.  
Vertical Datum: NAVD 88, feet.

PT# North      East      Elevation

24	667478.5	422614.7	5014.7
25	667473.1	422613.8	5014.9
26	667471.9	422620.1	5015.0
27	667477.6	422620.8	5014.0
96	667477.3	422620.1	5018.1
97	667473.4	422619.3	5017.6
98	667475.6	422617.9	5018.0
99	667477.4	422618.0	5018.2
100	667473.1	422617.3	5018.3
101	667475.2	422615.6	5018.0
102	667477.6	422615.5	5017.6

---

24

$\frac{\#155}{135}$

135

$\frac{\#122}{134}$

134

$\frac{\#69}{130}$

130

27

N

SCALE: 1"=1'

PITT

LAYER 3

$\frac{\#46}{132}$

132

$\frac{\#8}{133}$

133

25

26

COLD TEST PIT - 1996  
PIT C - LEVEL 3

---

Positions determined with Topcon electronic total station on 7-1-96  
by K. V. Beard.

Horizontal Datum: NAD 83, Idaho East Zone, State Plane Coordinates, feet.

Vertical Datum: NAVD 88, feet.

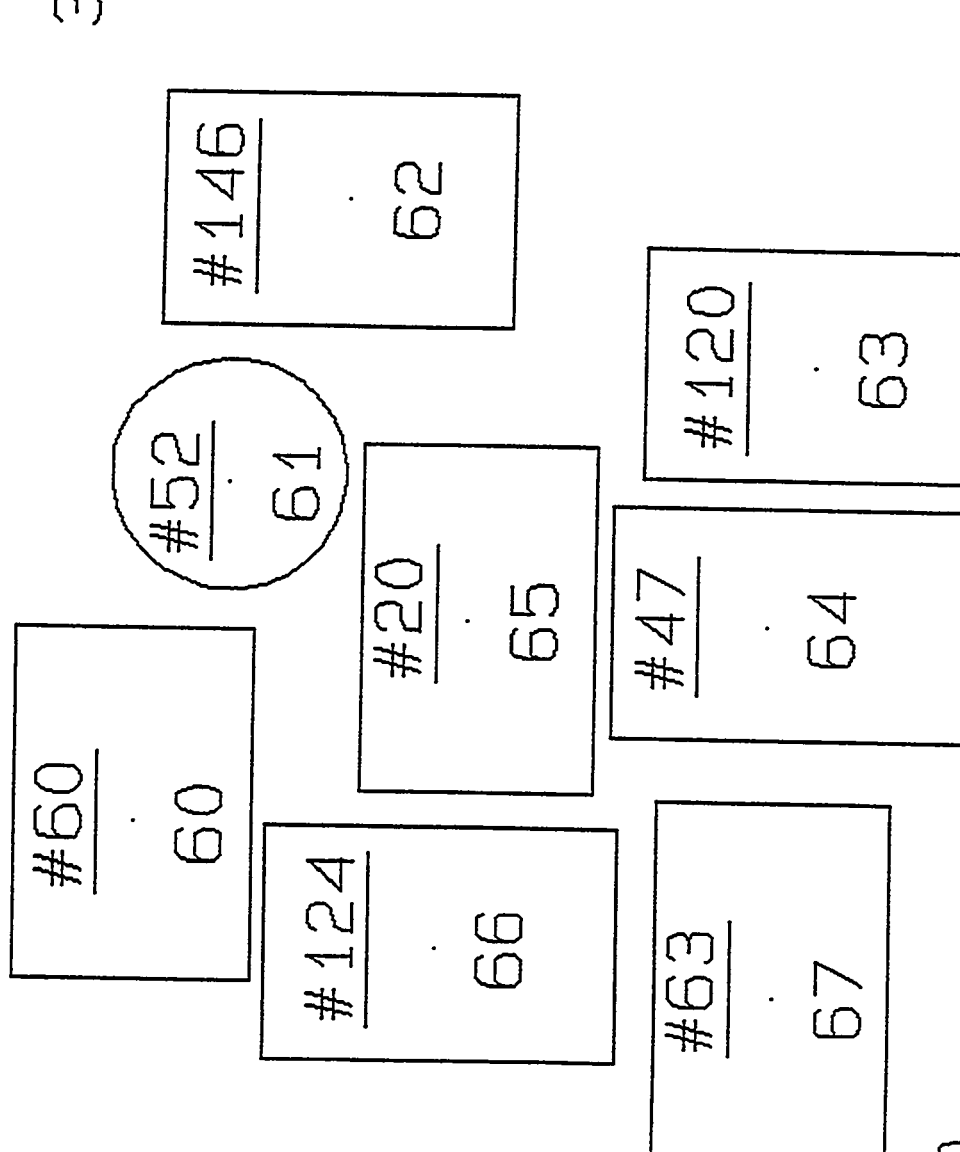
PT# North      East      Elevation

---

24	667478.5	422614.7	5014.7
25	667473.1	422613.8	5014.9
26	667471.9	422620.1	5015.0
27	667477.6	422620.8	5014.0
130	667477.4	422619.3	5019.6
131	667474.9	422619.4	5019.0
132	667473.4	422618.0	5019.6
133	667473.8	422615.6	5019.5
134	667475.8	422617.4	5019.4
135	667477.1	422615.9	5019.2

---

28



29

30

LD TEST PIT - 1996

T D

---

sitions determined with Topcon electronic total station on 6-24-96

K. V. Beard.

horizontal Datum: NAD 83, Idaho East Zone, State Plane Coordinates, feet.

vertical Datum: NAVD 88, feet.

# North      East      Elevation

---

667475.1	422640.0	5013.4
667469.6	422638.9	5014.1
667468.5	422644.0	5014.2
667474.0	422645.7	5013.8
667474.0	422640.9	5015.3
667473.5	422642.9	5016.1
667472.8	422644.5	5015.4
667470.2	422643.6	5015.6
667470.4	422642.1	5015.7
667472.1	422642.1	5015.4
667472.3	422640.2	5015.3
667470.4	422640.0	5015.4

---

四

31 .

#163  
103

#123  
110

#154  
109

#149	108	#165	106
#14	107	#6	105
#116			104

SCALE: 1" = 1'

8

三

## AYER 2

D TEST PIT - 1996  
D - LEVEL 2

---

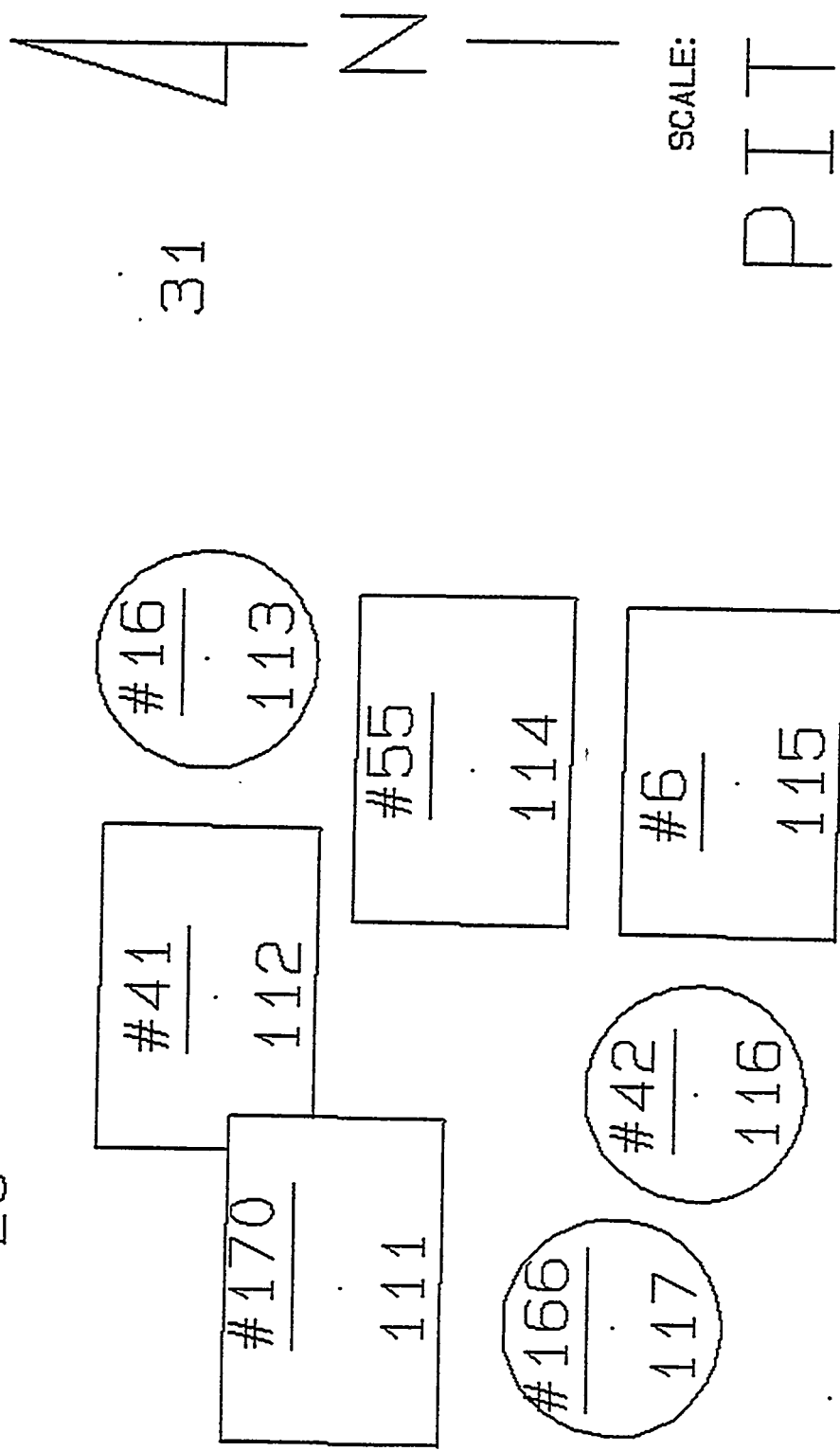
sitions determined with Topcon electronic total station on 6-27-96  
K. V. Beard.  
Horizontal Datum: NAD 83, Idaho East Zone, State Plane Coordinates, feet.  
Vertical Datum: NAVD 88, feet.

North      East      Elevation

---

667475.1	422640.0	5013.4
667469.6	422638.9	5014.1
667468.5	422644.0	5014.2
667474.0	422645.7	5013.8
667473.3	422644.5	5017.4
667471.2	422643.3	5017.1
667470.3	422642.8	5019.0
667470.0	422641.2	5017.4
667471.6	422641.2	5017.7
667471.1	422639.7	5016.9
667473.4	422640.3	5017.7
667473.9	422642.6	5018.7

---



8

११

SCALE: 1" = 1'

---

P T T D

---

LAYER

## Layer 3

OLD TEST PIT - 1996  
T D - LEVEL 3

---

positions determined with Topcon electronic total station on 7-1-96  
K. V. Beard.  
Horizontal Datum: NAD 83, Idaho East Zone, State Plane Coordinates, feet.  
Vertical Datum: NAVD 88, feet.

# North East Elevation

---

1	667475.1	422640.0	5013.4
1	667469.6	422638.9	5014.1
1	667468.5	422644.0	5014.2
	667474.0	422645.7	5013.8
1	667472.6	422639.5	5018.5
2	667473.4	422641.3	5019.8
3	667473.4	422643.4	5019.9
4	667471.8	422642.7	5019.3
5	667470.2	422642.7	5018.9
6	667470.4	422640.8	5020.4
7	667470.9	422639.3	5019.2

---

## **Appendix C**

### **Packer Test Data/Calculations and Falling Head Test Data**



## PACKER TESTING CALCULATIONS

Testing and data interpretation are accomplished following the techniques outlined in the U.S. Bureau of Reclamation's *Ground Water Manual* (Ref. 2). Hydraulic conductivity for the saturated grouted culvert will be calculated using the following formula:

$$K = Q/Cs r H$$

where:

$K$  = hydraulic conductivity in centimeters per second (cm/s)  
 $Q$  = flow rate into the test section in gallons in time (T)  
 $Cs$  = conductivity coefficient for semi-spherical flow in saturated material through partially penetrating cylindrical test wells (unitless)  
 $r$  = radius of the corehole in feet  
 $H$  = effective head in feet

Hydraulic conductivity for the unsaturated grouted culvert and implementation pits will be calculated using the following formula:

$$K = Q/Cs r H$$

where:

$K$  = hydraulic conductivity in centimeters per second (cm/s)  
 $Q$  = flow rate into the test section in gallons in time (T)  
 $Cs$  = conductivity coefficient for unsaturated materials with partially penetrating cylindrical test wells (unitless)  
 $r$  = radius of the corehole in feet  
 $H$  = effective head in feet

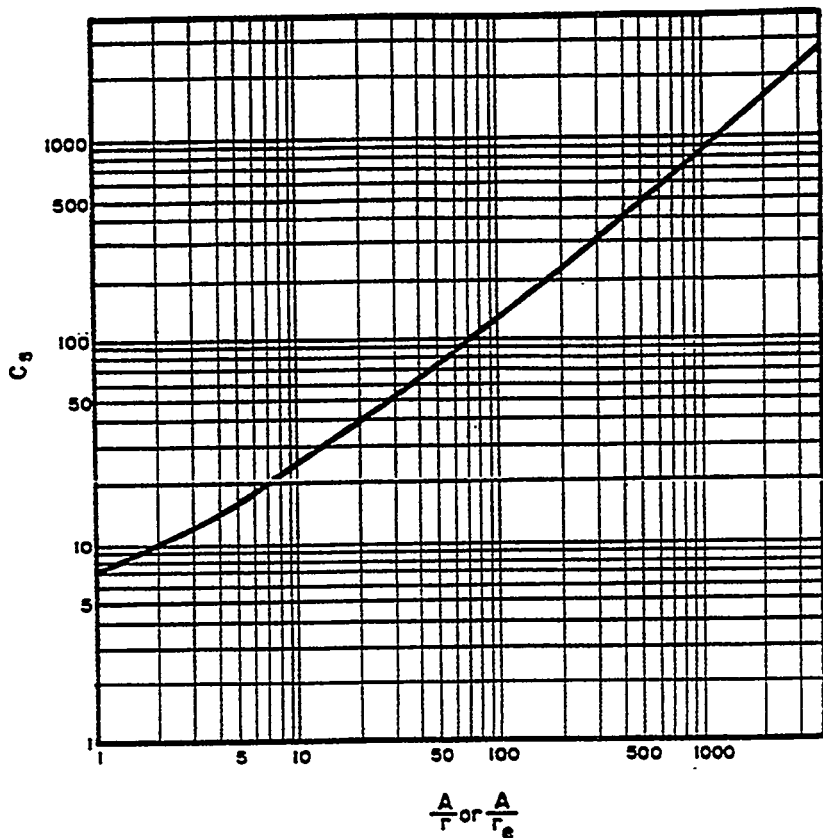


FIGURE 10-8.—Conductivity coefficients for semispherical flow in saturated materials through partially penetrating cylindrical test wells. 103-D-1477.

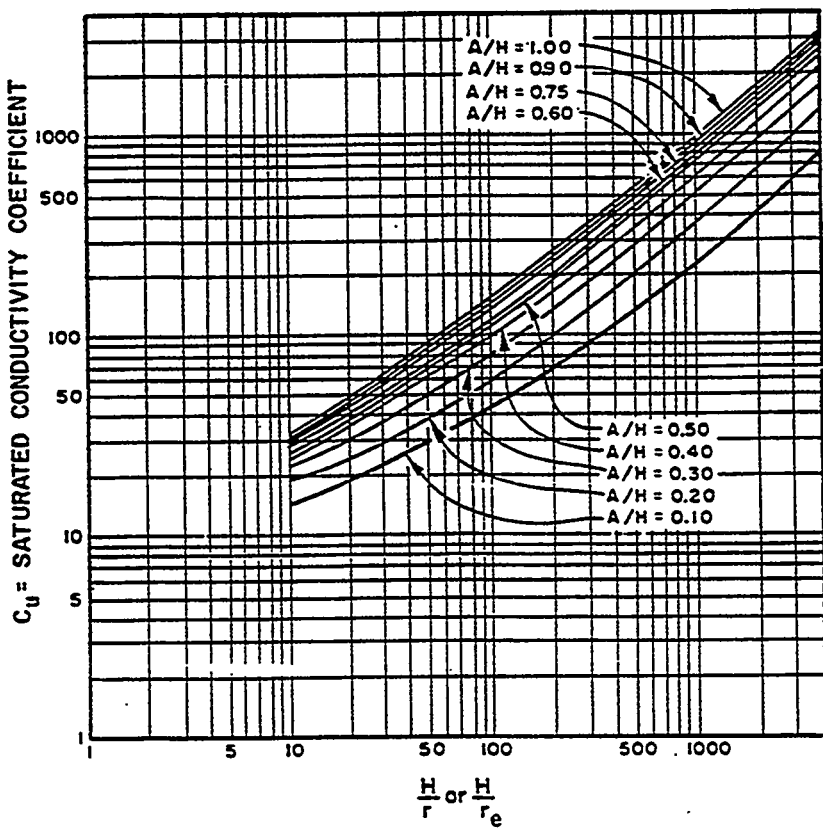


FIGURE 10-7.—Conductivity coefficients for permeability determination in unsaturated materials with partially penetrating cylindrical test wells. 103-D-1476

**HEAD TEST RESULTS**  
**BASELINE CULVERT**

Date	Time (hrs)	Outflow (gal)	Inflow (ft3)	Outflow			Inflow			Outflow			Inflow			
				L	A	H	LQ	AHT	LQ	AHT	LQ	AHT	LQ	AHT	LQ	
9/19/96	0:00	0	0.000	10	78.5	4	0	0	0	0	0	0	0	0	0	
9/19/96	4:43	16980	4.4	0.588	5.7	0.762	10	78.5	4	5.8192	5331720	7.61978	5331720	1.1E-06	3.36E-05	
9/20/96	22:46	818960	16.4	2.182	16.8	2.246	10	78.5	4	21.82352	25735440	22.45824	25735440	8.52E-07	8.73E-07	
9/20/96	24:31	88260	23.9	3.185	20.1	2.687	10	78.5	4	31.94952	27713840	26.886868	27713840	1.15E-06	3.51E-05	
9/23/96	98:31	3546869	82	10.982	63.7	8.515	10	78.5	4	109.8178	1.11E+08	85.15416	1.11E+08	9.84E-07	9.7E-07	
9/23/96	101:03	363780	83.6	11.176	0	0.000	10	78.5	4	111.7565	1.14E+08	0	1.14E+08	7.65E-07	2.33E-05	
10/2/96	102:05	36750	0	0.000	68.7	8.916	10	78.5	4	0	1.15E+08	89.16456	1.15E+08	0	0	
9/24/96	119:24	429840	97	12.967	0	0.000	10	78.5	4	128.6638	1.35E+08	0	1.35E+08	9.61E-07	2.36E-05	
9/24/96	119:59	431840	0	0.000	90.7	12.125	10	78.5	4	0	1.38E+08	121.2478	1.36E+08	0	0	
126/03	453160	110.5	14.772	0	0.000	10	78.5	4	147.7184	1.42E+08	0	1.42E+08	1.04E-06	3.16E-05		
126/21	454680	0	0.000	105.7	14.130	10	78.5	4	0	1.43E+08	141.2998	1.43E+08	0	0	0	
9/25/96	145:26	523560	124.6	16.857	0	0.000	10	78.5	4	166.5853	1.64E+08	0	1.64E+08	1.01E-06	3.09E-05	
9/25/96	146:09	526140	0	0.000	124.5	16.843	10	78.5	4	0	1.65E+08	168.4316	1.65E+08	0	0	0
150:34	542040	127.5	17.044	0	0.000	10	78.5	4	170.442	1.7E+08	0	1.7E+08	1E-06	3.07E-05		
150:40	542400	0	0.000	131.5	17.579	10	78.5	4	0	1.7E+08	175.7892	1.7E+08	0	0	0	
9/26/96	168:06	605160	139.5	18.848	0	0.000	10	78.5	4	188.4836	1.9E+08	0	1.9E+08	9.81E-07	3.02E-05	
9/26/96	168:45	60750	0	0.000	145	19.384	10	78.5	4	0	1.91E+08	193.838	1.91E+08	0	0	0
9/27/96	194:36	700560	157.3	21.028	161.3	21.563	10	78.5	4	210.2768	2.22E+08	215.8258	2.22E+08	9.58E-07	9.81E-07	
9/30/96	265:16	9546860	215.6	28.821	198.6	26.549	10	78.5	4	288.2141	3E+08	285.4885	3E+08	9.61E-07	8.85E-07	
10/1/96	291:57	1051020	219.3	29.316	216.6	28.985	10	78.5	4	293.1602	3.3E+08	289.5529	3.3E+08	8.88E-07	2.71E-05	
10/2/96	311:54	1122840	229.3	30.653	231.6	30.980	10	78.5	4	306.5282	3.53E+08	309.6029	3.53E+08	8.69E-07	8.77E-07	
10/2/96	313:42	1129320	236.5	31.615	235.4	31.468	10	78.5	4	316.1532	3.55E+08	314.6827	3.55E+08	8.92E-07	8.87E-07	
10/3/96	336:44	1212240	244.6	32.698	249.2	33.313	10	78.5	4	328.9813	3.81E+08	333.1306	3.81E+08	8.59E-07	2.72E-05	
10/4/96	340:51	1227080	253.4	33.875	255	34.088	10	78.5	4	338.77451	3.85E+08	340.884	3.85E+08	8.79E-07	8.75E-07	
10/4/96	359:35	1249450	257.9	34.476	264.5	35.358	10	78.5	4	344.7607	4.08E+08	353.5836	4.08E+08	8.48E-07	8.75E-07	
10/7/96	432:50	1558200	286.9	39.690	287.8	38.473	10	78.5	4	398.38959	4.89E+08	364.731	4.89E+08	8.11E-07	2.44E-05	
10/8/96	460:08	1658480	307.9	41.160	307.1	41.053	10	78.5	4	411.8007	5.2E+08	410.5313	5.2E+08	7.91E-07	2.41E-05	
10/8/96	480:58	1731480	317.9	42.497	318.1	42.524	10	78.5	4	424.9887	5.44E+08	425.2361	5.44E+08	7.82E-07	2.38E-05	
10/10/96	504:12	1815120	327.9	43.834	327.6	43.794	10	78.5	4	438.3387	5.72E+08	437.9357	5.72E+08	7.69E-07	2.34E-05	
10/11/96	527:23	1898580	337.9	45.170	335.6	44.863	10	78.5	4	451.7047	5.98E+08	448.6301	5.98E+08	7.58E-07	2.31E-05	
10/14/96	601:02	2163720	363.2	48.553	366.1	48.940	10	78.5	4	485.5258	6.79E+08	489.4025	6.79E+08	7.15E-07	2.18E-05	
10/15/96	623:47	2245620	371.9	49.716	378.6	50.611	10	78.5	4	497.1559	7.05E+08	506.1125	7.05E+08	7.05E-07	2.15E-05	
10/16/96	651:14	2344440	381.4	50.986	393.6	52.616	10	78.5	4	509.0555	7.36E+08	526.1645	7.36E+08	6.93E-07	2.11E-05	
10/17/96	673:23	2424180	387.4	51.788	413.6	55.280	10	78.5	4	517.8763	7.61E+08	552.8005	7.81E+08	6.8E-07	2.07E-05	
10/17/96	673:23	2424180	387.4	51.788	413.6	55.280	10	78.5	4	517.8763	7.61E+08	552.8005	7.81E+08	6.8E-07	2.07E-05	

**HEAD TEST RESULTS**  
**GROUTED CULVERT**

Date	Time (hrs)	Outflow (gal)	Inflow (ft3)			L	A	H	Outflow	Inflow	Outflow (ft/sec)	Inflow (ft/sec)
			(gal)	(ft3)	(ft3)							
9/19/98	0:00	0	0.000	0	0.000	10	78.5	4	0	0	0	0
	1:50	6600	1.7	0.227	1.4	0.187	10	78.5	4	2.272583	2072400	1.1E-06
9/20/98	20:30	75000	6.2	0.829	9.1	1.216	10	78.5	4	8.28818	235500000	3.52E-07
	22:00	78200	6.5	0.869	10.3	1.377	10	78.5	4	8.9892	24868800	3.49E-07
9/23/98	98:45	346900	14.5	1.938	24.9	3.329	10	78.5	4	19.3898	1.09E+08	1.09E-08
	98:11	353460	14.8	1.952	31.9	4.264	10	78.5	4	19.51728	1.11E+08	1.11E-08
9/24/98	117:16	422160	16.3	2.179	0	0.080	10	78.5	4	21.76884	1.335E+08	5.36E-08
	117:19	422340	0	0.000	39.4	5.267	10	78.5	4	0	1.33E+08	3.84E-07
123:39	445140	0	0.000	42.4	5.668	10	78.5	4	0	1.33E+08	52.66892	1.17E-05
123:45	445500	16.8	2.246	0	0.000	10	78.5	4	22.45824	1.4E+08	0	0
9/25/98	142:28	512880	18.5	2.473	0	0.000	10	78.5	4	24.7388	0	1.4E+08
	142:59	514740	0	0.000	48.4	6.470	10	78.5	4	0	1.61E+08	1.54E-07
147:32	531120	19	2.540	0	0.090	10	78.5	4	0	1.62E+08	0	0
	147:42	531720	0	0.000	50.9	6.804	10	78.5	4	25.3992	1.67E+08	1.67E-08
9/26/98	165:15	5894900	20.7	2.767	0	0.000	10	78.5	4	0	1.67E+08	4.89E-08
	165:34	5969040	0	0.000	58	7.488	10	78.5	4	27.67176	1.87E+08	0
9/27/98	191:15	6865500	22.7	3.035	64.8	8.662	10	78.5	4	0	1.87E+08	1.48E-07
6/30/98	261:15	840500	28.6	3.823	79.8	10.668	10	78.5	4	30.34538	2.16E+08	4.52E-08
	288:55	1040100	30.7	4.104	87.8	11.737	10	78.5	4	38.23246	2.65E+08	1.09E-07
10/2/98	308:38	1111080	32.3	4.318	93.8	12.512	10	78.5	4	41.03976	3.27E+08	1.17:371
	310:48	1118980	32.5	4.345	94.9	12.688	10	78.5	4	43.17884	3.49E+08	125.1245
10/3/98	333:05	11189100	34.1	4.558	100.9	13.488	10	78.5	4	43.446	3.51E+08	128.8823
	337:35	1215300	34.5	4.812	103.2	13.788	10	78.5	4	45.58488	3.77E+08	134.8831
10/4/98	356:30	1283400	36.3	4.853	107.8	14.411	10	78.5	4	48.1198	3.92E+08	137.9578
	428:21	1545660	41.7	5.574	120.8	16.149	10	78.5	4	48.52584	4.03E+08	144.107
10/8/98	458:55	1644800	43.8	5.855	129.1	17.258	10	78.5	4	55.74488	4.85E+08	161.4854
	477:49	1720140	45.6	6.098	134.7	18.007	10	78.5	4	58.55184	5.16E+08	172.5809
10/9/98	501:05	1803800	47.7	6.377	140.5	18.782	10	78.5	4	60.95888	5.4E+08	180.087
	525:18	1891080	50	6.884	146	19.517	10	78.5	4	63.76536	5.86E+08	187.8204
10/14/98	597:29	2150940	54.5	7.288	193.8	21.897	10	78.5	4	66.84	5.94E+08	195.1728
	620:26	2233580	55.8	7.459	172.3	23.033	10	78.5	4	72.8558	6.75E+08	218.8678
10/16/98	647:53	2332380	57	7.620	181.8	24.303	10	78.5	4	74.59344	7.01E+08	230.3308
	670:16	2412360	58.3	7.784	192.1	25.680	10	78.5	4	76.1978	7.32E+08	243.0302
10/17/98	670:16	2412360	58.3	7.784	192.1	25.680	10	78.5	4	77.93544	7.57E+08	256.7893

PACKER PERMEABILITY TESTING DATA									
TECT PIT			Test No. 1						
CH-1		Time	Q	r	H	A	h1	h2	L
(ft)	(ft3/sec)		Cu	(ft)	(ft)	(ft)	ft of H20	psi	(ft)
5.3 - 7.0		0 - 5	0.0011	45	0.16	20.04	1.7	8.5	11.54
		5 - 7.7	0.0055	59	0.16	31.57	1.7	8.5	23.07
		7.7 - 9.7	0.0066	80	0.16	45.41	1.7	8.5	36.91
		21 - 28	0.0018	55	0.16	18.73	1.7	9.5	9.23
PACKER PERMEABILITY TESTING DATA									
TECT PIT			Test No. 2						
CH-1		Time	Q	r	H	A	h1	h2	L
(ft)	(ft3/sec)		Cu	(ft)	(ft)	(ft)	ft of H20	psi	(ft)
5.3 - 7.0		0 - 16	2.9E-06	50	0.16	22.34	1.7	8.5	13.84
		16 - 37	2.2E-06	70	0.16	36.18	1.7	8.5	27.68
		37 - 55	2.7E-06	95	0.16	54.64	1.7	8.5	46.14
		55 - 58	0.0013	80	0.16	39.64	1.7	8.5	31.14
		58 - 60	0.0017	45	0.16	15.42	1.7	8.5	6.92
		60 - 75	0.00023	40	0.16	10.81	1.7	8.5	2.31
PACKER PERMEABILITY TESTING DATA									
TECT PIT			Test No. 3						
CH-1		Time	Q	r	H	A	h1	h2	L
(ft)	(ft3/sec)		Cu	(ft)	(ft)	(ft)	ft of H20	psi	(ft)
5.3 - 7.8		0 - 5	0.000037	50	0.16	13.91	2.4	9.3	4.61
		5 - 16	8.4E-06	51	0.16	25.45	2.4	9.3	16.15
		16 - 26	4.6E-06	80	0.16	41.60	2.4	9.3	32.30
		26 - 36	0.000023	100	0.16	57.75	2.4	9.3	48.45
		36 - 48	4.6E-06	80	0.16	43.91	2.4	9.3	34.61
		48 - 58	4.6E-06	56	0.16	27.76	2.4	9.3	18.46

PACKER PERMEABILITY TESTING DATA									
TECT PIT		CH-2		Test No. 1					
Test Interval (ft)	Time (min)	Q (ft <sup>3</sup> /sec)	Cu	r (ft)	H (ft)	A (ft)	h1 (ft)	h2 (ft)	L (ft)
5.3 - 8.5	0 - 5	0.000018	55	0.16	21.54	3.2	10	11.54	5
	5 - 10	0.000037	70	0.16	33.07	3.2	10	23.07	10
	10 - 11	0.000046	80	0.16	44.61	3.2	10	34.61	15
	11 - 15	0.006	100	0.16	56.14	3.2	10	46.14	20
PACKER PERMEABILITY TESTING DATA									
TECT PIT		CH-2		Test No. 2					
Test Interval (ft)	Time (min)	Q (ft <sup>3</sup> /sec)	Cu	r (ft)	H (ft)	A (ft)	h1 (ft)	h2 (ft)	L (ft)
5.0 - 7.3	0 - 16	2.9E-06	52	0.16	24.95	2.3	8.8	16.15	7
	16 - 19.5	0.00112	60	0.16	27.26	2.3	8.8	18.46	8
	19.5 - 28	0.00044	50	0.16	14.57	2.3	8.8	5.77	2.5
PACKER PERMEABILITY TESTING DATA									
TECT PIT		CH-2		Test No. 3					
Test Interval (ft)	Time (min)	Q (ft <sup>3</sup> /sec)	Cu	r (ft)	H (ft)	A (ft)	h1 (ft)	h2 (ft)	L (ft)
4.9 - 6.6	0 - 6	7.7E-06	47	0.16	15.02	1.7	8.1	6.92	3
	6 - 7.5	0.00046	55	0.16	26.56	1.7	8.1	18.46	8
PACKER PERMEABILITY TESTING DATA									
TECT PIT		CH-2		Test No. 4					
Test Interval (ft)	Time (min)	Q (ft <sup>3</sup> /sec)	Cu	r (ft)	H (ft)	A (ft)	h1 (ft)	h2 (ft)	L (ft)
4.9 - 6.7	0 - 1	0.0037	50	0.16	22.04	1.8	8.2	13.84	6
PACKER PERMEABILITY TESTING DATA									
TECT PIT		CH-2		Test No. 5					
Test Interval (ft)	Time (min)	Q (ft <sup>3</sup> /sec)	Cu	r (ft)	H (ft)	A (ft)	h1 (ft)	h2 (ft)	L (ft)
4.9 - 6.7	0 - 10	0.000069	42	0.16	17.43	1.8	8.2	9.23	4
	10 - 16.75	0.003	52	0.16	24.35	1.8	8.2	16.15	7

PACKER PERMEABILITY TESTING DATA									
TECT Pit			Test No. 1						
CH-3		Test No. 1							
Test Interval (ft)	Time (min)	Q (ft <sup>3</sup> /sec)	Cu (ft)	r (ft)	H (ft)	A (ft)	h1 (ft)	h2 (ft)	L (ft)
6.2 - 9.3	0 - 10	0.000023	100	0.16	54.63	3.1	10.8	43.83	19
	10 - 20	4.6E-06	90	0.16	47.71	3.1	10.8	36.91	16
	20 - 35	0.000023	140	0.16	80.01	3.1	10.8	69.21	30
	30 - 35	0.00062	110	0.16	63.86	3.1	10.8	53.06	23
PACKER PERMEABILITY TESTING DATA									

PACKER PERMEABILITY TESTING DATA									
Grouted Culvert - Portland									
CH-2		Test No. 1							
Test Interval (ft)	Time (min)	Q (ft <sup>3</sup> /sec)	C <sub>u</sub> (ft)	r (ft)	H (ft)	A (ft)	h <sub>1</sub> (ft)	h <sub>2</sub> (ft)	L (ft)
5.4 - 7.0	0 - 6	7.7E-06	46	0.16	15.42	1.6	8.5	6.92	3
	6 - 21	3.1E-06	50	0.16	22.34	1.6	8.5	13.84	6
	21 - 22	0.019	45	0.16	19.04	1.6	8.5	11.54	5
Test Interval (ft)	Time (min)	Q (ft <sup>3</sup> /sec)	C <sub>s</sub> (ft)	r (ft)	H (ft)	A (ft)	h <sub>1</sub> (ft)	h <sub>2</sub> (ft)	L (ft)
5.4 - 7.0	0 - 6	7.7E-06	25	0.16	15.42	1.6	8.5	6.92	3
	6 - 21	3.1E-06	25	0.16	22.34	1.6	8.5	13.84	6
	21 - 22	0.019	25	0.16	19.04	1.6	8.5	11.54	5
PACKER PERMEABILITY TESTING DATA									
Grouted Culvert - Portland									
CH-2		Test No. 2							
Test Interval (ft)	Time (min)	Q (ft <sup>3</sup> /sec)	C <sub>u</sub> (ft)	r (ft)	H (ft)	A (ft)	h <sub>1</sub> (ft)	h <sub>2</sub> (ft)	L (ft)
5.9 - 7.0	0 - 2	0.000023	39	0.16	13.11	1.1	8.5	4.61	2
	2 - 9	0.000032	54	0.16	26.96	1.1	8.5	18.46	8
	9 - 12	0.0044	70	0.16	31.57	1.1	8.5	23.07	10
Test Interval (ft)	Time (min)	Q (ft <sup>3</sup> /sec)	C <sub>s</sub> (ft)	r (ft)	H (ft)	A (ft)	h <sub>1</sub> (ft)	h <sub>2</sub> (ft)	L (ft)
5.9 - 7.0	0 - 2	0.000023	20	0.16	13.11	1.1	8.5	4.61	2
	2 - 9	0.000032	20	0.16	26.96	1.1	8.5	18.46	8
	9 - 12	0.0044	20	0.16	31.57	1.1	8.5	23.07	10

PACKER PERMEABILITY TESTING DATA									
GROUTED CULVERT - PORTLAND									
CH-2		Test No. 3							
Test Interval (ft)	Time (min)	Q (ft <sup>3</sup> /sec)	r (ft)	H (ft)	A (ft)	h1 (ft)	ft of H <sub>20</sub> psi	L (ft)	k (cm/sec)
5.8 - 7.0	0 - 10	4.6E-06	52	0.16	24.65	1.2	8.5	16.15	7
	10 - 20	4.6E-06	75	0.16	36.18	1.2	8.5	27.68	12
	20 - 28	5.8E-06	90	0.16	50.03	1.2	8.5	41.53	18
	28 - 38	4.6E-06	100	0.16	54.64	1.2	8.5	46.14	20
	38 - 50	4.6E-06	78	0.16	38.49	1.2	8.5	29.99	13
	50 - 65	4.6E-06	52	0.16	24.65	1.2	8.5	16.15	7
Test Interval (ft)	Time (min)	Q (ft <sup>3</sup> /sec)	r (ft)	H (ft)	A (ft)	h1 (ft)	ft of H <sub>20</sub> psi	L (ft)	k (cm/sec)
5.8 - 7.0	0 - 10	4.6E-06	21	0.16	24.65	1.2	8.5	16.15	7
	10 - 20	4.6E-06	21	0.16	36.18	1.2	8.5	27.68	12
	20 - 28	5.8E-06	21	0.16	50.03	1.2	8.5	41.53	18
	28 - 38	4.6E-06	21	0.16	54.64	1.2	8.5	46.14	20
	38 - 50	4.6E-06	21	0.16	38.49	1.2	8.5	29.99	13
	50 - 65	4.6E-06	21	0.16	24.65	1.2	8.5	16.15	7

PACKER PERMEABILITY TESTING DATA											
GROUTED CULVERT - PORTLAND											
CH-3 Test No. 1											
Test Interval (ft)	Time (min)	Q (ft <sup>3</sup> /sec)	r (ft)	H (ft)	A (ft <sup>2</sup> )	h1 (ft)	h2 ft of H <sub>20</sub>	psi	L (ft)	k (ft/sec)	k (cm/sec)
5.8 - 8.2	0 - 10	4.6E-06	50	0.16	16.62	2.4	9.7	6.92	3	NF	3.46E-08 1.055E-06
	10 - 25	0.000069	48	0.16	21.24	2.4	9.7	11.54	5	NF	4.23E-07 1.29E-05
	10 - 12	0.00046	52	0.16	23.54	2.4	9.7	13.84	6	NF	2.35E-06 7.16E-05
	12 - 25	3.5E-06	50	0.16	19.50	2.4	9.7	9.80	4.25	NF	2.24E-08 6.839E-07
	25 - 37	0.00044	55	0.16	30.46	2.4	9.7	20.76	9	NF	1.64E-06 5.004E-05
	37 - 51	3.3E-06	48	0.16	21.24	2.4	9.7	11.54	5	NF	2.02E-08 6.169E-07
Test Interval (ft)	Time (min)	Q (ft <sup>3</sup> /sec)	r (ft)	H (ft)	A (ft <sup>2</sup> )	h1 (ft)	h2 ft of H <sub>20</sub>	psi	L (ft)	k (ft/sec)	k (cm/sec)
5.8 - 8.2	0 - 10	4.6E-06	31	0.16	16.62	2.4	9.7	6.92	3	NF	5.58E-08 1.701E-06
	10 - 25	0.000069	31	0.16	21.24	2.4	9.7	11.54	5	NF	6.55E-07 1.897E-05
	10 - 12	0.00046	31	0.16	23.54	2.4	9.7	13.84	6	NF	3.94E-06 0.0001201
	12 - 25	3.5E-06	31	0.16	19.50	2.4	9.7	9.80	4.25	NF	3.62E-08 1.103E-06
	25 - 37	0.00044	31	0.16	30.46	2.4	9.7	20.76	9	NF	2.91E-06 8.878E-05
	37 - 51	3.3E-06	31	0.16	21.24	2.4	9.7	11.54	5	NF	3.13E-08 9.552E-07
PACKER PERMEABILITY TESTING DATA											
GROUTED CULVERT - PORTLAND											
CH-3 Test No. 2											
Test Interval (ft)	Time (min)	Q (ft <sup>3</sup> /sec)	r (ft)	H (ft)	A (ft <sup>2</sup> )	h1 (ft)	h2 ft of H <sub>20</sub>	psi	L (ft)	k (ft/sec)	k (cm/sec)
5.6 - 7.9	0 - 5	9.2E-06	48	0.16	18.63	2.3	9.4	9.23	4	NF	6.43E-08 1.961E-06
	5 - 20	3.1E-06	55	0.16	25.55	2.3	9.4	16.15	7	NF	1.38E-08 4.204E-07
	20 - 22	0.0044	57	0.16	26.70	2.3	9.4	17.30	7.5	NF	1.81E-05 0.0005508
	22 - 34	0.00069	50	0.16	22.09	2.3	9.4	12.69	5.5	NF	3.90E-06 0.000119
	22 - 28	7.7E-06	50	0.16	22.09	2.3	9.4	12.69	5.5	NF	4.36E-08 1.328E-06
	28 - 34	0.00016	50	0.16	22.09	2.3	9.4	12.69	5.5	NF	9.05E-07 2.761E-05
	34 - 35	0.0035	70	0.16	34.78	2.3	9.4	25.38	11	NF	8.99E-06 0.000274
	35 - 50.5	0.000003	55	0.16	27.86	2.3	9.4	18.46	8	NF	1.22E-08 3.731E-07
Test Interval (ft)	Time (min)	Q (ft <sup>3</sup> /sec)	r (ft)	H (ft)	A (ft <sup>2</sup> )	h1 (ft)	h2 ft of H <sub>20</sub>	psi	L (ft)	k (ft/sec)	k (cm/sec)
5.6 - 7.9	0 - 5	9.2E-06	28	0.16	18.63	2.3	9.4	9.23	4	NF	1.10E-07 3.361E-06
	5 - 20	3.1E-06	28	0.16	25.55	2.3	9.4	16.15	7	NF	2.71E-08 8.257E-07
	20 - 22	0.0044	28	0.16	26.70	2.3	9.4	17.30	7.5	NF	3.68E-05 0.0011214
	22 - 34	0.00069	28	0.16	22.09	2.3	9.4	12.69	5.5	NF	6.97E-06 0.0002126
	22 - 28	7.7E-06	28	0.16	22.09	2.3	9.4	12.69	5.5	NF	7.78E-08 2.372E-06
	28 - 34	0.00016	28	0.16	22.09	2.3	9.4	12.69	5.5	NF	1.62E-06 4.929E-05
	34 - 35	0.0035	28	0.16	34.78	2.3	9.4	25.38	11	NF	2.25E-05 0.0006849
	35 - 50.5	0.000003	28	0.16	27.86	2.3	9.4	18.46	8	NF	2.40E-08 7.329E-07

PACKER PERMEABILITY TESTING DATA									
Grouted Culvert - Portland				CH-3 Test No. 3					
Test Interval (ft)	Time (min)	Q (ft <sup>3</sup> /sec)	r (ft)	H (ft)	A (ft)	h1 (ft)	h2 (ft)	L (ft)	K (cm/sec)
5.6 - 7.9	0 - 2	0.000023	50	0.16	20.94	2.3	9.4	11.54	5
	2 - 15	0.000058	70	0.16	32.47	2.3	9.4	23.07	10
	2 - 10	0.000092	70	0.16	33.62	2.3	9.4	24.22	10.5
	10 - 15	9.2E-06	50	0.16	30.16	2.3	9.4	20.76	9
	15 - 25	0.000041	70	0.16	35.93	2.3	9.4	26.53	11.5
	15 - 16	0.00041	75	0.16	41.70	2.3	9.4	32.30	14
	16 - 25	5.1E-06	70	0.16	34.78	2.3	9.4	25.38	11
	26 - 28	0.0037	72	0.16	39.39	2.3	9.4	29.99	13
Test Interval (ft)	Time (min)	Q (ft <sup>3</sup> /sec)	r (ft)	H (ft)	A (ft)	h1 (ft)	h2 (ft)	L (ft)	K (cm/sec)
5.6 - 7.9	0 - 2	0.000023	28	0.16	20.94	2.3	9.4	11.54	5
	2 - 15	0.000058	28	0.16	32.47	2.3	9.4	23.07	10
	2 - 10	0.000092	28	0.16	33.62	2.3	9.4	24.22	10.5
	10 - 15	9.2E-06	28	0.16	30.16	2.3	9.4	20.76	9
	15 - 25	0.000041	28	0.16	35.93	2.3	9.4	26.53	11.5
	15 - 16	0.0041	28	0.16	41.70	2.3	9.4	32.30	14
	16 - 25	5.1E-06	28	0.16	34.78	2.3	9.4	25.38	11
	26 - 28	0.0037	28	0.16	39.39	2.3	9.4	29.99	13
PACKER PERMEABILITY TESTING DATA									
Grouted Culvert - Portland				CH-3 Test No. 4					
Test Interval (ft)	Time (min)	Q (ft <sup>3</sup> /sec)	r (ft)	H (ft)	A (ft)	h1 (ft)	h2 (ft)	L (ft)	K (cm/sec)
6.1 - 7.9	0 - 14	3.3E-06	48	0.16	20.94	1.8	9.4	11.54	5
	14 - 16	0.0014	68	0.16	31.89	1.8	9.4	22.49	9.75
	16 - 25	5.1E-06	62	0.16	29.59	1.8	9.4	20.19	8.75
	25 - 36	0.000555	89	0.16	47.47	1.8	9.4	38.07	16.5
	25 - 29	0.002	85	0.16	45.16	1.8	9.4	35.76	15.5
	29 - 36	6.6E-06	80	0.16	44.01	1.8	9.4	34.61	15
Test Interval (ft)	Time (min)	Q (ft <sup>3</sup> /sec)	r (ft)	H (ft)	A (ft)	h1 (ft)	h2 (ft)	L (ft)	K (cm/sec)
6.1 - 7.9	0 - 14	3.3E-06	28	0.16	20.94	1.8	9.4	11.54	5
	14 - 16	0.0014	28	0.16	31.89	1.8	9.4	22.49	9.75
	16 - 25	5.1E-06	28	0.16	29.59	1.8	9.4	20.19	8.75
	25 - 36	0.000555	26	0.16	47.47	1.8	9.4	38.07	16.5
	25 - 29	0.002	26	0.16	45.16	1.8	9.4	35.76	15.5
	29 - 36	6.6E-06	26	0.16	44.01	1.8	9.4	34.61	15

		Grouted Culvert - Portland									
		CH-3	Test No. 6								
Test Interval (ft)	Time (min)	Q (ft³/sec)	r (ft)	H (ft)	A (ft)	h1 (ft)	h2 (ft)	L (ft)	k (cm/sec)	k (cm/sec)	
5.4 - 7.9	0 - 10	4.6E-06	55	0.16	23.24	2.5	9.4	13.84	6	NF	2.25E-08
	10 - 20	0.00041	70	0.16	32.47	2.5	9.4	23.07	10	NF	1.13E-06
	20 - 21	0.0087	90	0.16	48.62	2.5	9.4	39.22	17	NF	3.437E-05
	10 - 11	0.0041	70	0.16	33.62	2.5	9.4	24.22	10.5	NF	1.24E-05
	11 - 20	5.1E-06	70	0.16	31.89	2.5	9.4	22.49	9.75	NF	0.0003319
	Time (min)	Q (ft³/sec)	r (ft)	H (ft)	A (ft)	h1 (ft)	h2 (ft)	psi (ft)	ft of H20 (ft)	psi (ft)	ft of H20 (ft)
5.4 - 7.9	0 - 10	4.6E-06	30	0.16	23.24	2.5	9.4	13.84	6	NF	4.12E-08
	10 - 20	0.00041	30	0.16	32.47	2.5	9.4	23.07	10	NF	2.63E-06
	20 - 21	0.0087	30	0.16	48.62	2.5	9.4	39.22	17	NF	8.02E-05
	10 - 11	0.0041	30	0.16	33.62	2.5	9.4	24.22	10.5	NF	3.73E-05
	11 - 20	5.1E-06	30	0.16	31.89	2.5	9.4	22.49	9.75	NF	0.0007745
	Time (min)	Q (ft³/sec)	r (ft)	H (ft)	A (ft)	h1 (ft)	h2 (ft)	psi (ft)	ft of H20 (ft)	psi (ft)	ft of H20 (ft)

PACKER PERMEABILITY TESTING DATA									
Grouted Culvert - Portland									
CH-6		Test No. 4							
Test Interval (ft)	Time (min)	Q (ft <sup>3</sup> /sec)	r (ft)	H (ft)	A (ft)	h1 (ft)	h2 ft of H20	psi	L (ft)
4.6 - 6.8	0 - 1	0.000046	47	0.16	12.91	2.2	8.3	4.61	2
	1 - 5	0.00012	49	0.16	17.53	2.2	8.3	9.23	4
	1 - 2	0.00046	49	0.16	17.53	2.2	8.3	9.23	4
	2 - 5	0.000015	49	0.16	17.53	2.2	8.3	9.23	4
	5 - 15	0.00037	55	0.16	25.60	2.2	8.3	17.30	7.5
	5 - 6	0.0037	54	0.16	24.45	2.2	8.3	16.15	7
	6 - 15	5.1E-06	55	0.16	25.60	2.2	8.3	17.30	7.5
	15 - 25	0.00053	80	0.16	40.60	2.2	8.3	32.30	14
	15 - 16	0.0053	80	0.16	40.60	2.2	8.3	32.30	14
	16 - 25	5.1E-06	80	0.16	40.60	2.2	8.3	32.30	14
	25 - 38	0.000046	100	0.16	56.75	2.2	8.3	48.45	21
	25 - 26	0.00046	100	0.16	56.75	2.2	8.3	48.45	21
	26 - 38	3.8E-06	100	0.16	56.75	2.2	8.3	48.45	21
	38 - 49	4.2E-06	80	0.16	40.60	2.2	8.3	32.30	14
	49 - 60	4.2E-06	54	0.16	40.60	2.2	8.3	32.30	14
Test Interval (ft)	Time (min)	Q (ft <sup>3</sup> /sec)	r (ft)	H (ft)	A (ft)	h1 (ft)	h2 ft of H20	psi	L (ft)
4.6 - 6.8	0 - 1	0.000046	28	0.16	12.91	2.2	8.3	4.61	2
	1 - 5	0.00012	28	0.16	17.53	2.2	8.3	9.23	4
	1 - 2	0.00046	28	0.16	17.53	2.2	8.3	9.23	4
	2 - 5	0.000015	28	0.16	17.53	2.2	8.3	9.23	4
	5 - 15	0.00037	28	0.16	25.60	2.2	8.3	17.30	7.5
	5 - 6	0.0037	28	0.16	24.45	2.2	8.3	16.15	7
	6 - 15	5.1E-06	28	0.16	25.60	2.2	8.3	17.30	7.5
	15 - 25	0.00053	28	0.16	40.60	2.2	8.3	32.30	14
	15 - 16	0.0053	28	0.16	40.60	2.2	8.3	32.30	14
	16 - 25	5.1E-06	28	0.16	40.60	2.2	8.3	32.30	14
	25 - 38	0.000046	28	0.16	56.75	2.2	8.3	48.45	21
	25 - 26	0.00046	28	0.16	56.75	2.2	8.3	48.45	21
	26 - 38	3.8E-06	28	0.16	56.75	2.2	8.3	48.45	21
	38 - 49	4.2E-06	28	0.16	40.60	2.2	8.3	32.30	14
	49 - 60	4.2E-06	28	0.16	40.60	2.2	8.3	32.30	14

PACKER PERMEABILITY TESTING DATA										
GROUTED CULVERT - PORTLAND			TEST NO. 5							
CH-6	Test No. 5									
Test Interval (ft)	Time (min)	Q (ft <sup>3</sup> /sec)	Cu	r (ft)	H (ft)	A (ft)	h1 (ft)	h2 (ft)	L (ft)	k (cm/sec)
4.6 - 6.8	0 - 5	0.00023	48	0.16	17.53	2.2	8.3	9.23	4	NF 1.71E-06 5.209E-05
	1 - 5	0.000012	48	0.16	17.53	2.2	8.3	9.23	4	NF 8.91E-08 2.718E-06
	5 - 15	0.00014	51	0.16	22.14	2.2	8.3	13.84	6	NF 7.75E-07 2.362E-05
	5 - 6	0.0014	51	0.16	22.14	2.2	8.3	13.84	6	NF 7.75E-06 0.0002362
	6 - 15	5.1E-06	51	0.16	22.14	2.2	8.3	13.84	6	NF 2.82E-08 8.606E-07
	15 - 30	0.00037	70	0.16	35.98	2.2	8.3	27.68	12	NF 9.18E-07 2.799E-05
	15 - 18	0.0018	70	0.16	35.98	2.2	8.3	27.68	12	NF 4.47E-06 0.0001362
	18 - 30	3.8E-06	69	0.16	34.83	2.2	8.3	26.53	11.5	NF 9.88E-09 3.013E-07
	30 - 40	0.000046	80	0.16	42.91	2.2	8.3	34.61	15	NF 8.38E-08 2.554E-06
	30 - 31	0.00046	80	0.16	42.91	2.2	8.3	34.61	15	NF 8.38E-07 2.554E-05
	31 - 40	5.1E-06	80	0.16	42.91	2.2	8.3	34.61	15	NF 9.29E-09 2.831E-07
	40 - 62	2.1E-06	100	0.16	56.75	2.2	8.3	48.45	21	NF 2.31E-09 7.052E-08
	62 - 73	4.2E-06	80	0.16	41.75	2.2	8.3	33.45	14.5	NF 7.86E-09 2.396E-07
	73 - 84	4.2E-06	55	0.16	26.76	2.2	8.3	18.46	8	NF 1.78E-08 5.438E-07
Test Interval (ft)	Time (min)	Q (ft <sup>3</sup> /sec)	Cs	r (ft)	H (ft)	A (ft)	h1 (ft)	h2 (ft)	L (ft)	k (cm/sec)
4.6 - 6.8	0 - 5	0.00023	28	0.16	17.53	2.2	8.3	9.23	4	NF 2.93E-06 8.93E-05
	1 - 5	0.000012	28	0.16	17.53	2.2	8.3	9.23	4	NF 1.53E-07 4.659E-06
	5 - 15	0.00014	28	0.16	22.14	2.2	8.3	13.84	6	NF 1.41E-06 4.303E-05
	5 - 6	0.0014	28	0.16	22.14	2.2	8.3	13.84	6	NF 1.41E-05 0.0004303
	6 - 15	5.1E-06	28	0.16	22.14	2.2	8.3	13.84	6	NF 5.14E-08 1.567E-06
	15 - 30	0.00037	28	0.16	35.98	2.2	8.3	27.68	12	NF 2.30E-06 6.997E-05
	15 - 18	0.0018	28	0.16	35.98	2.2	8.3	27.68	12	NF 1.12E-05 0.0003404
	18 - 30	3.8E-06	28	0.16	34.83	2.2	8.3	26.53	11.5	NF 2.44E-08 7.425E-07
	30 - 40	0.000046	28	0.16	42.91	2.2	8.3	34.61	15	NF 2.39E-07 7.296E-06
	30 - 31	0.00046	28	0.16	42.91	2.2	8.3	34.61	15	NF 2.39E-06 7.296E-05
	31 - 40	5.1E-06	28	0.16	42.91	2.2	8.3	34.61	15	NF 2.65E-08 8.089E-07
	40 - 62	2.1E-06	28	0.16	56.75	2.2	8.3	48.45	21	NF 8.26E-09 2.518E-07
	62 - 73	4.2E-06	28	0.16	41.75	2.2	8.3	33.45	14.5	NF 2.25E-08 6.846E-07
	73 - 84	4.2E-06	28	0.16	26.76	2.2	8.3	18.46	8	NF 3.50E-08 1.068E-06

## PACKER PERMEABILITY TESTING DATA

GROUTED CULVERT - PORTLAND

CH-3 Test No. 6

Test Interval (ft)	Time (min)	Q (ft <sup>3</sup> /sec)	Cu	r (ft)	H (ft)	A (ft)	h1 ft of H20	h2 ft of H20	psi	(ft)	L	K (ft/sec)	K (cm/sec)
5.4 - 7.9	0 - 5	0.0019	53	0.16	25.55	2.5	9.4	16.15	7	NF	8.77E-06	0.0002674	
5 - 16	0.02	75	0.16	39.39	2.5	9.4	29.99	13	NF	4.23E-05	0.00129		
16 - 18	0.0029	90	0.16	55.54	2.5	9.4	46.14	20	NF	3.63E-06	0.0001105		
18 - 26	0.00041	80	0.16	44.01	2.5	9.4	34.61	15	NF	7.28E-07	2.219E-05		
18 - 25	0.00046	80	0.16	44.01	2.5	9.4	34.61	15	NF	8.17E-07	2.49E-05		
26 - 38	0.0012	85	0.16	46.31	2.5	9.4	36.91	16	NF	1.91E-06	5.809E-05		
26 - 28	0.0045	100	0.16	60.15	2.5	9.4	50.75	22	NF	4.68E-06	0.0001425		
28 - 38	0.00053	90	0.16	48.62	2.5	9.4	39.22	17	NF	7.57E-07	2.308E-05		
28 - 36.7	0.0006	90	0.16	48.62	2.5	9.4	39.22	17	NF	8.57E-07	2.613E-05		
38 - 51	0.00081	92	0.16	53.23	2.5	9.4	43.83	19	NF	1.03E-06	3.152E-05		
38 - 39	0.0039	100	0.16	60.15	2.5	9.4	50.75	22	NF	4.05E-06	0.0001235		
39 - 51	0.00055	92	0.16	52.08	2.5	9.4	42.68	18.5	NF	7.17E-07	2.187E-05		
39 - 50	0.0006	92	0.16	52.08	2.5	9.4	42.68	18.5	NF	7.83E-07	2.386E-05		
51 - 52	Ran out of water												
Test Interval (ft)	Time (min)	Q (ft <sup>3</sup> /sec)	Cs	r (ft)	H (ft)	A (ft)	h1 ft of H20	h2 ft of H20	psi	(ft)	L	K (ft/sec)	K (cm/sec)
5.4 - 7.9	0 - 5	0.0019	30	0.16	25.55	2.5	9.4	16.15	7	NF	1.55E-05	0.0004724	
5 - 16	0.02	30	0.16	39.39	2.5	9.4	29.99	13	NF	1.06E-04	0.0032249		
16 - 18	0.0029	30	0.16	55.54	2.5	9.4	46.14	20	NF	1.09E-05	0.0003316		
18 - 26	0.00041	30	0.16	44.01	2.5	9.4	34.61	15	NF	1.94E-06	5.918E-05		
18 - 25	0.00046	30	0.16	44.01	2.5	9.4	34.61	15	NF	2.18E-06	6.64E-05		
26 - 38	0.0012	30	0.16	46.31	2.5	9.4	36.91	16	NF	5.40E-06	0.0001646		
26 - 28	0.0045	30	0.16	60.15	2.5	9.4	50.75	22	NF	1.56E-05	0.0004752		
28 - 38	0.00053	30	0.16	48.62	2.5	9.4	39.22	17	NF	2.27E-06	6.924E-05		
28 - 36.7	0.0006	30	0.16	48.62	2.5	9.4	39.22	17	NF	2.57E-06	7.838E-05		
38 - 51	0.00081	30	0.16	53.23	2.5	9.4	43.83	19	NF	3.17E-06	9.665E-05		
38 - 39	0.0039	30	0.16	60.15	2.5	9.4	50.75	22	NF	1.35E-05	0.0004118		
39 - 51	0.00055	30	0.16	52.08	2.5	9.4	42.68	18.5	NF	2.20E-06	6.708E-05		
39 - 50	0.0006	30	0.16	52.08	2.5	9.4	42.68	18.5	NF	2.40E-06	7.318E-05		
51 - 52	Ran out of water												

PACKER PERMEABILITY TESTING DATA									
Grouted Culvert - Portland									
CH-3		Test No. 7							
Test Interval (ft)	Time (min)	Q (ft <sup>3</sup> /sec)	Cu (ft)	r (ft)	H (ft)	A (ft)	h1 (ft)	h2 (ft)	L (ft)
5.4 - 7.1	0 - 2.78	0.000017	44	0.16	13.21	1.7	8.6	4.61	2
	2.78 - 7	0.000011	70	0.16	33.98	1.7	8.6	25.38	11
	7 - 14	6.6E-06	100	0.16	59.35	1.7	8.6	50.75	22
	14 - 21	6.6E-06	70	0.16	36.28	1.7	8.6	27.68	12
	21 - 27	7.7E-06	50	0.16	22.44	1.7	8.6	13.84	6
Test Interval (ft)	Time (min)	Q (ft <sup>3</sup> /sec)	Cs (ft)	r (ft)	H (ft)	A (ft)	h1 (ft)	h2 (ft)	L (ft)
5.4 - 7.1	0 - 2.78	0.000017	26	0.16	13.21	1.7	8.6	4.61	2
	2.78 - 7	0.000011	26	0.16	33.98	1.7	8.6	25.38	11
	7 - 14	6.6E-06	26	0.16	59.35	1.7	8.6	50.75	22
	14 - 21	6.6E-06	26	0.16	36.28	1.7	8.6	27.68	12
	21 - 27	7.7E-06	26	0.16	22.44	1.7	8.6	13.84	6

PACKER PERMEABILITY TESTING DATA									
Paraffin Pit			CH-1						
Test Interval		Time	Q	r	H	A	h1	h2	L
(ft)	(min)	(ft3/sec)	Cu	(ft)	(ft)	(ft)	ft of H20	psi	(ft)
6.2 - 7.8	0 - 0.5	0.000046	45	0.16	13.91	1.6	9.3	4.61	2
	0.5 - 3.5	0.00015	44	0.16	18.53	1.6	9.3	9.23	4
	3.5 - 18	0.00011	60	0.16	25.45	1.6	9.3	16.15	7
	18 - 20.5	0.003	75	0.16	39.29	1.6	9.3	29.99	13
PACKER PERMEABILITY TESTING DATA									
Paraffin Pit			CH-1						
Test Interval		Time	Q	r	H	A	h1	h2	L
(ft)	(min)	(ft3/sec)	Cu	(ft)	(ft)	(ft)	ft of H20	psi	(ft)
5.3 - 7.8	0 - 5	0.0022	50	0.16	16.22	2.5	9.3	6.92	3
PACKER PERMEABILITY TESTING DATA									
Paraffin Pit			CH-1						
Test Interval		Time	Q	r	H	A	h1	h2	L
(ft)	(min)	(ft3/sec)	Cu	(ft)	(ft)	(ft)	ft of H20	psi	(ft)
6.3 - 7.8	0 - 2	0.00013	42	0.16	16.22	1.5	9.3	6.92	3
	2 - 13	4.2E-06	55	0.16	27.76	1.5	9.3	18.46	8
	13 - 26	3.8E-06	85	0.16	47.37	1.5	9.3	38.07	16.5
	26 - 36	4.6E-06	100	0.16	62.36	1.5	9.3	53.06	23
	36 - 46	4.6E-06	85	0.16	46.21	1.5	9.3	36.91	16
	46 - 56	4.6E-06	55	0.16	28.91	1.5	9.3	19.61	8.5
PACKER PERMEABILITY TESTING DATA									
Paraffin Pit			CH-1						
Test Interval		Time	Q	r	H	A	h1	h2	L
(ft)	(min)	(ft3/sec)	Cu	(ft)	(ft)	(ft)	ft of H20	psi	(ft)
6.3 - 7.8	0 - 2	0.000023	40	0.16	13.91	1.5	9.3	4.61	2
	2 - 12.5	4.4E-06	52	0.16	26.60	1.5	9.3	17.30	7.5
	12.5 - 23	4.4E-06	82	0.16	42.75	1.5	9.3	33.45	14.5
	23 - 34	4.2E-06	100	0.16	60.05	1.5	9.3	50.75	22
	34 - 44	4.6E-06	82	0.16	41.60	1.5	9.3	32.30	14
	44 - 54	4.6E-06	52	0.16	25.45	1.5	9.3	16.15	7

PACKER PERMEABILITY TESTING DATA									
Paraffin Pit		CH-2		Test No. 1					
Test Interval (ft)	Time (min)	Q (ft <sup>3</sup> /sec)	r (ft)	H (ft)	A (ft)	h1 (ft)	h2 (ft)	L (ft)	k (cm/sec)
4.5 - 7.5	0 - 5	0.0072	55	0.16	13.61	3.0	9	4.61	2
PACKER PERMEABILITY TESTING DATA									
Paraffin Pit		CH-2		Test No. 2					
Test Interval (ft)	Time (min)	Q (ft <sup>3</sup> /sec)	r (ft)	H (ft)	A (ft)	h1 (ft)	h2 (ft)	L (ft)	k (cm/sec)
4.0 - 7.5	0 - 0.5	0.0023	62	0.16	13.61	3.5	9	4.61	2

## PACKER PERMEABILITY TESTING DATA

PACKER PERMEABILITY TESTING DATA									
Portland Field Trial									
Test Interval	Time	Q	r	H	A	h1	h2	L	K
ft)	(min)	(ft3/sec)	(ft)	(ft)	(ft)	(ft)	(ft)	(ft)	(cm/sec)
5.0 - 10.25	0 - 1	0.0095	100	0.16	57.89	5.25	11.75	46.14	1.03E-05
									0.0003127
PACKER PERMEABILITY TESTING DATA									
Portland Field Trial									
Test Interval	Time	Q	r	H	A	h1	h2	L	K
ft)	(min)	(ft3/sec)	(ft)	(ft)	(ft)	(ft)	(ft)	(ft)	(cm/sec)
5.0 - 7.0	0 - 1	0.0081	98	0.16	54.64	2.0	8.5	46.14	9.45E-06
	1 - 30	3.2E-06	140	0.16	82.324	2.0	8.5	73.824	0.0002882
	30 - 60	1.5E-06	160	0.16	100.78	2.0	8.5	92.28	1.74E-09
	60 - 110	1.5E-06	180	0.16	123.85	2.0	8.5	115.35	5.291E-08
	110 - 120	0.00018	210	0.16	156.148	2.0	8.5	147.648	4.21E-10
									1.282E-08
									3.43E-08
									1.046E-06

PACKER PERMEABILITY TESTING DATA									
TECT Field Trial			Test No. 1						
Test Interval	Time	Q	r	H	A	h1	h2	L	K
4.8 - 6.5	(min)	(ft <sup>3</sup> /sec)	Cu	(ft)	(ft)	(ft)	ft of H <sub>2</sub> O	(ft)	(cm/sec)
0 - 3	0 - 3	0.0081	50	0.16	21.84	1.7	13.84	6	4.64E-05
									0.0014133
PACKER PERMEABILITY TESTING DATA									
TECT Field Trial			Test No. 1						
Test Interval	Time	Q	r	H	A	h1	h2	L	K
4.7 - 6.4	(min)	(ft <sup>3</sup> /sec)	Cu	(ft)	(ft)	(ft)	ft of H <sub>2</sub> O	(ft)	(cm/sec)
0 - 2	0 - 2	0.00012	44	0.16	17.13	1.7	7.9	9.23	4
2 - 3.5	2 - 3.5	0.00011	55	0.16	26.36	1.7	7.9	18.46	8
3.5 - 5.5	3.5 - 5.5	0.0025	44	0.16	17.13	1.7	7.9	9.23	4
5.5 - 8.0	5.5 - 8.0	0.018	40	0.16	10.36	1.7	7.9	3.46	1.5
								1	2.71E-04
									0.0082767

PACKER PERMEABILITY TESTING DATA									
Paraffin Field Trial									
FT-1	Test No. 1								
Test Interval (ft)	Time (min)	Q (ft <sup>3</sup> /sec)	Cu (ft)	r (ft)	H (ft)	A (ft)	h1 (ft)	h2 ft of H <sub>2</sub> O (ft)	psi (cm/sec)
5.2 - 6.9	0 - 3	0.000069	44	0.16	17.63	1.7	8.4	9.23	4
	3 - 5	0.00012	60	0.16	29.16	1.7	8.4	20.76	9
	5 - 20	3.1E-06	75	0.16	38.39	1.7	8.4	29.99	13
	20 - 21.5	0.0072	116	0.16	63.77	1.7	8.4	55.37	24
PACKER PERMEABILITY TESTING DATA									
Paraffin Field Trial									
FT-1	Test No. 2								
Test Interval (ft)	Time (min)	Q (ft <sup>3</sup> /sec)	Cu (ft)	r (ft)	H (ft)	A (ft)	h1 (ft)	h2 ft of H <sub>2</sub> O (ft)	psi (cm/sec)
5.0 - 7.3	0 - 3.17	0.0012	52	0.16	21.49	2.3	8.8	12.69	5.5

**Appendix D**

**Results of Field-Scale Permeameter Water Emissions**



**MSE-HKM, Inc.**  
**Laboratory Services**

106 S. Parkmont  
(406) 494-1403

Butte, MT 591  
Fax (406) 494-11

October 23, 1996

Andy Zdinack  
MSE/TA  
WETO  
Butte, MT 59701

Dear Andy:

Please find enclosed analytical results for the water samples received at the MSE\HKM Laboratory October 3, 1996.

If you have any questions, please do not hesitate to call.

Sincerely,

  
Koen Kuyper

KEVIN KISSELL  
Laboratory Supervisor

**Enclosure**

KK/rbk

Ex - Baseline (Ungrafted) Colvent

SC - South (Created) Cult

CLIENT: ZDINACK,ANDY Report Date: 10/22/96 Page 1

DATE RECEIVED: 10/3/96

BF: 001794

Nitrate/Nitrite-N

Field ID	Sampled Date/Time	Results	Units	MSE Lab No.
IC-01	10/02/96 11:10:0	5360	mg/L	(W014932)
IC-01	10/02/96 11:40:0	3250	mg/L	(W014935)

MS

Review

10/22/96

1-423-HB003

MSE INC

4067236328

DATE RECEIVED: 10/3/96

BIF: 001794

## METALS TOTAL

Field ID	Sampled Date/Time	Results	Units	MSE Lab No.
Cerium				
SC-02	10/02/96 11:10:0	0.25	mg/L	(W014933)
BC-02	10/02/96 11:42:0	0.07	mg/L	(W014935)
Potassium				
SC-03	10/02/96 11:10:0	1570	mg/L	(W014934)
BC-03	10/02/96 11:47:0	1160	mg/L	(W014937)

  
Review

## **Appendix E**

### **Monitoring for Water Migration Following Jet Grouting**



## **Appendix E**

### **Monitoring for Water Migration Following Jet Grouting**

#### **ABSTRACT**

Pit D, located in disturbed sediments at the Cold Test Trench south of the Subsurface Disposal Area, was filled with simulated wastes and covered with 2.5 ft of soil. A total of 13 neutron-probe access tubes were drilled on three sides and in the center of the pit. On August 8, 1996, the pit was injected with Portland cement. This was followed by the drilling of two core holes in the pit and packer testing on August 22 and 23. Neutron moisture monitoring indicated that there were significant moisture content increases associated with the introduction of the water/grout mixture inside and to the north of the pit. Lesser moisture increases were noted in monitoring locations to the south and east. Water associated with the grout was bound in the cement monolith and had little or no influence on moisture contents in surrounding baseline sediments, suggesting that there is little danger of the mobilization or transport of waste components. Water introduced during the core drilling and packer tests had only a slight effect on moisture contents in sediments near the neutron monitoring sites.



# Monitoring for Water Migration Following Jet Grouting

## INTRODUCTION

In 1996, the Subsurface Contaminant Focus Area conducted the Innovative Subsurface Stabilization Project at the Cold Test Pit south of the Radioactive Waste Management Complex. The project involved field testing and evaluation of in situ waste encapsulation techniques. One objective of the field test was to investigate moisture movement at Pit D, a cold waste pit that had been jet grouted with Type-H Portland cement. Investigators wanted to know how moisture associated with the grout mixture affects moisture content in sediments near the pit and if water in the grout mixture was sufficient to mobilize waste constituents. This report documents results of that investigation.

## METHODS

### Pit Installation

Pit D was a 6-ft cube-configured pit dug in disturbed surficial sediments (Figure E-1). Simulated wastes, consisting of cardboard boxes, paper, plastic, 55-gal drums, wood, and assorted metal pieces, were placed in the pit and subsequently covered with 2.5 ft of overburden.

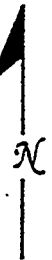
### NAT Hole Installation and Completion

Figure E-1 shows locations of the 13 neutron-probe access tube (NAT) holes drilled in and near the pit. A set of four holes extends laterally from each of three sides of the pit (north, east, and south). The first hole in each set is located 1 ft from the surveyed pit perimeter, with spacing of 1 ft, 1.5 ft, and 1.5 ft between holes (as shown in Figure E-1). One hole is located in the middle of the pit. Table E-1 is a listing of each NAT hole, depth, and location in relation to Pit D. Holes were drilled on July 10 and 11, 1996.

**Table E-1.** NAT hole name, depth, and location with respect to Pit D.

Name	Drilled Depth (ft)	Maximum Monitored Depth (ft)	Location
NAT 51	16.8	12	Center of pit
NAT 61	16.4	15.5	North of pit
NAT 62	17.2	16.5	North of pit
NAT 63	16.5	15.5	North of pit
NAT 64	17.6	16.5	North of pit
NAT 71	16.6	15.7	North of pit
NAT 72	17.4	16.5	South of pit
NAT 73	17.6	16.5	South of pit
NAT 74	15.6	14.5	South of pit
NAT 81	14.8	13.5	East of pit
NAT 82	15.5	14.5	East of pit
NAT 83	15.6	14.5	East of pit
NAT 84	16.1	15.5	East of pit

- 64
- 63
- 62
- 61



## Cold Test Pit #D

- 51

1' 1' 1.5' 1.5'

- 71
- 72
- 73
- 74

overburden 2.5'

Ground surface

51

63

64

84

Sediment/Basalt Interface

74

73

72

Figure E-1. Plan-view map and 3-D map of Pit D.

The NAT holes were drilled with a 2-in. auger to the underlying basalt. Carbon steel tubes, 1.9-in. outer diameter and 1.6-in. inner diameter with sealed bottoms, were placed in each hole. The hole in the center of Pit D (NAT-51) was drilled through the waste to the basalt. However, wastes caved into the bottom of the hole while the tube was being placed downhole, preventing full tube penetration. About 4 ft of the hole was lost.

Sediments recovered during drilling were finely sieved (<1/4 in.) and placed into the annular spaces of each hole. The sieved sediments were compacted by running a long wire up and down the annular spaces and by vibrating the carbon steel tube. This ensured a tight sediment backfill in each of the annular spaces. NAT-51, of course, was the exception. Wastes appeared to have blocked the annular space at the bottom of the hole and potentially obstructed some areas along the sides of the tube, preventing a tight tube seal to the formation. Approximately twice the usual volume of sieved sediments was placed in this hole, indicating that void spaces within the wastes were being filled. Once the backfilling was complete, the tube tops were cut such that they were 1 to 2 in. below land surface. Tube openings were taped and capped to prevent sediments from falling into the tubes.

### **Neutron-Probe Monitoring**

Neutron moisture monitoring used the CPN 503 hydroprobe with a 50-mCi Am/Be source, an emitter of fast neutrons. The fast neutrons are thermalized by collisions with hydrogen nuclei, usually associated with the presence of water. The probe counts the number of thermalized neutrons during a preselected monitoring period and, generally, the larger the count, the more water present.

Moisture monitoring is initiated by lowering the source into the NAT hole to the final cable stop near the bottom of the hole. A 16-second count is taken and entered into the probe's electronic storage. The source is pulled up 6 in. to the next cable stop, where the process is repeated. This process is continued until the entire depth of the NAT hole is logged in 6-in. intervals. Because the source is not waterproof, it cannot be placed in water (hence, the NAT tubes are sealed at the bottom).

The neutron count was calibrated to moisture content using a calibration equation developed for disturbed Subsurface Disposal Area surficial sediments (Bishop 1996). The disturbed sediment equation was used because the sediments in this area have been dug, worked, and redistributed several times. All holes were monitored at least once (in July) before jet grouting. Four holes were monitored twice before grouting to ensure that a stable baseline neutron moisture profile had been obtained. Table E-2 lists dates that each of the holes were monitored. Neutron monitoring data are available from Carolyn Bishop at the Idaho National Engineering Laboratory (INEL).

### **Jet Grouting**

On August 8, 1996, after the NAT holes were installed and initial moisture monitoring was completed, Pit D was jet grouted with a 1-to-1 mixture (mass) of Portland Type-H cement (also known as a 14-sack per cubic yard mix) and water. The cement/water mixture was about the same viscosity as water. The grout was injected into the pit from 18 grouting centers spaced in a

Table E-2. NAT holes and dates monitored.

NAT holes	Dates monitored
NAT-51	7/24/96, 8/12/96, 8/15/96, 8/19/96, 8/27/96, 9/4/96, 10/11/96
NAT-61	7/17/96, 8/12/96, 8/15/96, 8/19/96, 8/27/96, 9/4/96, 10/11/96
NAT-62	7/17/96, 8/12/96, 8/15/96, 8/19/96, 8/27/96, 9/4/96, 10/11/96
NAT-63	7/17/96, 7/24/96, 8/12/96, 8/15/96, 8/27/96, 9/4/96, 10/11/96
NAT-64	7/17/96, 7/24/96, 8/12/96, 8/15/96, 8/27/96, 9/4/96, 10/11/96
NAT-71	7/17/96, 8/12/96, 8/15/96, 8/19/96, 8/27/96, 9/4/96, 10/11/96
NAT-72	7/24/96, 8/12/96, 8/15/96, 8/27/96, 9/4/96, 10/11/96
NAT-73	7/17/96, 7/24/96, 8/12/96, 8/15/96, 8/27/96, 9/4/96, 10/11/96
NAT-74	7/17/96, 8/12/96, 8/15/96, 8/27/96, 9/4/96, 10/11/96
NAT-81	7/17/96, 7/24/96, 8/12/96, 8/15/96, 8/19/96, 8/27/96, 9/4/96, 10/11/96
NAT-82	7/17/96, 8/12/96, 8/15/96, 8/19/96, 8/27/96, 9/4/96, 10/11/96
NAT-83	7/17/96, 8/12/96, 8/15/96, 8/27/96, 9/4/96, 10/11/96
NAT-84	7/17/96, 8/12/96, 8/15/96, 8/27/96, 9/4/96, 10/11/96

triangular-pitch matrix 20 in. apart. A 19th grouting center outside and slightly south of the pit center on the western pit perimeter was also used to inject cement. Spacing for this center was 20 in. from the nearest center. Grouting was accomplished by placing a nozzle at the depth, injecting grout under 6,000 psi pressure, withdrawing the drill stem nozzle assembly, and continuing the process until the entire pit was grouted. Approximately 70 gal of grout was injected at each grouting center. A more detailed description of the grouting methods can be found in *Innovative Subsurface Stabilization Project—Final Report* (Loomis 1996).

Grouting has the potential to affect moisture contents when the water/cement mixture is introduced into the subsurface. The concern is the possibility that not all the water is tied up in the cement when the cement cures, and that the excess water might contribute to the mobilization and transport of waste constituents.

### Core Drilling

Core holes 1 and 2 were drilled through the grouted pit on August 22 and 23, 1996. The purpose for drilling these holes was to collect core data to ascertain grout hydraulic conductivity and provide a mechanism for performing subsequent packer tests. A 4 7/8-in. HX core pipe was used in the drilling. Core hole 1 was drilled to a depth of 8 ft in the southeast quadrant of the pit; core hole 2 was drilled to a depth of 8.1 ft in the northwest quadrant. The core indicated that the grout had not permeated the entire volume of material in the pit. Some cored intervals showed grout penetration; others were relatively untouched by the grout. More information on the drilling and grouting can be found in *Innovative Subsurface Stabilization Project—Final Report* (Loomis 1996).

The core drilling has the potential to affect moisture content by providing moisture to the Pit D area. Water was used during the core drilling. Loomis (1996) estimated that 10 gal/minute of water was used for 3 hours (1,800 gallons), while the driller estimated 400 to 500 gal of water used per hole. Some of this water entered the subsurface; some came back up the boreholes and drained into nearby low areas where it either seeped into the ground or evaporated.

### **Packer Testing**

On August 23, 1996, packer tests were performed in core holes 1 and 2. The objective for performing the packer tests was to determine the saturated hydraulic conductivity of the materials surrounding the core holes. Packers were set at selected intervals in the borehole, and water under a 2-to-8 psi pressure head was injected into core holes 1 and 2.

About 50 gal of water was injected into core hole 1 during two packer tests. The test interval for the single packer test was 60 to 118 in. below land surface (bls), and 20 gal of water was injected into this interval. The test interval for the double packer test was 60 to 81 in. bls. Thirty gal of water was injected into this interval before the test was stopped. Maximum pressure in both tests did not exceed 2 psi. Where the water went during both of these tests is unknown. Twenty-four gal of water was injected into core hole 2 under 8 psi pressure during a single packer test. The test interval was 60 to 96 in. bls. The water was observed to surface about 3 ft southeast of the injection site. When the water reached the land surface, the packer test in core hole 2 was discontinued.

The packer test has the potential to affect moisture content by providing water to the subsurface. Moisture monitoring was performed 4 days following injection of water during the packer tests.

## **MOISTURE MONITORING RESULTS**

The July monitoring was performed before the jet grouting conducted on August 8, 1996. The purpose for monitoring before the grouting was to establish a baseline moisture profile for each of the NAT holes. Although most holes were monitored only once before the injection of grout, that was sufficient to establish a baseline, as Figures E-2 and E-3 indicate. Figures E-2 and E-3 are baseline plots for NAT-63 and NAT-73, respectively. The figures show moisture profiles monitored on July 17 and 24, 1996. In both figures, the two profiles are nearly identical, indicating that moisture regimes near the pit did not vary for several weeks before the test. These data indicate that moisture profiles of the other holes are reasonable baseline data even though only one monitoring was performed.

### **Test Summary**

Table E-3 is a listing of estimated moisture increases (positive values) and decreases (negative values) derived from neutron-probe readings taken a few days after the August 8 grouting and the August 22-23 core drilling/packer tests. These estimates were obtained by integrating the differences between subsequent moisture content profiles over the length of the access tube. This technique results in an estimate for the amount of total moisture change in the

## NAT 63 (north)

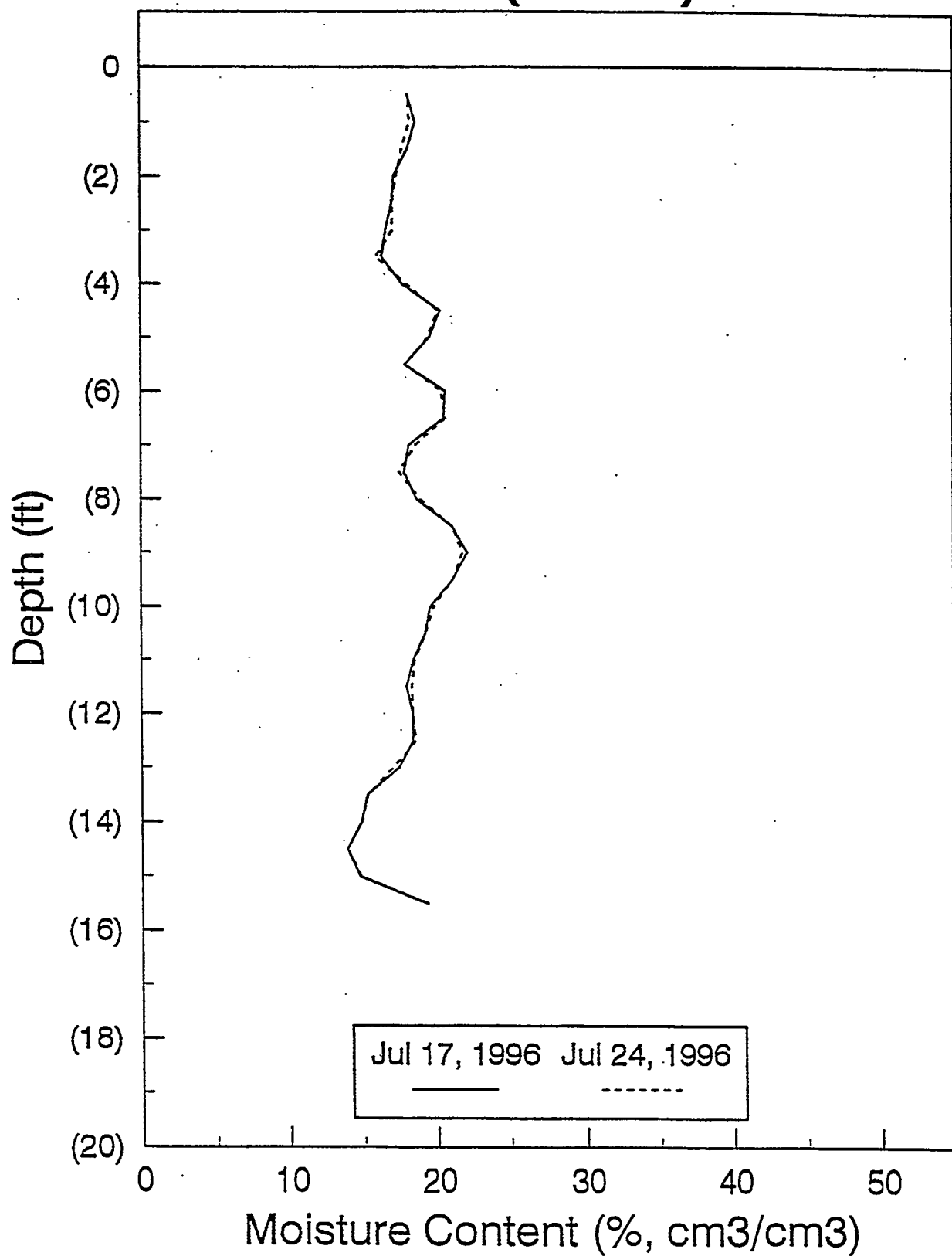


Figure E-2. Baseline moisture content profiles for NAT-63.

# NAT 73 (south)

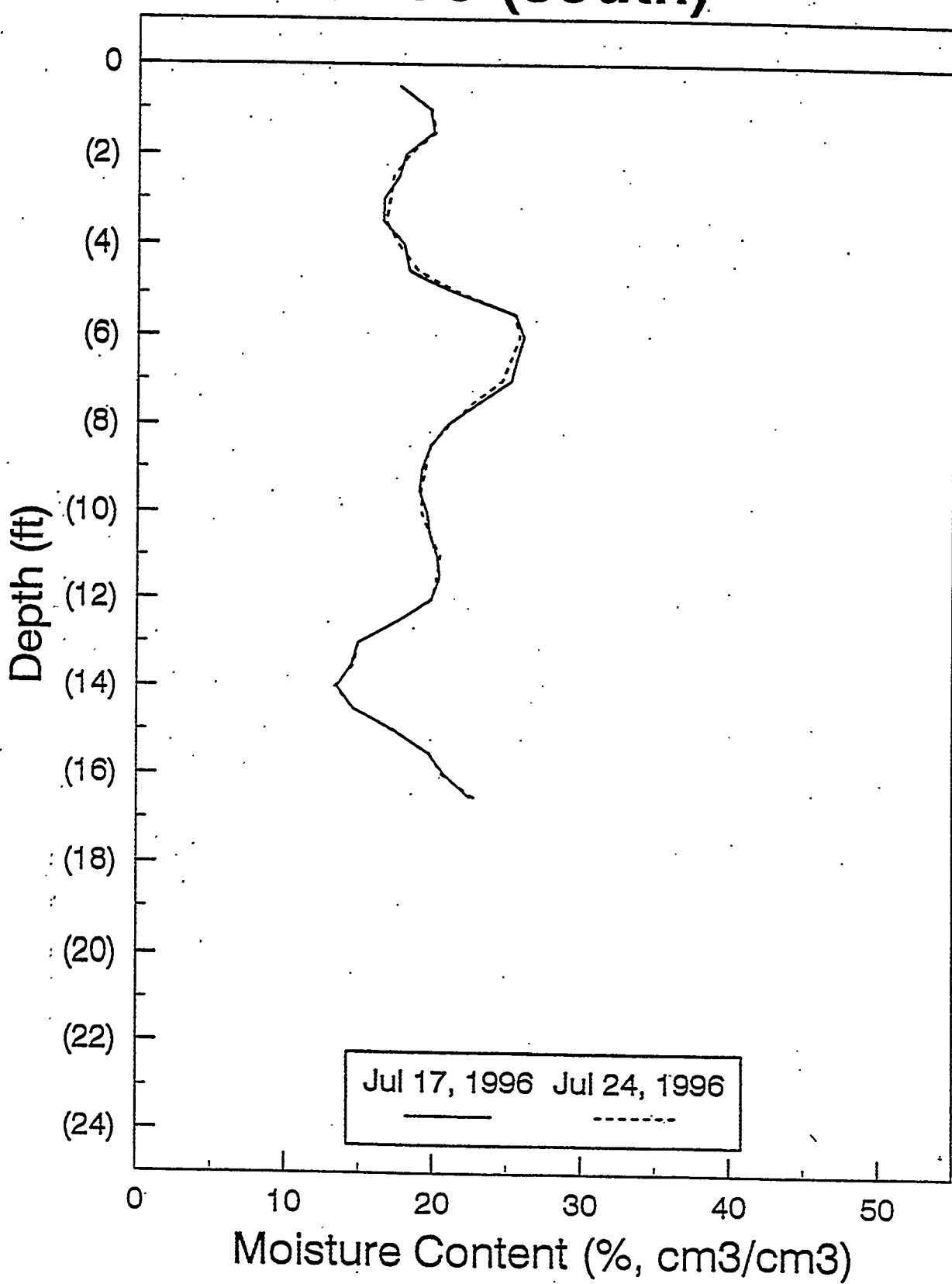


Figure E-3. Baseline moisture content profiles for NAT-73.

**Table E-3.** Estimated water increases and decreases resulting from moisture changes in sediments at NAT sites following grouting and drilling/packer testing.

NAT hole	Increases (-decreases) in moisture around each hole (inches of water)	
	Grouting (July 17/24-Aug 12)	Core drilling/packer test (Aug 19-27)
NAT-51	20.48	(-0.49)
NAT-61	5.02	(-0.113)
NAT-62	0.45	0.13
NAT-63	0.35	0.43
NAT-64	0.07	0.06
NAT-71	1.01	(-0.18)
NAT-72	0.43	0.06
NAT-73	0.11	0.13
NAT-74	(-0.02)	(-0.16)
NAT-81	0.58	0.14
NAT-82	0.27	(-0.02)
NAT-83	0.18	0.07
NAT-84	0.25	(-0.00)

vicinity of each NAT hole and does not reflect total amounts of moisture increases or decreases for the entire Pit D area. Copies of the computer output for each NAT hole are available from Carolyn Bishop at the INEL.

What follows is a discussion of moisture profile changes for each of the monitored holes: NAT-51, -61, -62, -63, -64, -71, -72, -73, -74, -81, -82, -83, and -84.

### NAT-51

Figure E-4 is a plot of all NAT-51 monitoring profiles. The background moisture profile (solid line) was measured on July 24. Often the profile can be used to determine soil structure. The sharp angles seen in the profile (1.5, 9, and 11 ft) are typical of Subsurface Disposal Area disturbed sediments and are usually in response to moisture increases resulting from textural and density changes in the soil, which is probably the case here. However, the moisture increase at the 5-ft level in NAT-51 is caused by an intrusion of sediments into the wastes. The profile

# NAT 51 (center)

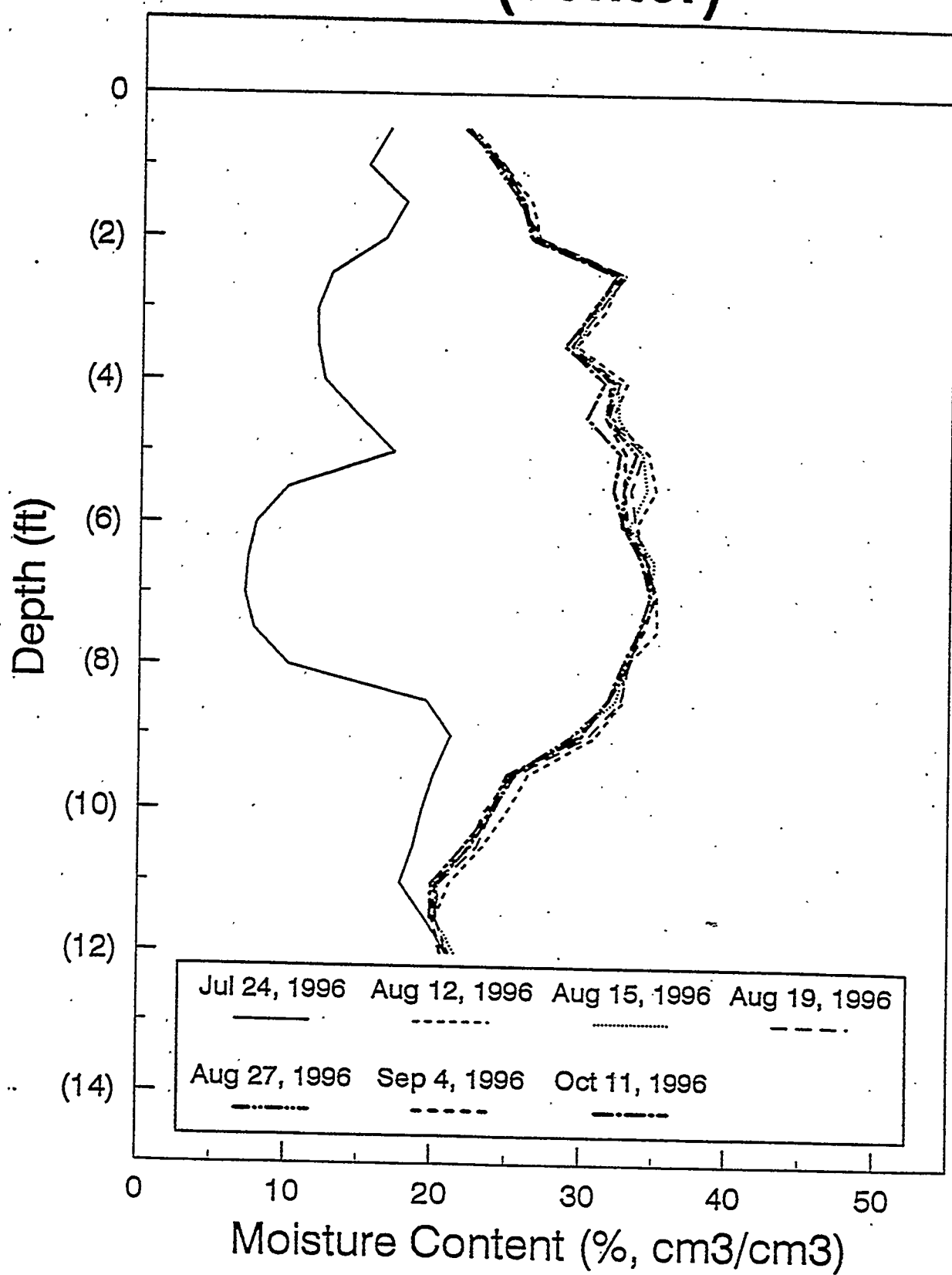


Figure E-4. Moisture content profiles for NAT-51.

indicates that wastes are encountered at about 2.5 to 8.5 ft. The 5 to 8.5-ft section is considerably drier than other areas in the hole. The higher moisture content in the 2.5 to 5-ft section results from a mixture of sediments and wastes. Sediments may have mixed with the wastes during emplacement of the overburden cover and/or during the completion of NAT-51.

The August 12 monitoring followed grouting by several days. Neutron monitoring indicates that the moisture content had increased along the entire profile except at the bottom of the hole. Moisture contents sharply increase in areas inside the pit where wastes were encountered starting at about 2.5 ft and ending at about 9 or 9.5 ft bls. The curve between about 2.5 and 6 ft bls is influenced by the sediments in the waste. The profile also indicates that grouting resulted in increased moisture contents (although well below saturation levels) in the sediments above and below the pit. This moisture increase is expected. Where the moisture contents after August 12 have not continued to change significantly over time, it can be assumed that the moisture contents for August 12 and afterward are associated with cured grout.

The August 12 monitoring shows the wettest conditions in this hole occurred from about 5 to 6 ft, and 7.5 ft bls. The August 15 monitoring indicates that only slight drying has occurred except at the bottom of the hole, where sediments are slightly wetter. All subsequent monitoring shows the profile to be slightly drier, approaching an equilibrium condition for the cement monolith. This result indicates that there is little or no free water in the cement/soil matrix. The October 11 monitoring shows drying at about 4 to 6 ft bls, another indication that soil is present in this area. The decrease in moisture at this interval also suggests that the interval is not thoroughly grouted; otherwise, this amount of moisture change would not be expected. However, grouting for most of the monolith around this hole is fairly thorough, because water introduced to the pit during the core drilling and packer tests (August 22-23) appears to have had very little influence on moisture contents that surround NAT-51. In areas where the grouting is not thorough, the moisture is not bound in the grout, and moisture contents would be expected to change, as seen at the 5.5-ft level in NAT-51.

#### **NAT-61**

Grouting also influenced moisture content to the north of Pit D (Figure E-5). Preferential flow from the pit to the north is evident during both grouting and packer testing. Moisture contents increased from the surface down to about 9.5 ft bls, which is an indication that the grout mixture injected into the pit has moved to the north in response to some preferential flow path. Surface wetting to about 1.5 ft is evident in the September 4 monitoring. This was probably caused by the core drilling/packer tests. Otherwise, neither the core drilling nor the packer testing appears to have affected the moisture content in the sediments surrounding this hole.

#### **NAT-62**

Figure E-6 shows the moisture profile for NAT-62, another hole located to the north of the pit. Grouting increased moisture content from about the 7 to 8.5-ft level bls. Otherwise, the profile is fairly consistent, indicating that while grouting had a small affect, core drilling and packer testing did not.

# NAT 61 (north)

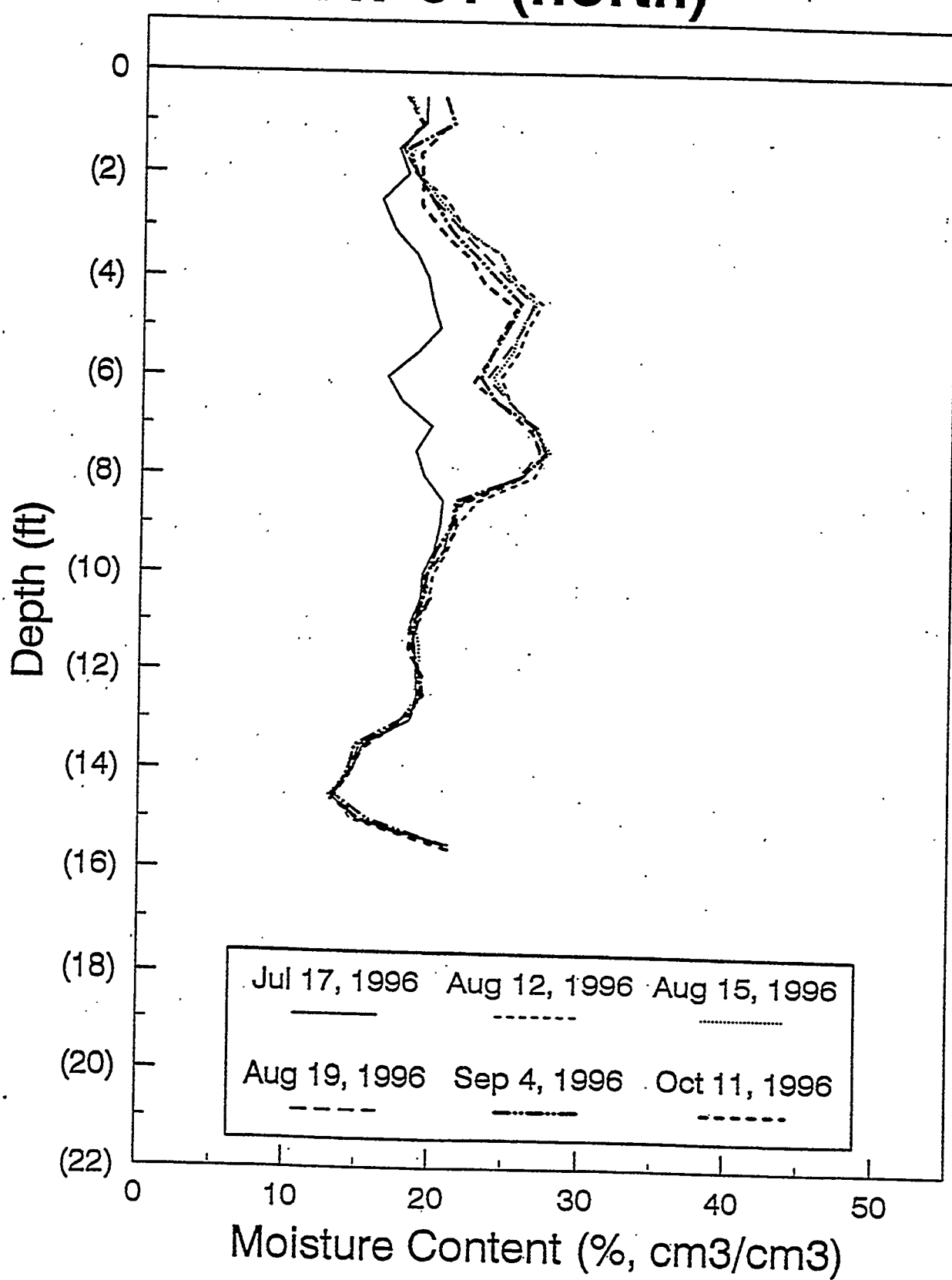


Figure E-5. Moisture content profiles for NAT-61.

## NAT 62 (north)

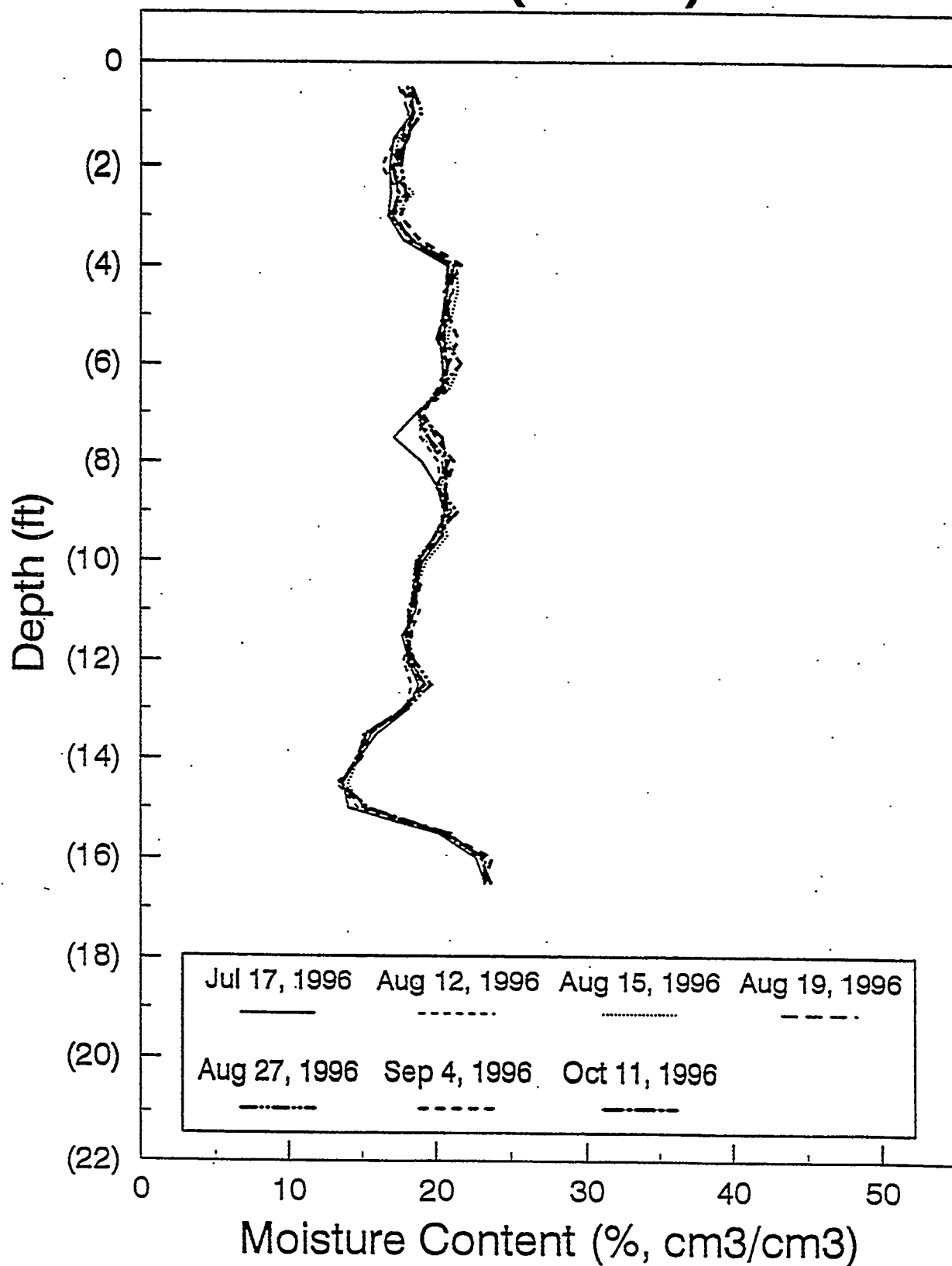


Figure E-6. Moisture content profiles for NAT-62.

## NAT-63

Moisture profiles for NAT-63 are shown in Figure E-7. Two small areas are influenced by grouting: about 5.5 ft and about 7 to 9.5 ft bls. Grouting influence in NAT-63 appears to be slightly greater than in NAT-62, which is surprising considering that NAT-62 is 1.5 ft closer to the northern perimeter of Pit D than NAT-63. This is another indication that some sort of preferential flow is occurring. Also interesting is that some of the wettest conditions measured in this interval are monitored on October 11. This result also indicates preferential flow; core drill and packer water may have moved in some unmonitored area following some preferential flow path or paths, and the wetting fronts from these areas are only now reaching NAT-63 where they can be monitored.

## NAT-64

Moisture content for NAT-64, the most northerly hole, is depicted in Figure E-8. Slight changes in moisture content are noted from the surface to about 5 ft, with the greatest change in mid-hole about 7 to 9 ft. Most of the increases in moisture are not attributable to effects of grouting, but appear to be related to the core drilling/packer testing. Preferential flow may influence this area; the wettest conditions occurring at the 8-ft level were monitored on October 11, 1996. Wetting at the surface (1 to 5 ft) also appears to be influenced by the core drilling/packer tests.

## NAT-71

NAT-71, -72, -73, and -74 are located to the south of Pit D. Moisture increases in this direction are much less pronounced than those monitored to the north. Moisture profiles for NAT-71 are shown in Figure E-9. Grouting caused moisture contents to increase from about 1.5 ft to 9 ft bls, with an additional slight increase about 11 ft bls. The moisture content increase noted at 5 to 5.5 ft appears to be a delayed response to the grouting.

## NAT-72

Moisture content increased in NAT-72 about 2.25 to 5.5 ft bls and again at 6.5 to 9 ft bls (Figure E-10). Both increases are slight and resulted from grouting. Core drilling/packer testing may have increased the response at 2.25 to 5.5 ft. In any event, the increases between the 2.25 and 5.5 levels are slight. Also, there appears to be a subtle increase in moisture content at the bottom of the hole at the sediment/basalt interface. Although this increase is very slight, it suggests that the water that went into the subsurface during the core drilling and packer tests descended to the sediment/basalt interface and moved along it.

## NAT-73

NAT-73 moisture profiles are depicted in Figure E-11. Again, as is noted in all the holes to the south of the pit, slight moisture level increases are observed in the first 5.5 ft of the hole. Below that level, moisture changes cannot be distinguished. Moisture changes are related to the grouting and perhaps the core drilling and packer tests. It should be noted that some of the responses attributed to packer testing may actually be delayed grout influences. Moisture may

## NAT 63 (north)

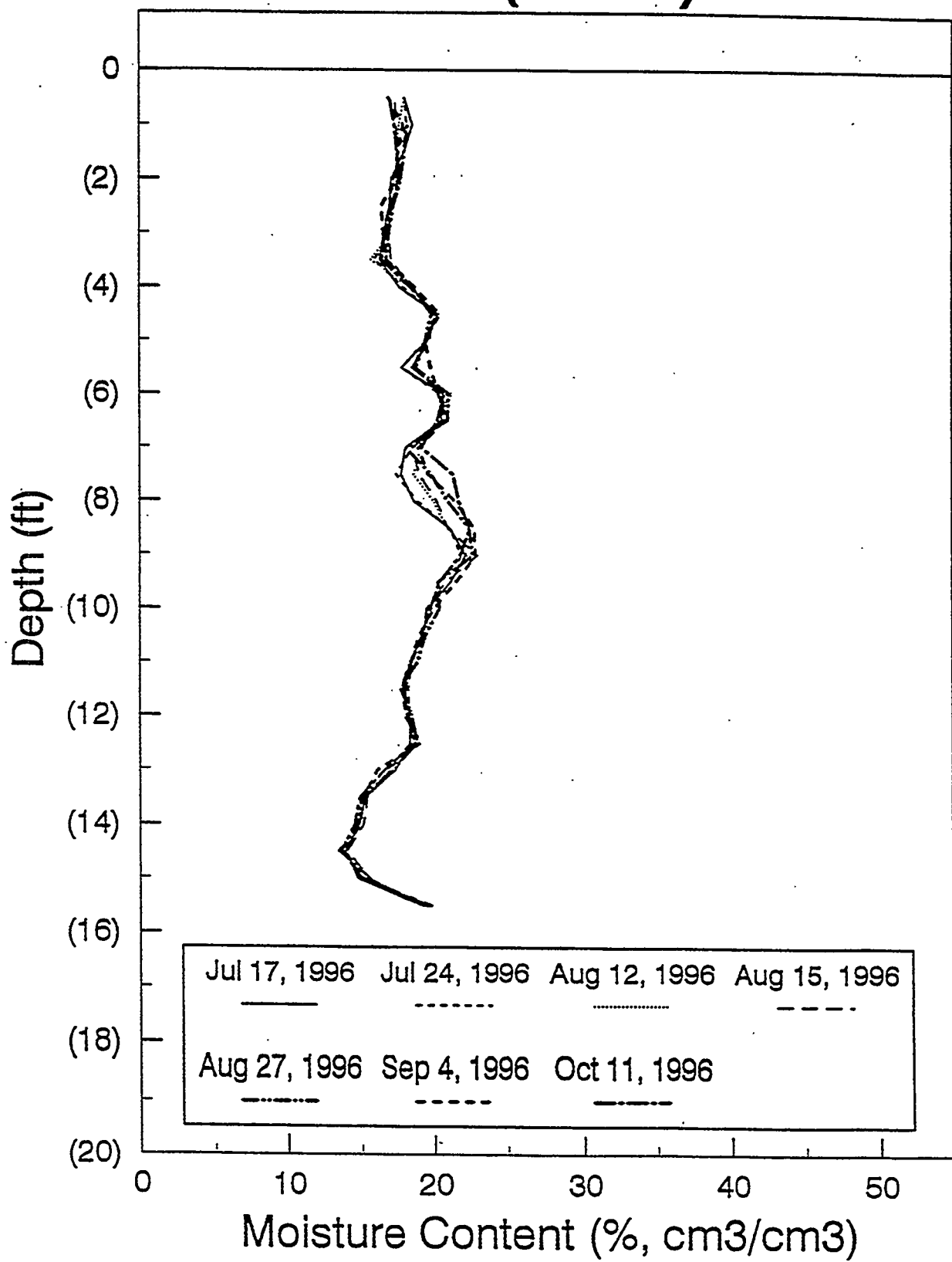


Figure E-7. Moisture content profiles for NAT-63.

# NAT 64 (north)

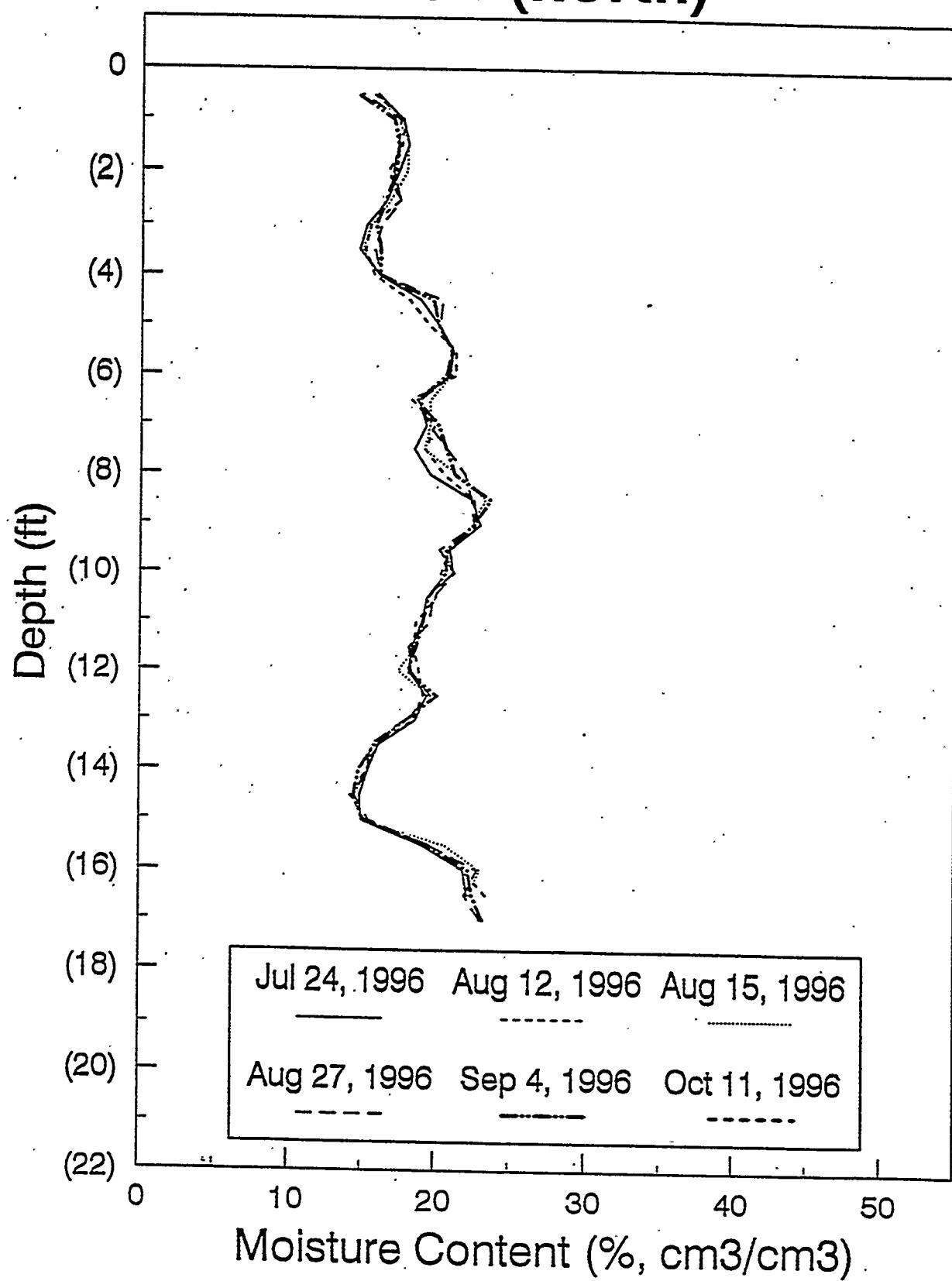


Figure E-8. Moisture content profiles for NAT-64.

# NAT 71 (south)

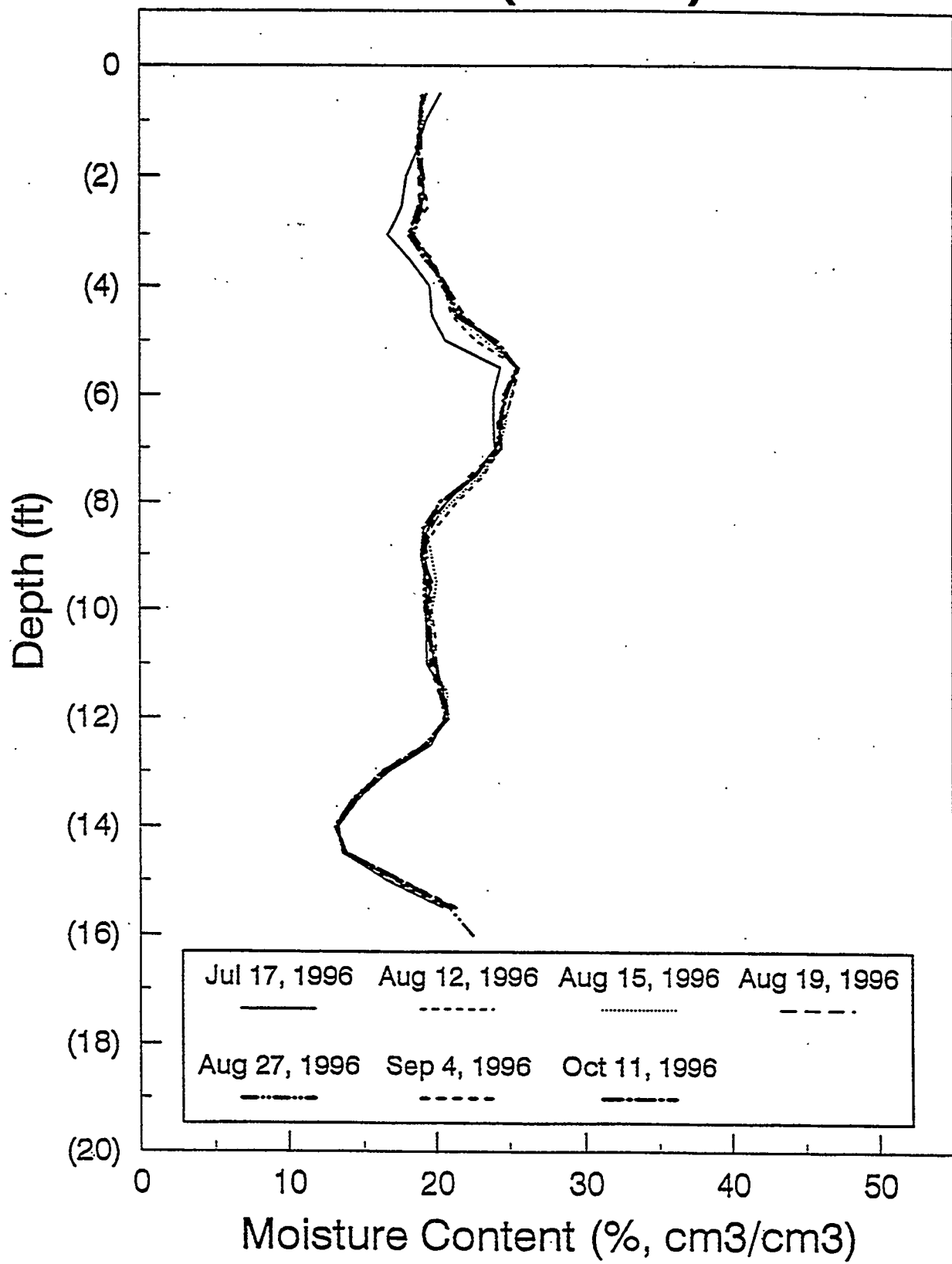


Figure E-9. Moisture content profiles for NAT-71.

# NAT 72 (south)

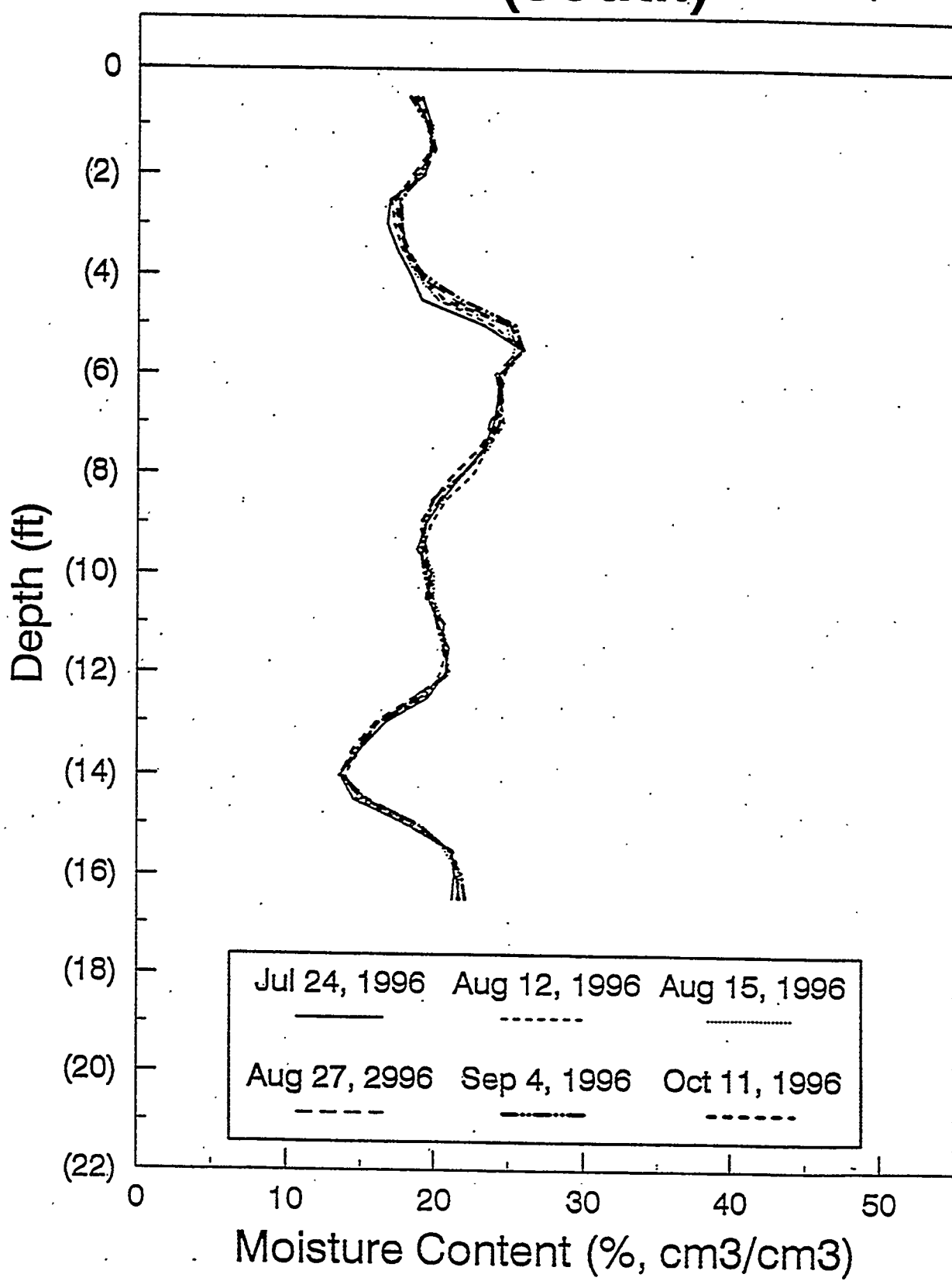


Figure E-10. Moisture content profiles for NAT-72.

# NAT 73 (south)

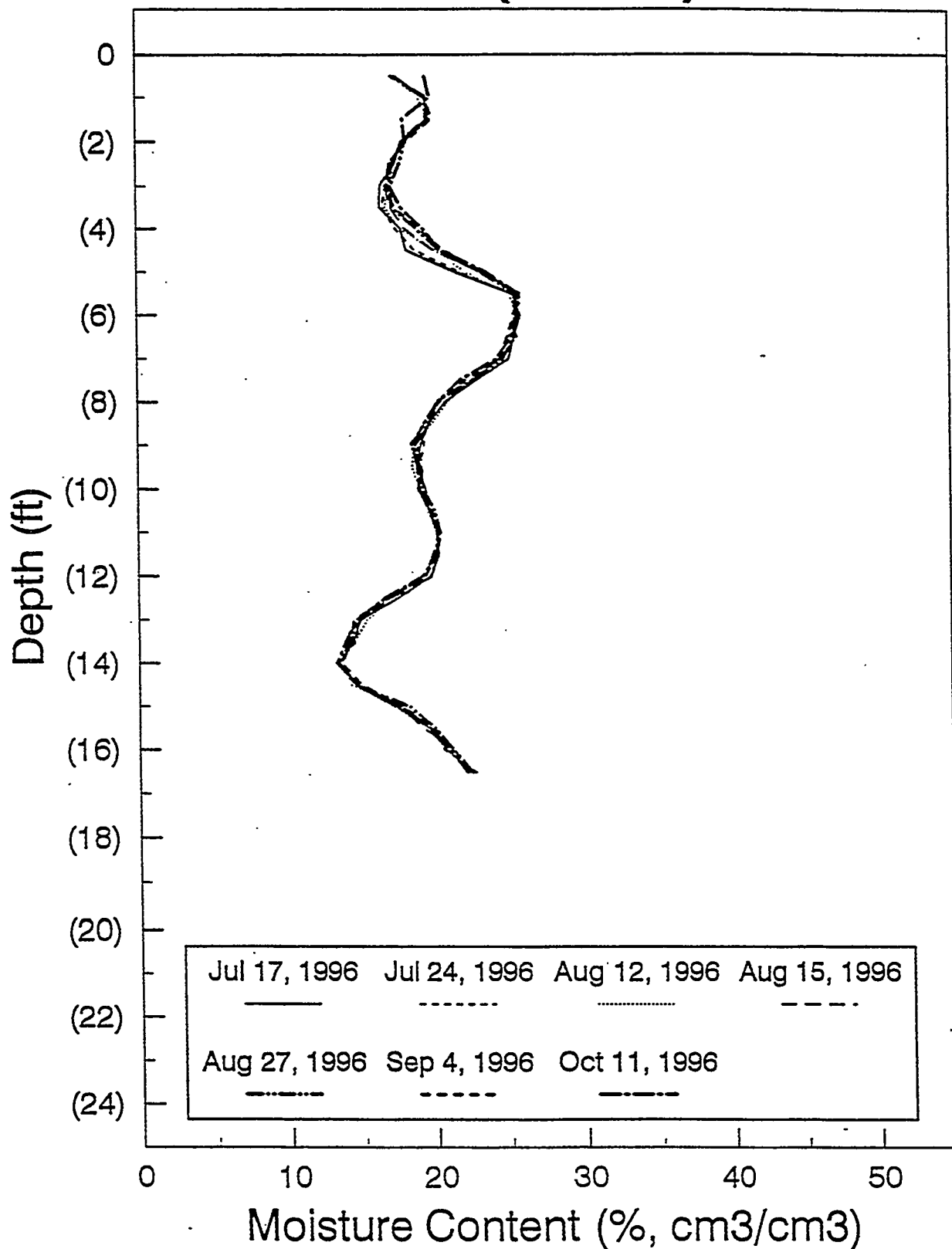


Figure E-11. Moisture content profiles for NAT-73.

move through preferential pathways fairly quickly, and moisture moving out as a wetting front from a source such as the grouted monolith may be delayed, yet both moisture increases can be related to a single event (the grouting).

#### **NAT-74**

Figure E-12 shows moisture profiles for NAT-74. Moisture changes were noted from about 3 to 5 ft bls. The majority of these influences can be related to effects of grouting. However, the bulge between 4.25 and 5 ft bls may be packer test influences. Profiles indicate that some drying of the sediments has occurred in the lower portions of the hole.

#### **NAT-81**

Moisture profiles for NAT-81 (east of the pit) indicate wetting in the interval from 5 to 9 ft bls (Figure E-13), and the wetting is greater than on the southern perimeter. Less than half of the moisture increases are attributed to grouting; the rest appear to be the result of water introduced during the core drilling and packer test. The October 11 profile shows the wettest conditions in the interval from 6.25 to 8 ft bls, which results from a wetting front moving from a source which could be the grouted monolith or introduced water. Because water from the packer test surfaced a few feet from this hole, it may be more reasonable to assume that the increased moisture content in this interval resulted from the packer tests. Surface moisture increases are mostly due to core drilling and packer testing.

After Pit D testing was complete, the sediments on the southeast side of the monolith were removed to permit examination of the grout. Slight increases in sediment moisture were observed in the vicinity of this hole (NAT-81). Apparently, a soil ramp angling down from the surface into the pit existed before and during pit construction. Traffic using the ramp compacted the soil, which created a path for the moisture to follow toward the surface. This may be the reason that moisture changes observed in the eastern NAT holes are higher in the profile (1 to 7 ft bls) than in NAT holes located either to the north or south. This may also be the explanation of why the packer test water (core hole 2) surfaced in this general direction.

#### **NAT-82**

NAT-82 shows wetting in the middle of the hole, similar to NAT-81, except that the amount of increase is much less (Figure E-14). The greatest increase was noted between the September 4 and October 11 monitoring, indicating that moisture moved into the area substantially after the event. Because moisture increases in NAT-81 are probably related to the packer test, it can be assumed that these increases are probably due to the packer test as well.

#### **NAT-83**

NAT-83 shows slight increases in the 5.5 to 8-ft levels (Figure E-15). Again, the wettest conditions in this interval were monitored on October 11 and are probably a result of moisture introduced during the packer test. The interval between about 8 and 9 ft bls indicates that slight drying of the sediments has occurred. Otherwise, the profiles indicate that moisture conditions changed very little from the mid-July background.

## NAT 74 (south)

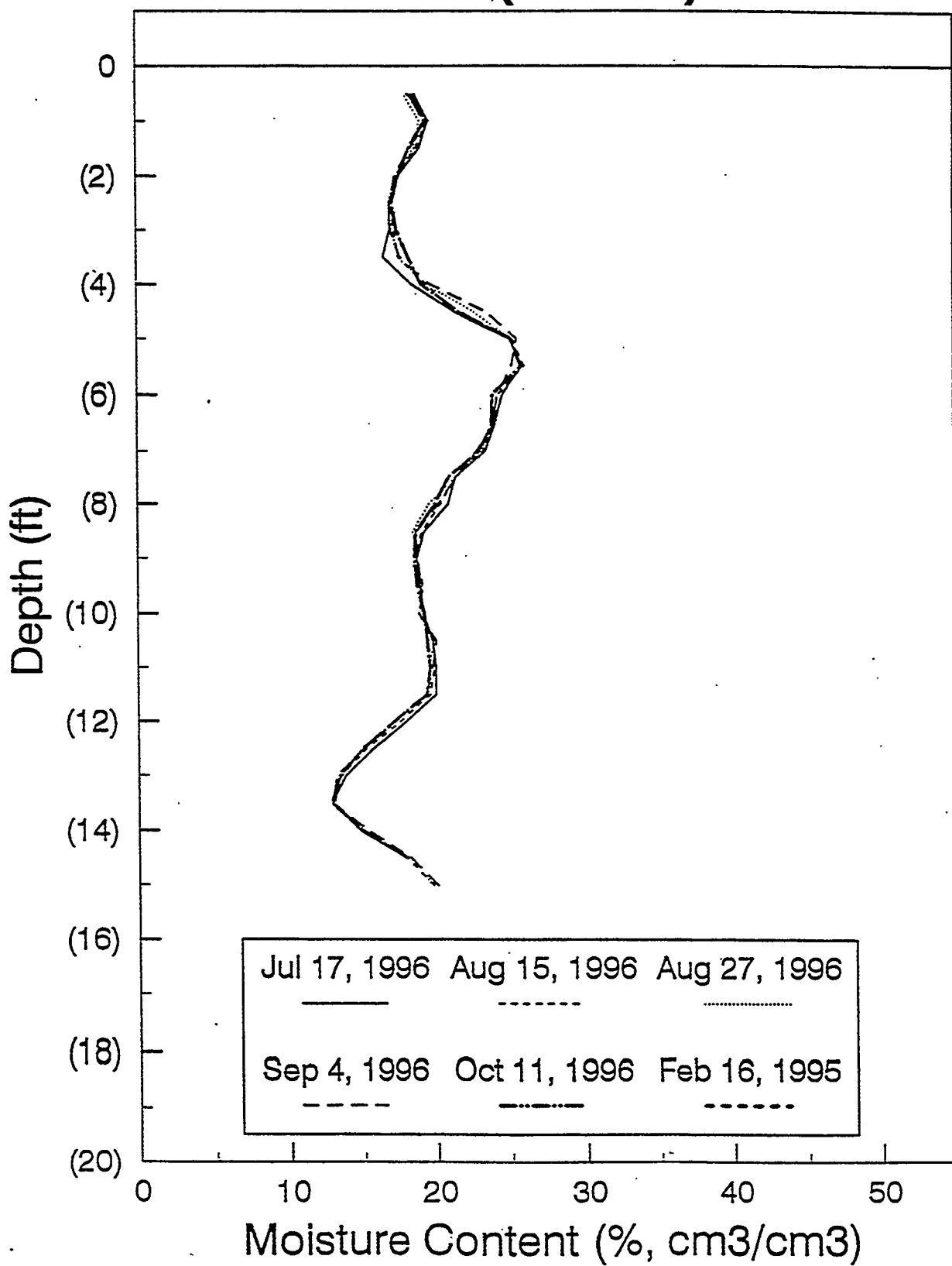


Figure E-12. Moisture content profiles for NAT-74.

# NAT 81 (east)

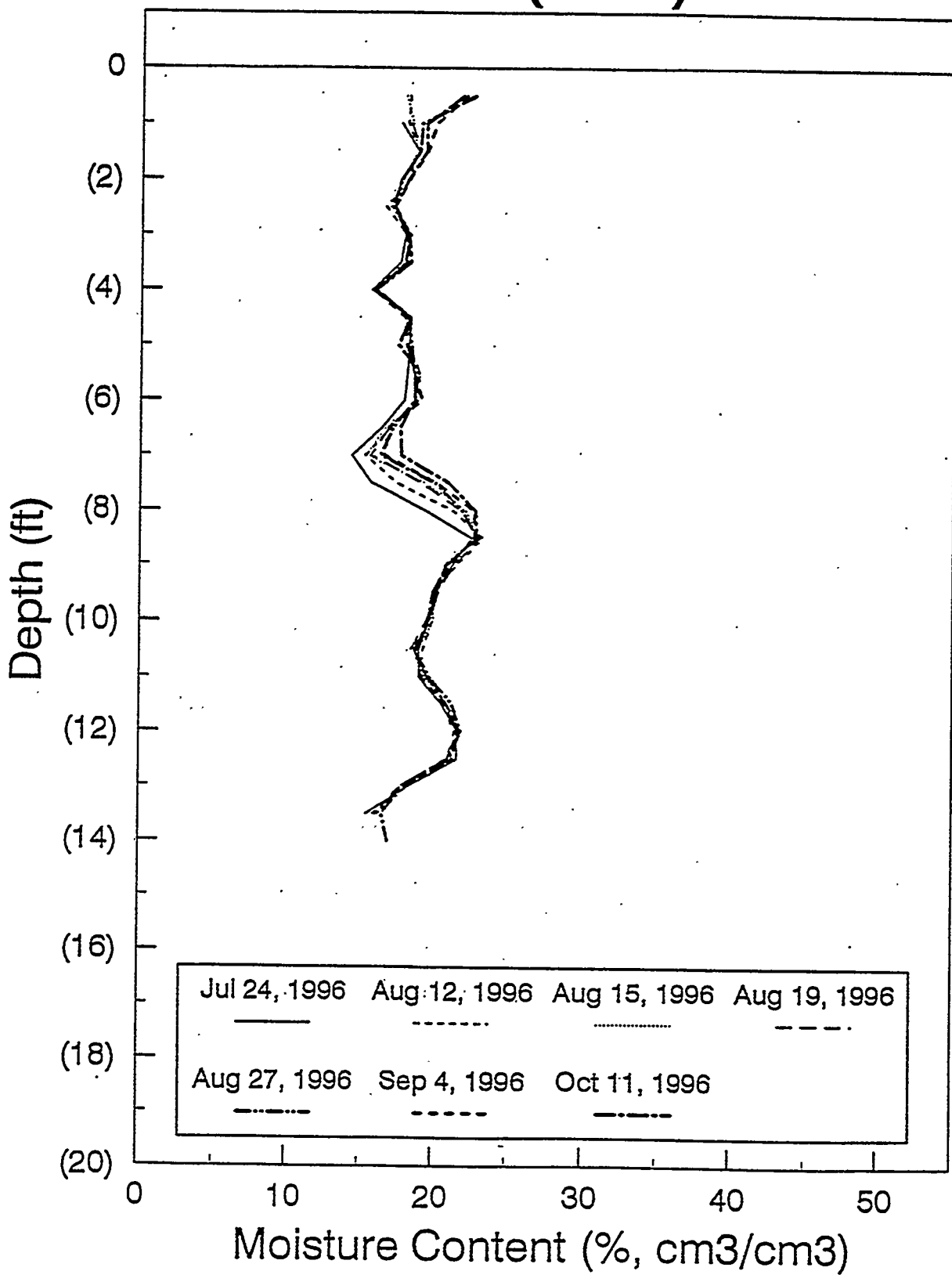


Figure E-13. Moisture content profiles for NAT-81.

## NAT 82 (East)

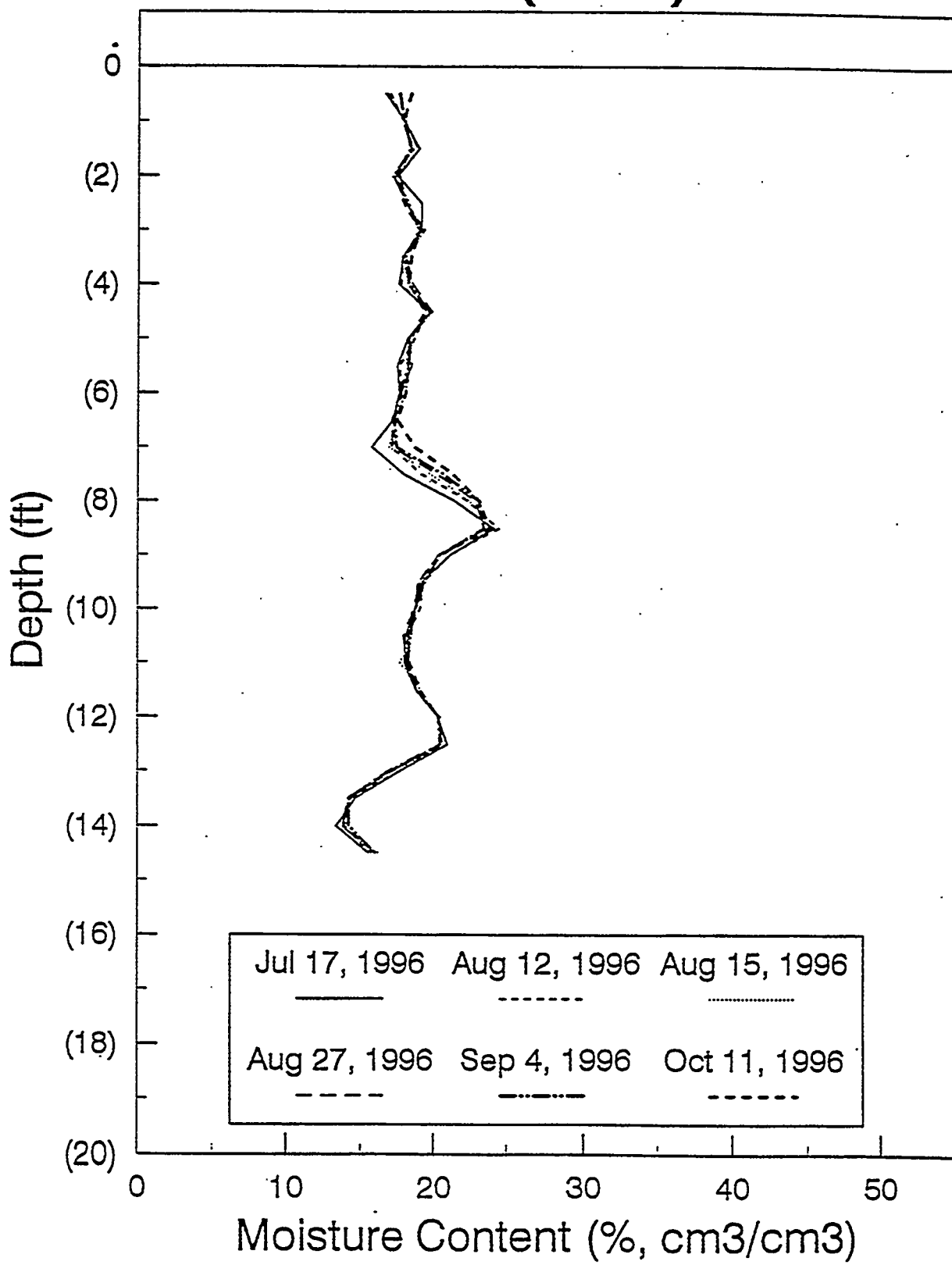


Figure E-14. Moisture content profiles for NAT-82.

# NAT 83 (east)

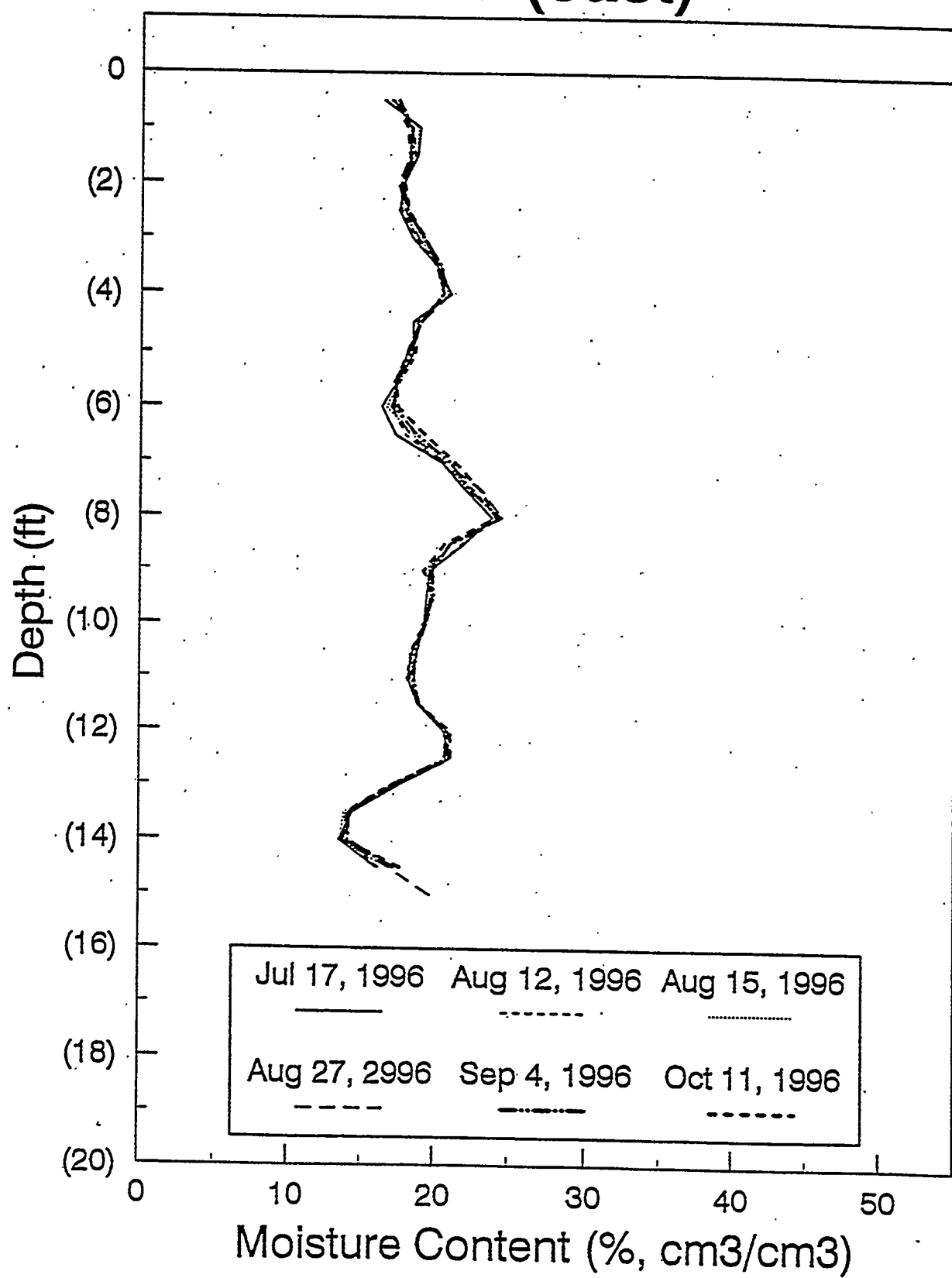


Figure E-15. Moisture content profiles for NAT-83.

## NAT-84

The moisture profiles monitored in NAT-84 (Figure E-16) are fairly static indicating that very little water from any source affected moisture content 5 ft east of the pit. Only slight wetting is evident about 5 to 8 ft bsl. The wettest conditions were monitored on October 11. The 7 to 8-ft interval shows some wetting from the grouting. Additional moisture increases are probably attributable to the packer test.

## CONCLUSIONS

The data indicate that water introduced to the pit and surrounding sediments as part of the grout mixture had little affect on moisture levels in ungrouted sediments outside the pit. In ungrouted sediments, slight increases and decreases in moisture content were observed, but in grouted sections, once equilibrium was reached, the moisture content did not change. This result suggests that most of the water in the grout mixture was bound in the grout monolith when it cured, and that there is little or no free water left over for possible mobilization and transport of waste constituents.

Of the moisture introduced to Pit D during testing and evaluation of in situ waste encapsulation techniques, the moisture associated with the grout far overshadowed any water introduced by the core drilling or packer testing at the NAT monitoring locations. Significant moisture increases associated with the grouting were monitored inside and to the north of the pit. Far lesser moisture increases were observed on either the southern or eastern sides of the pit. Preferential pathways to the north and southeast were evident during the grouting and subsequent testing. The western perimeter of the pit was unmonitored; therefore, no information about moisture movement in this direction is available. Moisture changes observed on the east side of the pit were the least and nearer the surface.

Increases in the sediment moisture content surrounding the pit following the drilling and packer testing were also slight. This may be a result of there being insufficient water because most of it returned to the surface, or it may be that the free-flowing water moved down preferential pathways to the sediment/basalt interface where it could move undetected by the neutron probe.

On the basis of this work, the data suggest that water associated with a grout mixture is not mobile and, therefore, does not transport waste components.

# NAT 84 (east)

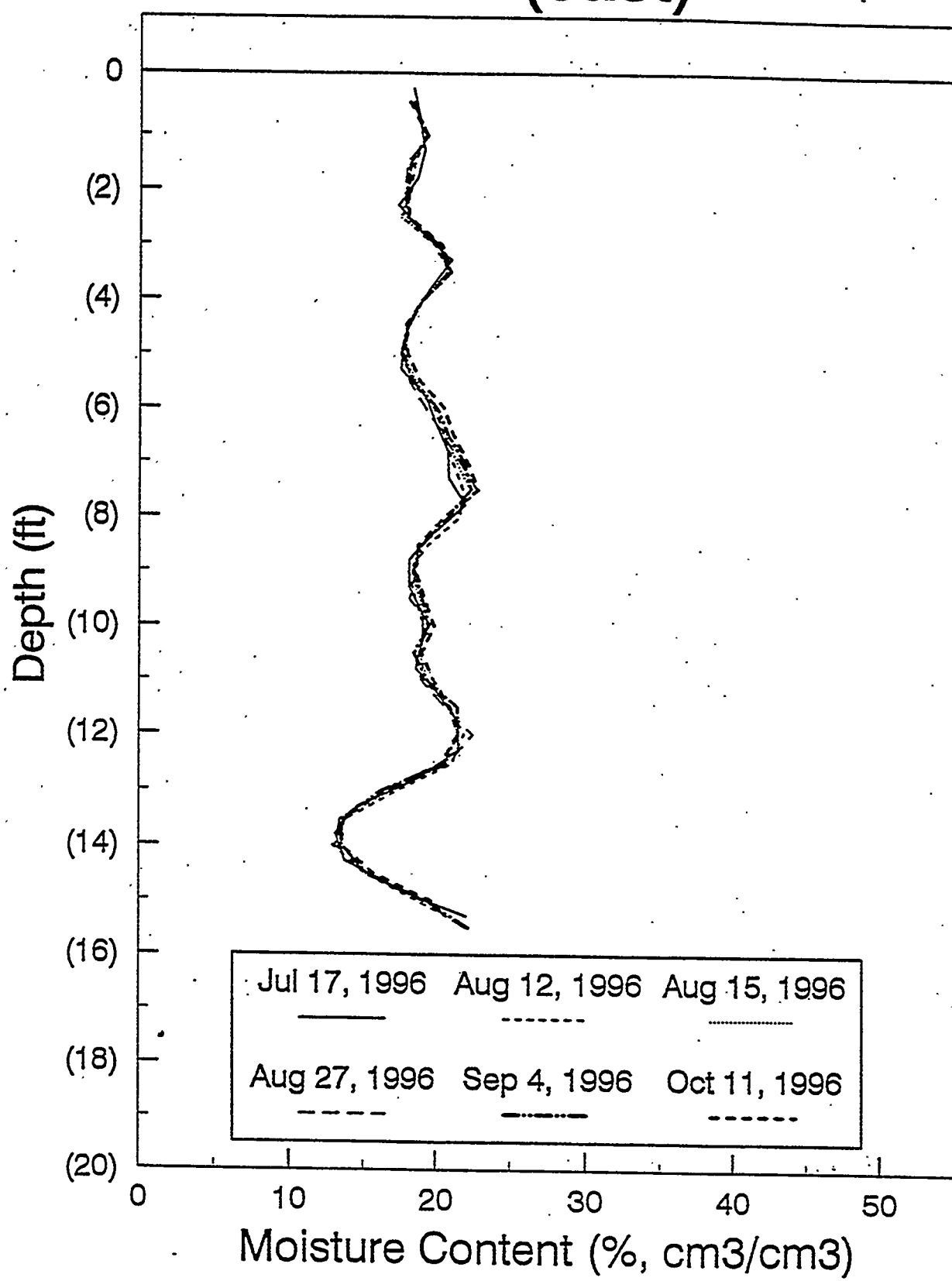


Figure E-16. Moisture content profiles for NAT-84.

## REFERENCES

Bishop, C. W., 1996, *Soil Moisture Monitoring Results at the Radioactive Waste Management Complex of the Idaho National Engineering Laboratory, FY-96, FY-95, and FY-94*, INEL-96/297.

Loomis, G. G., A. P. Zdinak, and C. W. Bishop, 1996, *Innovative Subsurface Stabilization Project—Final Report*, INEL-96/0439.